

**UNDERSTANDING LONG DISTANCE MIGRATION PATTERNS, TROPHIC
DYNAMICS, AND HABITAT USES OF MOLIDS IN THE WESTERN
PACIFIC OCEAN**

A DISSERTATION SUBMITTED TO THE GRADUATE DIVISION OF THE
UNIVERSITY OF HAWAII AT MĀNOA IN PARTIAL FULFILLMENT OF THE
REQUIREMENTS FOR THE DEGREE OF
DOCTOR OF PHILOSOPHY

IN

OCEANOGRAPHY

August 2024

By

Ching-Tsun Chang

Dissertation Committee:

Brian N. Popp, Chairperson

Jeffrey C. Drazen

Angelicque E. White

Kyle F. Edwards

Mark A. Hixon

Keywords: Molidae, tagging technique, stable isotope analysis, stomach content
analysis, isoscapes, compound specific isotope analysis of amino acids

© Copyright 20xx – Ching-Tsun Chang

All rights reserved.

DEDICATION

I dedicate this work to my mother, Shuo-Wen, and my family, for their endless support, love, and encouragement.

ACKNOWLEDGMENTS

First, I would like to express my deepest gratitude to my advisor, Dr. Brian Popp, for all the support and guidance throughout my Ph.D. I also extend my appreciation to my dissertation committee members: Dr. Jeffrey Drazen, for providing advice and great support on the diet research research direction and providing unwavering support; Dr. Mark Hixon, for his invaluable advice on my study of the diet of the Family Molidae; Dr. Angelicque White, for her thoughtful advice and support; and Dr. Kyle Edwards, for teaching me modeling and statistics.

I want to acknowledge the support from the Fisheries Research Institute and Eastern Fishery Research Center. I am grateful to Dr. Wei-Chuang Chiang, Jui-Hsein Wu, Hung-Hung Hsu, Qi-Xuan Chang, and Shian-Jhong Lin for their assistance in sample collection and experimental work.

Many thanks to Natalie Wallsgrove for always offering excellent advice and support during my experiments, and to Connor Shea, Michael Dowd, Lee Miller, Blake Stoner-Osborne, Migiwa Kawachi, Chris Wall, and Mario Kaluhiokalani for their support and advice throughout my research. I also wish to thank everyone in the Department of Oceanography office, including Kristin Momohara, Catalpa Kong, Lentina Villa, Mireya Inga, and Han Quach, for their unwavering support.

I appreciate Dr. Nakamura Itsumi at Nagasaki University, Dr. Marianne Nyegaard at Auckland War Memorial Museum, and Dr. Valérie Allain at The Pacific Community for their assistance in sample collection.

Finally, I would like to express my deep appreciation to my family: my mother and father, my grandparents, Shou-Wen, Ching-Han, Ching-Ren, and my parents-in-law. Your endless love and support have enabled me to complete my dissertation research and overcome all challenges.

ABSTRACT

Members of the family of Molidae have a circumglobal distribution from tropical to temperate regions and they can undergo long-distance migration in the western Pacific Ocean. Molids play a unique ecological role as predators of gelatinous zooplankton in the food web. Due to their slow growth rate and high bycatch, it is important to know Molidae trophic ecology across regions, which allows development of effective management strategies and policies. The overarching goal of this research is to explore the migration patterns, habitat use and feeding ecology of molids using electronic tagging, stomach content analysis (SCA) and stable carbon and nitrogen isotopic data (SIA) in the western Pacific Ocean. First, the tagging data revealed that molids made northward movements from Taiwan to Japan, and southward movements from Taiwan to the southern hemisphere. The N-S migrants demonstrate different habitat utilization patterns. Instead of using prevailing currents, the northward movements of molid cohorts exhibit extensive use of mesoscale eddies. Southward movement patterns are associated with major currents and thermal stratification of the water column. Second, isotope data suggested that some large molids found in Japan and Taiwan might have migrated from the warm pool region and one molid from New Caledonia might have migrated from Taiwan, consistent with satellite tagging data. Coupled with the captured timing of these large migrants and the spawning period of molids in Taiwan and Japan, it is suggested that the migration of the molids from the warm pool is likely related to spawning behavior. Third, a comprehensive diet description, breadth and overlap of each species in the Family Molidae were examined by literature review, SIA, and SCA. The literature review revealed that molids are predators of gelatinous plankton but exhibit broader diets than previously characterized as predators of gelatinous plankton almost exclusively. Ocean sunfish, bumphead sunfish, and hoodwinker sunfish reportedly consume prey from epi/mesopelagic

environments, while sharptail sunfish and slender sunfish consume prey from both epi/mesopelagic environments and benthic habitats. Off Taiwan, ocean sunfish and bumphead sunfish had similar and relatively narrow diet breadths, differing from sharptail sunfish, which exhibited a broader diet. Unlike other mollusks that typically feed on scyphozoans, sharptail sunfish primarily consumed tunicates. The diet of sharptail sunfish changed significantly with size and seasons. This study provides new insights into the movement and feeding ecology of mollusks in the western Pacific Ocean.

TABLE OF CONTENTS

ACKNOWLEDGMENTS	iv
ABSTRACT	v
LIST OF TABLES	xii
LIST OF FIGURES	xiv
CHAPTER 1 – INTRODUCTION AND RESEARCH RATIONALE	1
1.1 Introduction.....	1
1.2 Background.....	2
1.3 Research objectives and structure.....	4
1.4 References.....	6
CHAPTER 2 – WATER COLUMN STRUCTURE INFLUENCES LONG DISTANCE LATITUDINAL MIGRATION PATTERNS AND HABITAT USE OF BUMPHEAD SUNFISH MOLA ALEXANDRINI IN THE PACIFIC OCEAN	1
2.1 Abstract.....	11
2.2 Introduction.....	12
2.3 Materials and methods.....	13
2.3.1 Satellite Tagging.....	13
2.3.2 Geolocation Estimates.....	14
2.3.3 Environmental parameters.....	14
2.3.4 Data analysis.....	15
2.4 Results.....	15
2.4.1 Horizontal movements.....	16
2.4.2 Vertical habitat.....	16
2.4.3 Environmental variables influencing vertical activity.....	17

2.4.4 Movement behavior and oceanography.....	17
2.4.5 Dissolved oxygen.....	19
2.5 Discussion.....	19
2.5.1 Northward movement.....	20
2.5.2 Southward movement.....	22
2.6 Conclusion.....	23
2.7 References.....	24
CHAPTER 3 – UNDERSTANDING LONG-DISTANCE MIGRATION PATTERNS OF MOLIDS IN THE WESTERN PACIFIC OCEAN USING ISOTOPE ANALYSIS.....	45
3.1 Abstract.....	45
3.2 Introduction.....	46
3.3 Materials and methods.....	51
3.3.1 Sample collection.....	51
3.3.2 Bulk tissue stable isotope analysis.....	51
3.3.3 Nitrogen isotope analysis of individual amino acids.....	52
3.3.4 Reconstructing isoscapes of particulate organic matter and molids.....	52
3.3.4a Isoscape map of POM.....	52
3.3.4b Isoscape map of $\delta^{15}\text{N}$ in molids.....	54
3.3.4c Generating isoscapes.....	54
3.3.5 Comparing the predicted and measured $\delta^{15}\text{N}_{\text{molid}}$	55
3.3.6 Statistical analyses.....	55
3.3.6a Multivariate analyses.....	55
3.3.6b Bayesian mixing model.....	56
3.4 Results.....	57
3.4.1 Isoscapes of $\delta^{15}\text{N}_{\text{POM}}$ and $\delta^{15}\text{N}_{\text{molid}}$	57

3.4.2 Comparison of predicted and measured $\delta^{15}\text{N}_{\text{molid}}$ values.....	58
3.4.3 Isotopic composition in AAs of local residents and recent migrants.....	59
3.4.4 Bayesian mixing model.....	59
3.5 Discussion.....	60
3.5.1 Isoscapes of $\delta^{15}\text{N}_{\text{POM}}$ and $\delta^{15}\text{N}_{\text{molid}}$	60
3.5.2 Migrations pathway of molids in the western Pacific Ocean.....	62
3.6 Conclusion.....	66
3.7 References.....	66
CHAPTER 4 – DIET BREADTH AND OVERLAP IN THE FAMILY	
MOLIDAE.....	91
4.1 Abstract.....	91
4.2 Introduction.....	92
4.3 Materials and methods.....	94
4.3.1 Literature survey.....	94
4.3.2 Sample collection and processing.....	94
4.3.3 Stomach content analysis.....	96
4.3.4 Stable isotope analysis.....	97
4.4 Results.....	98
4.4.1 Diet composition from literature review and this study.....	98
4.4.2 Relationship between eye length/mouth gape and body length of sympatric molids.....	100
4.4.3 Diet composition of sympatric molids in eastern Taiwan.....	101
4.4.4 Isotopic composition of sympatric molids in eastern Taiwan.....	102
4.4.5 Bayesian mixing model.....	102
4.5 Discussion.....	103
4.5.1 Diet composition.....	103

4.5.2 Diets of sympatric species in eastern Taiwan.....	105
4.5.3 Diet breadth in SCA vs. SIA.....	107
4.5.4 Caveats.....	108
4.6 Conclusions.....	108
4.7 References.....	109
CHAPTER 5 – ONTOGENETIC AND SEASONAL SHIFTS IN DIETS OF SHARPTAIL SUNFISH MASTURUS LANCEOLATUS IN WATERS OFF TAIWAN.....	141
5.1 Abstract.....	141
5.2 Introduction.....	142
5.3 Materials and methods.....	144
5.3.1 Sample collection.....	144
5.3.2 Stomach content analysis.....	145
5.3.3 Bulk tissue stable isotope analysis.....	145
5.3.4 Nitrogen isotope analysis of individual amino acids.....	146
5.3.5 Data analysis.....	146
5.4 Results.....	149
5.4.1 Diet composition across size classes.....	149
5.4.2 Seasonal trend in diet composition across size classes.....	151
5.4.3 Seasonal variation in bulk isotope values across size classes.....	152
5.4.4 $\delta^{15}\text{N}$ values of amino acids and TP estimates.....	152
5.4.5 Isotopic niche width across size classes.....	153
5.4.6 Mixing models.....	153
5.5 Discussion.....	153
5.5.1 Diets of sharptail sunfish.....	154
5.5.2 Size effects.....	155

5.5.3 Seasonal effect.....	156
5.5.4 Integrating SCA and SIA in estimating diets of sharptail sunfish.....	157
5.6 Conclusions.....	160
5.7 References.....	160
CHAPTER 6 – CONCLUSIONS AND FUTURE DIRECTIONS.....	191
6.1 Research conclusion.....	192
6.2. Future Research.....	195
6.3 References.....	197

LIST OF TABLES

Table 2.1. Summary tag information of <i>Mola alexandrini</i>	31
Table 2.2. Mean day depth, night depth, depth range, and temperature range of <i>Mola alexandrini</i>	33
Table S2.1. Relative importance of each environmental variable to the final model, including Akaike information criterion, delta AIC, and Akaike weights.....	35
Table S2.2. Records of anticyclonic- and cyclonic eddies of fish 66588 and fish 195549 occurred.....	36
Table 3.1. Literature cited in development of the isoscape model of $\delta^{15}\text{N}_{\text{POM}}$	80
Table 3.2. The TP_{AA} of molids and TDF_{bulk} in each regions.....	81
Table 3.3. Isotopic compositions of local prey items in each region used for the Bayesian mixing model.....	82
Table 3.4. The isotopic compositions of potential residents and migrants of molids for CSIA-AA.....	83
Table S3.1. Isotopic compositions of local prey or other resident species used for LDA as training data.....	84
Table 4.1. Summary of diet studies of the Family Molidae.....	118
Table 4.2. Stomach contents of three collected sympatric species.....	124
Table 4.3. Diet breadth of three sympatric species.....	130
Table 4.4. Diet overlap of three sympatric species.....	131
Table S4.1. Sample size, body size range, and average size in both total length and standard length of three sympatric species.....	132
Table 5.1. Prey items of collected sharptail sunfish with stomach contents.....	169
Table 5.2. Percent similarity index values among size classes of sharptail sunfish and seasons.....	172
Table 5.3. Mean $\delta^{15}\text{N}$ values of trophic and source amino acids, and trophic positions	

across size classes of sharptail sunfish.....174

Table S5.1. Habitat and functional groups for prey items of sharptail sunfish.....175

Table S5.2. Prey tables for stomach contents of sharptail sunfish177

Table 6.1. The overlap of marine protected areas with mollids' distributions.....203

LIST OF FIGURES

Fig. 2.1. Most probable tracks of <i>Mola alexandrini</i>	37
Fig. 2.2. Depth profile of <i>Mola alexandrini</i> in daytime and nighttime with ambient water temperature and dissolved oxygen.....	38
Fig 2.3. Time-at-depth distribution of fish 66588 in different time periods.....	39
Fig. 2.4. Cluster analysis dendrogram of movement behavior patterns for <i>Mola alexandrini</i> in different periods.....	40
Fig. 2.5. Time-at-depth distribution of tag 195550 and tag 195553 in different time periods.....	41
Fig. 2.6. Vertical movement of fish 195550 and fish 195553 in different time periods with water temperature.....	42
Fig. S2.1. Generalized additive mixed models plots showing the effects of environmental variables on daily maximum depth, daytime depth and nighttime depth of <i>Mola alexandrini</i>	43
Fig. S2.2. Diagnostic plots for GAMM models.....	44
Fig. 3.1. Sampling map of molids in the western Pacific Ocean.....	85
Fig. 3.2. Map of $\delta^{15}\text{N}_{\text{POM}}$ and predicted $\delta^{15}\text{N}_{\text{molids}}$ isoscapes.....	86
Fig. 3.3. A: The relationship of measured $\delta^{15}\text{N}_{\text{molids}}$ values with molids size and the predicted $\delta^{15}\text{N}_{\text{molids}}$ values. B. The schematic of residency and migratory patterns of molids in the western Pacific Ocean.....	87
Fig. 3.4. Cluster analysis dendrogram of residents and migrants.....	88
Fig. 3.5. Linear discriminant function analysis of residents and migrants.....	89
Fig. 3.6. Estimated contribution of regional prey to diets of residents and migrants based on Bayesian isotope mixing models.....	90
Fig. 4.1. Map of the fishing grounds for set-net and longline fishing operations in eastern Taiwan for three sympatric species.....	133

Fig. 4.2. Linear relationships between gape width and standard body length, and eye length and body length of three sympatric species.....	134
Fig. 4.3. Numeric and gravimetric diet compositions of three sympatric species....	135
Fig. 4.4. Biplot of $\delta^{13}\text{C}$ and $\delta^{15}\text{N}$ values from three sympatric species.....	136
Fig. 4.5. Estimated contribution of common prey species to the diets of three sympatric species.....	137
Fig. S4.1. The number of studies that report different prey types in diet composition of mollids.....	138
Fig. S4.2. Cumulative prey curves of three sympatric species.....	139
Fig. S4.3. Linear relationships between standard body length and $\delta^{15}\text{N}$, and body length and $\delta^{13}\text{C}$ of three sympatric species.....	140
Fig. 5.1. Sharptail sunfish fishing grounds for set-net and longline fishing operations in eastern Taiwan.....	182
Fig. 5.2. Numerical and gravimetric diet compositions of sharptail sunfish for each size class.....	183
Fig. 5.3. Seasonal diet composition of sharptail sunfish <80 cm and 80–120 cm in terms of numerical and gravimetric indices.....	184
Fig. 5.4. Biplot of $\delta^{13}\text{C}$ and $\delta^{15}\text{N}$ values from sharptail sunfish and their prey items off eastern Taiwan and trophic position estimates in bulk tissues of sharptail sunfish and their prey items.....	185
Fig. 5.5. Estimated contribution of common prey species to sharptail sunfish diet based on Bayesian isotope mixing models.....	186
Fig. S5.1. Relationships between standard length and values of $\delta^{13}\text{C}$ and $\delta^{15}\text{N}$ of sharptail sunfish.....	187
Fig. S5.2. Cumulative prey curves of sharptail sunfish across sizes and seasons.....	188
Fig. S5.3. Numerical and gravimetric diet compositions of sharptail sunfish among	

seasons.....189

Fig. S5.4. Bayesian standard ellipse areas of each size class.....190

CHAPTER 1 – Introduction and Research Rationale

1.1 Introduction

The Family Molidae (known as molids), including three genera and five species (ocean sunfish *Mola mola*, bumphead sunfish *M. alexandrini*, hoodwinker sunfish *M. tecta*, sharptail sunfish *Masturus lanceolatus*, and slender sunfish *Ranzania laevis*), are distributed worldwide from tropical to temperate regions. The family, including the world's heaviest bony fish, *M. alexandrini* (2.7 tonnes, Gomes-Pereira et al. 2023), play an important ecological role as predators in the gelatinous food web. Most species are regarded as obligate gelativores and typically feed on scyphozoa (Fraser-Brunner 1951, Hooper et al. 1973). Molids comprise a large percentage of bycatch in longline, gillnet, and trawling fisheries in the Mediterranean Sea and Atlantic Ocean. Additionally, molids are captured as target food-fish species in the western Pacific Ocean (Pope et al. 2010). Given these anthropogenic pressures on molid populations, they are expected to decline globally in the coming decades due to their slow growth rate and high catch abundance (Liu et al. 2015, Phillips et al. 2023). Knowing their trophic ecology across the regions will explain how ocean sunfish interact with the environment under long-distance migrations and aid the development of effective management strategies and policies.

The spatiotemporal size distributions of *M. mola* and *M. alexandrini* suggest they undergo long-distance migration in the Pacific Ocean. Differences in size distributions of both species have been documented in Taiwan (~23°N), Japan (~35°N) and the Southern Hemisphere (~23°S). Most specimens found in Taiwan were intermediate in length (~1.6 m) (Chang et al. 2018). The individuals found in the waters off Japan and Australia were both small (< 1 m total length) and large (> 2 m) (Sawai et al. 2011, Nyegaard 2018). The timing of large sunfish occurrence also differs between regions,

occurring in April-May off Taiwan and July-August off Japan and Australia (Nakatsubo et al. 2007, Nyegaard 2018). This timing difference, coupled with the presence of large mature sunfish off Japan suggests that sunfish migrate from Taiwan to Japan and the Southern Hemisphere during summer for foraging or spawning.

Coupling tagging technology, stomach content analysis, and isotopic data allow study of migration patterns and trophic ecology of mollids in the Pacific Ocean. Tagging techniques including conventional tags and pop-up satellite archival tags, can be used to track the movement behavior and migration path of pelagic fishes. Pelagic fishes often migrate long distances in the ocean and display different habitat uses across their life histories, linked to foraging, spawning, or behavior seeking thermal preferences (Block et al. 2011). Several electronic tracking studies revealed that mollids (including *M. mola* and *M. alexandrini*) undergo long-distance seasonal migrations (Sousa et al. 2016a, b; Thys et al. 2016, 2017, Chang et al. 2020), suggesting mollids might move across different ocean basins.

1.2 Background

Tagging techniques; including conventional tags, implantable archival tags, pop-up satellite archival tags (PSATs), acoustic tags, and acceleration data loggers can also provide valuable data to study the physiology, behavioral ecology, and population structure of animals in relation to environmental variables (Ropert-Coudert & Wilson, 2005; Neilson et al., 2009; Block et al., 2011). PSATs transmit precise pop-off locations as well as archiving information on ambient water temperature, light intensity (used to approximate daily geolocations) and pressure (depth) via the Argos system of satellites. However, electronic tagging is limited to studying individual movements and is difficult to reveal the movement patterns and habitat uses at population levels. The movement ecology of animals can be further resolved and studied by using both extrinsic

(electronic and conventional tags) and intrinsic tags (e.g., stable isotopes, elemental otolith composition, genetic markers) (Graham et al., 2010; Madigan et al., 2012). Tagging studies can be used to validate the results from stable isotope data and provide a comprehensive perspective on species movement patterns and interactions with environments.

Stable isotope analysis (SIA) of bulk tissue is an effective tool for studying diets and migration of animals in many food-web studies (Hobson et al. 2006, Miller et al. 2010, Madigan et al. 2012). The stable isotope composition ($\delta^{15}\text{N}$ and $\delta^{13}\text{C}$) of animal tissues can be regarded as intrinsic tags that can be used to elucidate migration patterns and trophic dynamics of highly migratory species across ocean basins. Isotope ratios ($^{13}\text{C}/^{12}\text{C}$ and $^{15}\text{N}/^{14}\text{N}$) in predator tissues reflect their diets and food assimilation over the previous weeks to months (Hobson 1999). In particular, $\delta^{15}\text{N}$ values are frequently used to examine trophic dynamics and trophic position of animals. An increase in $\delta^{15}\text{N}$ values of 2~4‰ has been observed with each trophic level (Vander Zanden & Rasmussen 2001, Post 2002). The $\delta^{15}\text{N}$ and $\delta^{13}\text{C}$ values of the base of the food web can vary greatly across regions due to several factors including phytoplankton community composition, nutrient sources, and biological transformation of the nutrients (Altabet 2001, Sigman & Casciotti 2001). These spatial gradients in the base of the food web propagate up to the consumers via foraging. Thus, the isotopic compositions of resident predators reflect the values of local prey whereas recent migrants in a new environment may have $\delta^{15}\text{N}$ and $\delta^{13}\text{C}$ values very different than local prey (Graham et al. 2010, Madigan et al. 2014). Thus, constructing maps of the spatial distribution of primary producer isotope values (isoscapes) and comparing the isotopic differences between predator and local prey can be used to understand the movement ecology of animals (Logan et al. 2020, Madigan et al. 2014, 2016). However, it is challenging to determine the values of $\delta^{15}\text{N}$ and $\delta^{13}\text{C}$ at the base of food web.

Compound-specific isotope analysis of amino acids (CSIA-AA) is a new tool that overcomes the limitations of bulk SIA and can differentiate between the migratory and trophic effects. The $\delta^{15}\text{N}$ values in source amino acids (e.g., glycine, lysine, phenylalanine, serine, tyrosine) change little with increasing trophic level and reflect $\delta^{15}\text{N}$ values of the base of food webs, whereas other amino acids, the trophic amino acids (e.g., alanine, glutamic acid, leucine, proline, valine) change from prey to predator and reflect an organism's trophic level. Differences in the $\delta^{15}\text{N}$ values of source and trophic amino acids can thus be used to identify migrants versus local residents in a marine environment (Madigan et al. 2014, 2016).

1.3 Research objectives and structure

The overarching goal of this research is to explore the migration patterns, habitat use and feeding ecology of molids using electronic tagging, stomach content and isotopic analyses in the western Pacific Ocean. First, I explore the migration patterns and habitat uses of *M. mola* and *M. alexandrini* using electronic tags. Second, I examine the migration patterns of molids using a combination of approaches - isoscapes, CSIA-AA, and Bayesian mixing models. Third, I discuss the diet breadth and overlap of each species in the Family Molidae using a review of literature data, SIA, and stomach contents analysis (SCA). Last, the feeding ecology of the most common species off eastern Taiwan, sharptail sunfish *Masturus lanceolatus*, is examined using a combination of SIA, SCA and CSIA-AA. The study provides important insights into the trophic dynamics and habitat uses of molids under long-distance migrations in the western Pacific Ocean.

Chapter 2 explores the migration patterns of *M. alexandrini* and the relationships of environmental variables using pop-up satellite archival tags (PSATs) in the western Pacific Ocean. Four *M. alexandrini* off Taiwan recorded with pop-up satellite archival

tags in 2019–2020. Two individuals moved northward and travel to Okinawa Island and Kyushu, Japan and two moved southwards; crossing the equator, to Papua New Guinea and New Caledonia. The N–S migrants demonstrate different habitat utilization patterns. Instead of using prevailing currents, the cohort moving northward exhibited extensive use of mesoscale eddies. Southward movement patterns were associated with major currents and thermal stratification of the water column. These results present important insights into different habitat use patterns and the ability to undergo long-distance migrations of molids. Chapter 2 has been published in *Scientific Reports 11:21934* (Chang et al. 2021).

In Chapter 3, we combine isoscapes with bulk tissue, CSIA-AA, and Bayesian mixing models to elucidate migration patterns of molids in the western Pacific Ocean. The $\delta^{15}\text{N}$ values of molids sampled from Japan, Taiwan, New Caledonia (NC), and New Zealand (NZ) are measured and compared to the predicted $\delta^{15}\text{N}_{\text{molids}}$ values based on an isoscape of $\delta^{15}\text{N}$ values of particulate organic matter. We hypothesized that the $\delta^{15}\text{N}_{\text{molid}}$ values of resident molids should align with the predicted $\delta^{15}\text{N}_{\text{molid}}$ isoscapes; discrepancies could indicate a possibility of a migrant population that had been feeding elsewhere. Most molids found in Japan and Taiwan are residents, and some large individuals with high $\delta^{15}\text{N}$ values might be the recent migrants from the warm pool regions. The NC and NZ molid are non-residents that migrated from regions with similar $\delta^{15}\text{N}$ values.

Chapter 4 review the diets of each species in the Family Molidae as described in the literature. We additionally examined diet breadth and overlap among sympatric species – *M. mola*, *M. alexandrini*, and *M. lanceolatus* – through stomach content analysis (SCA) and stable isotope analysis (SIA) in fish collected in waters off eastern Taiwan. The literature review revealed that molids exhibited a broader diet than generally recognized. Results about the diets and niches of three sympatric species

suggested resource partitioning and niche separation among ocean sunfish, bumphead sunfish, and sharptail sunfish in waters off eastern Taiwan. Chapter 2 has been submitted to *Environmental Biology of Fishes*.

Next, in Chapter 5, the ontogenetic and seasonal shifts in diets of common molid *M. lanceolatus* in eastern Taiwan are examined using SCA, SIA, and CSIA-AA. Sharptail sunfish mainly consume tunicates with smaller amounts of diverse prey from epi- and mesopelagic, coastal, and benthic habitats. The diet of sharptail sunfish changes significantly at ~80 cm standard length. The results provide important insights into the trophic dynamics of sharptail sunfish and suggest that their foraging behavior varies across life-history stages and seasons, possibly reflecting resource partitioning and different habitat utilization than ocean sunfish. Chapter 5 has been published in *Marine Ecology Progress Series 715: 113–127* (Chang et al. 2023).

Finally, in **Chapter 6**, the last chapter of this dissertation provides conclusions and implications of this research. Additionally, the significance of the research and ideas for future research are discussed in this chapter.

1.4. References

- Altabet MA (2001) Nitrogen isotopic evidence for micronutrient control of fractional NO_3^- utilization in the equatorial Pacific. *Limnol Oceanogr* 46: 368-380.
- Block BA, Jonsen ID, Jorgensen SJ, Winship AJ, Shaffer SA, Bograd SJ, Hazen EL, Foley DG, Breed GA, Harrison AL, Ganong JE, Swithenbank A, Castleton M, Dewar H, Mate BR, Shillinger GL, Schaefer KM, Benson SR, Weise MJ, Henry RW, Costa DP (2011) Tracking apex marine predator movements in a dynamic ocean. *Nature* 475, 86-90.
- Chang CT, Drazen JC, Chiang WC, Madigan DJ, Carlisle AB, Wallsgrove NJ, Hsu HH, Ho YH, Popp BN (2023) Ontogenetic and seasonal shifts in diets of sharptail

- mola *Masturus lanceolatus* in waters off Taiwan. *Mar Ecol Prog Ser* 715, 113-127.
- Chang CT, Chiang WC, Musyl MK, Popp BN, Lam CH, Lin SJ, Watanabe YY, Ho YH, Chen JR (2021) Water column structure influences long-distance latitudinal migration patterns and habitat use of bumphead sunfish *Mola alexandrini* in the Pacific Ocean. *Sci Rep* 11:21934.
- Chang CT, Lin SJ, Chiang WC, Musyl MK, Lam CH, Hsu HH, Chang YC, Ho YS (2020) Horizontal and vertical movement patterns of sunfish off eastern Taiwan. *Deep-Sea Res II: Top Stud Oceanogr* 175:104683.
- Chang CT, Chih CH, Chang YC, Chiang WC, Tsai FY, Hsu HH, Wu JH, Ho YH (2018) Seasonal variations of species, abundance and size composition of Molidae in eastern Taiwan. *J Taiwan Fish Res* 26: 27-42.
- Fraser-Brunner A (1951) The ocean sunfishes (Family Molidae). *Bull Br Mus Nat Hist* 1:87–121.
- Graham BS, Koch P, Newsome S, MaMahon K, Aurioles D (2010) Using isoscapes to trace the movements and foraging behavior of top predators in oceanic ecosystems. In *Isoscapes: understanding movement, pattern and process on earth through isotope mapping*. (West JB, Bowen GJ, Dawson TE, Tu KP, eds). Springer, New York.
- Gomes-Pereira JN, Pham CK, Miodonski J, Santos MA, Dionísio G, Catarino D, Nyegaard M, Sawai E, Afonso P (2023) The heaviest bony fish in the world: A 2744-kg giant sunfish *Mola alexandrini* (Ranzani, 1839) from the North Atlantic. *J Fish Biol* 102: 290-293.
- Hobson KA (1999) Tracing origins and migration of wildlife using stable isotopes: a review. *Oecologia* 120: 314-326.
- Hooper SN, Paradis M, Ackman RG (1973) Distribution of trans-6-hexadecenoic acid, 7-methyl-7-hexadecenoic acid and common fatty acids in lipids of ocean sunfish

Mola mola. *Lipids* 8:509–516.

- Liu J, Zapfe G, Shao KT, Leis JL, Matsuura K, Hardy G, Liu M, Robertson R, Tyler J (2015) *Mola mola* (errata version published in 2016). The IUCN Red List of Threatened Species 2015: e.T190422A97667070. Accessed on 17 October 2023.
- Logan JM, Pethybridge H, Lorrain A, Somes CJ, Allain V (2020) Global patterns and inferences of tuna movements and trophodynamics from stable isotope analysis. *Deep-Sea Res II: Top Stud Oceanogr* 175: 104775.
- Madigan DJ, Chiang WC, Wallsgrove NJ, Popp BN, Kitagawa T (2016) Intrinsic tracers reveal recent foraging ecology of giant Pacific bluefin tuna at their primary spawning grounds. *Mar Ecol Prog Ser*: 553, 253-266.
- Madigan DJ, Baumann Z, Carlisle AB, Hoen DK, Popp BN, Dewar H, Snodgrass OE, Block BA, Fisher NS (2014) Reconstructing transoceanic migration patterns of Pacific bluefin tuna using a chemical tracer toolbox. *Ecology* 95: 1674-1683.
- Madigan DJ, Carlisle AB, Dewar H, Snodgrass OE, Litvin SY, Micheli F, Block BA (2012) Stable isotope analysis challenges wasp-waist food web assumptions in an upwelling pelagic ecosystem. *Sci Rep* 2: 1-10.
- Madigan DJ, Litvin SY, Popp BN, Carlisle AB, Farwell CJ, Block BA (2012) Tissue turnover rates and isotopic trophic discrimination factors in the endothermic teleost, Pacific bluefin tuna (*Thunnus orientalis*). *PLoS One* 7, e49220.
- Miller TW, Brodeur RD, Rau G, Omori K (2010) Prey dominance shapes trophic structure of the northern California Current pelagic food web: evidence from stable isotopes and diet analysis. *Mar Ecol Prog Ser* 420: 15–26.
- Neilson JD, Smith S, Royer F, Paul SD, Porter JM, Lutcavage M (2009) Investigations of horizontal movements of Atlantic swordfish using pop-up satellite archival tags. In: *Tagging and tracking of marine animals with electronic devices*. (Neilson JD, Arrizabalaga H, Hobday NFA, Lutcavage M, Sibert J, eds.). Springer, New York.

- Nyegaard M, Loneragan N, Hall S, Andrew J, Sawai E, Nyegaard M (2018) Giant jelly eaters on the line: Species distribution and bycatch of three dominant sunfishes in the Southwest Pacific. *Estuar Coast Shelf Sci* 207:1-15.
- Phillips N, Nyegaard M, Sawai E, Chang CT, Baptista M, Thys T (2023) The ocean sunfishes (family Molidae): Recommendations from the IUCN molidae review panel. *Mar Policy* 155: 105760.
- Pope EC, Hays G, Thys T, Doyle T, Sims D, Queiroz N (2010) The biology and ecology of the ocean sunfish *Mola mola*: A review of current knowledge and future research perspectives. *Rev Fish Biol Fish* 20:471–487.
- Post DM (2002) Using stable isotopes to estimate trophic position: Models, methods, and assumptions. *Ecology* 83:703–718.
- Ropert-Coudert Y, Wilson RP (2005) Trends and perspectives in animal-attached remote sensing. *Front. Ecol. Environ.* 3, 437-444.
- Sawai E, Yamanoue Y, Yoshita Y, Sakai Y, Hashimoto H (2011) Seasonal occurrence patterns of *Mola* sunfishes (*Mola* spp. A and B; Molidae) in waters off the Sanriku region, eastern Japan. *Japan. J Ichthyol* 58: 181–187.
- Sigman DM, Casciotti KL (2001) Nitrogen isotopes in the ocean. *Encyclopedia of ocean sciences* 3: 1884-1894.
- Sousa LL, Lopez-Castejon F, Gilabert J, Relvas P, Couto A, et al. (2016a) Integrated monitoring of *Mola mola* behaviour in space and time. *PLOS one* 11: e0160404.
- Sousa LL, Queiroz N, Mucientes G, Humphries NE, Sims DW (2016b) Environmental influence on the seasonal movements of satellite-tracked ocean sunfish *Mola mola* in the north-east Atlantic. *Anim Biotelemetry* 4: 1-19.
- Thys TM, Hearn AR, Weng KC, Ryan JP, Penaherrera-Palma C (2017) Satellite tracking and site fidelity of short ocean sunfish, *Mola ramsayi*, in the Galapagos Islands. *J Mar Biol* 2017: 7097965.

Thys TM, Ryan JP, Weng KC, Erdmann M, Tresnati J (2016) Tracking a marine ecotourism star: Movements of the short ocean sunfish *Mola ramsayi* in Nusa Penida, Bali, Indonesia. *J Mar Biol* 2016: 8750193.

Vander Zanden MJ, Rasmussen JB (2001) Variation in $\delta^{15}\text{N}$ and $\delta^{13}\text{C}$ trophic fractionation: Implications for aquatic food web studies. *Limnol Oceanogr* 46: 2061-2066.

CHAPTER 2 – Water column structure influences long-distance latitudinal migration patterns and habitat use of bumphead sunfish *Mola alexandrini* in the Pacific Ocean

CTChang, WC Chiang, MK Musyl, BN Popp, CH Lam, SJ Lin, YW, YH Ho, JR Chen (2021) Scientific Reports 11:21934.

2.1 Abstract

Satellite-tracking of adult bumphead sunfish, *Mola alexandrini*, revealed long-distance latitudinal migration patterns covering thousands of kilometers. Horizontal and vertical movements of four bumphead sunfish off Taiwan were tagged with pop-up satellite archival tags in 2019-2020. Two individuals moved northward and traveled to Okinawa Island and Kyushu, Japan and two moved southwards; crossing the equator, to Papua New Guinea and New Caledonia. During daytime, bumphead sunfish descended below the thermocline and ascended to mixed layer depths (MLD) during nighttime. The N-S migrants, however, demonstrated different habitat utilization patterns. Instead of using prevailing currents, the northward movements of sunfish cohorts exhibited extensive use of mesoscale eddies. Fish in anticyclonic eddies usually occupied deeper habitats whereas those in cyclonic eddies used near-surface habitats. On northward excursions, fish spent most of their time in regions with high dissolved oxygen concentrations. Southward movement patterns were associated with major currents and thermal stratification of the water column. In highly stratified regions, fish stayed below the thermocline and frequently ascended to MLD during daytime either to warm muscles or repay oxygen debts. These results for bumphead sunfish present important insights into different habitat use patterns and the ability to undergo long-distance migrations over varying spatial-temporal scales and features.

2.2 Introduction

Bumphead sunfish *Mola alexandrini* are widely distributed throughout tropical and temperate regions. Several satellite tracking studies of sunfish species have been completed in the North Pacific and Atlantic Oceans (Sims et al. 2009a, b, Dewar et al. 2010, Thys et al. 2015, Sousa et al. 2016a, b, Chang et al. 2020). Studies have shown that bumphead sunfish apparently prefer warmer waters compared to their congener (ocean sunfish, *M. mola*) (Sawai et al. 2011, Chang et al. 2020) but movement studies are limited (Chang et al. 2020, Thys et al. 2016, 2017) (Table 2.1), and movement corridors and behaviors in the Pacific Ocean are not well characterized. Prior satellite tagging data indicated that bumphead sunfish traveled thousands of kilometers near the equatorial front and dove into mesopelagic depths (1,112 m) in the Galapagos Islands (Thys et al. 2017). A clear diel vertical movement pattern was described where tagged fish descended to the mesopelagic zone during daytime and ascended to the epipelagic zone during nighttime (Thys et al. 2016, 2017).

Oceanographic characteristics including temperature, dissolved oxygen, thermal structure, eddies and prey availability; drive the movement and distribution of many pelagic fishes (Aspillaga et al. 2017, Gaube et al. 2018). Tracking studies of ocean sunfish indicated seasonal migration patterns to high latitudes in summer to locate preferred water temperatures and/or areas with high prey productivity (Dewar et al. 2010, Sousa et al. 2016a). The shift of temperatures in water structure often constrains the vertical movement of fishes. The thermocline segregates warm water near the surface from deeper and cooler water; limiting oxygen transport and influencing thermal structure and gradients. Results of tagging studies showed that some predators have the ability to descend at depth for exploiting prey organisms on an ephemeral basis but need to return to the surface to warm muscles and/or to repay oxygen debts (Nakamura et al. 2015, Tolotti et al. 2017) while other species are largely confined to

MLD due to temperature and concomitant physiological limitations (Musyl et al. 2011, Furukawa et al. 2014). Furthermore, mesoscale eddies and frontal areas influence movement behaviors for many pelagic fishes and mammals (Gaube et al. 2017, 2018, Braun et al. 2019). Mixing processes of anticyclonic eddies and cyclonic eddies influence chlorophyll *a* concentration and create enhanced foraging opportunities for different sized predator and prey species in the oligotrophic open ocean (Gaube et al. 2017).

Correlating vertical movements and the relationships to oceanographic characteristics provides insights into habitat utilization in the migration patterns for many pelagic fishes and sharks. Herein, we used pop-up satellite archival tags (PSATs) to study the horizontal and vertical movements of bumphead sunfish. Specifically, the influence of water temperature, thermal stratification, dissolved oxygen, and eddies on movement patterns and habitat uses of bumphead sunfish were investigated.

2.3 Materials and methods

2.3.1 Satellite Tagging

Four tags were deployed on bumphead sunfish by harpoon and longline fisheries from September 2019 to January 2020 off Taiwan (Table 2.1). Pop-up satellite archival tags (PSATs; miniPAT, Wildlife Computer, Redmond, WA, U.S.A.) were programmed to release after 150 to 240 days. PSATs were tethered with 300-lb test monofilament and stainless steel darts (Chang et al. 2020). Before tagging, the darts were treated with a broad-spectrum antibiotic to prevent infection and the tag was affixed beneath the dorsal fin. Round body weight was estimated by the captain and the body length was estimated from weight-length relationships (Chang, unpublished data). Pressure (converted to depth) and temperature were recorded every 10 minutes, and the MLD temperature and profiles of depth and temperature were summarized every 12 hours.

Two tags were physically recovered and provided archival data every 3 seconds (632,840 records) for fish 195550 and every 5 seconds (6,948,813 records) for fish 195549.

2.3.2 Geolocation Estimates

After pop-off, PSATs transmitted archived data via Argos, including times of sunrise and sunset, pressure (depth), temperature, light proxy, and MLD. Geolocations were estimated using Wildlife Computers GPE3 cloud-based software (Wildlife Computers 2019) on the transmitted data from detached tags, or from the full archival data record from recovered tags. The GPE3 software uses a proprietary state-space, hidden Markov model that includes ambient light, sea surface temperature, bathymetry, and Argos location to estimate most probable tracks. Location estimates were refined using the species' swimming speeds (Nakamura & Sato 2014). The most probable tracks were created with QGIS (QGIS Development Team 2016).

2.3.3 Environmental parameters

To better understand the movement patterns and relationships of environmental variables, we used sea level anomalies (SLA, global, 0.25° resolution), geostrophic currents, SST (global, 0.01° resolution), and topography from the NOAA CoastWatch ERDDAP server (<http://coastwatch.pfeg.noaa.gov/erddap>). Dissolved oxygen concentration (DO) was estimated from World Ocean Atlas 2013 (WOA, global, 1° resolution). The DO data provided monthly means in 5-m bins for 0-100m, in 25-m bins for 100-500 m, and then 50-m bins for 500-1,150 m. Mesoscale eddies were identified from SLA (Gaube et al. 2018, Chelton et al. 2011) and data from the Ocean Data Bank of the Ministry of Science and Technology, Republic of China (<http://www.odb.ntu.edu.tw/>). The depth of the MLD and thermocline in the water column were used to characterize and investigate the vertical movement behavior of tagged fish. The depth ranges between 20 °C isotherm and 14 °C isotherm was used to

represent the approximate depth range of thermocline (Fiedler et al. 2010).

2.3.4 Data analysis

Day and night differences in temperature and depth distributions were compared using non-parametric Kruskal-Wallis tests and non-parametric two-sample Kolmogorov-Smirnov tests (Zar 1999). The time-at-depth and time-at-temperature datasets were calculated from time series data. Diel periods were split by the time of local sunset and sunrise by the NOAA Solar Calculator (<https://gml.noaa.gov/grad/solcalc/>). Diel depth and temperature were plotted as frequency histograms. Depth and temperature distributions associated with anticyclonic/cyclonic eddies and different current regions were calculated. To quantify and classify movement behavior and water column use during different periods; depth and temperature distributions, maximum and minimum depth/temperature, MLD, and thermocline were used to generate similarity trees with Euclidean distances for hierarchical cluster analysis (Clarke & Gorley 2006).

Generalized additive mixed models (GAMMs, R package, mgcv and MuMIn) were used to determine potential factors that influenced vertical movements. Three GAMMs were fit separately to daily maximum depth, daytime mean depth and nighttime mean depth and tagged individuals were set as random effects. To understand the effects of water column structure on vertical movement, five environmental variables were set as fixed effects including SLA, SST, dissolved oxygen at 100 m depth, MLD, and thermocline. Each variable was included in a stepwise manner and the AICc, delta AIC, and Akaike weights were calculated. The final GAMM model was selected by lowest AICc and highest Akaike weights. We used F tests to determine whether the models were well fitted (Wood 2013).

2.4 Results

2.4.1 Horizontal movements

From 2019 to 2020, four PSATs were deployed on bumphead sunfish ranging from 160-220 cm total length (Table 2.1) and PSATs stayed attached for 78 to 240 days at liberty. Fish 66588 and 195549 moved northwards from the tagging location and traveled straight-line distances of 1,079 km and 542 km with average speeds of 6 and 7 km day⁻¹, respectively (Fig. 2.1A). Fish 66588, the largest individual (Table 2.1), moved to Okinawa Island, Japan in May, and then to Kyushu Island, Japan in August and September (Fig. 2.1C). Fish 195549 moved northwards to Okinawa Island in January (Fig. 2.1A). Both individuals experienced ambient water temperatures ranging from 7 to 30°C. The migratory pathway appeared to follow the Ryukyu Trench.

Two smaller individuals, fish 195550 and 195553 traveled 6,952 km and 5,183 km from tagging locations to Papua New Guinea and New Caledonia with speeds of 29 and 35 km day⁻¹, respectively. These individuals moved southward to the east of the Philippines in January and February, and then moved closer to the equator in April and May, and finally to New Caledonia in August and September (Fig. 2.1B, C). These fish experienced water temperatures ranging from 5 to 31°C.

2.4.2 Vertical habitat

Tagged individuals exhibited diel vertical movement patterns (Table 2.2). All individuals dove deeper in daytime than nighttime (Kruskal-Wallis: $p < 0.05$) where individuals stayed mainly in and/or above the thermocline during nighttime and below the thermocline during daytime (Fig. 2.2). Individuals (fish 66588 & 195549) that moved northward spent more time near the surface (15-20%) compared to individuals that moved southward (1-3%, fish 195550 & 195553). Average sea surface temperatures (SST) visited by fish moving northward (fish 66588: 24 ± 3 °C SD; fish 195549: 23 ± 1 °C) were significantly cooler than fish moving southward (fish 195550: 26 ± 2 °C; fish 195553: 28 ± 1 °C) ($p < 0.05$).

Fish 66588 spent most of its time within/above the thermocline, where water temperature ranged from 15 to 23 °C in both daytime and nighttime. Fish 195549 spent about 73% of time above 200 m during nighttime in comparison to 20% during daytime. Fish 195550 and fish 195553 both spent 40 to 58% of their time below 400 m during daytime with temperatures <10 °C and 85% of time >250 m during nighttime (15 to 28 °C).

2.4.3 Environmental variables influencing vertical activity

Results from the GAMM models (Fig. S2.1, S2.2) indicated the relationships between depth and environmental variables. The best fit models were selected based on Akaike information criterion (AICc) and Akaike weights (Table S2.1). The maximum depths visited were significantly influenced by thermocline, MLD, dissolved oxygen concentration (DO), and SST (best-fit model, adjusted $R^2 = 32\%$). Dissolved oxygen had a negative effect and the thermocline had positive effect on the maximum depth visited by tagged individuals (Fig. S2.1A). For tagged individuals that moved northwards, daytime movements (adjusted $R^2 = 79\%$) were significantly correlated with DO, sea level anomalies (SLA), MLD, thermocline depth, and SST. Nighttime movements were mainly influenced by thermocline and MLD, and SLA (adjusted $R^2 = 37\%$). Both DO and MLD had negative effects on the mean daytime and mean nighttime depth (Fig. S2.1B, C). Response plots showed a dome-shaped relationship between depth and SLA, with shallower depths occurring at the SLA was about -0.8 m. For tagged individuals that moved southwards, daytime depths were related to DO, SLA, thermocline, and SST (adjusted $R^2 = 36\%$). Nighttime depth (adjusted $R^2 = 54\%$) was highly related with dissolved oxygen, MLD, thermocline, and SST. Thermocline was positively correlated with the depth of tagged individuals (Fig. S2.1D, E).

2.4.4 Movement behavior and oceanography

Tagged bumphead sunfish showed distinct movement patterns related to

oceanographic characteristics. During northward movements, tagged individuals did not travel with the Kuroshio Current for an assist but instead extensively used the periphery of mesoscale eddies (Fig. 2.3A). In sunfish-associated eddies (Table S2.2), MLD and thermocline were shallower in cyclonic eddies (cold-core) than anticyclonic eddies (warm-core). Fish 66855 spent 6% and 9% of its time in cyclonic and anticyclonic eddies, respectively. Fish 195549 spent 6% of its time in only anticyclonic eddies. Both individuals showed different vertical movements when associated with anticyclonic and cyclonic eddies (Fig. 2.4A). Fish 66588 showed different depth distributions in cyclonic and anticyclonic eddies during daytime and nighttime (Kolmogorov-Smirnov: $p < 0.05$). When occupying cyclonic eddies, fish 66588 made frequent vertical movements and spent more time ($> 40\%$) at the surface to 200 m in daytime and nighttime with water temperature ranging from 17 to 23 °C (Fig. 2.3B, C). In the proximity of anticyclonic eddies, tagged individuals spent less time near the surface and went to greater depths (~600 m) and experienced water temperatures ranging from 10 to 32 °C.

By contrast, the southwest movements of fish 195550 and 195553 were not eddy-associated, but instead appeared to be influenced by ocean currents. Both individuals moved southward in the North Equatorial Current (NEC) in February (S2) and traveled a southwest course in the Equatorial Counter Current (ECC) in March (S3), and then moved southward in the South Equatorial Current (SEC) in May (S4) (Fig. 2.5). Tagged individuals mainly stayed below MLD. In S1 and S5 (the periods not influenced by major currents), MLD and thermocline were deeper than when associated with currents (Fig. 2.5). Tagged individuals spent most time below 400 m (bottom of thermocline) with water temperatures from 10 to 15 °C during daytime and occupied the 150-250 m strata (18 to 25 °C) during nighttime. Moving from the NEC to the ECC, and finally to the SEC; thermal stratification increased (average MLD increased from 33 to 94 m).

Tagged individuals mainly stayed at 100-200 m during nighttime and shifted to 350-400 m with water temperatures < 10 °C during daytime. During both daytime and nighttime, tagged individuals made frequent vertical forays within the MLD (Fig. 2.6). In the ECC, fish 195550 spent 9% of its time near the surface (0-50 m) at nighttime with a shallow MLD (33 m). The depth and temperature distribution patterns in SEC and ECC regions were similar (Fig. 2.4B).

2.4.5 Dissolved oxygen

Dissolved oxygen concentration was related to water column structure and DO was the highest in the MLD and decreased with depth (Fig. 2.2). For tagged individuals that moved northward, they experienced DO ranging from 2 to 5 ml L⁻¹ and they spent most time ($> 90\%$) above 400 m and with DO of 4-5 ml L⁻¹. Fish 195550 and 195553, which moved southward, experienced DO of 1 to 5 ml L⁻¹. They spent 35 to 46% of their time in higher DO environments (4-5 ml L⁻¹) during the night and spent 26-33% in 2 ml L⁻¹ DO environments during the day.

2.5 Discussion

This study documented the first long-distance latitudinal movement patterns of bumphead sunfish. Two bumphead sunfish moved against the prevailing current to the southern hemisphere and traveled 6,952 km and 5,183 km to New Caledonia and Papua New Guinea, respectively, and undertook the longest migration recorded for Molidae. Despite being released a month apart, they showed temporal synchronicity, and took similar movement paths along the coast of the Philippines and crossed the equator in April and May. Thys et al. (2017) recorded one bumphead sunfish travelled 2,700 km to the equatorial front and suggested equatorial upwelling might provide suitable foraging areas. Two larger individuals in our study (fish 66588 and 195549) moved northward and exhibited eddy-associated behavior which to our knowledge is the first

observation of the species utilizing mesoscale eddies. Our findings suggest that understanding movement patterns and effects of oceanographic characteristics requires detailed investigation along latitudinal routes to adequately characterize both the vertical and horizontal habitat requirements to predict movements.

2.5.1 Northward movement

Two individuals (fish 66588 and 195549) moved to high latitudes in summer paralleling the direction and course of the Kuroshio Current but they tended to avoid the current. Both individuals migrated to Okinawa Island, consistent with fisheries catch records (Sawai et al. 2018, Sawai & Yamada 2020) and previous tagging studies (Chang et al. 2020). Tagged individuals also moved to Kyushu Island, Japan in summer where similar routes were reported for skipjack tuna in terms of thermal preference and food availability (Kiyofujia et al. 2019). The high productivity and plankton biomass in the Kuroshio Current, the continental shelf, and its neighboring water mass have been reported (Fujioka et al. 2018, Kobari et al. 2019), suggesting a preferred corridor with sufficient food availability for pelagic fishes in the northwestern Pacific Ocean. Several studies on *M. mola* (Dewar et al. 2010, Sousa et al. 2015a, b), blue shark (Queiroz et al. 2010), and leatherback sea turtle (McMahon & Hays 2006) documented meridional movements during summer where movements to higher latitudes might be related to thermal preferences and food availability. Another movement interpretation suggests northward migration and the September occurrence in Japanese waters might be driven by reproduction. Mature female sunfish were found in summer (July to October) off Japan (Nakatsubo et al. 2007, Sawai et al. 2011), implying an important spawning ground. Comparable spawning migration patterns have been observed in Pacific bluefin tuna (Ashida et al. 2015, Watai et al. 2018).

When fish 66588 moved northward, it spent 20% of its time near the surface within a narrow range of ambient water temperatures (23-24 °C). Bumphead sunfish displayed

similar preferences in water temperature from 14-24 °C in Taiwan (Chang et al. 2020) and from 20-25 °C off Indonesia (Thys et al. 2017). By contrast, *M. mola* spent most time near the surface with temperature from 12-17 °C in the northeast Atlantic (Sousa et al. 2016a), from 15-17 °C in Japan (Dewar et al. 2010), and from 12-20 °C in Taiwan (Chang et al. 2020). Based on fisheries reports in Japan, bumphead sunfish mainly occurred in waters from 16-26 °C and *M. mola* occurred in water from 15 to 21 °C (Sawai et al. 2011). Together these findings suggest that bumphead sunfish may prefer higher temperatures than *M. mola*.

Sunfish generally stayed below the thermocline during the daytime and in/or above the thermocline during nighttime. Blue shark (*Prionace glauca*), bigeye tuna (*Thunnus obesus*), and swordfish (*Xiphias gladius*) also demonstrated similar vertical movement patterns that exploited resources in the thermocline during daytime (Stevens et al. 2010, Musyl et al. 2003, 2011, Lin et al. 2020). These movements probably mirrored those of vertically migrating organisms of the deep scattering layer for enhanced foraging opportunities.

Bumphead sunfish exhibited different vertical movement patterns and habitat utilization between southward and northward migrations. During northward movements, fish mainly stayed above 200 m in daytime and nighttime and were associated with mesoscale eddies. Pelagic species such as sharks, anchovy, salmon, mackerel, skipjack tuna, and sea turtles utilize eddies and perform distinct movement behaviors in anticyclonic and cyclonic eddies (Yasuda et al. 1996, Gaube et al. 2017, Bruan et al. 2019). Anticyclonic eddies enhance foraging opportunities compared to cyclonic eddies due to the warmer temperatures, upwelling of nutrients and high prey densities (Waite et al. 2019). Eddies are also influenced by the expansion and contraction of thermal structures which might affect the habitat preference and movement behavior of sunfish (Gaube et al. 2018).

2.5.2 Southward movement

Unlike northward migrations, bumphead sunfish that moved southwards did not display distinct vertical movements in or near eddy features. Instead, fish exploited geostrophic currents where depth distributions in the NEC, ECC, and SEC were shallower than other regions. Similar movement patterns were also found in sea turtles (Polovina et al. 2004). Bumphead sunfish often made deep excursions to the thermocline and ascended to MLD in highly stratified waters. The behavior can be regarded as a trade-off between physiological limitations and energy demands. Sunfish dove deep experiencing lower temperature and oxygen during daytime for foraging excursions and ascended to the surface to warm muscles and/or to repay oxygen debts. Many oceanic predators have similar strategies where they maintain warm body temperatures near the surface and exploit food resources at deeper depths (Sbragaglia et al. 2019). For *M. mola* (Nakamura et al. 2015), the thermal environment for foraging (5-12 °C) was lower than the average body temperature (16-17 °C). Whole-body heat-transfer coefficients were larger during the warming process than the cooling process. The large body size and surface area and thick skin might reduce the loss of heat, allowing fish to increase foraging time in cold water. Similar physiological mechanisms were found in sharks (Kohler et al. 1995, Nakamura et al. 2019). The cycles of deep foraging excursions and surface rewarming is possibly related to optimal foraging behavior.

Bumphead sunfish spent more time near the surface in the ECC areas characterized by wind-induced upwelling and shallow thermocline structure. Upwelling brings cold, nutrient-rich water to the surface attracting larger prey organisms, possibly allowing sunfish to feed at shallower depths.

The limitation of DO on the vertical movements and distribution of pelagic fishes has been demonstrated where oxygen minimum zones constrained vertical movements

and habitat use (Brill et al. 2005, Stramma et al. 2012, Thys et al. 2015). It has been reported that many pelagic fishes tend to show avoidance responses to hypoxia zones with minimum oxygen concentrations $< 2.5 \text{ ml L}^{-1}$ (Brill 1994). Although bumphead sunfish displayed a wide range in vertical movements, they preferred to stay in regions with high DO concentration ($4\text{-}5 \text{ ml L}^{-1}$) which is similar to other epipelagic predators, e.g., dolphinfish and billfish (Lam et al. 2015, Carlisle et al. 2017, Madigan et al. 2020). During northward migrations, bumphead sunfish spent most of their time in high DO environments where water temperature and mixing of eddies influenced DO concentrations (Schlitzer 2004, Thomsen et al. 2016). Bumphead sunfish experienced a wide range of DO concentration from 2 to 5 ml L^{-1} and during southward migration, fish remained in low DO depth during the daytime. Like *M. mola*, they probably experienced lower DO concentrations as they moved nearshore (Thys et al. 2015). The results suggested that sunfish can tolerate low DO concentrations on an ephemeral basis for feeding or to escape predators, also a pattern observed in striped marlin (Lam et al. 2015).

2.6 Conclusion

Satellite studies of bumphead sunfish demonstrated N-S migration patterns in the Pacific Ocean. Generally, vertical habitat use was related to the depth of the thermocline and MLD. Tagged fish stayed beneath the thermocline during daytime and above the thermocline or close to MLD during nighttime. Bumphead sunfish exhibited different habitat utilization patterns between southward and northward migrations. The northward movement behaviors showed an affinity to mesoscale eddies and thermal preferences while the southward movements were possibly related to the ocean currents and thermal stratification of the water column.

2.7 References

- Ashida H, Suzuki N, Tanabe T, Suzuki N, Aonuma Y (2015) Reproductive condition, batch fecundity, and spawning fraction of large Pacific bluefin tuna *Thunnus orientalis* landed at Ishigaki Island, Okinawa, Japan. *Environ Biol Fishes* 98: 1173-1183.
- Aspillaga E, Bartumeus F, Starr RM, López-Sanz A, Linares C, Díaz D, Garrabou J, Zabala M, Hereu B (2017) Thermal stratification drives movement of a coastal apex predator. *Sci Rep* 7: 526.
- Braun CD, Gaube P, Sinclair-Taylor TH, Skomal GB, Thorrold SR (2019) Mesoscale eddies release pelagic sharks from thermal constraints to foraging in the ocean twilight zone. *PNAS* 116: 17187-17192.
- Brill RW (1994) A review of temperature and oxygen tolerance studies of tunas pertinent to fisheries oceanography, movement models and stock assessments. *Fish Oceanogr* 3: 204-216.
- Brill RW, Bigelow KA, Musyl MK, Fritsches KA, Warrant EJ (2005) Bigeye tuna (*Thunnus obesus*) behavior and physiology and their relevance to stock assessments and fishery biology. *Collective Volumes of Scientific Papers ICCAT* 57: 142–161.
- Carlisle AB, Kochevar RE, Arostegui MC, Ganong JE, Castleton M, Schratwieser J, Block BA (2017) Influence of temperature and oxygen on the distribution of blue marlin (*Makaira nigricans*) in the Central Pacific. *Fish Oceanogr* 26: 34–48.
- Chang CT, Lin SJ, Chiang WC, Musyl MK, Lam CH, Hsu HH, Chang YC, Ho YS (2020) Horizontal and vertical movement patterns of sunfish off eastern Taiwan. *Deep-Sea Res II: Top Stud Oceanogr* 175: 104683.
- Chelton DB, Gaube P, Schlax MG, Early JJ, Samelson RM (2011) The influence of nonlinear mesoscale eddies on near-surface oceanic chlorophyll. *Science* 334:

328–332.

Clarke KR, Gorley RN (2006) PRIMER v6: user manual/tutorial. PRIMER-E, Plymouth.

Dewar H, Thys T, Teo SLH, Farwell C, O'Sullivan J, Tobayama T, Soichi M, Nakatsubo T, Kondo Y, Okada Y, Lindsay DJ, Hays GC, Walli A, Weng K, Streelmanand JT, Karl SA (2010) Satellite tracking the world's largest jelly predator, the ocean sunfish, *Mola mola*, in the Western Pacific. *J Exp Mar Biol Ecol* 393: 32–42.

Fiedler PC (2010) Comparison of objective descriptions of the thermocline. *Limnol Oceanogr: Methods* 8: 313–325.

Fujioka K, Fukuda H, Tei Y, Okamoto S, Kiyofuji H, Furukawa S, Takagi J, Estess E, Farwell CJ, Fuller DW, Suzuki N, Ohshimo S, Kitagawa T (2018) Spatial and temporal variability in the trans-Pacific migration of Pacific bluefin tuna (*Thunnus orientalis*) revealed by archival tags. *Prog Oceanogr* 162: 52-65.

Furukawa S, Tsuda Y, Nishihara GN, Fujioka K, Ohshimo S, Tomoe S, Nakatsuka N, Kimura H, Aoshima T, Kanehara H, Kitagawa T, Chiang WC, Nakata H, Kawabe R (2014) Vertical movements of Pacific bluefin tuna (*Thunnus orientalis*) and dolphinfish (*Coryphaena hippurus*) relative to the thermocline in the northern East China Sea. *Fish Res* 149: 86-91.

Gaube P, Barceló C, McGillicuddy Jr DJ, Domingo A, Miller P, Giffoni B, Marcovaldi N, Swimmer Y (2017) The use of mesoscale eddies by juvenile loggerhead sea turtles (*Caretta caretta*) in the southwestern Atlantic. *PLoS ONE* 12: e0172839.

Gaube P, Braun CD, Lawson GL, McGillicuddy Jr DJ, Penna AD, Skomal GB, Fischer C, Thorrold SR (2018) Mesoscale eddies influence the movements of mature female white sharks in the Gulf Stream and Sargasso Sea. *Sci Rep* 8: 7363.

Kiyofujia H, Aoki Y, Kinoshita J, Okamoto S, Masujima M, Matsumoto T, Fujioka K, Ogata R, Nakao T, Sugimoto N, Kitagawa T (2019) Northward migration dynamics

of skipjack tuna (*Katsuwonus pelamis*) associated with the lower thermal limit in the western Pacific Ocean. *Prog Oceanogr* 175: 55-67.

Kobari T, Kobari Y, Miyamoto H, Okazaki Y, Kume G, Kondo R, Habano A (2019) Variability in taxonomic composition, standing stock, and productivity of the plankton community in the Kuroshio and its neighboring waters. In: Nagai T, Saito H, Suzuki K, Takahashi M (eds) *Kuroshio Current: Physical, Biogeochemical, and Ecosystem Dynamics*, John Wiley & Sons, NJ, p 223-243.

Kohler NE, Casey JG, Turner PA (1995) Length-weight relationships for 13 species of sharks from the western North Atlantic. *Fish Bul* 93: 412-418.

Lam CH, Kiefer DA, Domeier ML (2015) Habitat characterization for striped marlin in the Pacific Ocean. *Fish Res* 166: 80-91.

Lin SJ, Musyl MK, Chiang WC, Wang SP, Su NJ, Chang CT, Chang QX, Ho YS, Kawabe R, Yeh HM, Tseng CT (2020) Vertical and horizontal movements of bigeye tuna (*Thunnus obesus*) in southeastern Taiwan. *Mar Freshw Behav Physiol* 54: 1-21.

Madigan DJ, Richardson AJ, Carlisle AB, Weber SB, Brown J, Hussey NE (2020) Water column structure defines vertical habitat of twelve pelagic predators in the South Atlantic. *ICES J Mar Sci: fsaa222*.

McMahon CR, Hays GC (2006) Thermal niche, large-scale movements and implications of climate change for a critically endangered marine vertebrate. *Glob Change Biol* 12: 1330–8.

Musyl MK, Brill R, Curran DS, Fragoso NM, McNaughton L, Nielsen A, Kikkawa BS, Moyes CD (2011) Postrelease survival, vertical and horizontal movements, and thermal habitats of five species of pelagic sharks in the central Pacific Ocean. *Fish Bull* 109: 341–368.

Musyl MK, Brill RW, Boggs CH, Curran DS, Kazama TK, Seki MP (2003) Vertical

- movements of bigeye tuna (*Thunnus obesus*) associated with islands, buoys, and seamounts near the main Hawaiian Islands from archival tagging data. *Fish Oceanogr* 12: 152–169.
- Nakamura I, Goto Y, Sato K (2015) Ocean sunfish rewarm at the surface after deep excursion to forage for siphonophores. *J Anim Ecol* 84: 590–603.
- Nakamura I, Mastumoto R, Sato K (2019) Body temperature stability in the whale shark, the world's largest fish. *J Exp Biol* 223: jeb210286.
- Nakamura I, Sato K (2014) Ontogenetic shift in foraging habit of ocean sunfish *Mola mola* from dietary and behavioral studies. *Mar Biol* 161: 1263–1273.
- Nakatsubo T, Kawachi M, Mano N, Hirose H (2007) Spawning period of ocean sunfish *Mola mola* in waters of the eastern Kanto region, Japan. *Aqua Sci* 55: 613-618.
- Polovina JJ, Balazs GH, Howell EA, Parker DM, Seki MP, Dutton PH (2004) Forage and migration habitat of loggerhead (*Caretta caretta*) and olive ridley (*Lepidochelys olivacea*) sea turtles in the central North Pacific Ocean. *Fish Oceanogr* 13: 36-51.
- QGIS Development Team (2016) Quantum GIS Geographic Information System. Open Source Geospatial Foundation Project. <http://www.qgis.org/en/site/>.
- Queiroz N, Humphries NE, Noble LR, Santos AM, Sims DW (2010) Short-term movements and diving behaviour of satellite-tracked blue sharks *Prionace glauca* in the northeastern Atlantic Ocean. *Mar Ecol Prog Ser* 406: 265–79.
- Sawai E, Yamada M (2020) Bump-head sunfish *Mola alexandrini* photographed in the north-west Pacific Ocean mesopelagic zone. *J Fish Biol* 96: 278–280.
- Sawai E, Yamanoue Y, Nyegaard M, Sakai Y (2018) Redescription of the bump-head sunfish *Mola alexandrini* (Ranzani 1839), senior synonym of *Mola ramsayi* (Giglioli 1883), with designation of a neotype for *Mola mola* (Linnaeus 1758) (Tetraodontiformes: Molidae). *Ichthyol Res* 65: 142-160.

- Sawai E, Yamanoue Y, Yoshita Y, Sakai Y, Hashimoto H (2011) Seasonal occurrence patterns of *Mola* sunfishes (*Mola* spp. A and B; Molidae) in waters off the Sanriku region, eastern Japan. *J Ichthyol* 58: 181–187.
- Sbragaglia V, Nuñez JD, Dominoni D, Coco S, Fanelli E, Azzurro E, Marini S, Noguerras M, Ponti M, del Rio Fernandez J, Aguzzi J (2019) Annual rhythms of temporal niche partitioning in the Sparidae family are correlated to different environmental variables. *Sci Rep* 9: 1708.
- Schlitzer R (2004) Export production in the equatorial and North Pacific derived from dissolved oxygen, nutrient and carbon data. *J Oceanogr* 60: 53–62.
- Sims DW, Queiroz N, Doyle TK, Houghton JDR, Hays GC (2009a) Satellite tracking of the world's largest bony fish, the ocean sunfish (*Mola mola* L.) in the North East Atlantic. *J Exp Mar Biol Ecol* 370: 127–133.
- Sims DW, Queiroz N, Humphries NE, Lima FP, Hays GC (2009b) Long-term GPS tracking of ocean sunfish *Mola mola* offers a new direction in fish monitoring. *PLOS ONE* 4: e7351.
- Sousa LL, Queiroz N, Mucientes G, Humphries NE, Sims DW (2016a) Environmental influence on the seasonal movements of satellite-tracked ocean sunfish *Mola mola* in the north-east Atlantic. *Anim Biotelemetry* 4: 7.
- Sousa LL, Lopez-Castejon F, Gilabert J, Relvas P, Couto A, Queiroz N, Caldas R, Dias PS, Dias H, Faria M, Ferreira F, Ferreira AS, Fortuna J, Gomes RJ, Loureiro B, Martins R, Madureira L, Neiva J, Oliveira M, Pereira J, Pinto J, Py F, Queirós H, Silva D, Sujit PB, Zolich A, Johansen TA, de Sousa JB, Rajan K (2016b) Integrated monitoring of *Mola mola* behaviour in space and time. *PLOS ONE* 11: e0160404.
- Stevens JD, Bradford RW, West GJ (2010) Satellite tagging of blue sharks (*Prionace glauca*) and other pelagic sharks of eastern Australia: depth behaviour, temperature experience and movements. *Mar Biol* 157: 575-591.

- Stramma L, Prince ED, Schmidtko S, Luo J, Hoolihan JP, Visbeck M, Wallace DW, Brandt P, Körtzinger A (2012) Expansion of oxygen minimum zones may reduce available habitat for tropical pelagic fishes. *Nat Clim Change* 2: 33–37.
- Thomsen S, Kanzow T, Krahnemann G, Greatbatch RJ, Dengler M, Lavik G (2016) The formation of a subsurface anticyclonic eddy in the Peru-Chile Undercurrent and its impact on the near-coastal salinity, oxygen, and nutrient distributions. *J Geophys Res* 121: 476–501.
- Thys TM, Hearn AR, Weng KC, Ryan JP, Penaherrera-Palma C (2017) Satellite tracking and site fidelity of short ocean sunfish, *Mola ramsayi*, in the Galapagos Islands. *J Mar Biol* 2017: 7097965.
- Thys TM, Ryan JP, Dewar H, Perle CR, Lyons K (2015) Ecology of the ocean sunfish, *Mola mola*, in the southern California Current System. *J Exp Mar Biol Ecol* 471: 64–76.
- Thys TM, Ryan JP, Weng KC, Erdmann M, Tresnati J (2016) Tracking a marine ecotourism star: Movements of the short ocean sunfish *Mola ramsayi* in Nusa Penida, Bali, Indonesia. *J Mar Biol* 2016: 8750193.
- Tolotti M, Bauer R, Forget F, Bach P, Dagorn L, Travassos P (2017) Fine-scale vertical movements of oceanic whitetip sharks (*Carcharhinus longimanus*). *Fish Bull* 115: 380–402.
- Waite AM, Raes E, Beckley LE, Thompson PA, Griffin D, Saunders M, Sävström C, O’Rourke R, Wang M, Landrum JP, Jeffs A (2019) Production and ecosystem structure in cold-core vs. warm-core eddies: Implications for the zooplankton isoscape and rock lobster larvae. *Limnol Oceanogr* 64: 2405-2423.
- Watai M, Hiraoka Y, Ishihara T, Yamasaki I, Ota T, Ohshimo S, Strüssmann CA (2018) Comparative analysis of the early growth history of Pacific bluefin tuna *Thunnus orientalis* from different spawning grounds. *Mar Ecol Prog Ser* 607: 207-220.

Wood SN (2013) On p-values for smooth components of an extended generalized additive model. *Biometrika* 100: 221–228.

Yasuda I, Kitagawa D (1996) Locations of early fishing grounds of saury in the northwestern Pacific. *Fish Oceanogr* 5: 63–69.

Zar JH (1999) *Biostatistical Analysis*. Prentice Hall, NJ.

Table 2.1. Summary tag information of *Mola alexandrini* from current and earlier studies

Electronic device	ID	Body weight and length	Location	Tagging date	Tagging location	Pop off location	Pop off date	Duration (days)	Distance (km)/ speed (km day ⁻¹)	References
PSAT	66588	450 kg, 220 cm	Taiwan	2019/4/2	24°04'N, 121°37'E	29°20' N, 130°46' E	2019/9/24	178	1,079 km 6.06 km · day ⁻¹	This study
PSAT	195549	290 kg, 180 cm	Taiwan	2019/12/16	22°52'N, 123°09'E	26°35' N, 127°04' E	2020/2/21	78	542 km 6.95 km · day ⁻¹	This study
PSAT	195553	240 kg, 170 cm	Taiwan	2019/12/11	22°50' N, 122°07' E	00°52' S, 164°35' E	2020/5/9	150	5,183 km 34.55 km · day ⁻¹	This study
PSAT	195550	225 kg, 160 cm	Taiwan	2020/1/8	22°35' N, 122°41' E	21°44' S, 168°16' E	2020/9/4	240	6,952 km 28.97 km · day ⁻¹	This study
PSAT	45923	400-450 kg, > 200 cm	Taiwan	2018/3/28	24°13' N, 121°46' E	24°06' N, 121°38' E	2018/4/14	18	54 km 3 km · day ⁻¹	Chang et al. (2020)
Ultrasonic tag, GPS	31738- 31741	98-165 cm	Galapagos Islands	2011/9/26	-	-	2011/10/1 2011/11/19	4 53	2,740 km 51.7 km · day ⁻¹	Thys et al. (2017)

Table 2.1. (Continued) Summary tag information of *Mola alexandrini* from current and earlier studies

Electronic device	ID	Body weight and length	Location	Tagging date	Tagging location	Pop off location	Pop off date	Duration (days)	Distance (km)/ speed (km day ⁻¹)	References
PSAT	52918-89298	100-150 cm	Indonesia	2004-2008	8°42' S-8°42' N, 115°26' E-115°27' E	8°40' S-10°34' S, 114°17' E-121°25' E	2004-2009	7-188	8.4-747 km 0.04-20.3 km · day ⁻¹	Thys et al. (2016)

Table 2.2. Mean day depth, night depth, depth range, and temperature range of *Mola alexandrini*

Fish	Day depth (m)	Night depth (m)	Depth range (m)	Temperature range (°C)	Reference
66588	212.2±144.2	145.2±89.3	3-670	6.8-29.5 (18.7±4.1)	This study
195549	328±118.7	170.7±99	0.5-623	7.1-25.7 (17.9±4.4)	This study
195550	385.3±119.5	169.1±74.8	4-1,100	4.9-30.8 (16.9±6.3)	This study
195553	328.6±142.1	167.6±71	1-1,052	5.1-30 (18.5±4.7)	This study
45923	232.5±106.9	93.2±63.5	0-486	7.7-34.1 (16.2±4.2)	Chang et al. (2020)
31739	-	-	-1,112	4.5-23.2	Thys et al. (2017)
52918	-	-	0-450	10.27.5	Thys et al. (2016)

Table S2.1. Relative importance of each environmental variable to the final model, including Akaike information criterion (AICc), delta AIC (Δ AIC), and Akaike weights (wAIC).

	AIC	Δ AIC	wAIC
<hr/>			
Maximum depth			
<hr/>			
Full	9467.9	0	0.56
No DO	9475.5	7.62	0.01
No SLA	9468.5	0.65	0.41
No MLD	9478.7	10.88	0.00
No thermocline	9585.9	118.06	0.00
No SST	9474.5	6.59	0.02
<hr/>			
Northward movement	-	Mean daytime depth	
<hr/>			
Full	2173.7	0.00	1.00
No DO	2204.0	30.24	0.00
No SLA	2195.8	22.05	0.00
No MLD	2185.4	11.70	0.00
No thermocline	2213.4	39.72	0.00
No SST	2220.2	46.43	0.00
<hr/>			
Northward movement	-	Mean nighttime depth	
<hr/>			
Full	2128.3	0.00	0.58
No DO	2129.7	1.32	0.30
No SLA	2132.8	4.46	0.06
No MLD	2141.8	13.43	0.00
No thermocline	2166.9	38.56	0.00
No SST	2133.1	4.76	0.06

Table S2.1. (Continued) Relative importance of each environmental variable to the final model, including Akaike information criterion (AICc), delta AIC (Δ AIC), and Akaike weights (wAIC).

<hr/>			
Southward movement	-	Mean daytime depth	
<hr/>			
Full	6452.1	0.00	0.55
No DO	6486.8	34.72	0.00
No SLA	6460.8	8.70	0.00
No MLD	6452.4	0.39	0.45
No thermocline	6512.6	60.50	0.00
No SST	6465.5	13.42	0.00
<hr/>			
Southward movement	-	Mean nighttime depth	
<hr/>			
Full	5804.0	0.00	0.94
No DO	5815.6	11.64	0.00
No SLA	5809.7	5.71	0.06
No MLD	5843.9	39.87	0.00
No thermocline	5986.8	182.79	0.00
No SST	5817.7	13.69	0.00
<hr/>			

Table S2.2. Records of anticyclonic- and cyclonic eddies of fish 66588 and fish 195549 occurred. Center SSHa represents sea surface height anomaly of the eddy center

Fish	Type	Radius (km)	Amplitude (cm)	Center SSHa (m)
66588	anticyclonic	101.7	16.5	0.45
66588	cyclonic	48.6	6.4	-0.05
66588	cyclonic	83.8	21.3	-0.2
66588	anticyclonic	100.9	6.4	0.3
66588	cyclonic	82.6	7.3	-0.15
66588	anticyclonic	126.2	16	0.4
66588	cyclonic	70.7	14.6	-0.15
66588	cyclonic	127.6	20.1	-0.1
66588	anticyclonic	236.1	27.1	0.5
66588	cyclonic	69.2	24.4	-0.5
195549	anticyclonic	191.2	6.9	0.2

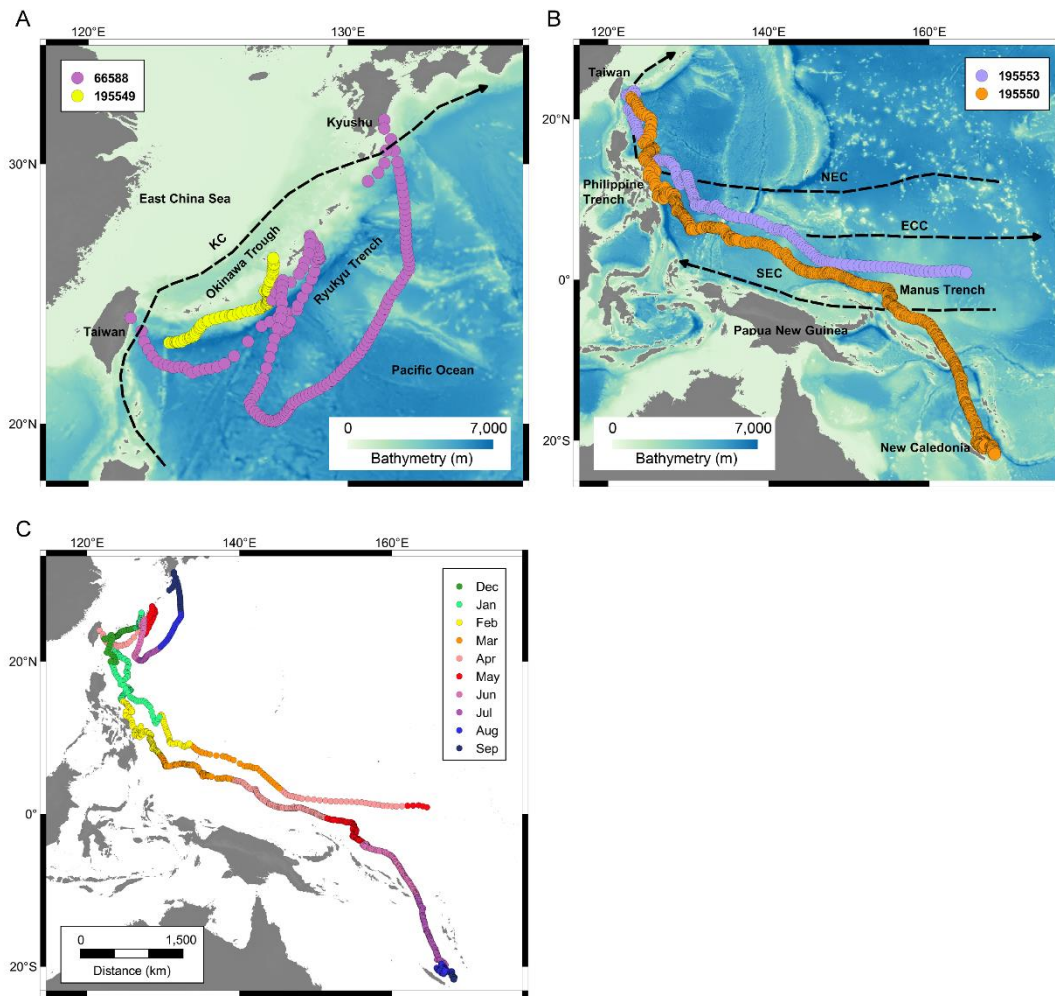


Fig. 2.1. Most probable tracks of *Mola alexandri*. (A) Tracks of fish 66588 and fish 195549 with bathymetry. (B) Tracks of fish 195550 and fish 195553 with bathymetry (C) Track of all individuals color-coded by months. KC: Kuroshio Current. NEC: North Equatorial Current. ECC: Equatorial Counter Current. SEC: South Equatorial Current.

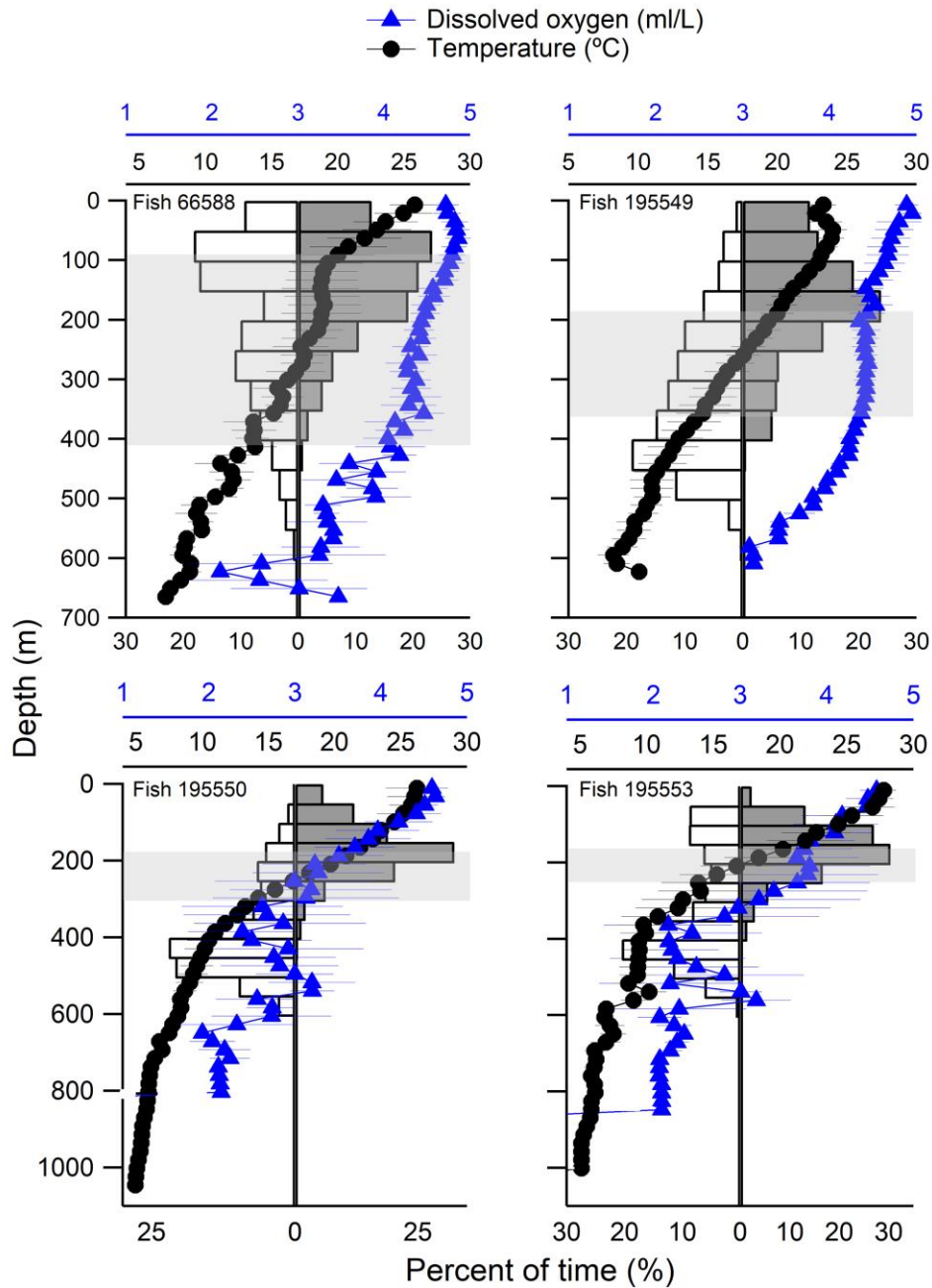


Fig. 2.2. Depth profile of *Mola alexandrini* in daytime (white bar) and nighttime (dark gray bar) with ambient water temperature (circle) and dissolved oxygen (triangle). Error bars in profile indicate standard deviations in temperature and dissolved oxygen. Shaded areas show approximate temperature at thermocline top (20 °C) and bottom (14 °C).

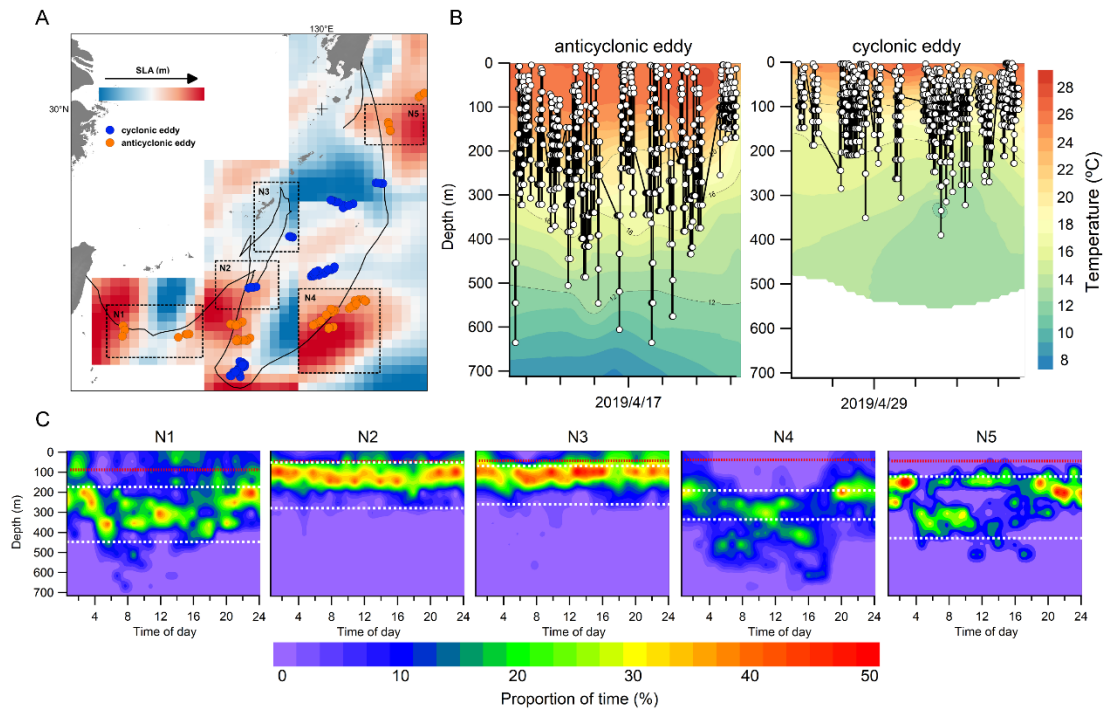


Fig 2.3. Time-at-depth distribution of fish 66588 in different time periods. N1: 4/8-20; N2: 4/25-30; N3: 5/27-31; N4: 8/1-25; N5: 9/11-15. (A) The most probable track of fish 66588 and the presence of anticyclonic eddies (red circle) and cyclonic eddies (blue circle). (B) vertical movements and the water temperature in depth profiles of anticyclonic- and cyclonic eddies. (C) The time-at-depth distribution in different time periods. White dash-line represents the depth range of thermocline and red dash-line represents the depth of mixed layer depth.

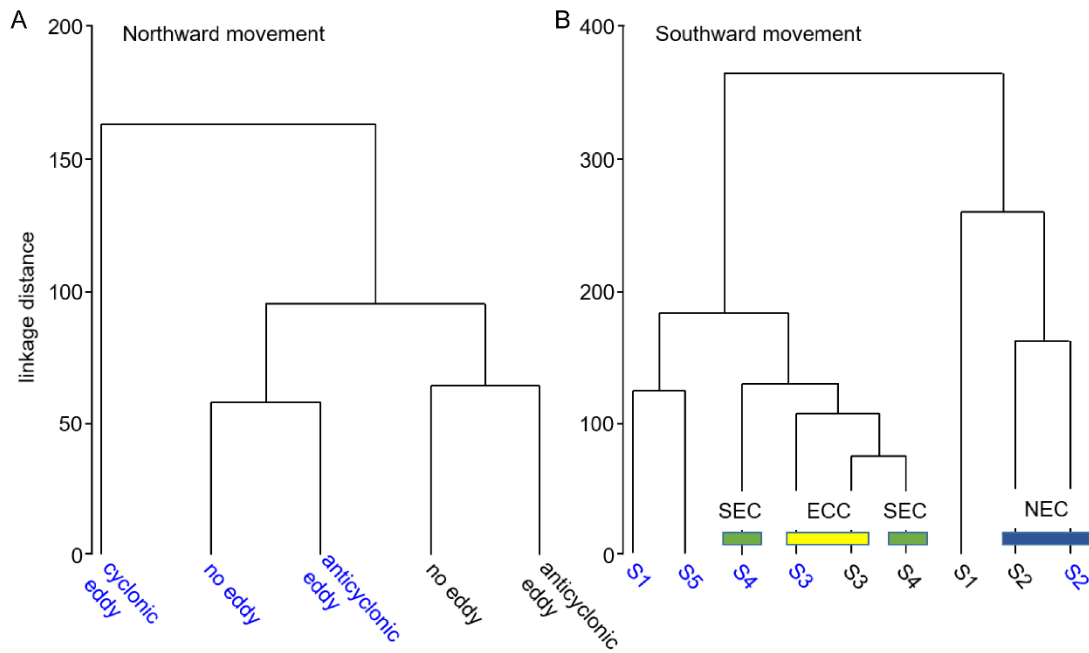


Fig. 2.4. Cluster analysis dendrogram of movement behavior patterns for *Mola alexandrini* in different periods. (A) The northward movement behavior patterns of fish 66588 (blue) and fish 195549 (black) in anticyclonic eddies, cyclonic eddies, and absence of eddies (cophenetic correlation = 0.83). (B) The southward movement behavior patterns of fish 195550 (blue) and fish 195553 (black) in different current regions (cophenetic correlation = 0.82). NEC: North Equatorial Current. ECC: Equatorial Counter Current. SEC: South Equatorial Current.

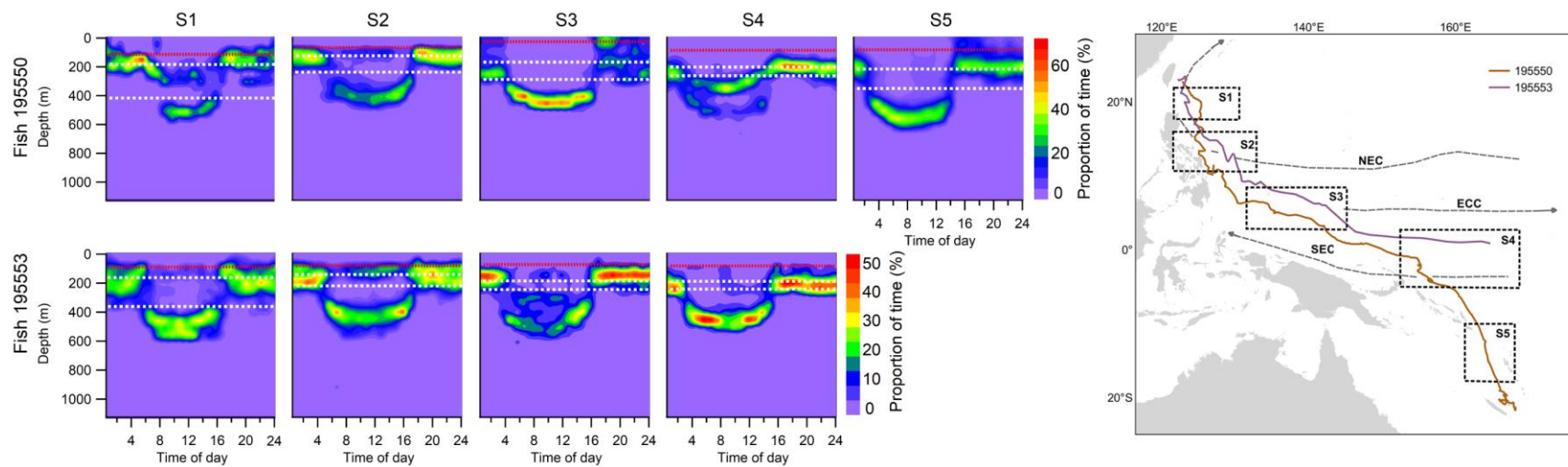


Fig. 2.5. Time-at-depth distribution of tag 195550 and tag 195553 in different time periods. White dash-line represents the depth range of thermocline and red dash-line represents the depth of mixed layer. S1 (fish 195550: 1/11-14; fish 195553: 12/18-1/16) represents the tagged individuals that moved southward. S2 (fish 195550: 2/10-25; fish 195553: 1/26-2/25) represents the tagged individuals that swam cross the North Equatorial Current. S3 (fish 195550: 3/4-18; fish 195553: 3/15-4/3) represents the tagged individuals that moved along the Equatorial Counter Current. S4 (fish 195550: 5/8-20; fish 195553: 4/11-4/30) represents the tagged individuals that moved cross the South Equatorial Current. S5 (fish 195550: 7/1-31) represents the tagged individuals that moved to southern hemisphere. NEC is North Equatorial Current. ECC is Equatorial Counter Current. SEC is South Equatorial Current. Orange line in the right bottom plot represents the most probable track of tag 195550 and purple line represents the most probable track of tag 195553.

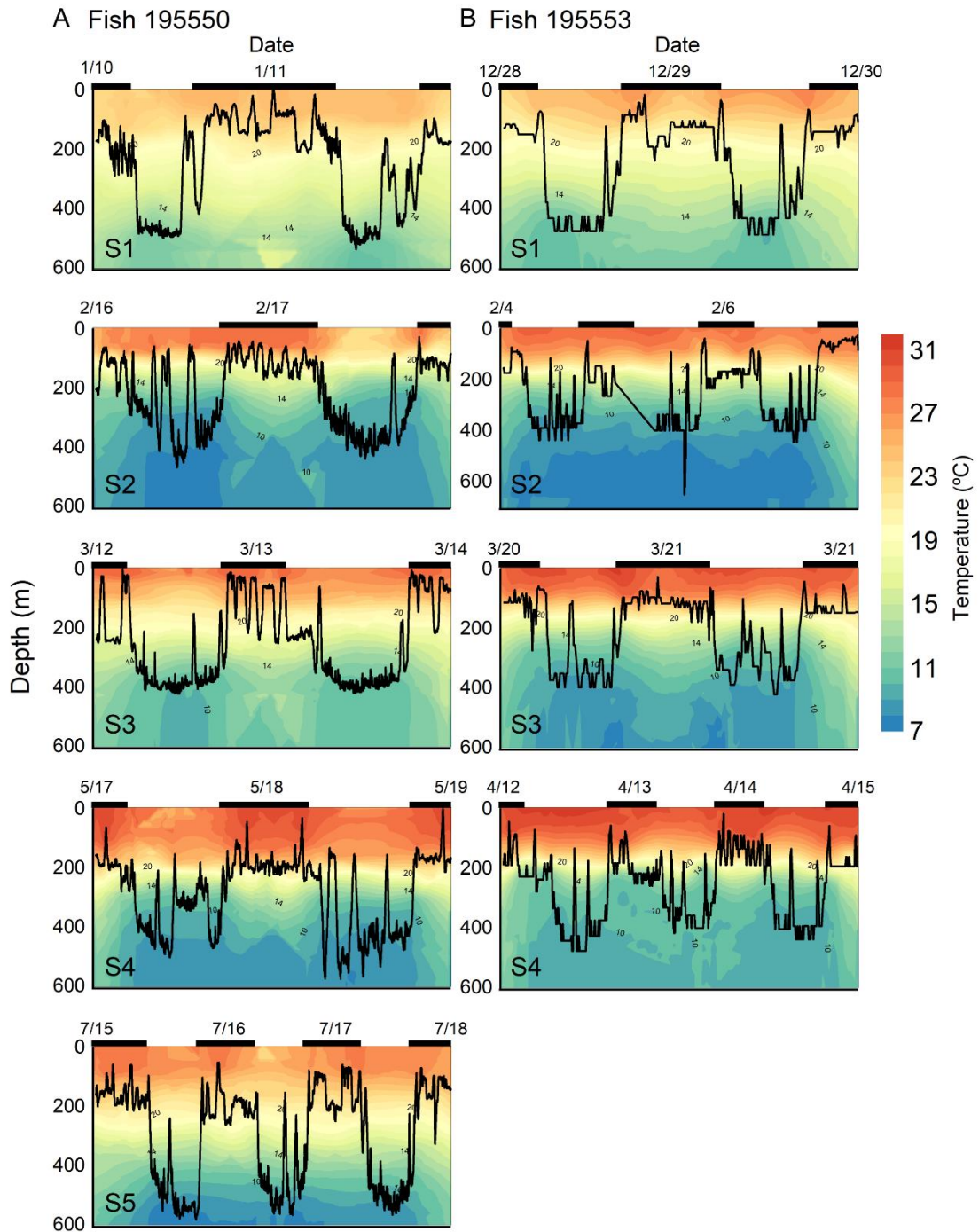


Fig. 2.6. Vertical movement of fish 195550 (A) and fish 195553 (B) in different time periods with water temperature.

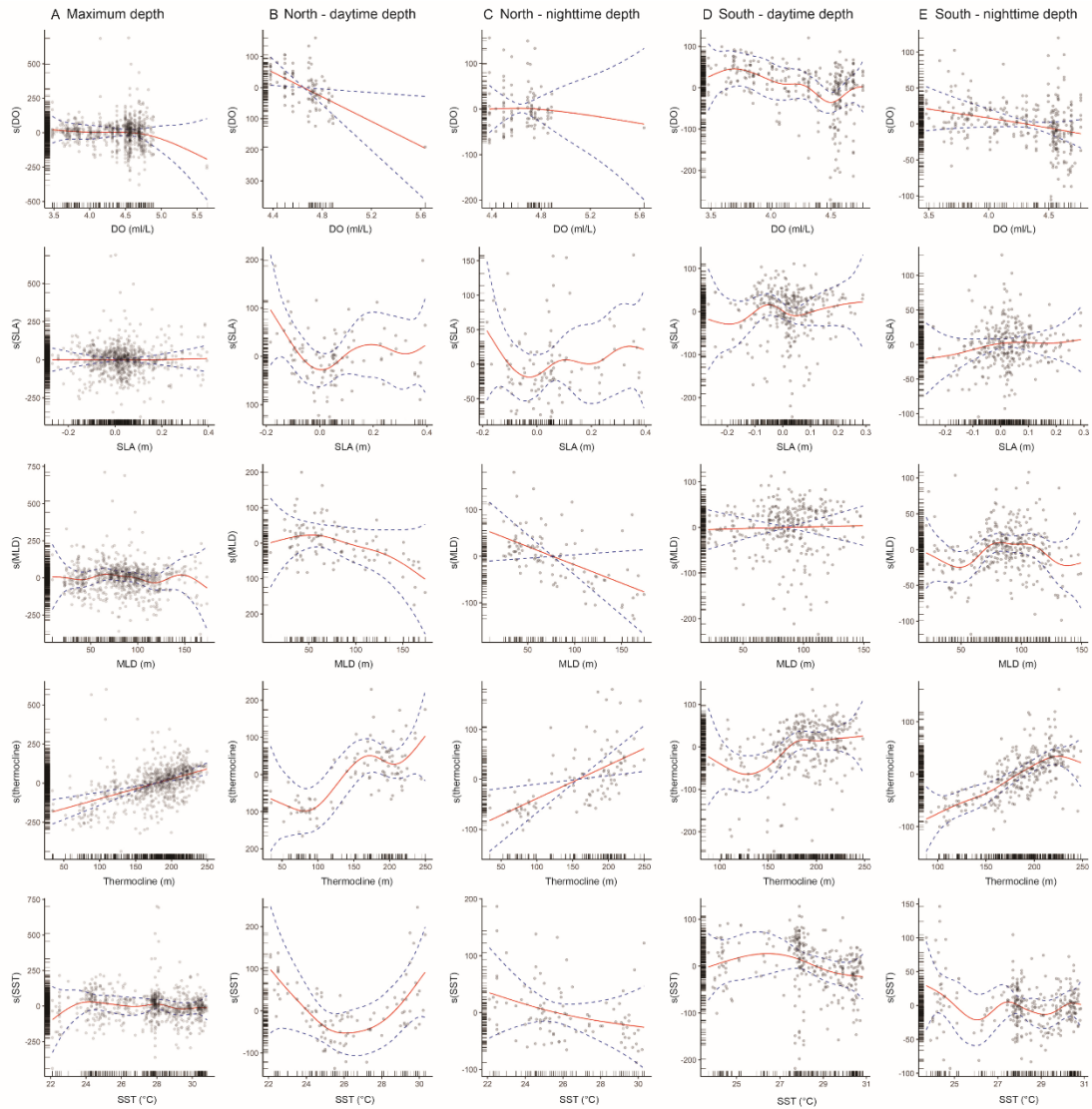


Fig. S2.1. Generalized additive mixed models plots showing the effects of environmental variables on daily maximum depth, daytime depth and nighttime depth of *Mola alexandrini*. Five plots are available for each model (from up to down): (1) DO: dissolved oxygen, (2) SLA: sea surface anomalies, (3) MLD: mixed layer depth, (4) thermocline, and (5) SST: sea surface temperature. Red solid lines show the predicted values from fitted models and dashed blue lines 95% confidence intervals

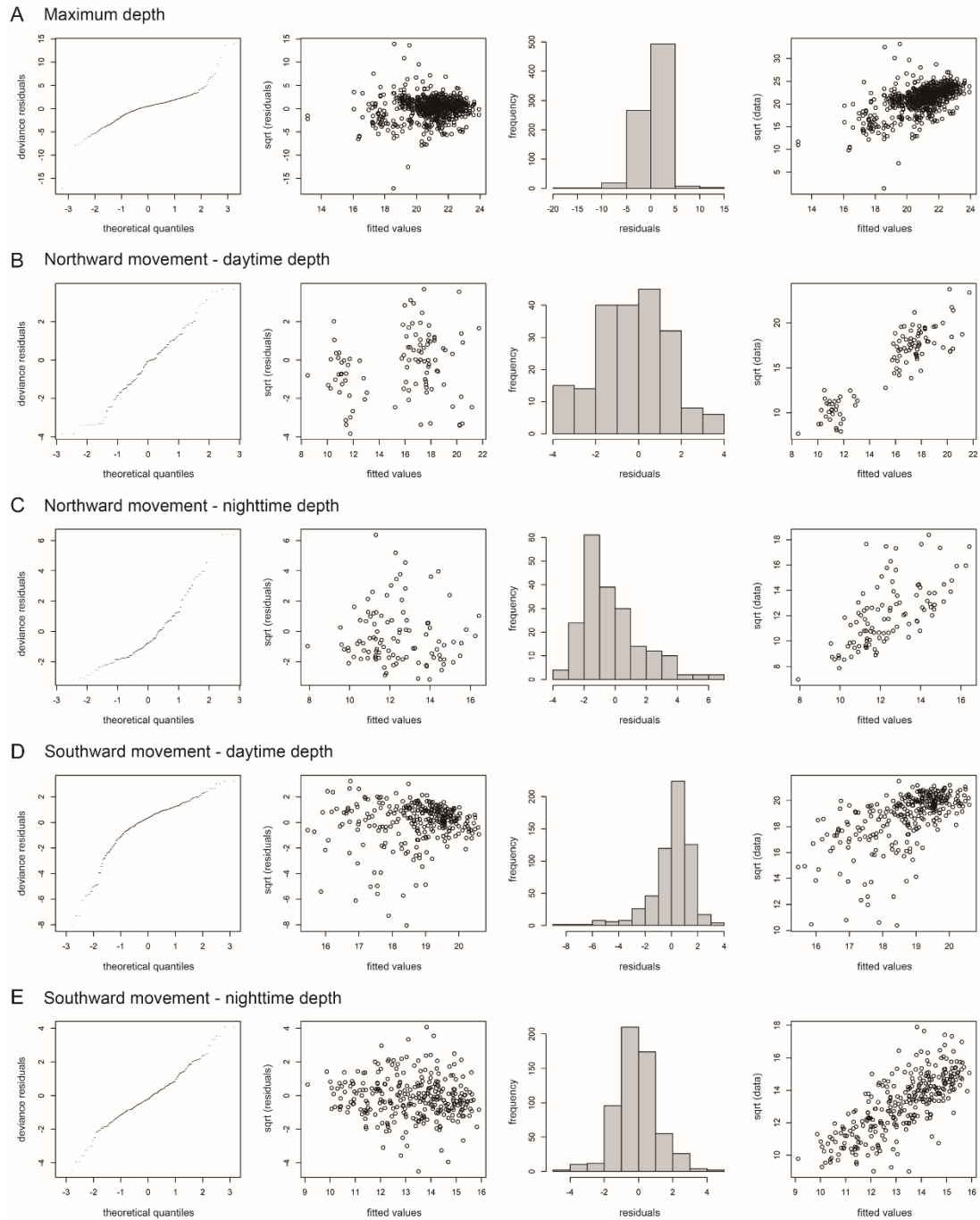


Fig. S2.2. Diagnostic plots for GAMM models on daily vertical activity (maximum depth, daytime depth, nighttime depth) of *Mola alexandrini*. Four plots are available for each model (from left to right): (1) Q-Q plot for deviance residuals of the full model, (2) fitted values versus square-root-transformed residuals, (3) distribution of residuals, (4) fitted values versus square-root-transformed observed values.

CHAPTER 3 – Understanding long-distance migration patterns of molids in the western Pacific Ocean using isotope analysis

3.1 Abstract

Combining isoscapes with bulk tissue, compound specific isotope analysis of amino acids (CSIA-AA), and a Bayesian mixing model can elucidate migration patterns of pelagic fishes at a population level. Electronic tracking studies and the spatiotemporal size distributions of molids (*Mola* spp.) suggest they undergo long-distance migration in the western Pacific Ocean. This study aims to explore the migration patterns of molids in the western Pacific Ocean using a combination of approaches. We hypothesized that the $\delta^{15}\text{N}_{\text{molid}}$ values of resident molids should align with the predicted $\delta^{15}\text{N}_{\text{molid}}$ isoscapes; discrepancies could indicate a possibility of a migrant population that had been feeding elsewhere. The predicted $\delta^{15}\text{N}_{\text{molid}}$ isoscapes was reconstructed from $\delta^{15}\text{N}$ values at the base of the food web. The measured $\delta^{15}\text{N}$ values of molids sampled from Japan, Taiwan, New Caledonia (NC), and New Zealand (NZ) when compared to the predicted $\delta^{15}\text{N}_{\text{molids}}$ values of isoscapes, shows that most molids in Japan, Taiwan and NC overlapped with the predicted values. However, some large individuals found in Japan (29%) and Taiwan (6%) with distinctly high measured values were observed, suggesting they are potential recent migrants over several months. The measured values of molids in NZ did not overlap with the predicted values, indicating they are likely non-residents. Results of multivariate analysis and Bayesian mixing model based on source amino acid $\delta^{15}\text{N}$ values provided evidence that diets of local residents in Japan and Taiwan had a high contribution from local prey. Diets of potential migrants with high $\delta^{15}\text{N}_{\text{molid}}$ values in Japan and Taiwan are consistent with high contributions from warm pool prey, indicating they might migrate from the warm pool regions. Molids found in waters of NC and NZ could potentially migrate from areas with isotopic values distinct from the local food web base. This study offers important insights into the

migration patterns of molids, suggesting they frequently migrate across different regions in the western Pacific Ocean.

3.2 Introduction

The Family Molidae, known as ocean sunfishes or molids, are globally distributed from tropical to temperate regions, playing important ecological roles as predators of gelatinous zooplankton. Like many highly migratory fish, such as tunas, billfishes, and oceanic sharks, molids travel long distances and often exhibit diverse habitat uses throughout their life histories, related to foraging, spawning, or maintenance of thermal preferences (Block et al. 2011). These highly migratory species travel various ocean basins and are frequently targeted by commercial or recreational fisheries worldwide. Molids are a food-fish species in the Pacific Ocean and comprise a significant proportion of bycatch in the Mediterranean Sea and Atlantic Ocean (Pope et al. 2010, Chang et al. 2018). Given these anthropogenic pressures on molid populations, a global decline is expected due to molid's slow growth rate and high bycatch (Liu et al. 2015). Therefore, gaining insight into the migration patterns and their interactions with the environment during long-distance migrations can help the development of effective management strategies and policies.

Observed spatiotemporal variability in size distributions of *M. mola* and *M. alexandrini* (referred to as *Mola* spp. or molids here) suggest that they undergo long-distance migration in the western Pacific Ocean. Small molids, due to their smaller size and weaker swimming abilities, are less likely to undertake basin-scale migrations. In contrast, medium to large molids, which have stronger swimming capabilities, can undergo long-distance migrations (Dewar et al. 2010, Chang et al. 2020). Differences in size distributions have been documented in both species across various habitats, including Taiwan (~23°N), Japan (~35°N) and the Southern Hemisphere (23-40°S).

Most specimens found in Taiwan had a median in total length of ~1.6 m total length (TL) (Chang et al. 2018). The individuals found in the waters off Japan and Australia varied in size, with some being small (less than 1 m) and others being large (> 2 m) (Sawai et al. 2011, Nyegaard 2018). Additionally, the timing of large mature molid occurrence differs between regions, occurring in April-May off Taiwan (Chang et al. 2018) and in July-August off Japan (Nakatsubo et al. 2007) and Australia (Nyegaard 2018). This timing difference, coupled with the presence of large mature molids, suggests that molids migrate among ocean basins, likely for foraging and/or spawning.

Tagging techniques, including conventional tags and pop-up satellite archival tags, can be used to track the movement behavior and migration path of pelagic fishes, including molids (Sibert & Nielsen 2001). Several electronic tracking studies have revealed that molids undergo long-distance seasonal migrations (Dewar et al. 2010, Sousa et al. 2016a, b, Thys et al. 2016, 2017, Chang et al. 2020, 2021). In the northwestern Pacific Ocean, twelve small *M. mola* (87 to 133 cm TL) were tagged off Japan and then migrated along the coast of Japan, likely driven by seasonal changes in temperature and prey availability (Dewar et al. 2010). Four molids tagged with pop-up satellite archival tags off Taiwan showed different migratory patterns (Chang et al. 2021). Two large individuals moved northward and traveled to Okinawa Island and Kyushu, Japan and two moved southwards; crossing the equator, to Papua New Guinea and New Caledonia. The N–S migrants demonstrated different habitat utilization patterns. Instead of using prevailing currents, the tagged fish that moved north exhibited extensive use of mesoscale eddies. The movements of the fish that moved south were associated with major currents and influenced by thermal stratification of the water column. These studies provided important insights into variability in habitat use and migratory patterns in molids and demonstrated that these animals are capable of undergoing long-distance migrations (Chang et al. 2020, 2021). However, electronic

tagging is limited to studying individual movements due to its high cost. It is generally cost prohibitive to tag enough animals to robustly characterize movement patterns and habitat use at the population level.

Stable isotope analysis (SIA) of bulk tissue is an effective tool for studying diets and migration of animals (Hobson et al. 2006, Miller et al. 2010a, Madigan et al. 2012). The stable isotope composition ($\delta^{15}\text{N}$ and $\delta^{13}\text{C}$ values) of animal tissues can be regarded as intrinsic tags that can be used to elucidate migration patterns and trophic dynamics of highly migratory species across ocean basins. Isotope ratios ($^{13}\text{C}/^{12}\text{C}$ and $^{15}\text{N}/^{14}\text{N}$) in predator tissues reflect their diets and food assimilation over the previous weeks to months, depending on the tissue type (Hobson 1999). In particular, $\delta^{15}\text{N}$ values are frequently used to examine trophic dynamics and trophic position of animals. An increase of 2~4‰ has been observed with each trophic level (Vander Zanden & Rasmussen 2001, Post 2002).

Isotopic turnover rate in animal tissue can be used to constrain the diet, migration patterns, and habitat uses over time. Isotopic turnover is a measure of how quickly isotopic compositions in consumers are replaced or renewed. Turnover rate is often expressed as isotopic half-life, which is the time it takes for 50% of the tissue's isotopic composition to reflect a new diet. When an animal consumes prey with distinct isotopic values from a new environment, its tissues gradually incorporate the new isotopic composition from prey and reflect the prey isotopic values over several months (Hesslein et al. 1993, MacAvoy et al. 2006, Madigan et al. 2012). In migration studies, both 50% and 95% turnover (~3 half-lives) are typically used to estimate when an organism's tissues have reached a steady-state with the isotopic composition in the new environment. The isotopic half-life of ^{15}N in various tissues of many pelagic fishes have been studied, including the Pacific Bluefin Tuna *Thunnus orientalis* (white muscle, 50%: 167 days, 95%: 1103 days), California yellowtail *Seriola dorsalis* (white muscle,

50%: 181 days, 95%: 784 days), nursehound *Scyliorhinus stellaris* (plasma, 50%: 39-135 days, 95%: 476 days), and smallnose fanskate *Sympterygia bonapartii* (blood, 50%: 65 days, 95%: 290 days) (Madigan et al. 2012, Kim et al. 2012, Caut et al. 2013, Galván et al. 2016). Although the ^{15}N turnover rate of molid white muscle tissue has not been studied, we estimate that their 50% and 95% turnover rates are about 300 and 1000 days, respectively (Madigan et al. 2012, Malpica-Cruz et al. 2012, Vander Zanden et al. 2015). A previous tagging study indicated that molids spend about 150 and 180 days migrating from Taiwan to Japan and the warm pool region, respectively (Chang et al. 2021). Thus, assuming the first-order reaction rate applies to ^{15}N turnover in molid white muscle tissue, a recent migrant should retain at least some of the isotopic composition of the environment from which it originated. This would depend on how much the migrant fed along the migration route and the $\delta^{15}\text{N}$ values of prey along that route. For example, a molid that migrated from the western pool with a $\delta^{15}\text{N}$ value of 14.6‰ through an environment that had a $\delta^{15}\text{N}$ value similar to Taiwan (12‰) after 180 days would have a $\delta^{15}\text{N}$ value of ~ 13.6 ‰. While this example is extreme, it shows that the migrant should retain a $\delta^{15}\text{N}$ value characteristic of the environment from which it migrated. Conversely, the isotopic composition of molid should reach 95% of the $\delta^{15}\text{N}$ value of the new environment in ~ 1000 days. Coupling tagging data with isotopic turnover rates can provide insight into molid recent foraging and migration patterns over several months/years.

The $\delta^{15}\text{N}$ and $\delta^{13}\text{C}$ values of the base of the food web can vary greatly across regions due to many factors including phytoplankton community composition, nutrient sources, and biological transformation of the nutrients (Altabet 2001, Sigman & Casciotti 2001). These spatial gradients in stable isotope composition of the base of the food web propagate up to the consumers via foraging. The isotopic compositions of resident predators reflect the values of local prey whereas recent migrants in a new environment

may have $\delta^{15}\text{N}$ and $\delta^{13}\text{C}$ values that can be very different than local prey (Graham et al. 2010, Madigan et al. 2014). Thus, constructing maps of the spatial distribution of primary producer $\delta^{15}\text{N}$ and $\delta^{13}\text{C}$ values (isoscapes) and comparing the isotopic differences between predator and local prey can be used to understand the movement ecology of animals (Logan et al. 2020, Madigan et al. 2014, 2016). However, it can be challenging to determine the values of $\delta^{15}\text{N}$ and $\delta^{13}\text{C}$ at the base of food web and understand how those baseline values propagate up through the different trophic level of the local food web (Arnoldi et al. 2023).

Compound-specific isotope analysis of amino acids (CSIA-AA) is a new tool that overcomes some of the limitations of bulk SIA and discerns migratory from trophic effects. In particular, CSIA-AA is useful for understanding how variation in movements (i.e., foraging across isotopically distinct food webs) or trophic ecology (i.e., spatiotemporal shifts in trophic level) impacts the stable isotope composition of consumers (Popp et al. 2007, Madigan et al. 2016, Matsubayashi et al. 2020). The $\delta^{15}\text{N}$ values in source amino acids (source AAs: glycine, lysine, phenylalanine, serine, tyrosine) change little with increasing trophic level and reflect $\delta^{15}\text{N}$ values of the base of food webs, whereas other amino acids, the trophic amino acids (trophic AAs: alanine, glutamic acid, leucine, proline, valine) change from prey to predator and reflect an organism's trophic level. Differences in the $\delta^{15}\text{N}$ values of source and trophic amino acids can thus be used to identify migrants versus local residents in a marine environment (Madigan et al. 2014, 2016).

The available tagging data confirms molids can migrate long distances in the western Pacific Ocean. This study aimed to explore migration patterns of molids in the western Pacific Ocean using a combination of approaches, including isoscapes, CSIA-AA, and Bayesian mixing models. Our objectives were to (i) reconstruct a nitrogen isotope isoscape for molids from $\delta^{15}\text{N}$ values at the base of the food web (ii) compare

measured $\delta^{15}\text{N}$ values of sampled molids to their predicted $\delta^{15}\text{N}$ value based on the isoscapes and, (iii) examine the migratory and trophic effects of molids using the CSIA-AA and Bayesian mixing models. We expected that molids frequently migrate in the western Pacific Ocean and demonstrate similar patterns to those observed in previous tagging studies at the population level.

3.3 Materials and methods

3.3.1 Sample collection

We collected muscle tissue and measured the total length (TL, from the tip of snout to the end to the caudal fin) of molids (*M. mola* and *M. alexandrini*) in Taiwan (n = 95, 68-257 cm TL), Japan (n = 14, 31-201 cm TL), New Caledonia (NC, n = 1, 136 cm TL), and New Zealand (NZ, n = 10, 42-127 cm TL) from 2012 to 2022 for bulk SIA and CSIA-AA (Fig. 3.1). We combined *M. mola* and *M. alexandrini* (known as *Mola* spp. or molids) in this study because they share similar feeding habits (Chang et al. in review) and movement behaviors, and there are no significant differences in their isotopic compositions of nitrogen (one-way ANOVA: $F_{1, 93} = 0.400, p = 0.528$) and carbon ($F_{1, 93} = 2.326, p = 0.131$). The muscle samples were frozen at -80°C before SIA processing. Scyphozoa (*Atolla* spp.), a major prey item of molids, in Taiwan (n = 8) and Japan (n = 9) were also collected during 2019 to 2021.

3.3.2 Bulk tissue stable isotope analysis

Muscle tissue and prey items were rinsed with distilled water and freeze-dried for 48h at -55°C . The dried tissue was ground into a homogeneous powder. Approximately 0.4-0.8 mg of powder was packed into ultra-clean tin capsules. The values of $\delta^{13}\text{C}$ and $\delta^{15}\text{N}$ were determined using an elemental analyzer (Costech ECS 4010 Elemental Combustion System using a Zero Blank Autosampler) coupled to a mass spectrometer (Thermo-Delta V Advantage or Delta Plus XP). The isotope values were expressed in standard ‰ notation relative to Vienna Pee Dee belemnite (V-PDB) for carbon and

atmospheric N₂ for nitrogen. The analytical error derived from multiple analyses of reference materials for both $\delta^{13}\text{C}$ and $\delta^{15}\text{N}$ was <0.2‰. Because lipids have lower $\delta^{13}\text{C}$ values relative to other animal tissues, and the variability in tissue lipid content can affect $\delta^{13}\text{C}$ values (Focken & Becker 1998), the $\delta^{13}\text{C}$ values of muscle (C:N > 3.5) and invertebrate prey items (C:N > 3.8) were normalized using lipid normalization algorithms for muscle from Atlantic bluefin tuna *Thunnus thynnus* (Logan et al. 2008) and from zooplankton (Syväranta & Rautio 2010), respectively

3.3.3 Nitrogen isotope analysis of individual amino acids

We selected for CSIA-AA some individuals identified as residents over months (including the small and large size individuals) based on overlapping measured $\delta^{15}\text{N}_{\text{molids}}$ and predicted $\delta^{15}\text{N}_{\text{molids}}$ values, and potential migrants over months (mostly large individuals) with measured $\delta^{15}\text{N}_{\text{molids}}$ values distinctly different from that predicted from our isoscape. The preparation for CSIA-AA followed the methods of Hannides et al. (2009). Approximately 10–15 mg of homogenized white muscle tissue were hydrolyzed, then esterification and trifluoroacetylation were undertaken. The $\delta^{15}\text{N}$ values of individual amino acids were analyzed using a Delta V Plus mass spectrometer interfaced to a Trace GC gas chromatograph. The measured $\delta^{15}\text{N}$ values were corrected using the linear regression of the measured versus known curves derived from the analysis of 14 AAs with known isotopic compositions. All samples were analyzed in triplicate. The $\delta^{15}\text{N}$ of norleucine and aminoadipic acid of known isotopic composition and co-injected with samples were used as a measure of accuracy and precision. Standard deviation for triplicate injections of each sample averaged 0.55‰ ($\pm 0.3\%$) and ranged from 0.03 to 1.95‰.

3.3.4 Reconstructing isoscapes of particulate organic matter (POM) and molids

3.3.4a Isoscape map of POM

We constructed isoscape maps of $\delta^{15}\text{N}_{\text{POM}}$ in the western Pacific Ocean using both

sampling data and data obtained from literature (Table 3.1). Several assumptions were made during the construction of the isoscape map. Firstly, we assumed that the trophic discrimination factor (TDF) between each trophic position was the same. Secondly, we assumed the isoscapes of POM and molids did not change over time; therefore, we collected data from various time points to mitigate temporal variability. Thirdly, we assumed that the trophic position (TP) of POM was TP 1 and POM represents the $\delta^{15}\text{N}$ values at the base of the food web, in effect primary producers.

The data of $\delta^{15}\text{N}_{\text{POM}}$ isoscapes were extracted from published $\delta^{15}\text{N}$ values of nitrate, POM, zooplankton, and forage fish (Table 3.1). For the nitrate data, we assumed that the nitrate was completely utilized by primary producers and the $\delta^{15}\text{N}$ values of nitrate can represent the $\delta^{15}\text{N}$ values of POM in the oligotrophic regions (i.e., eastern Taiwan). We compared the $\delta^{15}\text{N}$ values of nitrate and those estimated for POM from forage fish (see method below) in the oligotrophic regions and found that the measured $\delta^{15}\text{N}$ values of nitrate and estimated POM were similar. For the POM data, we selected the size of POM ($<330 \mu\text{m}$). In the zooplankton data, we selected copepod samples collected in the euphotic zone (0-200 m). In the fish data, we selected the fish with TP < 4 , habitat depth $< 200 \text{ m}$, and no diel vertical migration (e.g. anchovy, Scombridae). The ecological information of the TP and habitat depth of fish were collected from Fishbase.

For the data of zooplankton and forage fish, we estimated the $\delta^{15}\text{N}$ values of primary producers (i.e., POM) by subtracting the TDF_{bulk} between the consumer and phytoplankton using the equation:

$$\delta^{15}\text{N}_{\text{POM}} = \delta^{15}\text{N}_{\text{consumer}} - \text{TDF}_{\text{bulk}} \times (\text{TP}_{\text{consumer}} - \text{TP}_{\text{POM}}) \quad (1)$$

where $\delta^{15}\text{N}_{\text{POM}}$ represents the estimated $\delta^{15}\text{N}$ values of POM, $\delta^{15}\text{N}_{\text{consumer}}$ represents the $\delta^{15}\text{N}$ values of consumers (i.e. zooplankton and forage fish) obtained from literature reviews. TDF_{bulk} represents the difference between $\delta^{15}\text{N}$ values of a consumer and its

diet. The values of TDF_{bulk} varied in each region (Table 3.2). $TP_{consumer}$ and TP_{POM} were the trophic positions of consumers and POM, respectively. We compared the observed values of $\delta^{15}N_{POM}$ from POM and estimated values from nitrate, zooplankton, and fish in the regions with similar latitude and longitude. The outliers (identified as observations more than 2.5 standard deviations away from the mean) were excluded because the outliers appear unrealistic.

3.3.4b Isoscape map of $\delta^{15}N$ in molids

A constant increase in $\delta^{15}N$ values between a consumer and its prey allows for constructing the $\delta^{15}N_{molids}$ isoscape from the $\delta^{15}N_{POM}$ isoscape. We built the isoscape maps of $\delta^{15}N_{molids}$ by adding the $\delta^{15}N$ values between POM and molids to the $\delta^{15}N_{POM}$ isoscapes using the equation:

$$\delta^{15}N_{molid} = \delta^{15}N_{POM} + TDF_{bulk} \times (TP_{molid} - TP_{POM}) \quad (2)$$

where $\delta^{15}N_{molid}$ represents the predicted value of molids. The TP of molids (TP_{molid}) was calculated from the $\delta^{15}N$ values of amino acids using the equation:

$$TP_{molid} = 1 + \frac{\delta^{15}N_{Trp} - \delta^{15}N_{Src} - \beta}{TDF_{AA}} \quad (3)$$

In this equation, $\delta^{15}N_{Trp}$ and $\delta^{15}N_{Src}$ represent the weighed averaged of trophic (alanine, aspartic acid, glutamic acid) and source (glycine, serine, phenylalanine, lysine) amino acids. β (3.6‰; Bradley et al. 2015) represents the difference between the $\delta^{15}N$ values of trophic and source amino acids in primary producers. TDF_{AA} (5.7‰; Bradley et al. 2015) represents the TDF for the $\delta^{15}N$ values of trophic and source amino acids for each trophic level.

3.3.4c Generating isoscapes

We generated the $\delta^{15}N_{POM}$ and $\delta^{15}N_{molid}$ isoscapes using Ocean Data View version 5.0.0 (Schlitzer 2018) with data interpolating variational analysis (DIVA). We set the DIVA parameters for interpolation to get high-quality estimates. We used length scales

(x, y) = 28, 21. Large length scales result in a smooth field while small length scale can preserve more of the data's structure. The quality limit was set to 2, with estimates considered problematic if the quality limit exceeds 3. The signal-to-noise ratio, which measures the quality of the data relative to background noise, was set to 30. The depth of isosurface was set to 200 m, representing the depth at which a particular parameter (such as temperature, salinity, or density) is constant throughout a vertical water column.

3.3.5 Comparing the predicted and measured $\delta^{15}\text{N}_{\text{molid}}$

After generating the $\delta^{15}\text{N}_{\text{molid}}$ isoscapes, we resampled $\delta^{15}\text{N}_{\text{molid}}$ values of potential habitats for molids, including Japan (37-41.4 °N, 141-143.1 °E), Taiwan (23-25.4 °N, 121.4-122.8 °E), warm pool (1.7 °N -14 °S, 145-179.9 °E), NC (18.6-22.4 °S, 159.8-166.4 °E), and NZ (40.9-45 °S, 173.6-178.6 °E), from the sampling values in isoscape using an iterative bootstrapping approach (10000 iterations, Mooney et al. 1993). We generated a sampling distribution by repeatedly taking random samples from known sampling values. This allowed us to generate estimates of population-wide resident molid SIA values for each region. Then, we compared the predicted $\delta^{15}\text{N}_{\text{molid}}$ values from isoscapes to the measured $\delta^{15}\text{N}_{\text{molid}}$ values from sampled molids in each region. The comparison allows us to identify residents and recent migrants, as well as potential regions where the migrants traveled from. We hypothesized that the measured $\delta^{15}\text{N}$ values of resident molid populations should match predicted $\delta^{15}\text{N}$ values based on isoscapes; discrepancies could suggest a possibility of a migrant population that had been feeding elsewhere.

3.3.6 Statistical analyses

3.3.6a Multivariate analyses

To assess whether residents utilize local prey, linear discriminant function analysis (LDA, Izenman 2013) was applied using $\delta^{15}\text{N}_{\text{Src}}$ values of prey for molids or other resident species in Japan (Japanese horse mackerel and Japanese anchovy), Taiwan

(jellyfish, small sharptail sunfish), the warm pool (yellowfin tuna), and NZ (POM) as training data. Then, we applied multivariate analysis of variance (MANOVA) to test whether the groupings were significantly different from one another. The $\delta^{15}\text{N}_{\text{Src}}$ of residents should be similar to the $\delta^{15}\text{N}_{\text{Src}}$ of local prey or other local resident species if residents use the local prey. The $\delta^{15}\text{N}_{\text{Src}}$ values of jellyfish in Taiwan were measured in this study, and the values of other local resident species in Japan, the warm pool, and NZ were obtained from previous studies (Lorrain et al. 2015, Miyachi et al. 2015, Sabadel et al. 2022, Chang et al. 2023, Xing et al. 2023). Two source AAs (glycine, phenylalanine) were used when we set prey and other resident species as training data (Table S3.1) since not all source AAs were reported in the previous studies. The testing results (grouping accuracy: 61%, $p < 0.001$) showed that most Japan residents and Taiwan residents were grouped with the $\delta^{15}\text{N}_{\text{Src}}$ values of prey and other local resident species from Japan and Taiwan, respectively. Japan migrants and Taiwan migrants were grouped with the $\delta^{15}\text{N}_{\text{Src}}$ values of other local resident species from the warm pool region. The NC group fell between the Taiwan and Japan residents. NZ groups were grouped with $\delta^{15}\text{N}_{\text{Src}}$ values of Taiwan and Japan residents. The grouping results suggested that Japan and Taiwan residents might use their local prey, and the migrants that captured in Japan and Taiwan might use the prey from the warm pool region. Based on the testing results, we applied LDA and cluster analysis to classify the groupings of molids (no prey here) using more isotopic tracers, including $\delta^{13}\text{C}_{\text{bulk}}$, $\delta^{15}\text{N}_{\text{bulk}}$, and $\delta^{15}\text{N}_{\text{Src}}$ (glycine, serine, phenylalanine, lysine). Cluster analysis used similarity trees based on Euclidean distances to classify molids. The statistical tests were undertaken using R version 4.0.4.

3.3.6b Bayesian mixing model

Bayesian mixing models were used to quantify inputs of regional prey by foraging regions for potential migrants and residents. Prey were categorized into 4 broad regions,

including Japan, Taiwan, warm pool, and NZ. The 4 regional prey groups were used as diet inputs for potential molid migrants and residents. In the model, we used $\delta^{13}\text{C}_{\text{bulk}}$, $\delta^{15}\text{N}_{\text{bulk}}$, and $\delta^{15}\text{N}_{\text{Src}}$ (phenylalanine) values as tracers (Table 3.3). The endmembers were the values of $\delta^{13}\text{C}_{\text{bulk}}$, $\delta^{15}\text{N}_{\text{bulk}}$, and $\delta^{15}\text{N}_{\text{Src}}$ for potential residents and migrants in Japan, Taiwan, NC, and NZ. For the diets of potential residents and migrants in Japan, Taiwan, and NC, we used 3 regional prey groups (Japan, Taiwan and warm pool region) as input data based on the LDA results and movement tracks in previous study of molids (Chang et al. 2021). In the diets of molids in NZ, we used 2 regional prey sources (warm pool region, and NZ). The prey from Japan and Taiwan were not considered because the NZ molids (~42 cm) were assumed to too small to undertake long-distance migration across ocean basins (Dewar et al. 2010). The $\delta^{13}\text{C}_{\text{bulk}}$ and $\delta^{15}\text{N}_{\text{bulk}}$ values of jellyfish from Taiwan and Japan were measured in this study. The $\delta^{13}\text{C}_{\text{bulk}}$ and $\delta^{15}\text{N}_{\text{bulk}}$ values of jellyfish in WP and NZ were calculated from invertebrates and POM in reference papers by adding TDF_{bulk} ($\Delta\delta^{15}\text{N} = 2.09\text{‰}$, $\Delta\delta^{13}\text{C} = 1.19\text{‰}$) from laboratory experiment of jellyfish (Lorrain et al. 2015, Schaub et al. 2021, St John Glew et al. 2021, Sabadel et al. 2022, Kolodzey et al. 2023). The priors for those local prey were uninformative. The TDF_{bulk} for bulk values that we used varied across regions (Table 3.2). We assumed that TDF for phenylalanine is 0 due to the little fractionation of the source amino acids. Each mixing model with 3 Markov chain Monte Carlo simulations of 25000 iterations (burn-in = 10000 and thinning rate = 10). All statistical tests were undertaken using R version 4.0.4.

3.4 Results

3.4.1 Isoscapes of $\delta^{15}\text{N}_{\text{POM}}$ and $\delta^{15}\text{N}_{\text{molid}}$

The predicted $\delta^{15}\text{N}_{\text{POM}}$ and $\delta^{15}\text{N}_{\text{molid}}$ isoscapes showed clear spatial variations in the western Pacific Ocean (Fig. 3.2). Specifically, the warm pool region had the

highest values of $\delta^{15}\text{N}_{\text{POM}}$ (range from 0.3 to 10.9‰), followed by values of Taiwan (0.8-5.6‰), Japan (0.7-7.1‰), New Caledonia (0.4-5.3‰), and New Zealand (0.01-8.7‰). In predicted $\delta^{15}\text{N}_{\text{molid}}$ isoscapes, molids from the warm pool (7.3-17.9‰) had the highest predicted $\delta^{15}\text{N}$ values, followed by those in Taiwan (9.8-14.6‰), NC (7.4-12.3‰), NZ (7.1-15.8‰), and Japan (4.6-12.7‰). The mean value of bootstrapping $\delta^{15}\text{N}_{\text{molid}}$ was 9.6‰ (± 0.4 S.D.) in Japan, 12.0‰ (± 0.5) in Taiwan, 14.6‰ (± 0.4) in warm pool, 10.1‰ (± 0.3) in NC, and 10.2‰ (± 0.2) in NZ.

3.4.2 Comparison of predicted and measured $\delta^{15}\text{N}_{\text{molid}}$ values

The values of predicted and measured $\delta^{15}\text{N}_{\text{molid}}$ were compared in each region (Fig. 3.3A). The measured $\delta^{15}\text{N}_{\text{molid}}$ values of individuals sampled in Japan ranged from 6.5 to 12.2‰ (9.9 ± 1.8 ‰), showing a wider range compared to the predicted $\delta^{15}\text{N}_{\text{molid}}$ values for this region. Most of the measured $\delta^{15}\text{N}_{\text{molid}}$ values in Japan (10 of 14 samples, ~71%, 31-201 cm TL, Fig. 3.3B) overlapped with the predicted $\delta^{15}\text{N}_{\text{molid}}$ values, suggesting they were local residents in Japan (identified as Japan resident over months). Some large individuals (>180 cm, ~29%) in Japan captured in July with high measured $\delta^{15}\text{N}_{\text{molid}}$ values (11.5 to 12.2‰) did not overlap with the predicted $\delta^{15}\text{N}_{\text{molid}}$ values, indicating they were potential recent migrants (Japan migrant).

The measured range of $\delta^{15}\text{N}_{\text{molid}}$ values in Taiwan spanned 9.5 to 15.7‰ (11.7 ± 1.2 ‰). Most molids overlapped with predicted values (89 of 95 samples, ~94%, 80-257 cm TL, Fig. 3.3B), suggesting they were local residents in Taiwan (Taiwan resident over months). Some individuals (>150 cm, ~6%) from Taiwan mostly captured between April and June with high measured $\delta^{15}\text{N}_{\text{molids}}$ values (13.7 to 15.7‰) that overlapped with the predicted values from the warm pools, suggesting they were potential recent migrants from this region (Taiwan migrant over months).

The measured $\delta^{15}\text{N}_{\text{molid}}$ value of one specimen collected in February from NC was 9.6‰ (136 cm TL), and this value fell within the lower bound of the predicted values,

suggesting it might be local resident of NC (NC group over months).

The measured $\delta^{15}\text{N}_{\text{molid}}$ of individuals captured in NZ ranged from 11.6 to 12.7‰ ($12.1 \pm 0.3\text{‰}$). All measured $\delta^{15}\text{N}_{\text{molid}}$ sampling data (42-127 cm TL) were higher than predicted values for NZ, suggesting they were non-residents in NZ and were migrating from somewhere with high $\delta^{15}\text{N}$ values (NZ group over months).

3.4.3 Isotopic composition in AAs of local residents and potential recent migrants

Potential molid residents and recent migrants in each region were identified for CSIA-AA based on the above analysis (Table 3.4). The potential local residents and recent migrants in Japan, Taiwan, NC, and NZ clustered into four groups: (i) Japan and Taiwan migrants, (ii) Japan residents, (iii) Taiwan residents and NC individual, and (iv) NZ group. The potential migrants in Japan and Taiwan were the most distinct and isolated group from other three groups (Fig. 3.4).

In LDA, all five groups of potential residents and migrants clustered separately based on their $\delta^{13}\text{C}_{\text{bulk}}$, $\delta^{15}\text{N}_{\text{bulk}}$, $\delta^{15}\text{N}_{\text{Src}}$. The groups included: (i) Japan resident group, which clustered with other Japan residents in the testing results; (ii) Taiwan resident group, which clustered with Taiwan prey; (iii) Taiwan and Japan migrant group, which clustered with local residents from the warm pool region; (iv) NC group, and (v) NZ group (Fig. 3.5; grouping accuracy: 81%, $p < 0.001$). Overall, LD1 (47%) separated the residents of Japan and Taiwan, and the NC group, from Japan and Taiwan migrants, and the NZ group. This separation was mainly driven by $\delta^{15}\text{N}$ of phenylalanine. LD2 (35%) separated the NZ group and Japan residents from residents and migrants of Taiwan. This separation was driven by bulk $\delta^{13}\text{C}$, and $\delta^{13}\text{C}$ of glycine, serine, and lysine. The NC group fell between the 95% confidence interval of Taiwan residents and Japan resident. The NZ group showed some overlapped with Taiwan migrants and Japan migrants (Fig. 3.5).

3.4.4 Bayesian mixing model

The mixing model results indicated the regional prey input to recent feeding of local residents and potential recent migrants in each area (Fig. 3.6). Japan residents showed high foraging on local prey from Japan (64%). Taiwan residents had higher regional prey input from Taiwan (42%) than other regional prey from Japan (37%) and the warm pool (19%). The potential recent migrants in Japan, captured in July, had high foraging on regional prey from the warm pool (46%), followed by Taiwan (32%) and Japan (22%). The potential migrants in Taiwan, captured from April to June, had the highest regional prey input from the warm pool (58%). High contribution of regional prey from warm pool to the recent foraging of potential migrants captured in Japan and Taiwan, suggesting they might migrate from the warm pool region. The NC specimen showed a high contribution of regional prey from Taiwan (49%) and Japan (44%). The NZ group had higher regional prey input from NZ (79%) than from the warm pool regions.

3.5 Discussion

This study provides insight into the migration patterns of molids, which are known to undertake long-distance migrations across ocean basins in the western Pacific Ocean, but for which little data exist. The evidence suggests that most molids in waters of Taiwan and Japan are local residents and some large molids may be recent migrants from warm pool regions. The molids occurring in waters of NC and NZ could potentially migrate from areas with isotopic values distinct from the base of local food webs.

3.5.1 Isoscapes of $\delta^{15}\text{N}_{\text{POM}}$ and $\delta^{15}\text{N}_{\text{molid}}$

The $\delta^{15}\text{N}$ isoscapes of POM vary spatially across the study regions, likely due to the various oceanographic and biogeochemical processes affecting nitrogen cycling across regions (Somes et al. 2010). The warm pool regions had the highest $\delta^{15}\text{N}$ values

of POM. Similar patterns of higher $\delta^{15}\text{N}$ values of POM and forage fishes near the equator compared to neighboring regions (10°N) has been observed in previous studies (Houssard et al. 2017, Ohshimo et al. 2019). These high $\delta^{15}\text{N}$ values are likely to result from sinking and remineralization of particles and equatorial upwelling of nitrate with high- $\delta^{15}\text{N}$ values (Rafter et al. 2013; Lehmann et al. 2018). Intermediate $\delta^{15}\text{N}$ values of POM were found near the coastal waters of Japan, and lower $\delta^{15}\text{N}$ values were observed in the offshore regions, similar to previous studies of forage fishes and squid in Japan (Takai et al. 2000, 2007, Tanaka et al. 2008, Ohshimo et al. 2019). The waters of eastern Taiwan and New Caledonia are characterized as nutrient-limited and are dominated by diazotroph, nitrogen-fixing bacteria (Le Borgne et al. 2011, Chan et al. 2019, Lin et al. 2022). The strong nitrogen fixation process observed in those regions leads to low $\delta^{15}\text{N}$ values of POM, consistent with previous studies of POM and zooplankton (Ryabenko 2013, Hunt et al. 2015). The $\delta^{15}\text{N}$ values of POM in New Zealand from our study were similar to those in a previous study (St John Glew et al. 2021), related to nitrate availabilities and nitrogen cycles (Somes et al. 2010). The spatial differences in $\delta^{15}\text{N}_{\text{POM}}$ across the western Pacific are sufficiently significant to distinguish potential migrants from the local residents in the studied regions.

The isoscapes of molids showed spatial variations across the western Pacific region, and the variations are due to changes in $\delta^{15}\text{N}$ of POM and TP_{AA} of molids. The high predicted $\delta^{15}\text{N}$ values of molids in the warm pool region resulted from the high $\delta^{15}\text{N}_{\text{POM}}$ isoscapes near the equator. The predicted $\delta^{15}\text{N}$ values of molids in Taiwan were higher than other regions, except for the molids in the warm pool region, which was inconsistent with the $\delta^{15}\text{N}_{\text{POM}}$ isoscapes. The inconsistency is influenced by TP_{AA} of molids. In the study, the TP_{AA} of molids varied in each region, with the highest TP_{AA} in Taiwan, and these variations may be related to nutrient availability and its affect on food web length. The availability of nutrients determines the length of the food chain,

further influencing the TP of predators (Post 2002). Recent studies using CSIA-AA indicated that heterotrophic protists play an important role in transferring nutrients in oligotrophic food webs, leading to an increase of one TP in higher predators (Landry & Décima 2017, Shea et al. 2023). Eastern Taiwan, along with the Kuroshio Current, is considered a region with low nutrient concentration and strong nitrogen fixation. In this area, protists play important roles in transferring nutrients to higher TP consumers through the predation of pico/nanoplankton (Chan et al. 2019, Lin et al. 2022). Thus, the molids in Taiwan had higher TP_{AA}, leading to higher predicted $\delta^{15}\text{N}$ values from the isoscapes.

3.5.2 Migrations pathway of molids in the western Pacific Ocean

The isotope results provide evidence of the frequent migrations of molids in the western Pacific Ocean, offering insight into migration and a plausible explanation for their migratory behavior at a population level.

In this study, most molids found in Japan and Taiwan are local residents (including small and large molids) with similar measured $\delta^{15}\text{N}$ values to $\delta^{15}\text{N}_{\text{molid}}$ isoscapes. We observed that certain large molids (>150 cm) in Japan (~29%) and Taiwan (~6%) had (i) high measured $\delta^{15}\text{N}$ values that were different from the predicted values of isoscapes, (ii) isotopic compositions of source amino acids that are similar to those of warm pool prey and dissimilar to those of local molid residents, and (iii) high diet contributions from the warm pool prey. Several factors might lead to the difference, including dietary ontogenetic shifts and vertical or horizontal migration. Previous studies on molids revealed dietary ontogenetic shifts might affect the difference in isotopic compositions of large and small molids (Syväranta et al. 2012, Nakamura & Sato 2014). Additionally, the vertical migration of molids might result in this difference because large predators with stronger swimming ability could dive into deeper depths and feed on mesopelagic prey, which have higher $\delta^{15}\text{N}$ values (Choy et al. 2015, Gloeckler et al. 2018). However,

little ontogenetic variation in diets of *Mola* spp. (Chang et al. in review) and the results of CSIA-AA in this study suggested that horizontal migration of molids influenced the variability of $\delta^{15}\text{N}$ more. In the resident groups, most large molids showed similar isotopic compositions to small molids, indicating they are less affected by dietary shifts in ontogeny or vertical movement in this size range. Instead, the large molids with dissimilar isotopic compositions are most likely caused by horizontal migration. These findings suggest these molids may be potential migrants from warm pool regions. Additionally, the spawning period of molids is estimated to occur from March to June in Taiwan (Sawai & Chang 2018, Chang unpublished data) and from August to October in Japan (Nakatsubo et al. 2007), based on gonadal indices and the histological observation of gonad tissues. The captured time of these large potential migrants aligns with the occurrence of large mature molids in Japan and Taiwan, implying that migration may be related to spawning behavior.

The molid collected in NC (136 cm TL) might be non-resident based on the isotopic compositions of source AAs, Bayesian mixing model, and published tagging results (Chang et al. 2021), despite its measured $\delta^{15}\text{N}$ value falling within the lower bound of the predicted values. Molids accounted for only 1% (499 tonnes) of the bycatch in tuna or tuna-like species from longline fisheries in the western and central Pacific Ocean from 1994 to 2009 (Clarke et al., 2014); further suggesting that they are not common species in those regions. The isotopic compositions of source AAs of the NC molid were grouped together with those of Taiwan residents, and prey from Taiwan had a higher contribution to its diet than prey from other regions. This suggests the possibility that the molid in NC might have migrated from Taiwan, or a region with similar isotopic values such as the central Pacific Ocean. Chang et al. (2021) tagged one molid (160 cm TL) that migrated from Taiwan to NC and remained in the waters of NC for a month. This finding was consistent with our isotopic results of the molid

captured in NC and provides further evidence that molids are able to migrate from Taiwan to NC. More tagging studies of molids would better refine their migration routes and prey from a greater geographic range would assist in isoscape interpretation.

Our results suggest that molids sampled in NZ (ranging from 42 to 127 cm TL) may be potential recent migrants, even though the NZ prey had a high contribution to the diets of NZ group in the Bayesian mixing model. The small individuals (42-45 cm TL) in NZ had similar isotopic compositions of source AAs to those of intermediate-sized individuals (90 and 127 cm), suggesting no dietary ontogenetic shift exists in this size range. Thus, the inconsistency between the predicted and measured values is not driven by the ontogenetic shift in diets of molids. Furthermore, the diet contributions of Bayesian analysis are estimated based on the source inputs. In other words, the source inputs have a large influence on the estimation. In this study, we only used prey from two regions (the warm pool region and NZ) and the results suggested that the diets of NZ molids had high contributions from local prey. If we include more prey data from other potential habitats of molids (i.e. Australia), the results might be different. In our isoscape map of $\delta^{15}\text{N}_{\text{molid}}$, Taiwan, the warm pool region and eastern Australia have high-predicted $\delta^{15}\text{N}$ values comparable to the measured values of NZ specimens, indicating potential habitats for these migrants. However, a previous tagging study in the northwestern Pacific Ocean indicated that small molids (87-113 cm TL) undertook seasonal migrations along the coast of Japan and did not appear to make long basin-scale migrations (Dewar et al. 2010). Thus, Taiwan and the warm pool region might not be the potential habitats for NZ molids due to the long distance between those regions. Conversely, according to fishery data, molids were found in waters of eastern Australia and New Zealand throughout the year (Nyegaard 2018). The NZ molids possibly migrate from Australia or regions with similarly high $\delta^{15}\text{N}$ background values based on the isoscapes and the fishery data.

This study has potential limitations. First, the isoscapes of POM were reconstructed from different sampling materials (i.e., POM, nitrate, zooplankton, forage fish) without considering the time scales. Several studies indicate that the $\delta^{15}\text{N}$ values of POM can vary temporally due to changing nitrogen cycles and nutrient availability (McMahon et al. 2013, Kodama et al. 2021, Yoshikawa et al. 2022), suggesting the predicted values of isoscapes might be influenced by time scales. Second, the predicted values of isoscapes in the study were constructed, and the molids were sampled based on the tagging studies (Chang et al. 2020, 2021). There might be other potential migration pathways or habitats of molids that we did not consider in our study that future tagging studies could identify. For example, Taiwan is less likely to be the potential habitat for NZ molids, especially the small molids, even though the measured $\delta^{15}\text{N}$ values of the NZ group overlapped with the predicted $\delta^{15}\text{N}$ values in Taiwan. Instead, Australia might be the potential habitat for the NZ molids due to the similar isotope values and the reasonable distance. Thus, it is important to undertake literature reviews (including fishery data, spatiotemporal size distributions, and tagging data) and combine those ecological studies into the study. Third, the influences of molid vertical migrations are not considered when constructing the isoscapes. Molids exhibit vertical movement behaviors (Dewar et al. 2010, Thys et al. 2015, Chang et al. 2020, 2021), and their vertical migration during foraging affects the $\delta^{15}\text{N}$ values in their tissue due to the high $\delta^{15}\text{N}$ values of mesopelagic prey (Choy et al. 2015, Gloeckler et al. 2018). The influences of horizontal and vertical migrations of molids on variabilities in $\delta^{15}\text{N}_{\text{molid}}$ isoscapes can be explained by the CSIA-AA results. If variations in the $\delta^{15}\text{N}$ values of the small molids and large molids are influenced more by vertical movement, the isotopic compositions in $\delta^{15}\text{N}_{\text{Src}}$ of large and small molids will not be grouped together in cluster analysis or LDA. Large molids and small molids were grouped together, indicating that the variability of $\delta^{15}\text{N}_{\text{molid}}$ isoscapes is more influenced by

horizontal migrations than vertical movements of mollids. Additionally, the source inputs might lead to variabilities across the dietary proportion estimates in the Bayesian mixing model. For example, there is a discrepancy between the isoscapes, CSIA-AA, and the Bayesian mixing model results regarding NZ mollids, where the isoscapes and CSIA-AA results suggested that NZ mollids may be potential migrants, while the Bayesian mixing model indicated them as residents. This discrepancy might be related to the source inputs of the Bayesian mixing model that a single missing source of the potential habitats for mollids may cause biases in estimates of dietary proportion (Parnell et al. 2013; Stock et al. 2018).

3.6 Conclusion

This study revealed that mollids frequently migrate across regions in the western Pacific Ocean using a combination of approaches, including isoscapes, CSIA-AA, and Bayesian mixing model. Isotopic data indicate that large mollids found in Taiwan and Japan may migrate from the warm pool region, and one NC mollid could be a migrant from Taiwan. These findings are in agreement with results of tagging studies that demonstrated large mollids were observed undertaking long-distance migrations, to the southern hemisphere from Taiwan. The NZ mollids might be non-local residents and migrating from regions with high $\delta^{15}\text{N}$ values. Overall, this study offers insight into the migratory patterns of mollids in the western Pacific Ocean, enhancing the ecological understanding of migration pathway of mollids and may support the sustainable fisheries management globally.

3.7 References

Altabet MA (2001) Nitrogen isotopic evidence for micronutrient control of fractional NO_3^- utilization in the equatorial Pacific. *Limnol Oceanogr* 46: 368-380.

- Altabet MA, Francois R (1994) Sedimentary nitrogen isotopic ratio as a recorder for surface ocean nitrate utilization. *Global Biogeochem Cycles* 8: 103–116.
- Arnoldi NS, Litvin SY, Madigan DJ, Micheli F, Carlisle A (2023) Multi-taxa marine isoscapes provide insight into large-scale trophic dynamics in the North Pacific. *Prog Oceanogr* 213: 103005.
- Block BA, Jonsen ID, Jorgensen SJ, Winship AJ, Shaffer SA, Bograd SJ, Hazen EL, Foley DG, Breed GA, Harrison AL, Ganong JE, Swithenbank A, Castleton M, Dewar H, Mate BR, Shillinger GL, Schaefer KM, Benson SR, Weise MJ, Henry RW, Costa DP (2011) Tracking apex marine predator movements in a dynamic ocean. *Nature* 475: 86-90.
- Bradley CJ, Wallsgrave NJ, Choy CA, Drazen JC, Hetherington ED, Hoen DK, Popp BN (2015) Trophic position estimates of marine teleosts using amino acid compound specific isotopic analysis. *Limnol Oceanogr: Methods* 13: 476-493.
- Caut S, Jowers MJ, Michel L, Lepoint G, Fisk AT (2013) Diet-and tissue-specific incorporation of isotopes in the shark *Scyliorhinus stellaris*, a North Sea mesopredator. *Mar Ecol Prog Ser* 492: 185-198.
- Carassou L, Kulbicki M, Nicola TJ, Polunin NV (2008) Assessment of fish trophic status and relationships by stable isotope data in the coral reef lagoon of New Caledonia, southwest Pacific. *Aquat Living Resour* 21: 1-12.
- Chan YF, Chung CC, Gong GC, Hsu CW (2020) Spatial variation of abundant picoeukaryotes in the subtropical Kuroshio Current in winter. *Mar Ecol* 41: e12579.
- Chang CT, Drazen JC, Chiang WC, Madigan DJ, Carlisle AB, Wallsgrave NJ, Hsu HH, Ho YH, Popp BN (2023) Ontogenetic and seasonal shifts in diets of sharptail mola *Masturus lanceolatus* in waters off Taiwan. *Mar Ecol Prog Ser* 715: 113-127.
- Chang CT, Chiang WC, Musyl MK, Popp BN, Lam CH, Lin SJ, Watanabe YY, Ho YH, Chen JR (2021) Water column structure influences long-distance latitudinal

- migration patterns and habitat use of bumphead sunfish *Mola alexandrini* in the Pacific Ocean. *Sci Rep* 11: 21934.
- Chang CT, Lin SJ, Chiang WC, Musyl MK, Lam CH, Hsu HH, Chang YC, Ho YS (2020) Horizontal and vertical movement patterns of sunfish off eastern Taiwan. *Deep-Sea Res II: Top Stud Oceanogr* 175: 104683.
- Chang CT, Chih CH, Chang YC, Chiang WC, Tsai FY, Hsu HH, Wu JH, Ho YH (2018) Seasonal variations of species, abundance and size composition of Molidae in eastern Taiwan. *J Taiwan Fish Res* 26: 27-42.
- Chiba S, Sugisaki H, Kuwata A, Tadokoro K, Kobari T, Yamaguchi A, Mackas DL (2012) Pan-North Pacific comparison of long-term variation in *Neocalanus* copepods based on stable isotope analysis. *Prog Oceanogr* 97: 63-75.
- Choy CA, Popp BN, Hannides CC, Drazen JC (2015) Trophic structure and food resources of epipelagic and mesopelagic fishes in the North Pacific Subtropical Gyre ecosystem inferred from nitrogen isotopic compositions. *Limnol Oceanogr* 60: 1156-1171.
- Clarke S, Sato M, Small C, Sullivan B, Inoue Y, Ochi D (2014) Bycatch in longline fisheries for tuna and tuna-like species: a global review of status and mitigation measures. *FAO Fish Tech Pap* 588: 1-199.
- DeVries T, Deutsch C, Rafter PA, Primeau F (2013) Marine denitrification rates determined from a global 3-D inverse model. *Biogeosciences* 10: 2481-2496.
- Dewar H, Thys T, Teo SLH, Farwell C, O'Sullivan J, Tobayama T, Soichi M, Nakatsubo T, Kondo Y, Okada Y, Lindsay DJ, Hays GC, Walli A, Weng K, Streelmanand JT, Karl SA (2010) Satellite tracking the world's largest jelly predator, the ocean sunfish, *Mola mola*, in the Western Pacific. *J Exp Mar Biol Ecol* 393: 32–42.
- DiFiore PJ, Sigman DM, Trull TW, Lourey MJ, Karsh K, Cane G, Ho R (2006) Nitrogen isotope constraints on subantarctic biogeochemistry. *J Geophys Res Oceans* 111:

C8.

Gaston TF, Suthers IM (2004) Spatial variation in $\delta^{13}\text{C}$ and $\delta^{15}\text{N}$ of liver, muscle and bone in a rocky reef planktivorous fish: the relative contribution of sewage. *J Exp Mar Biol Ecol* 304: 17-33.

Galvan DE, Jañez J, Irigoyen AJ (2016) Estimating tissue-specific discrimination factors and turnover rates of stable isotopes of nitrogen and carbon in the smallnose fanskate *Sympterygia bonapartii* (Rajidae). *J Fish Biol* 89: 1258-1270.

Gloeckler K, Choy CA, Hannides CC, Close HG, Goetze E, Popp BN, Drazen JC (2018) Stable isotope analysis of micronekton around Hawaii reveals suspended particles are an important nutritional source in the lower mesopelagic and upper bathypelagic zones. *Limnol Oceanogr* 63: 1168-1180.

Graham BS, Koch P, Newsome S, MaMahon K, Aurioles D (2010) Using isoscapes to trace the movements and foraging behavior of top predators in oceanic ecosystems. In: West JB, Bowen GJ, Dawson TE, Tu KP (eds) *Isoscapes: understanding movement, pattern and process on earth through isotope mapping*. Springer, NY, p 299-318.

Fripiat F, Marconi D, Rafter PA, Sigman DM, Altabet MA, Bourbonnais A, Brandes J, Casciotti KL, Deman F, Dehairs F, Emeis KC, Fawcett S, Galbraith ED, Gaye B, Granger J, Harms N, Haug GH, Kemeny PC, Kienast M, Knapp AN, Kopf S, Lehmann MF, Luu VH, Martin T, Martínez-García A, Pantoja S, Peng X, Peters B, Smart S, Trull TW, Van Oostende N, Voss M, Yoshikawa C, Zhang R, Dähnke K (2021) Compilation of nitrate $\delta^{15}\text{N}$ in the ocean [dataset]. PANGAEA. <https://doi.org/10.1594/PANGAEA.936484>.

Hannides CC, Popp BN, Landry MR, Graham BS (2009) Quantification of zooplankton trophic position in the North Pacific Subtropical Gyre using stable nitrogen isotopes. *Limnol Oceanogr* 54: 50-61.

- Hesslein RH, Hallard KA, Ramlal P (1993) Replacement of sulfur, carbon, and nitrogen in tissue of growing broad whitefish (*Coregonus nasus*) in response to a change in diet traced by $\delta^{34}\text{S}$, $\delta^{13}\text{C}$, and $\delta^{15}\text{N}$. *Canadian Journal of Fisheries and Aquatic Sciences* 50: 2071-2076.
- Hobson KA (1999) Tracing origins and migration of wildlife using stable isotopes: a review. *Oecologia* 120: 314-326.
- Hobson KA, Cherel Y (2006) Isotopic reconstruction of marine food webs using cephalopod beaks: new insight from captive raised *Sepia officinalis*. *Can J Zool* 84: 766–770.
- Houssard P, Lorrain A, Tremblay-Boyer L, Allain V, Graham BS, Menkes CE, Pethybridge H, Couturier LIE, Point D, Leroy B, Receveur A, Hunt BPV, Vourey E, Bonnet S, Rodier M, Raimbault P, Feunteun E, Kuhnert PM, Munaron JM, Lebreton B, Otake T, Letourneur Y (2017) Trophic position increases with thermocline depth in yellowfin and bigeye tuna across the Western Central Pacific Ocean. *Progr Oceanogr* 154: 49–63.
- Hunt BP, Allain V, Menkès C, Lorrain A, Graham B, Rodier M, Pag M, Carlotti F (2015) A coupled stable isotope-size spectrum approach to understanding pelagic food-web dynamics: a case study from the southwest sub-tropical Pacific. *Deep-Sea Res II: Top Stud Oceanogr* 113: 208-224.
- Izenman AJ (2008) Linear discriminant analysis. In: Izenman AJ (ed) *Modern multivariate statistical techniques: regression, classification, and manifold learning*. Springer, NY, p 237-280.
- Kang CK, Kim JB, Lee KS, Kim JB, Lee PY, Hong JS (2003) Trophic importance of benthic microalgae to macrozoobenthos in coastal bay systems in Korea: dual stable C and N isotope analyses. *Mar Ecol Prog Ser* 259: 79-92.
- Kienast M, Lehmann MF, Timmermann A, Galbraith E, Bolliet T, Holbourn A,

- Normandeau C, Laj C (2008) A mid-Holocene transition in the nitrogen dynamics of the western equatorial Pacific: Evidence of a deepening thermocline? *Geophys Res Lett* 35: L23610.
- Kim SL, del Rio CM, Casper D, Koch PL (2012) Isotopic incorporation rates for shark tissues from a long-term captive feeding study. *J Exp Biol* 215: 2495-2500.
- Kodama T, Nishimoto A, Horii S, Ito D, Yamaguchi T, Hidaka K, Setou T, Ono T (2021) Spatial and seasonal variations of stable isotope ratios of particulate organic carbon and nitrogen in the surface water of the Kuroshio. *J Geophys Res Oceans* 126: e2021JC017175.
- Landry MR, Décima MR (2017) Protistan microzooplankton and the trophic position of tuna: Quantifying the trophic link between micro- and mesozooplankton in marine foodwebs. *ICES J Mar Sci* 74: 1885–1892
- Le Borgne R, Allain V, Griffiths SP, Matear RJ, McKinnon AD, Richardson AJ, Young JW (2011) Vulnerability of open ocean food webs in the tropical Pacific to climate change. In: Bell JD, Johnson JE, Hobday AJ (eds) *Vulnerability of Tropical Pacific Fisheries and Aquaculture to Climate Change*. Secretaria to the Pacific Community, Noumea, NC, p 189–249.
- Lehmann N, Granger J, Kienast M, Brown KS, Rafter PA, Martínez-Méndez G, Mohtadi M (2018) Isotopic evidence for the evolution of subsurface nitrate in the Western Equatorial Pacific. *J Geophys Res: Oceans* 123: 1684-1707.
- Lin YC, Chin CP, Yang JW, Chiang KP, Hsieh CH, Gong GC, Shih CY, Chen SY (2022) How communities of marine stramenopiles varied with environmental and biological variables in the Subtropical Northwestern Pacific Ocean. *Microb ecol*: 1-13.
- Liu J, Zapfe G, Shao KT, Leis JL, Matsuura K, Hardy G, Liu M, Robertson R, Tyler J (2015) *Mola mola* (errata version published in 2016). The IUCN Red List of

- Threatened Species 2015: e.T190422A97667070. Accessed on 17 October 2023.
- Liu KK, Su MJ, Hsueh CR, Gong GC (1996) The nitrogen isotopic composition of nitrate in the Kuroshio Water northeast of Taiwan: Evidence for nitrogen fixation as a source of isotopically light nitrate. *Mar Chem* 54: 273-292.
- Logan JM, Pethybridge H, Lorrain A, Somes CJ, Allain V (2020) Global patterns and inferences of tuna movements and trophodynamics from stable isotope analysis. *Deep-Sea Res II: Top Stud Oceanogr* 175: 104775.
- Logan JM, Jardine TD, Miller TJ, Bunn SE, Cunjak RA, Lutcavage ME (2008) Lipid corrections in carbon and nitrogen stable isotope analyses: comparison of chemical extraction and modelling methods. *J Anim Ecol*: 838-846.
- Lourey MJ, Trull TW, Tilbrook B (2004) Sensitivity of $\delta^{13}\text{C}$ of Southern Ocean suspended and sinking organic matter to temperature, nutrient utilization, and atmospheric CO_2 . *Deep-Sea Res I: Oceanogr Res Paper* 51: 281–305.
- MacAvoy SE, Arneson LS, Bassett E (2006) Correlation of metabolism with tissue carbon and nitrogen turnover rate in small mammals. *Oecologia* 150: 190-201.
- Madigan DJ, Chiang WC, Wallsgrove NJ, Popp BN, Kitagawa T (2016) Intrinsic tracers reveal recent foraging ecology of giant Pacific bluefin tuna at their primary spawning grounds. *Mar Ecol Prog Ser* 553: 253-266.
- Madigan DJ, Baumann Z, Carlisle AB, Hoen DK, Popp BN, Dewar H, Snodgrass OE, Block BA, Fisher NS (2014) Reconstructing transoceanic migration patterns of Pacific bluefin tuna using a chemical tracer toolbox. *Ecology* 95: 1674-1683.
- Madigan DJ, Carlisle AB, Dewar H, Snodgrass OE, Litvin SY, Micheli F, Block BA (2012) Stable isotope analysis challenges wasp-waist food web assumptions in an upwelling pelagic ecosystem. *Sci Rep* 2: 1-10.
- Malpica-Cruz L, Herzka SZ, Sosa-Nishizaki O, Lazo JP (2012) Tissue-specific isotope trophic discrimination factors and turnover rates in a marine elasmobranch:

- empirical and modeling results. *Can J Fish Aquat Sci* 69: 551-564.
- Matsubayashi J, Osada Y, Tadokoro K, Abe Y, Yamaguchi A, Shirai K, Honda K, Yoshikawa C, Ogawa NO, Ohkouchi N, Ishikawa NF, Nagata T, Miyamoto H, Nishino S, Tayasu I (2020) Tracking long-distance migration of marine fishes using compound-specific stable isotope analysis of amino acids. *Ecol Lett* 23: 881-890.
- Matsubayashi J, Osada Y, Tadokoro K, Abe Y, Yamaguchi A, Shirai K, Honda K, Yoshikawa C, Ogawa NO, Ohkouchi N, Ishikawa NF, Nagata T, Miyamoto H, Nishino S, Tayasu I (2020) Tracking long-distance migration of marine fishes using compound-specific stable isotope analysis of amino acids. *Ecol Lett* 23: 881-890.
- McMahon KW, Hamady LL, Thorrold SR (2013) Ocean ecogeochemistry: a review. *Oceanogr Mar Biol: An Annu Rev* 51: 327-374.
- Miller TW, Brodeur RD, Rau G, Omori K (2010a) Prey dominance shapes trophic structure of the northern California Current pelagic food web: evidence from stable isotopes and diet analysis. *Mar Ecol Prog Ser* 420: 15–26.
- Miller TW, Omori K, Hamaoka H, Shibata JY, Hidejiro O (2010b) Tracing anthropogenic inputs to production in the Seto Island Sea, Japan - a stable isotope approach. *Mar Pollut Bull* 60: 1803-1809.
- Miyachi S, Mayahara T, Tsushima K, Sasada K, Kohno E, Ogawa NO, Chikaraishi Y, Ohkouchi N (2015) Approach to determine individual trophic level and the difference in food sources of Japanese anchovy *Engraulis japonicas* in Sagami Bay, based on compound-specific nitrogen stable isotope analysis of amino acids. *Fish Sci* 81: 1053-1062.
- Mooney CZ, Duval RD, Duvall R (1993) *Bootstrapping: A nonparametric approach to statistical inference*. SAGE.
- Nakatsubo T, Kawachi M, Mano N, Hirose H (2007) Spawning period of ocean sunfish *Mola mola* in waters of the eastern Kanto Region, Japan. *Aquac Sci* 55: 613-618.

- Nakamura I, Sato K (2014) Ontogenetic shift in foraging habit of ocean sunfish *Mola mola* from dietary and behavioral studies. *Mar Biol* 161:1263-1273.
- Nyegaard M, Loneragan N, Hall S, Andrew J, Sawai E, Nyegaard M (2018) Giant jelly eaters on the line: Species distribution and bycatch of three dominant sunfishes in the Southwest Pacific. *Estuar Coast Shelf Sci* 207:1-15.
- Ohshimo S, Madigan DJ, Kodama T, Tanaka H, Komoto K, Suyama S, Ono T, Yamakawa T (2019) Isoscapes reveal patterns of $\delta^{13}\text{C}$ and $\delta^{15}\text{N}$ of pelagic forage fish and squid in the Northwest Pacific Ocean. *Prog Oceanogr* 175: 124-138.
- Olson RJ, Popp BN, Graham BS, López-Ibarra GA, Galván-Magaña F, LennertCody CE, Bocanegra-Castillo N, Wallsgrove NJ, Gier E, Alatorre-Ramírez V, Ballance LT, Fry B (2010) Food-web inferences of stable isotope spatial patterns in copepods and yellowfin tuna in the pelagic eastern Pacific Ocean. *Prog Oceanogr* 86: 124-138.
- Parnell AC, Phillips DL, Bearhop S, Semmens BX, Ward EJ, Moore JW, Jackson AL, Inger R (2013) Bayesian stable isotope mixing models. *Environmetrics* 24: 387-399.
- Phillips ND, Elliott Smith EA, Newsome SD, Houghton JDR, Carson CD, Alfaro-Shigueto J, Mangel JC, Eagling LE, Kubicek L, Harrod C (2020) Bulk tissue and amino acid stable isotope analyses reveal global ontogenetic patterns in ocean sunfish trophic ecology and habitat use. *Mar Ecol Prog Ser* 633: 127-140.
- Pope EC, Hays G, Thys T, Doyle T, Sims D, Queiroz N (2010) The biology and ecology of the ocean sunfish *Mola mola*: A review of current knowledge and future research perspectives. *Rev Fish Biol Fish* 20:471–487.
- Popp BN, Graham BS, Olson RJ, Hannides CCS, Lott MJ, Lopez-Ibarra GA, Galvan-Magana F, Fry B (2007) Insight into the trophic ecology of yellowfin tuna, *Thunnus albacares*, from compound-specific nitrogen isotope analysis of proteinaceous

- amino acids. In: Dawson TE, Siegwolf RTW (eds) Stable isotopes as indicators of ecological change. Elsevier, Amsterdam, p 173-190.
- Post DM (2002) Using stable isotopes to estimate trophic position: Models, methods, and assumptions. *Ecology* 83: 703–718.
- Primavera HJ (1996) Stable carbon and nitrogen isotope ratios of penaeid juveniles and primary producers in a riverine mangrove in Guimaras, Philippines. *Bull Mar Sci* 58: 675-683.
- Rafter PA, DiFiore PJ, Sigman DM (2013) Coupled nitrate nitrogen and oxygen isotopes and organic matter remineralization in the Southern and Pacific Oceans. *J Geophys Res: Oceans* 118: 4781-4794.
- Rafter PA, Sigman DM (2016) Spatial distribution and temporal variation of nitrate nitrogen and oxygen isotopes in the upper equatorial Pacific Ocean. *Limnol Oceanogr* 61: 14-31.
- Rafter PA, Sigman DM, Charles CD, Kaiser J, Haug GH (2012) Subsurface tropical Pacific nitrogen isotopic composition of nitrate: Biogeochemical signals and their transport. *Global Biogeochem Cycles* 26: GB1003
- Ryabenko E (2013) Stable isotope methods for the study of the nitrogen cycle. *Topics Oceanogr*: 1-40.
- Sabadel AJM, Décima M, McComb K, Meyers M, Barr N, Gall M, Law CS (2022) Amino acid nitrogen stable isotopes as biomarkers of coastal phytoplankton assemblages and food web interactions. *Mar Ecol Prog Ser* 690: 1-13.
- Saino T, Hattori A (1987) Geographical variation of the water column distribution of suspended particulate organic nitrogen and its ^{15}N natural abundance in the Pacific and its marginal seas. *Deep-Sea Res* 34: 807–827.
- Sawai E, Chang YC (2018) A rare record of the bump-head sunfish, *Mola alexandrini* (Tetraodontiformes: Molidae) with a 117 kg ovary from Hualien, Taiwan.

Biogeography 20: 73-77.

Sawai E, Yamanoue Y, Yoshita Y, Sakai Y, Hashimoto H (2011) Seasonal occurrence patterns of Mola sunfishes (*Mola* spp. A and B; Molidae) in waters off the Sanriku region, eastern Japan. *Japan. J Ichthyol* 58: 181–187.

Schaub J, McLaskey AK, Forster I, Hunt BP (2021) Experimentally derived estimates of turnover and modification for stable isotopes and fatty acids in scyphozoan jellyfish. *J Exp Mar Biol Ecol* 545: 151631.

Schell DM, Barnett BA, Vinette KA (1998) Carbon and nitrogen isotope ratios in zooplankton of the Bering, Chukchi and Beaufort seas. *Mar Ecol Prog Ser* 162: 11-23.

Schlitzer R (2018) Ocean Data View. <https://odv.awi.de>

Shadsky IP, Romankevich EA, Grinchenko Y (1982) Isotopic composition of carbon in lipids from suspended matter and bottom sediments east of the Kuril Islands. *Oceanology* 22: 301-304.

Shea CH, Wojtal PK, Close HG, Maas AE, Stamieszkin K, Cope JS, Steinberg DK, Wallsgrove N, Popp BN (2023) Small particles and heterotrophic protists support the mesopelagic zooplankton food web in the subarctic northeast Pacific Ocean. *Limnol oceanogr* 68: 1949-1963.

Sibert JR, Nielsen JL (2001) *Electronic Tagging and Tracking in Marine Fisheries: Proceedings of the Symposium on Tagging and Tracking Marine Fish with Electronic Devices*. Springer Science & Business Media, HI.

Sigman DM, Casciotti KL (2001) Nitrogen isotopes in the ocean. *Encyclopedia of Ocean Sciences* 3: 1884-1894.

Somes CJ, Schmittner A, Galbraith ED, Lehmann MF, Altabet MA, Montoya JP, Letelier RM, Mix AC, Bourbonnais A, Eby M (2010) Simulating the global distribution of nitrogen isotopes in the ocean. *Global Biogeochem Cycles* 24:

GB4019.

Sousa LL, Lopez-Castejon F, Gilabert J, Relvas P, Couto A, Queiroz N, Caldas R, Dias PS, Dias H, Faria M, Ferreira F, Ferreira AS, Fortuna J, Gomes RJ, Loureiro B, Martins R, Madureira L, Neiva J, Oliveira M, Pereira J, Pinto J, Py F, Queirós H, Silva D, Sujit PB, Zolich A, Johansen TA, de Sousa JB, Rajan K (2016a) Integrated monitoring of *Mola mola* behaviour in space and time. PLOS ONE 11: e0160404.

Sousa LL, Queiroz N, Mucientes G, Humphries NE, Sims DW (2016b) Environmental influence on the seasonal movements of satellite-tracked ocean sunfish *Mola mola* in the north-east Atlantic. Anim Biotelemetry 4: 1-19.

St John Glew K, Espinasse B, Hunt BPV, Pakhomov EA, Bury SJ, Pinkerton M, Nodder SD, Gutiérrez-Rodríguez A, Safi K, Brown JCS, Graham L, Dunbar RB, Mucciarone DA, Magozzi S, Somes C, Trueman CN (2021) Isoscape models of the Southern Ocean: Predicting spatial and temporal variability in carbon and nitrogen isotope compositions of particulate organic matter. Global Biogeochem Cycles 35: e2020GB006901.

Stock BC, Jackson AL, Ward EJ, Parnell AC, Phillips DL, Semmens BX (2018) Analyzing mixing systems using a new generation of Bayesian tracer mixing models. PeerJ 6: e5096.

Syväranta J, Harrod C, Kubicek L, Cappanera V, Houghton JDR (2012) Stable isotopes challenge the perception of ocean sunfish *Mola mola* as obligate jellyfish predators. J Fish Biol 80:225-231.

Takai N, Hirose N, Osawa T, Hagiwara K, Kojima T, Okazaki Y, Kuwae T, Taniuchi T, Yoshihara K (2007) Carbon source and trophic position of pelagic fish in coastal waters of south-eastern Izu Peninsula, Japan, identified by stable isotope analysis. Fish Sci 73: 593–608.

Takai N, Onaka S, Ikeda Y, Yatsu A, Kidokoro H, Sakamoto W (2000) Geographical

variations in carbon and nitrogen stable isotope ratios in squid. *J Mar Biol Assoc UK* 80: 675-684.

Tanaka H, Takasuka A, Aoki I, Ohshimo S (2008) Geographical variations in the trophic ecology of Japanese Anchovy, *Engraulis japonicus*, inferred from carbon and nitrogen stable isotope ratios. *Mar Biol* 154: 557–568.

Thys TM, Hearn AR, Weng KC, Ryan JP, Penaherrera-Palma C (2017) Satellite tracking and site fidelity of short ocean sunfish, *Mola ramsayi*, in the Galapagos Islands. *J Mar Biol* 2017: 7097965.

Thys TM, Ryan JP, Weng KC, Erdmann M, Tresnati J (2016) Tracking a marine ecotourism star: Movements of the short ocean sunfish *Mola ramsayi* in Nusa Penida, Bali, Indonesia. *J Mar Biol* 2016: 8750193.

Thys TM, Ryan JP, Dewar H, Perle CR, Lyons K, O'Sullivan J, Farwell C, Howard MJ, Weng KC, Lavaniegos BE, Gaxiola-Castro G, Bojorquez LEM, Hazen EL, Bograd SJ (2015) Ecology of the ocean sunfish, *Mola mola*, in the southern California Current System. *J Exp Mar Biol Ecol* 471: 64-76.

Usui T, Nagao S, Yamamoto M, Suzuki K, Kudo I, Montani S, Minagawa M (2006) Distribution and sources of organic matter in surficial sediments on the shelf and slope off Tokachi, western North Pacific, inferred from C and N stable isotopes and C/N ratios. *Mar Chem* 98: 241-259.

Vander Zanden MJ, Rasmussen JB (2001) Variation in $\delta^{15}\text{N}$ and $\delta^{13}\text{C}$ trophic fractionation: Implications for aquatic food web studies. *Limnol Oceanogr* 46: 2061-2066.

Wada E, Hattori A (1976) Natural abundance of ^{15}N in particulate organic matter in the North Pacific Ocean. *GCA* 40: 249-251.

Xing D, Takizawa Y, Yanagisawa M, Chikaraishi (2023) Tissue-specific $\delta^{15}\text{N}$ values of amino acids in aquatic organisms: Comparison between muscle and others for

ecological food web studies. *Res Org Geochem* 39: 13-20.

Yamamuro M, Kayanne H, Minagawao M (1995) Carbon and nitrogen stable isotopes of primary producers in coral reef ecosystems. *Limnol Oceano* 40: 617-621.

Yñiguez AT, Apego GCM, Mendoza N, Gomez NC, Jacinto GS (2022) Nearshore to offshore trends in plankton assemblage and stable isotopes in reefs of the west Philippine Sea. *Front Mar Sci* 8: 724504.

Yoshikawa C, Ogawa NO, Chikaraishi Y, Makabe A, Matsui Y, Sasai Y, wakita M, Honda MC, Mino Y, Aita MN, Fujiki T, Nunoura T, Harada N, Ohkouchi N (2022) Nitrogen isotopes of sinking particles reveal the seasonal transition of the nitrogen source for phytoplankton. *Geophys Res Lett* 49: e2022GL098670.

Yoshikawa C, Yamanaka Y, Nakatsuka T (2005) An ecosystem model including nitrogen isotopes: perspectives on a study of the marine nitrogen cycle. *J Oceanogr* 61: 921-942.

Table 3.1. Literature cited in development of the isoscape model of $\delta^{15}\text{N}_{\text{POM}}$.

Type	Reference
Nitrate	Liu et al. (1996), Yoshikawa et al. (2005), DiFiore et al. (2006), Kienast et al. (2008), Rafter et al. (2012), DeVries et al. (2013), Rafter & Sigman (2016), Fripiat et al. (2021)
POM	Wada & Hattori (1976), Shadsky et al. (1982), Saino & Hattori (1987), Altabet & Francois (1994), Yamamuro et al. (1995), Primavera (1996), Kang et al. (2003), Gaston & Suthers (2004), Lourey et al. (2004), Usui et al. (2006), Carassou et al. (2008), Lorrain et al. (2015), St John Glew et al. (2021), Yñiguez et al. (2022),
Zooplankton	Schell et al. (1998), Miller et al. (2010b), Chiba et al. (2012), Matsubayashi et al. (2020)
Fish	Takai et al. (2007), Tanaka et al. (2008), Ohshimo et al. (2019), This study

Table 3.2. The TP_{AA} of molids and TDF_{bulk} in each regions. The value in the parenthesis of TDF_{bulk} represents the standard error.

Region	TP_{AA} of molid	TDF_{bulk}	References
Japan	3.3	2.8 (0.4)	Madigan et al. (2021)
Taiwan	4	2.4 (1.3)	Philips et al. (2020), this study
Warm pool	3.3	3.2 (-)	Post (2002), Olson et al. (2010), Lorrain et al. (2015)
New Caledonia	3.3	3.2 (-)	Post (2002), Olson et al. (2010), Lorrain et al. (2015)
New Zealand	3.3	3.4 (-)	Post (2002)

Table 3.3. Isotopic compositions, including bulk $\delta^{15}\text{N}$, $\delta^{13}\text{C}$, and $\delta^{15}\text{N}_{\text{Ser}}$ values (from phenylalanine), of local prey items in each region used for the Bayesian mixing model.

Prey	Species used for $\delta^{15}\text{N}_{\text{Ser}}$ values	$\delta^{15}\text{N}$ of bulk tissue	$\delta^{13}\text{C}$ of bulk tissue	$\delta^{15}\text{N}$ of phenylalanine	References
Japan	Chum salmon, Japanese horse mackerel, Japanese anchovy	7.8 ± 1.1	-20.6 ± 1.5	4.4 ± 2.4	This study, Miyachi et al. (2015), Matsubayashi et al. (2020), Xing et al. (2023)
Taiwan	Jellyfish, sharptail sunfish	8.2 ± 1.0	-17.4 ± 0.5	4.1 ± 2.1	This study, Chang et al. (2023)
Warm pool	Yellow tuna	10 ± 1	-16.3 ± 0.9	9.4 ± 3.6	Schaub et al. (2021), Lorrain et al. (2015)
New Zealand	POM	7.3 ± 2.3	-21.12 ± 2.3	6.6 ± 1.4	Sabadel et al. (2022), Schaub et al. (2021), Kolodzey et al. (2023), St John Glew et al. (2021)

Table 3.4. The isotopic compositions of potential residents and migrants of molluscs for CSIA-AA, including $\delta^{15}\text{N}$ and $\delta^{13}\text{C}$ of bulk tissues and $\delta^{15}\text{N}$ of glutamic acid, glycine, serine, phenylalanine, and lysine.

Group	n	$\delta^{15}\text{N}$ of bulk tissue	$\delta^{13}\text{C}$ of bulk tissue	$\delta^{15}\text{N}$ of glutamic acid	$\delta^{15}\text{N}$ of glycine	$\delta^{15}\text{N}$ of serine	$\delta^{15}\text{N}$ of phenylalanine	$\delta^{15}\text{N}$ of lysine
JP resident	6	9.3 ± 1.6	-19.0 ± 1.3	21.3 ± 1.5	1.7 ± 1.5	7.4 ± 1.6	4.7 ± 1.6	4.1 ± 0.8
JP migrant	3	11.9 ± 0.2	-17.4 ± 0.9	23.4 ± 0.8	5.4 ± 0.6	9.4 ± 0.8	9.1 ± 2.2	6.7 ± 0.2
TW resident	4	11.9 ± 1.9	-17.1 ± 1.1	26.3 ± 2.0	4.4 ± 0.9	3.6 ± 0.3	4.4 ± 1.3	6.5 ± 0.9
TW migrant	2	15.6 ± 0.2	-17.2 ± 0.3	29.9 ± 1.5	8.2 ± 1.2	7.1 ± 1.1	7.4 ± 1.9	8.1 ± 1.0
NC group	1	9.6	-19.1	23.3	2.4	3.6	4.8	4.3
NZ group	5	12.2 ± 0.5	-20.9 ± 0.4	21.7 ± 0.5	3.4 ± 1.1	4.9 ± 1.8	7.1 ± 1.2	6.2 ± 0.8

Table S3.1. Isotopic compositions of local prey or other resident species used for LDA as training data.

Species	Region	$\delta^{15}\text{N}$ of phenylalanine	$\delta^{15}\text{N}$ of glycine	References
Japanese horse mackerel	Japan	5	-1.9	Xing et al. (2023)
Japanese anchovy	Japan	1.3	-1.8	Miyachi et al. (2015)
Japanese anchovy	Japan	2.4	0.6	Miyachi et al. (2015)
Jellyfish	Taiwan	2.06	4.91	This study
Jellyfish	Taiwan	6.83	5.39	This study
Sharptail sunfish	Taiwan	2.82	3.37	Chang et al. (2023)
Sharptail sunfish	Taiwan	4.78	3.73	Chang et al. (2023)
Yellowfin tuna	Warm pool	5.3	-7.4	Lorrain et al. (2015)
Yellowfin tuna	Warm pool	11.6	-2.1	Lorrain et al. (2015)
Yellowfin tuna	Warm pool	11.4	4.9	Lorrain et al. (2015)
POM	New Zealand	6	5.5	Sabadel et al. (2022)
POM	New Zealand	7.9	6.8	Sabadel et al. (2022)
POM	New Zealand	5.8	6.3	Sabadel et al. (2022)

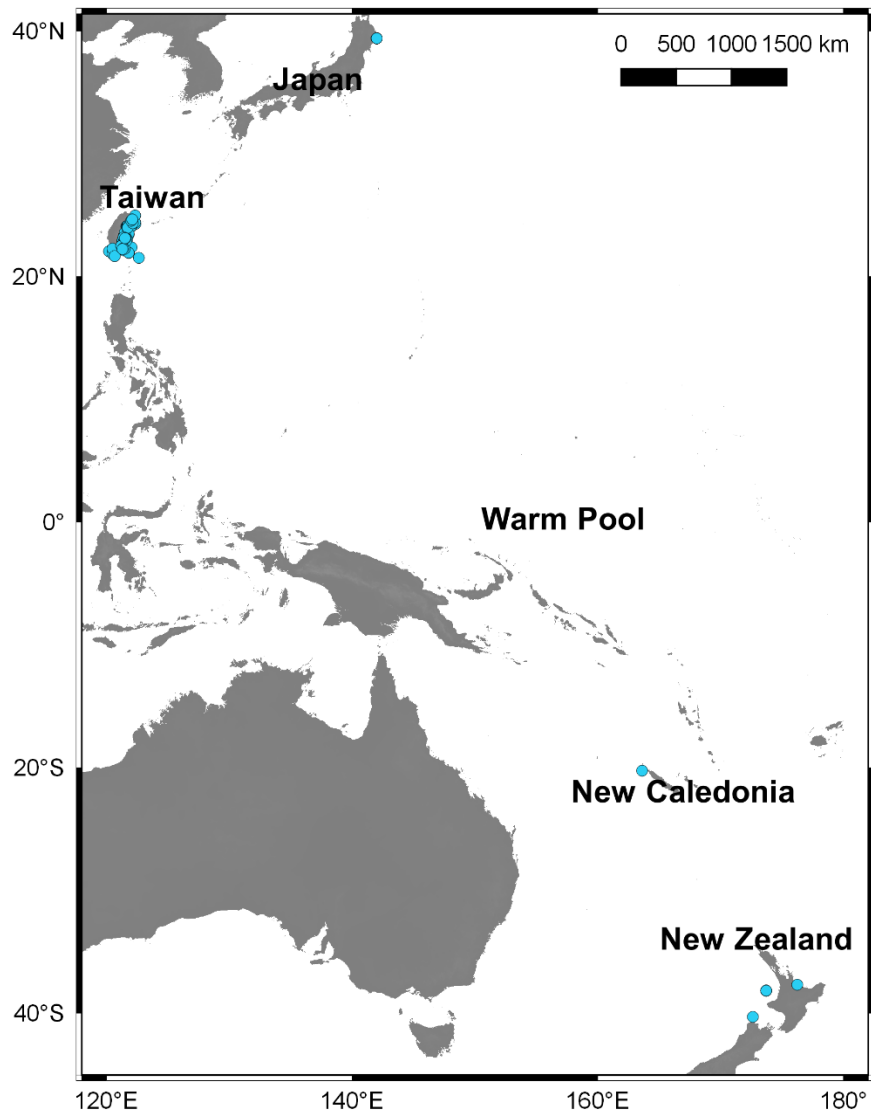


Fig. 3.1. Sampling map (blue solid circles) of molidis in the western Pacific Ocean, the sampling areas included Japan, Taiwan, New Caledonia (NC), and New Zealand (NZ).

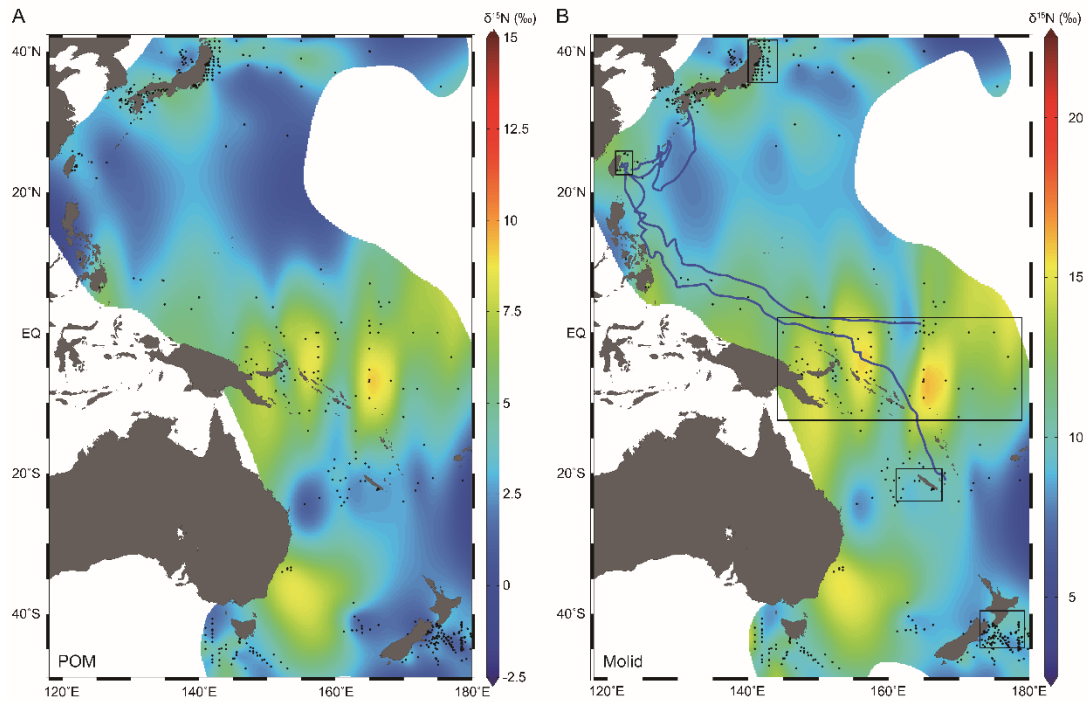


Fig. 3.2. Map of $\delta^{15}\text{N}_{\text{POM}}$ (A) and predicted $\delta^{15}\text{N}_{\text{molids}}$ (B) isoscapes showing the location of sampling sites (black dots). The blue lines and black boxes in Fig. 3.2B represent the tracks of tagged molids in Chang et al. (2021) and the sampling values in isoscape used in the bootstrapping approach, respectively.

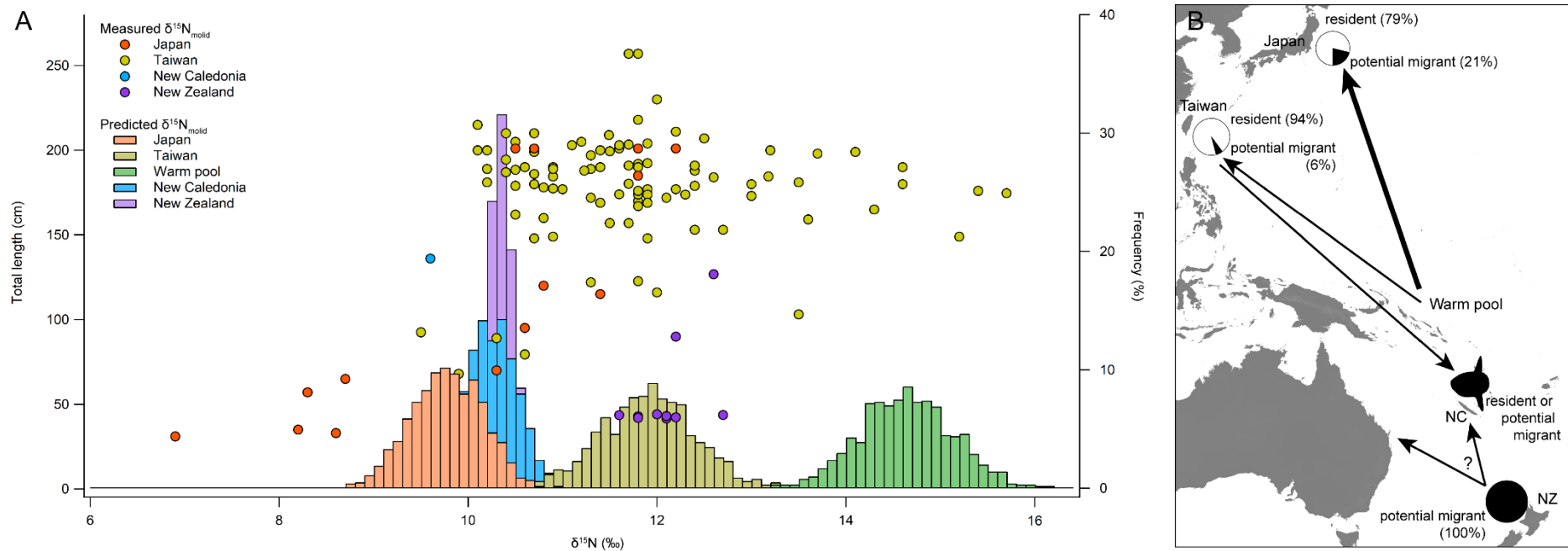


Fig. 3.3. The relationship of measured $\delta^{15}\text{N}_{\text{molid}}$ values with molid size (left axis) and the frequency distribution of predicted $\delta^{15}\text{N}_{\text{molid}}$ values (right axis) in Taiwan, Japan, warm pool region, New Caledonia, and New Zealand (A). Solid circles represent the measured $\delta^{15}\text{N}_{\text{molid}}$ values from sampling data. Bootstrapping histograms represent the predicted $\delta^{15}\text{N}_{\text{molid}}$ values from isoscapes. The schematic of residency and migratory patterns of molids in each regions of the western Pacific Ocean (B). The pie charts represent the percentages of residents (white) and potential migrants (black) based on Fig. 3.3A. The arrow lines represent the possible direction of migratory patterns.

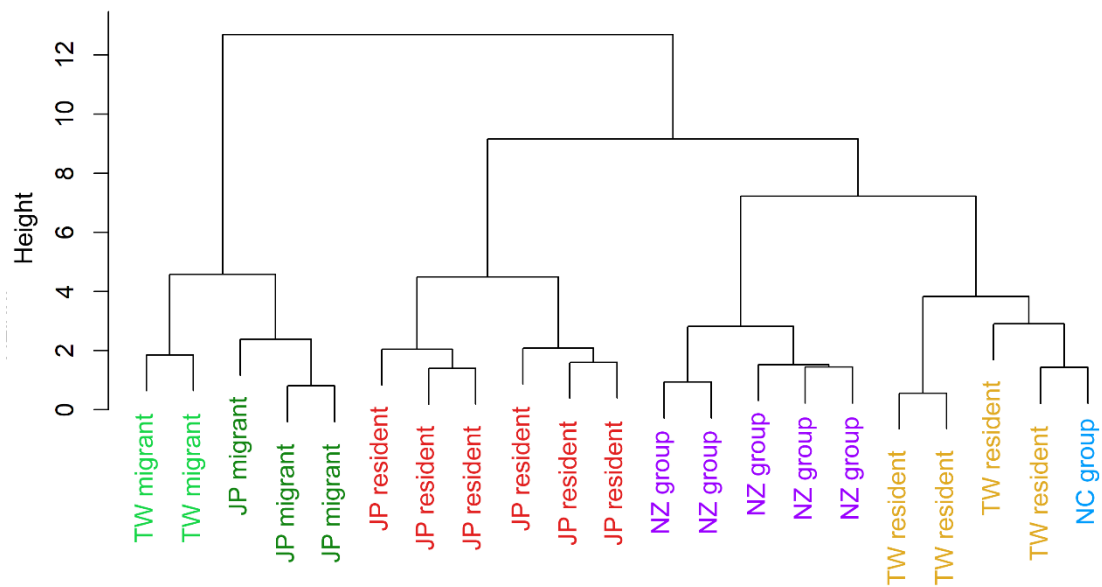


Fig. 3.4. Cluster analysis dendrogram of potential residents and migrants of molids in each regions based on bulk $\delta^{13}\text{C}$, $\delta^{15}\text{N}$, and $\delta^{15}\text{N}_{\text{Src}}$ values (glycine, serine, phenylalanine, lysine).

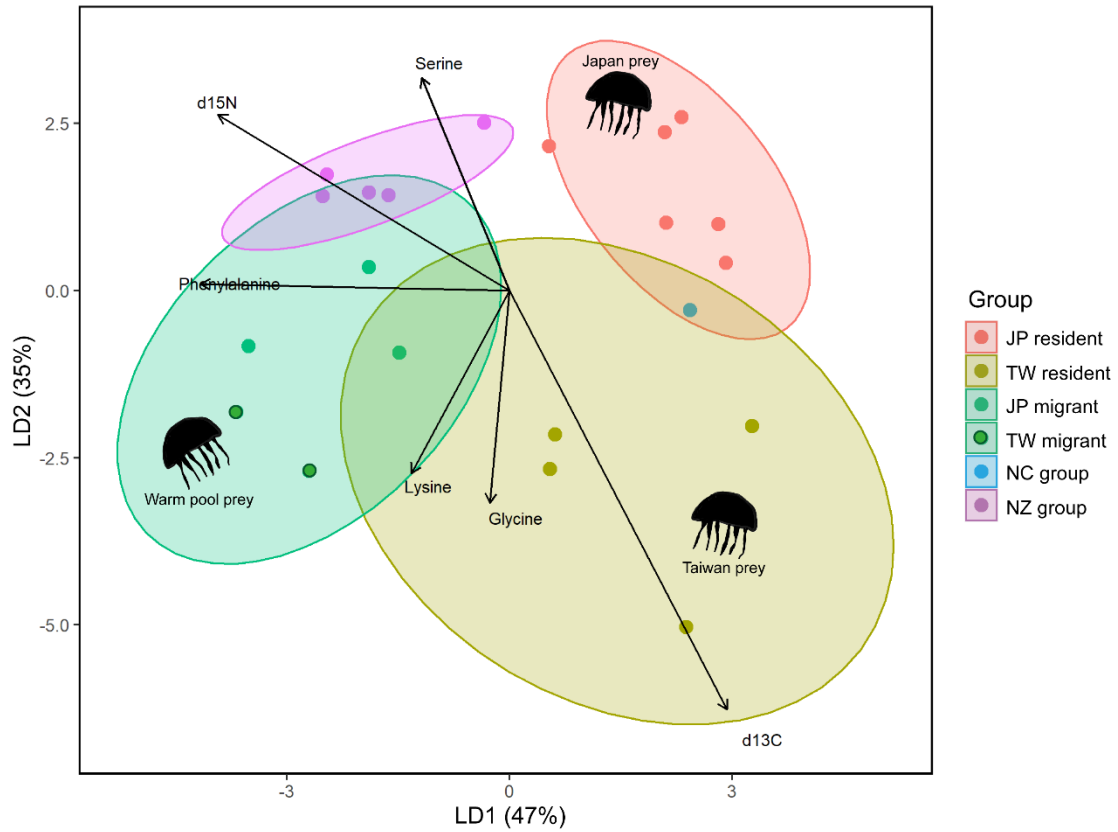


Fig. 3.5. Linear discriminant function analysis of potential residents and migrants of molids based on their bulk $\delta^{13}\text{C}$, $\delta^{15}\text{N}$, and $\delta^{15}\text{N}_{\text{Src}}$ values (glycine, serine, phenylalanine, lysine). The ellipses represent 95% confidence intervals of each endmember, and the arrows represent the relative weightings of the independent variables.

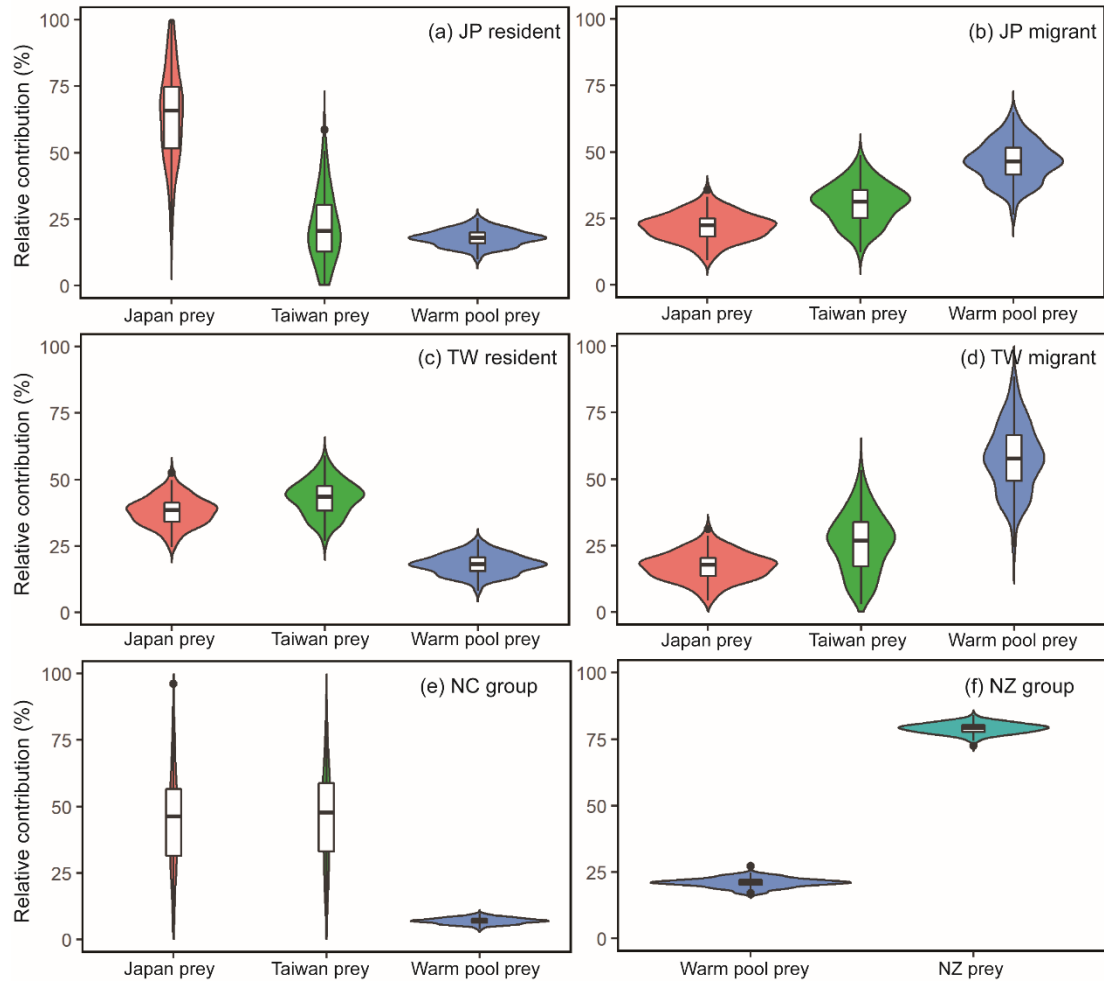


Fig. 3.6. Estimated contribution of regional prey to diets of potential residents and migrants based on Bayesian isotope mixing models. Boxplots represent the 25th, median, and 75th quartiles of data; whiskers represent $1.5\times$ the interquartile range; and solid circles represent outliers.

CHAPTER 4 – Diet breadth and overlap in the Family Molidae

Chang CT, Drazen JC, Hixon MA, Nyegaard M, Phillips ND, Chiang WC, Ho YH,

Popp BN (2023) Environmental Biology of Fishes (in revision)

4.1 Abstract

Marine sunfishes (also known as molids) of the Family Molidae are widely distributed from tropical to temperate waters and are typically recognized as predators of gelatinous plankton almost exclusively. Despite similar morphological features and behaviors, the trophic ecology and potential interactions among species of molids remain largely unknown. We reviewed literature on the diets of each species and conducted diet analyses of three species sampled off the east coast of Taiwan. We examined diet separation among sympatric species – ocean sunfish *Mola mola*, bumphead sunfish *Mola alexandrini*, and sharptail sunfish *Masturus lanceolatus* – through stomach content and stable isotope analyses. The literature review revealed that the Family Molidae exhibits broader diets than previously characterized. *Mola mola*, *M. alexandrini*, and *M. tecta* consume prey from epi/mesopelagic environments, while *M. lanceolatus* and slender sunfish *Ranzania laevis* consume prey from both epi/mesopelagic environments and benthic habitats. No gelatinous prey were found in the stomachs of *R. laevis*. Off Taiwan, *M. mola* and *M. alexandrini* had similar and relatively narrow diet breadths, primarily feeding on scyphozoans, suggesting similar trophic niches. In contrast, *M. lanceolatus* displayed a broader diet, mainly consuming tunicates and augmenting their diet from epi- and mesopelagic, coastal, and benthic habitats. Dietary differences between *M. lanceolatus* and the other species might be linked to morphological differences such as gape size and eye length. *Mola mola* and *M. alexandrini* tend to have larger gapes and eyes and our diet analysis shows that they forage on larger-sized prey and at greater depths.

4.2 Introduction

The marine Family Molidae (often known as molids or marine sunfishes) includes three genera (*Mola*, *Masturus*, and *Ranzania*) and five species: ocean sunfish *Mola mola*, bumphead sunfish *M. alexandrini*, hoodwinker sunfish *M. tecta*, sharptail sunfish *Masturus lanceolatus*, and slender sunfish *Ranzania laevis*. They are distributed worldwide from tropical to temperate waters. Molids comprise a large percentage of bycatch in set-net, longline, gillnet, and trawling fisheries in the Mediterranean Sea and Atlantic Ocean (Pope et al. 2010, Nyegaard et al. 2020). Additionally, molids are targeted fishery species in some regions of the Pacific Ocean (Pope et al. 2010, Chang et al. 2018). Due to the impact of fishing pressure and their potentially slow growth rate (Liu et al. 2009), their populations are expected to decline globally (Liu et al. 2015, Phillips et al. 2023). Documenting the ecology of molids provides important information for managing their populations and implementing ecosystem-based fishery management (Francis et al. 2007, Essington & Punt 2011).

Molids are typically considered to be gelatinous plankton feeders that prey on scyphozoan jellyfishes, siphonophores, or tunicates (Fraser-Brunner 1951, Hooper et al. 1973, Nakamura et al. 2015, Sousa et al. 2016, Chang et al. 2023). Recent studies have indicated a wider dietary range, including pelagic, neritic and benthic prey, such as megalops, amphipods, and squids (Syväranta et al. 2012, Harrod et al. 2013, Nakamura & Sato 2014, Phillips et al. 2020, Chang et al. 2023).

Molids share similar physical and behavioral characteristics. They have specialized morphologies, including a round body shape, elongated dorsal fins, and a clavus (rudder-like caudal fin). They also display similar movement patterns, mostly staying at deep depths during daytime and near the surface at night (Seitz et al. 2002, Dewar et al. 2010, Chang et al. 2020, 2021). With similar physical features and movement

behaviors, how species of mollids interact with each other and possibly partition resources remains unknown.

When organisms share the same habitat or food resources, competition will result if those resources are in short supply. When competition occurs, organisms may separate their ecological niches by partitioning resources. Resource partitioning among sympatric organisms may reduce the intensity of competition and allow coexistence (Schoener 1974). The species might develop strategies to take advantage of different resources (i.e., habitats, food, or activity time) or increase the variety of those resources (Roughgarden 1976). Arostegui et al. (2020) concluded that mollids were partially separated geographically in the eastern North Pacific. In this region, *M. mola* and *M. alexandrini* preferred temperate regions while *M. lanceolatus* and *R. laevis* preferred sub- and tropical regions. However, several fishery records showed that these species all co-occurred in the same regions (Sawai et al. 2011, 2019, Chang et al. 2018). Therefore, the mechanisms through which species of mollids with comparable physical traits and movement patterns interact and potentially divide resources are still uncertain. Thus, more diet studies are required to understand the trophic ecology of mollids and whether they partition food resources.

Multiple approaches have been used to quantify diet partitioning, including stomach content analysis (SCA) and stable isotope analysis (SIA). Coupling SCA and SIA provides detailed insight into diets. SCA provides short-term diet information of consumers from hours to days/weeks and identifies specific prey items to the lowest possible taxonomic level (Cortés 1997). SCA is typically expressed by four diet indices, including frequency of occurrence (%FO), gravimetric importance (%W), numeric abundance (%N), and index of relative importance (IRI). Those indices can be used to estimate the diet breadth of each species, such as Levin's (Levins 1968) and Shannon-Wiener's diversity measures (Smith 1982), as well as diet overlap among species

(Hurlbert 1978). SIA provides time-integrated information on assimilated prey (Peterson & Fry 1987). Stable isotope ratios of carbon and nitrogen have been commonly used to explore the trophic dynamics and trophic position of animals that are integrated over time scales longer than SCA (Vander Zanden & Rasmussen 2001, Post 2002). Diet breadth and overlap can be calculated using isotopic values (Layman et al. 2007, Jackson et al. 2011) complementing SCA data.

In this study, we explored the trophic ecology and potential food resource partitioning among species of molids. First, we conducted a literature review to describe diets of molids and determine whether differences in diet exist among all species. Second, we used SCA and SIA to explore whether there is dietary partitioning among three molids occurring in the same region off Taiwan, testing whether these sympatric species provide evidence of diet partitioning.

4.3 Materials and methods

4.3.1 Literature survey

The literature review of diet studies of molids was conducted using Google Scholar and Web of Science search engines. We recorded the species of molid, specimen status (i.e., collected from fishing activity or from stranded specimens), fishery region, sample size, and diet composition from each study. A total of 20 reports (including this study) focused on the diet composition of molids using visual analysis or DNA meta-barcoding of stomach contents. For this part of our study, we did not include diet studies using stable isotope analysis or other chemical tracers because diets from those analyses cannot provide direct diet observation of molids.

4.3.2 Sample collection and processing

For our diet study, muscle tissue from the abdomen of fish for SIA and stomach samples for SCA were collected from the most common species, including *M. mola*, *M.*

alexandrini, and *M. lanceolatus*, at fish markets in eastern Taiwan from 2017 to 2021. We could not collect stomach contents from every individual because some stomach contents were removed and discarded by fishers before landing. Samples of the most common prey (based on cumulative %IRI > 95% in this diet study) for SIA, including scyphozoans (*Atolla* spp.), tunicates (Salpidae and *Pyrosoma* spp.), pteropods, and amphipods (*Phronima* spp. and *Lestrigonus* spp.), were collected in eastern Taiwan during the same periods. Scyphozoa (n = 8) were collected with a hand-net. Undigested tunicates (n = 16), pteropods (n = 10), *Phronima* spp. (n = 7), and *Lestrigonus* spp. (n = 6) were collected directly from stomach contents of molids. All molids were caught off eastern Taiwan by set-net and longline fisheries (Fig. 4.1), and brought back to the fish market on ice for sale on the same day.

Four physical features of molids were measured, including total length (TL, from the tip of snout to the end of caudal fin), standard length (SL, from the tip of the snout to the flexible crease of the caudal fin), eye length, and gape width. We used SL in analyses because caudal fins of some specimens had been removed and discarded by fishers.

For SCA, the stomachs of molids with prey items were collected. Prey items were identified to the lowest possible taxon in the laboratory, and their abundance and wet weight were measured. Cephalopods were identified from beaks. The prey items were preserved in 95% ethanol after measurements.

For SIA, white muscle tissue samples of molids were collected. Muscle tissue and prey items were rinsed with distilled water and dried for 48h at 60°C. The dried tissue was ground into a homogeneous powder. Approximately 0.4-0.8 mg of powder was packed into ultra-clean tin capsules. The values of $\delta^{13}\text{C}$ and $\delta^{15}\text{N}$ were determined using an elemental analyzer (Costech ECS 4010 Elemental Combustion System using a Zero Blank Autosampler) coupled to a mass spectrometer (Thermo-Delta V Advantage). The

isotope values were expressed in standard ‰ notation relative to Vienna Pee Dee belemnite (V-PDB) for carbon and atmospheric N₂ for nitrogen. The analytical error derived from multiple analyses of reference materials for both $\delta^{13}\text{C}$ and $\delta^{15}\text{N}$ was <0.2‰.

To quantify diet partitioning of these sympatric species, we limited data analysis to species that co-occurred at the same time, capture depth (hook depth of longline fisheries or the depth of set-net), and location (referred to as unrestricted data). Additionally, we controlled the size of three species between 120-160 cm SL (referred to as size-restricted data) to minimize any body size effect since the average SL of captured *M. mola* (161 ± 27 cm, 106 to 249 cm) and *M. alexandrini* (161 ± 40 cm, 63 to 301 cm) were larger than the size of *M. lanceolatus* (91 ± 21 cm, 42 to 151 cm). The sample size and size range of each species in both unrestricted and size-restricted data for SCA and SIA are described in Table S4.1. The relationships between the eye length/gape width and body length were examined by species using linear regression. Differences of eye length and gape width among species in the same range (120-160 cm SL) of body length were tested using one-way ANOVA.

4.3.3 Stomach content analysis

Cumulative prey curves were used to determine whether there was a sufficient number of stomachs analyzed to describe the diets of the three species in both unrestricted and size-restricted data. Four diet indices were calculated: frequency of occurrence as proportion of predator stomachs containing a prey item (%FO), numerical abundance as the proportion of the number of a prey item in the total number of all prey (%N), gravimetric importance as the proportion of the weight of a prey item in the total weight of all prey items (%W), and the index of relative importance as a combination of these 3 metrics (expressed as a percentage, %IRI) (Pianka 1973). The diet compositions (%N and %W) among three species were compared using analysis of

similarities (ANOSIM, 9999 permutations) with pairwise tests based on a Bray-Curtis similarity matrix.

To estimate diet breadth and overlap among the three sympatric species, Levin's measure (B, Levins 1968, Krebs 1999) and a percent similarity index (PSI, Hurlbert 1978) were calculated based on %N and %W:

$$B = \frac{1}{\sum p_i^2} \quad (1)$$

$$PSI = \sum \min p_i \quad (2)$$

where B is the diet breadth, PSI is the diet overlap, and p_i is the proportion (in %N and %W) of prey i found in the diets of a consumer. Species that use many resources have B values (which can range from 0 to 1) close to 1, indicating a generalist pattern of resource use. The PSI ranges from 0 to 100%, with a higher PSI value indicating a greater resource overlap in the diet between two species.

4.3.4 Stable isotope analysis

Linear regression was used to test for significant relationships between $\delta^{13}\text{C}$ and $\delta^{15}\text{N}$ values and SL. Differences in $\delta^{13}\text{C}$ and $\delta^{15}\text{N}$ values among species were tested using one-way ANOVA with Tukey's post-hoc tests in both unrestricted and size-restricted data. The diet breadth (a corrected standard ellipse area, SEAc) and diet overlap among species were calculated using Stable Isotope Bayesian Ellipse (SIBER, Jackson et al. 2011) in both unrestricted and size-restricted data. A Bayesian mixing model was used to estimate the relative contributions of prey taxa to three sympatric species in both data sets. The most common (the cumulative %IRI >90%) prey items found in the stomach contents were analyzed. Informative priors were used based on the diet composition (%W) in this study because the gravimetric importance (%W) represents the total mass or energy transferred from prey to predator. The trophic discrimination factor values ($\Delta^{13}\text{C} = 2 \pm 1.3\text{‰}$ and $\Delta^{15}\text{N} = 3 \pm 1.2\text{‰}$; Phillips et al.

2020) were used. We ran each mixing model with 3 Markov chain Monte Carlo simulations of 25000 iterations (burn-in = 10000 and thinning rate = 10). Both Gelman-Rubin (Gelman et al. 2013) and Geweke diagnostics (Geweke 1991) were used to test for model convergence. All statistical tests, isotopic diet breadth, overlap and Bayesian mixing model were undertaken using R version 4.0.4.

4.4 Results

4.4.1 Diet composition from literature review and this study

The literature review of diet studies of molids included *M. mola* (Reuvens 1897, Nakamura & Sato 2014, Nakamura et al. 2015, Bakenhaster & Knight-Gray 2016, Sousa et al. 2016, this study), *M. alexandrini* (this study), *M. tecta* (Nyegaard et al. 2018), *M. lanceolatus* (Yabe 1950, Bakenhaster & Knight-Gray 2016, Sawai et al. 2019, Chang et al. 2023), and *R. laevis* (Plancus 1746, Donovan & Rivington 1803, Steenstrup & Lütken 1898, Barnard 1927, 1935, Fitch 1969, Robison 1975, Smith et al. 2010, Purushottama et al. 2016, Nyegaard et al. 2017) (Table 4.1). Diet composition reported in the literature was examined by stomach content analysis, DNA meta-barcoding analysis, and bio-logging devices. In these studies, the body size range (TL) of *M. mola* was 37-279 cm, *M. alexandrini* 79-322 cm, *M. tecta* 65-196 cm, *M. lanceolatus* 3.7-250 cm, and *R. laevis* 10-70 cm.

Overall, the literature survey on the diets of molids showed a wide variety of prey, including species ranging from the epi/mesopelagic zones to benthic habitats. *Mola mola* were collected mostly from fisheries, one study from stranding samples, and one used only a bio-logging device. The reported diets of *M. mola* were composed of a wide variety of prey from nearshore (i.e., seagrass, epiphytic diatoms) to epi/mesopelagic environments (i.e., scyphozoan, siphonophores) (Fig. S4.1). Cnidarians were the most common prey for *M. mola* recorded in most diet studies, except for studies with a

sample size of 1 (Reuvens 1897) or with stranded specimens (Bakenhaster & Knight-Gray 2016). Nakamura et al. (2015) used bio-logging devices to observe the foraging behavior of 7 *M. mola* off Japan and found that 4 of them approached and captured gelatinous plankton (e.g., siphonophores, scyphozoans). In the studies with quantitative estimates (i.e., %FO, %N, %W, %IRI, or by volume %V), scyphozoans, amphipods (Gammaridae, Lestrigonidae), macroalgae and fishes were the most important prey in *M. mola* (Nakamura & Sato 2014, Bakenhaster & Knight-Gray 2016, this study). The stomach contents of 57 *M. mola* that were caught by set net off southern Portugal were identified by DNA meta-barcoding (Sousa et al. 2016). Malacostraca crustaceans had the highest percent occurrence in the stomachs of these *M. mola* (37%), followed by bony fishes (24%), and hydrozoans (15%). Moreover, an ontogenetic shift in diet of *M. mola* was found in two studies (Nakamura & Sato 2014, Sousa et al. 2016) where large individuals had a more pelagic diet (i.e., Hydrozoa and Scyphozoa) and small individuals had a more benthic diet (i.e., Malacostraca, Gammaridae, Bivalvia).

Only our study examined the diet of *M. alexandrini*. Various prey categories were found, including scyphozoans and amphipods (Hyperiidia, Lestrigonidae), but also pteropods, tunicates and fishes (FO%, in Table 4.2, see detailed information in section 3.3).

A single study mentioned the diet of *M. tecta*, with one stranded specimen and two fresh specimens collected from fisheries (Nyegaard et al. 2018). Tunicates (*Thetys vagina* and *Pyrosoma* sp.) and nektonic siphonophores were found in the stomachs of three specimens.

Two diet studies of *M. lanceolatus* were of stranded specimens, and two additional studies were based on fisheries samples. The diet was composed of prey from both benthic habitats (i.e., annelids, sponges, and various sand-dwelling animals) and epi/mesopelagic habitats (i.e., tunicates, cephalopods). In the studies with quantitative

values (Bakenhaster & Knight-Gray 2016, Chang et al. 2023), tunicates were the most important prey (55%V in Bakenhaster & Knight-Gray 2016, 81%W in Chang et al. 2023). Notably, some remains of terrestrial plants were found in *M. lanceolatus* in Japan (Sawai et al. 2019).

Most diet studies of *R. laevis* were recorded in the early 1900s from fisheries and one study from stranded specimens. The diet of *R. laevis* was composed of prey from nearshore (i.e., seagrass), benthic (i.e., sponge) to epi/mesopelagic environments (i.e., cephalopods, fishes, some crustaceans). Robison (1975) investigated the diet compositions of 7 juvenile *R. laevis* (10-11 cm TL) collected by a mid-water trawl in the eastern Pacific Ocean, revealing the presence of copepods, ostracods, and amphipods in their stomachs. In a subsequent study (Nyegaard et al. 2017), crustaceans and cephalopods were identified as the predominant prey for a *R. laevis* captured in deep water off eastern Australia. The investigation with quantitative data (Smith et al. 2010) found that the stomachs of 4 *R. laevis*, stranded on sandy beaches of Western Australia, contained unidentified digested material (77% by volume), seagrass (19%), and invertebrates (1%). In contrast to other species, no gelatinous prey (i.e., scyphozoan or tunicates) were reported in the stomachs of *R. laevis*.

4.4.2 Relationship between eye length/gape width and body length of sympatric molids

Differences in the morphological traits among three sympatric species could be related to their dietary differences. The relationship between gape width and body length of each species was positive and linear ($p < 0.05$) (Fig. 4.2A). In the same size range, the average gape of *M. lanceolatus* (4.5 ± 1.2 cm) was smaller than that of *M. mola* (6.8 ± 1) and *M. alexandrini* (6.8 ± 1.5) ($F_{2,71} = 25.186$, $p < 0.001$). The relationship between eye length and body length of each species was also significantly positive ($p < 0.05$) (Fig. 4.2B). The average eye length of *M. lanceolatus* (4.3 ± 1.1) was smaller than that of *M. mola* (6.1 ± 1.3) and *M. alexandrini* (6.6 ± 1.9) ($F_{2,71} =$

18.033, $p < 0.001$).

4.4.3 Diet composition of sympatric molids in eastern Taiwan

A total of 159 stomachs with prey items were analyzed, including 85 *M. lanceolatus*, 34 *M. mola* and 40 *M. alexandrini* (Table S4.1). Cumulative prey curves indicated that sample sizes for *M. mola*, *M. alexandrini* and *M. lanceolatus* in both unrestricted and size restricted data were sufficient to describe their diets (Fig. S4.2). Overall, the diets of the three species showed significant differences in terms of %N (ANOSIM: unrestricted: $R = 0.47$, $p < 0.001$; size-restricted: $R = 0.296$, $p < 0.001$) and %W (unrestricted: $R = 0.458$, $p < 0.001$; size-restricted: $R = 0.302$, $p < 0.001$). In pairwise tests, diets of *M. mola* and *M. alexandrini* were similar (unrestricted: %N: $p = 0.126$, %W: $p = 0.180$; size-restricted: %N: $p = 0.476$, %W: $p = 0.201$), and both of their diets were different from the diet of *M. lanceolatus* (unrestricted: %N and %W: $p < 0.001$; size-restricted: %N and %W: $p < 0.001$). The most abundant and important prey in stomachs of *M. mola* and *M. alexandrini* were scyphozoans of the genus *Atolla* (Fig. 4.3, Table 4.2). The diet of *M. lanceolatus* varied widely, including some cephalopods, gastropods, crustaceans, and fishes. Further, the most abundant prey of *M. lanceolatus* were tunicates, followed by pteropods (Fig. 4.3, Table 4.2). All three species fed frequently on hyperiidean amphipods (high %FO) even though the contributions of %W and %N were low. *Masturus lanceolatus* primarily fed on amphipods from the genus *Phronima*, whereas *M. mola* and *M. alexandrini* commonly fed on amphipods from the genus *Lestrignonus* (Table 4.2).

The diet breadth of *M. lanceolatus* (unrestricted Levine's B: %N: 0.10, %W: 0.15; size-restricted: %N: 0.26, %W: 0.02) was wider than that of *M. mola* (unrestricted: %N: 0.01, %W: 0.00; size-restricted: %N: 0.02, %W: 0.00) and *M. alexandrini* (unrestricted: %N: 0.01, %W: 0.00; size-restricted: %N: 0.02, %W: 0.00) in terms of %N and %W (Table 4.3). Diet overlap between *M. mola* and *M. alexandrini* was high (unrestricted:

%N: 98.2, %W: 99.8; size-restricted: %N: 97.9, %W: 99.7), whereas diet overlap between *M. mola* and *M. lanceolatus* was low (unrestricted: %N: 7.7, %W: 3.3; size-restricted: %N: 1.0, %W: 0.2), as was that between *M. alexandrini* and *M. lanceolatus* (unrestricted: %N: 6.2, %W: 3.2; size-restricted: %N: 0.8, %W: 0.04) (Table 4.4).

4.4.4 Isotopic composition of sympatric mollids in eastern Taiwan

A total of 264 tissue samples were collected, including 176 *M. lanceolatus*, 28 *M. mola*, and 60 *M. alexandrini* (Table S4.1). Linear regressions of SIA revealed an increase in values of $\delta^{15}\text{N}$ and $\delta^{13}\text{C}$ values with SL in *M. lanceolatus* ($\delta^{15}\text{N}$: $p = 0.002$, $\delta^{13}\text{C}$: $p = 0.049$) but there was no increase with SL in either *M. mola* ($\delta^{15}\text{N}$: $p = 0.356$, $\delta^{13}\text{C}$: $p = 0.419$) or *M. alexandrini* ($\delta^{15}\text{N}$: $p = 0.895$, $\delta^{13}\text{C}$: $p = 0.091$) across their full size ranges (Fig. S4.3). Both values of $\delta^{15}\text{N}$ (one-way ANOVA: $F_{2, 261} = 48.365$, $p < 0.001$) and $\delta^{13}\text{C}$ ($F_{2, 261} = 9.915$, $p < 0.001$) had significant differences among the three mollid species. In size-restricted data, $\delta^{15}\text{N}$ values were different among species ($F_{2, 89} = 14.780$, $p < 0.001$) but $\delta^{13}\text{C}$ values were not ($F_{2, 89} = 2.087$, $p = 0.13$). The $\delta^{15}\text{N}$ values of *M. mola* and *M. alexandrini* were similar and significantly higher than the values of *M. lanceolatus* in both data sets. The $\delta^{13}\text{C}$ values of *M. mola* and *M. lanceolatus* were lower than the values of *M. alexandrini* in the unrestricted data (Fig. 4.4).

In both data sets, *M. mola* had the largest isotopic diet breadth, followed by *M. alexandrini* and then *M. lanceolatus* (Fig. 4.4). The diet overlap between *M. mola* and *M. alexandrini* was high (unrestricted and size-restricted: 71%), whereas that between *M. lanceolatus* and both *M. mola* (unrestricted: 38%; size-restricted: 30%) and *M. alexandrini* (unrestricted: 38%; size-restricted: 36%) was relatively low.

4.4.5 Bayesian mixing model

Mixing model results indicated that prey contributions varied among three sympatric species (Fig. 4.5). The most important prey (median) for *M. mola* and *M. alexandrini* were scyphozoans of the genus *Atolla* in both the unrestricted (*M. mola*:

100%, *M. alexandrini*: 30%) and size-restricted datasets (*M. mola*: 90%, *M. alexandrini*: 100%). In unrestricted data, *Atolla* (30%) and amphipods of the genus *Phronima* (22%) had high contributions to diets of *M. alexandrini*. Unlike *M. mola* and *M. alexandrini*, the most important prey for *M. lanceolatus* were tunicates in both the unrestricted (98%) and size-restricted data (92%).

4.5 Discussion

Our literature review revealed that gelatinous organisms were the primary prey for four of the five molid species, yet they all augmented their diets with prey from other taxa. *Ranzania laevis* did not feed on gelatinous prey, suggesting substantial niche partitioning from the other species. For three sympatric species captured off the eastern coast of Taiwan, *M. mola* and *M. alexandrini* showed great diet overlap, whereas the diet of *M. lanceolatus* was significantly different. Instead of consuming scyphozoan, the *M. lanceolatus* fed mainly on tunicates and augmented their diets from epi/mesopelagic and benthic habitats. Thus, overall there is evidence for partial partitioning in diets of these sympatric species off the eastern Taiwan.

4.5.1 Diet composition

Our literature review and diet study further demonstrated that molids can have broad diets and are not necessarily obligate consumers of gelatinous prey. Compiled studies of diet composition suggested some differences among species, yet the reviewed studies were not conducted at the same time and in the same geographic areas (which our dietary study was able to provide). Our review revealed that *Mola mola*, *M. alexandrini*, and *M. tecta* (*Mola* spp.) reportedly consumed more prey items from epi/mesopelagic environments, while *M. lanceolatus* and *R. laevis* consumed prey items from both epi/mesopelagic and benthic habitats. In studies with quantitative dietary analysis (i.e., %FO, %W, %N, %N, %IRI), the most important prey were

different among species: *M. mola* and *M. alexandrini* consumed mostly scyphozoans and hyperiid amphipods, *M. lanceolatus* mostly tunicates, and *R. laevis* mostly squid and seagrasses. For the latter species, at least 4 non-quantitative studies found small crustaceans as prey, including crab megalops, copepods and ostracods. Small crustaceans, namely hyperiid amphipods, were important for the other molids but these are parasites of the gelatinous plankton, providing further evidence that *M. mola* and *M. alexandrini* mainly consume gelatinous prey (Crossley et al. 2009). Notably, no gelatinous plankton was found in the stomachs of *R. laevis*, even in the studies where specimens were freshly collected from fishery activities.

It remains unclear whether differences in diet composition among molid species are due to ecological resource partitioning of space or food caused by present or past competition (Connell 1980). Data limitations, including the variable status of specimens (i.e., fresh samples from fishing activity or stranded specimens) or small sample size, could lead to spurious differences in diet composition. The status of specimens would affect the precision in diet compositions due to differential digestion rates of different prey, especially gelatinous plankton (Arai et al. 2003). In previous studies (Table 4.1), some specimens were collected from fishery activities, and their stomachs were processed immediately after collection. Some diet studies were recorded by bio-logging devices or DNA meta-barcoding, and other studies examined stranded specimens. Gelatinous plankton were mainly found in the stomachs collected from fishery activities, bio-logging devices, and DNA meta-barcoding, suggesting the prey with a rapid digestion rate are better documented from fresh specimens compared to the stranded specimens. Prey in the diet of stranded specimens could be identified only from hard parts (e.g., crustaceans, fishes, and squid beaks), with sand and algae in the stomachs possibly coming from stranding on beaches. Stranded specimens also provided very low detection of gelatinous prey (i.e., scyphozoans and tunicates),

suggesting that gelatinous prey are rapidly digested and underestimated in stomachs from stranding samples. Systematically underestimating soft-bodied prey is a well-documented problem in diet studies based on SCA (Symondson 2002).

Additionally, small sample sizes affect the interpretation of fish diets. In our literature review, the sample size was sometimes 1 and sometimes more than 30. A small sample size obviously makes it difficult to represent the diet of a population (Tirasin & Jørgensen 1999). Based on the specimen status and sample sizes, the diet composition of *M. mola* was documented more comprehensively than other species. Clearly, more study is needed on the diets of these fishes throughout their ranges, particularly the *M. alexandrini* and *M. tecta*, for which only one sample exists each.

Nonetheless, our data are consistent with the hypothesis that the differences in diet composition of molid species is related to resource partitioning caused by competition. The spatiotemporal segregation of molid species in a previous study (Arostegui et al. 2020) suggested that diet composition might differ among them due to the distinct prey sources in different habitats. Additionally, the diet composition of molid species might be linked to their diet preferences among potential prey species. In studies with quantitative values, the *M. mola*, *M. alexandrini*, and *M. lanceolatus* consume mostly gelatinous plankton and augment their diets from diverse array of other prey (Nakamura & Sato 2014, Bakenhaster & Knight-Gray 2016, Chang et al. 2023). Notably, no evidence suggested that *R. laevis* are predators of gelatinous plankton. From limited data, they consume mostly cephalopods and crustaceans (Donovan & Rivington 1803, Barnard 1935, Fitch 1969, Robison 1975, Nyegaard et al. 2017).

4.5.2 Diets of sympatric species in eastern Taiwan

Both SCA and SIA of three sympatric species suggested that the *M. mola*, *M. alexandrini*, and *M. lanceolatus* exhibit food resource partitioning between most species pairs. Both *M. mola* and *M. alexandrini* showed low diet overlap with *M.*

lanceolatus. High diet overlap between *M. mola* and *M. alexandrini* mainly feeding on scyphozoans (high %W and %IRI) suggested they had similar feeding habits despite occupying similar habitats. *Masturus lanceolatus* had a broad diet, mainly consuming tunicates and augmenting their diet from epipelagic, mesopelagic, coastal, and benthic habitats, consistent with previous studies (Bakenhaster & Knight-Gray 2016, Chang et al. 2023). Results from SIA and a Bayesian mixing model reinforce these findings. *Mola mola* and *M. alexandrini* had high $\delta^{15}\text{N}$ values and high diet contribution from scyphozoans, suggesting that they consumed and assimilated prey with high $\delta^{15}\text{N}$ values. In contrast, *M. lanceolatus* had a high diet contribution from tunicates, which are filter feeding organisms with low $\delta^{15}\text{N}$ values (Bone et al. 2003).

The occurrence and size distributions of *M. mola* and *M. alexandrini* in waters off Taiwan are similar (Chang et al. 2018). A potential partitioning in space (feeding depth range) or a limited interaction between these two species might result in their similar and high overlap diets. *Mola mola* and *M. alexandrini* experienced wide geographic and temperature ranges yet have slightly different thermal preferences (Chang et al. 2020, 2021), perhaps allowing them to reduce competition and coexist with each other. Another explanation for these two species having highly similar diets is that competition may be weak or nonexistent. The density of *M. mola* and *M. alexandrini* in waters off Taiwan are low (Chang et al. 2018, Fisheries Agency 2022), perhaps allowing both species to obtain sufficient food. On the contrary, the abundance of *M. lanceolatus* is high, so this sympatric species may avoid competition by consuming different food resources than the other molids.

Morphological traits play an important role in determining the feeding ability of fish species (Wainwright & Richard 1995). The partial partitioning in diets of three sympatric molids off eastern Taiwan might be linked to the differences in their morphological traits such as gape size and eye length. The gape size of *M. mola* and *M.*

alexandrini are notably larger than those of *M. lanceolatus* in the same body size range. This large gape size allows *M. mola* and *M. alexandrini* to consume larger prey, such as scyphozoans (Ménard et al. 2006). Conversely, the smaller gape size of *M. lanceolatus* restricts it to smaller prey like tunicates. Eye length may be related to the foraging depth of molids. *Mola mola* and *M. alexandrini* had larger eye lengths than *M. lanceolatus*, suggesting that *Mola* species forage at deeper depths (Braun et al. 2022, Warrant 2004, Warrant & Locket 2004). Kröger et al. (2009) measured the eye structure of twelve large predators. They found that some deep-diving fishes, such as the swordfish *Xiphias gladius*, the bigeye tuna *Thunnus obesus*, and the escolar *Lepidocybium flavobrunneum*, had large eye lengths, helping them detect prey at depth. These morphological differences suggest that two *Mola* species are adapted to foraging on larger prey and potentially at greater depths, while *M. lanceolatus* is better suited for consuming smaller prey in shallower waters.

4.5.3 Diet breadth in SCA vs. SIA

SCA and SIA detected differences in diet breadth within species, indicating the importance of integrating both approaches in studying foraging ecology. Diet breadth of *M. mola* and *M. alexandrini* were narrower than that of *M. lanceolatus*, while isotopic diet breadth of *M. mola* and *M. alexandrini* were broader than that of *M. lanceolatus*. SCA results provided contemporary diets of predators that reflect recently consumed items from hours to days or weeks (Cortés 1997), while SIA provides long-term assimilated prey of predators that reflect diets integrated across time and perhaps space (Peterson & Fry 1987). In SCA, we could easily determine that the diets of *M. mola* and *M. alexandrini* were less diverse than those of *M. lanceolatus*. The discrepancy in SIA-derived diet breadth might have resulted from variations in isotopic compositions of prey (Newsome et al. 2007). For example, *M. lanceolatus* feeding on a variety of prey with similar isotopic compositions would result in a small diet breadth.

Alternatively, *M. mola* and *M. alexandrini* may consume similar prey from different habitats (e.g., water depths) that have different isotopic baseline values and could result in a large isotopic diet breadth (Burgess et al. 2016, Gloeckler et al. 2018, Shipley et al. 2019).

4.5.4 Caveats

Our study has several limitations that should be acknowledged. First, we assumed that prey availability was similar across years and we did not consider interannual variation in diet due to the small sample sizes. Second, a wide range of $\delta^{15}\text{N}$ and $\delta^{13}\text{C}$ values of *M. mola* and *M. alexandrini* might be related not only to the isotopic compositions of prey sources but also to the migration patterns of molids. Previous tagging studies revealed that *M. mola* and *M. alexandrini* undergo both horizontal migrations and diel vertical movements (Cartamil & Lowe 2004, Dewar et al. 2010, Chang et al. 2021). During the migration, the fish could consume prey from regions with distinct baselines of isotopic values, resulting in a wide range of dietary isotopic values. Third, the diet contributions estimated from mixing models were influenced by the wide range of $\delta^{15}\text{N}$ and $\delta^{13}\text{C}$ values of *M. alexandrini*. The prey contributions could not fully explain the diet of *M. alexandrini*.

4.6 Conclusions

Our literature review and diet studies indicate that molids have broader diets than traditionally described, and notably that all but *R. laevis* principally feed on gelatinous prey. *Mola mola*, *M. alexandrini*, and *M. tecta* consumed more prey from pelagic environments, while *M. lanceolatus* consumed prey from both pelagic and benthic habitats. *Ranzania laevis* showed a distinct diet that mainly included cephalopods, benthic species, and no gelatinous plankton. Three sympatric species off the eastern coast of Taiwan exhibited partial food resource partitioning in that the diet of *M.*

lanceolatus was significantly different from that of *M. mola* and *M. alexandrini*, which overlapped greatly in diet. Overall, this study offers insight into the diet and trophic role of a family of understudied, yet globally distributed marine predators. These results increase ecological understanding. These insights could inform future efforts towards sustainable fisheries management, especially given the lack of fisheries regulations for molids across their broad geographic range.

4.7 References

- Arai MN, Welch DW, Dunsmuir AL, Jacobs MC, Ladouceur AR (2003) Digestion of pelagic Ctenophora and Cnidaria by fish. *Can J Fish Aquat Sci* 60:825–829. <https://doi.org/10.1139/f03-07>
- Arostegui MC, Braun CD, Woodworth-Jefcoats PA, Kobayashi DR, Gaube P (2020) Spatiotemporal segregation of ocean sunfish species (Molidae) in the eastern North Pacific. *Mar Ecol Prog Ser* 654:109-125. <https://doi.org/10.3354/meps13514>
- Bakenhaster MD, Knight-Gray JS (2016) New diet data for *Mola mola* and *Masturus lanceolatus* (Tetraodontiformes: Molidae) off Florida’s Atlantic coast with discussion of historical context. *Bull Mar Sci* 92:497-511. <https://doi.org/10.5343/bms.2016.1059>
- Barnard KH (1935) Notes on South African marine fishes. *Ann S Afr Mus* 30:645–658.
- Barnard KH (1927) A monograph of the marine fishes of South Africa. *Ann S Afr Mus* 21:419–1065.
- Bone Q, Carre C, Chang P (2003) Tunicate feeding filters. *J Mar Biol Assoc U K* 83:907-919. <https://doi.org/10.1017/S002531540300804Xh>
- Braun CD, Arostegui MC, Thorrold SR, Papastamatiou YP, Gaube P, Fontes J, Afonso P (2022) The functional and ecological significance of deep diving by large marine predators. *Annu Rev Mar Sci* 14:129-159. <https://doi.org/10.1146/annurev-marine-109>

032521-103517

Burgess KB, Couturier LI, Marshall AD, Richardson AJ, Weeks SJ, Bennett MB (2016)

Manta birostris, predator of the deep? Insight into the diet of the giant manta ray through stable isotope analysis. *R Soc Open Sci* 3:160717.
<https://doi.org/10.1098/rsos.160717>

Cartamil DP, Lowe CG (2004) Diel movement patterns of ocean sunfish *Mola mola* off

southern California. *Mar Ecol Prog Ser* 266:245-253.
<https://doi.org/10.3354/meps266245>

Chang CT, Drazen JC, Chiang WC, Madigan DJ, Carlisle AB, Wallsgrove NJ, Hsu HH,

Ho YH, Popp BN (2023) Ontogenetic and seasonal shifts in diets of sharptail mola *Masturus lanceolatus* in waters off Taiwan. *Mar Ecol Prog Ser* 715:113-127.
<https://doi.org/10.3354/meps14356>

Chang CT, Chiang WC, Musyl MK, Popp BN, Lam CH, Lin SJ, Watanabe YY, Ho YH,

Chen JR (2021) Water column structure influences long-distance latitudinal migration patterns and habitat use of bumphead sunfish *Mola alexandrini* in the Pacific Ocean. *Sci Rep* 11:21934. <https://doi.org/10.1038/s41598-021-01110-y>

Chang CT, Lin SJ, Chiang WC, Musyl MK, Lam CH, Hsu HH, Chang YC, Ho YS

(2020) Horizontal and vertical movement patterns of sunfish off eastern Taiwan. *Deep Sea Res Part II Top Stud Oceanogr* 175:104683.
<https://doi.org/10.1016/j.dsr2.2019.104683>

Chang CT, Chih CH, Chang YC, Chiang WC, Tsai FY, Hsu HH, Wu JH, Ho YH (2018)

Seasonal variations of species, abundance and size composition of Molidae in eastern Taiwan. *J Taiwan Fish Res* 26:27-42.

Connell JH (1980) Diversity and coevolution of competitors, or the ghost of

competition past. *Oikos* 35:131-138. <https://doi.org/10.2307/3544421>

Cortés E (1997) A critical review of methods of studying fish feeding based on analysis

of stomach contents: application to elasmobranch fishes. *Can J Fish Aquat Sci* 54:726-738. <https://doi.org/10.1139/f96-316>

Crossley SM, George AL, Keller CJ (2009) A method for eradicating amphipod parasites (Hyperiididae) from host jellyfish, *Chrysaora fuscescens* (Brandt, 1835), in a closed recirculating system. *J Zoo Wildl Med* 40:174-180. <https://doi.org/10.1638/2008-0100.1>

Dewar H, Thys T, Teo SLH, Farwell C, O'Sullivan J, Tobayama T, Soichi M, Nakatsubo T, Kondo Y, Okada Y, Lindsay DJ, Hays GC, Walli A, Weng K, Streelmanand JT, Karl SA (2010) Satellite tracking the world's largest jelly predator, the ocean sunfish, *Mola mola*, in the Western Pacific. *J Exp Mar Biol Ecol* 393:32–42. <https://doi.org/10.1016/j.jembe.2010.06.023>

Donovan E, Rivington FCJ (1803) The natural history of British fishes, including scientific and general descriptions of the most interesting species and an extensive selection of accurately finished coloured plates. Naturalis Biodiversity Center, London.

Essington TE, Punt AE (2011) Implementing ecosystem-based fisheries management: advances, challenges, and emerging tools. *Fish Fish* 12:123–124. <https://doi.org/10.1111/j.1467-2979.2011.00407.x>

Fisheries Agency (2022) Fisheries statistical yearbook—Taiwan, Kinmen and Matsu Area, 2022. Fisheries Agency, Council of Agriculture, Taipei.

Fitch JE (1969) A second record of the slender Mola, *Ranzania laevis* (Pennant), from California. *Bull South Calif Acad Sci* 68:115–188. <https://doi.org/10.3160/0038-3872-68.2.115>

Francis RC, Hixon MA, Clarke ME, Murawski SA, Ralston S (2007) Ten commandments for ecosystem-based fisheries scientists. *Fisheries* 32:217-233. [https://doi.org/10.1577/1548-8446\(2007\)32\[217:TCFBFS\]2.0.CO;2](https://doi.org/10.1577/1548-8446(2007)32[217:TCFBFS]2.0.CO;2)

- Fraser-Brunner A (1951) The ocean sunfishes (Family Molidae). *Bull Br Mus Nat Hist* 1: 87–121.
- Gelman A, Carlin JB, Stern HS, Dunson DB, Vehtari A, Rubin DB (2013) Bayesian data analysis. CRC Press, Boca Raton, Florida.
- Geweke J (1991) Evaluating the accuracy of sampling-based approaches to the calculation of posterior moments. Federal Reserve Bank of Minneapolis, Minneapolis, Minnesota.
- Gloeckler K, Choy CA, Hannides CC, Close HG, Goetze E, Popp BN, Drazen JC (2018) Stable isotope analysis of micronekton around Hawaii reveals suspended particles are an important nutritional source in the lower mesopelagic and upper bathypelagic zones. *Limnol Oceanogr* 63:1168-1180. <https://doi.org/10.1002/lno.10762>
- Harrod C, Syväranta J, Kubicek L, Cappaneraand V, Houghton JDR (2013) Reply to Logan & Dodge: ‘Stable isotopes challenge the perception of ocean sunfish *Mola mola* as obligate jellyfish predators’. *J Fish Biol* 82:10–16. <https://doi.org/10.1111/j.1095-8649.2012.03485.x>
- Hooper SN, Paradis M, Ackman RG (1973) Distribution of trans-6-hexadecenoic acid, 7-methyl-7-hexadecenoic acid and common fatty acids in lipids of ocean sunfish *Mola mola*. *Lipids* 8:509–516. <https://doi.org/10.1007/BF02531986>
- Hurlbert SH (1978) The measurement of niche overlap and some relatives. *Ecology* 59:67–77. <https://doi.org/10.2307/1936632>
- Jackson AL, Inger R, Parnell AC, Bearhop S (2011) Comparing isotopic niche widths among and within communities: SIBER-Stable Isotope Bayesian Ellipses in R. *J Anim Ecol* 80:595–602. <https://doi.org/10.1111/j.1365-2656.2011.01806.x>
- Krebs GJ (1999) Niche measures and resource preferences. In: Krebs GJ (ed) *Ecological methodology*. Addison-Welsey Educational Publishers, Menlo Park,

California, pp 455–495.

- Kröger RH, Fritsches KA, Warrant EJ (2009) Lens optical properties in the eyes of large marine predatory teleosts. *J Comp Physiol A* 195:175-182. <https://doi.org/10.1007/s00359-008-0396-1>
- Layman CA, Arrington DA, Montaña CG, Post DM (2007) Can stable isotope ratios provide for community-wide measures of trophic structure? *Ecology* 88:42-48. [https://doi.org/10.1890/0012-9658\(2007\)88\[42:csirpf\]2.0.co;2](https://doi.org/10.1890/0012-9658(2007)88[42:csirpf]2.0.co;2)
- Levins R (1968) Evolution in changing environments: some theoretical explorations. *Monogr Popul Biol* 2:1-122. <https://doi.org/10.2307/j.ctvx5wbbh>
- Liu KM, Lee ML, Joung SJ, Chang YC (2009) Age and growth estimates of the sharptail mola, *Masturus lanceolatus*, in waters of eastern Taiwan. *Fish Res* 95:154-160. <https://doi.org/10.1016/j.fishres.2008.08.013>
- Liu J, Zapfe G, Shao KT, Leis JL, Matsuura K, Hardy G, Liu M, Robertson R, Tyler J (2015) *Mola mola* (errata version published in 2016). The IUCN Red List of Threatened Species 2015: e.T190422A97667070. Accessed on 17 October 2023.
- Ménard F, Labrune C, Shin YJ, Asine AS, Bard FX (2006) Opportunistic predation in tuna: a size-based approach. *Mar Ecol Prog Ser* 323:223-231. <https://doi.org/10.3354/meps323223>
- Nakamura I, Goto Y, Sato K (2015) Ocean sunfish rewarm at the surface after deep excursions to forage for siphonophores. *J Anim Ecol* 84:590-603. <https://doi.org/10.1111/1365-2656.12346>
- Nakamura I, Sato K (2014) Ontogenetic shift in foraging habit of ocean sunfish *Mola mola* from dietary and behavioral studies. *Mar Biol* 161:1263-1273. <https://doi.org/10.1007/s00227-014-2416-8>
- Newsome SD, Martinez del Rio C, Bearhop S, Phillips DL (2007) A niche for isotopic ecology. *Front Ecol Environ* 5:429-436. <https://doi.org/10.1890/060150.01>

- Nyegaard M, García-Barcelona S, Phillips ND, Sawai E (2020) Fisheries interactions, distribution modelling and conservation issues of the ocean sunfishes. In: Thys TM, Hays GC, Houghton JDR (eds) *The Ocean Sunfishes: Evolution, Biology and Conservation*, CRC Press. Boca Raton, Florida, pp 216-242.
- Nyegaard M, Loneragan NR, Santos MB (2017) Squid predation by slender sunfish *Ranzania laevis* (Molidae). *J Fish Biol* 90:2480-2487. <https://doi.org/10.1111/jfb.13315>
- Nyegaard M, Sawai E, Gemmell N, Gillum J, Loneragan NR, Yamanoue Y, Stewart A. L (2018) Hiding in broad daylight: molecular and morphological data reveal a new ocean sunfish species (Tetraodontiformes: Molidae) that has eluded recognition. *Zool J Linn Soc* 182:631-658. <https://doi.org/10.1093/zoolinnean/zlx040>
- Peterson BJ, Fry B (1987) Stable isotopes in ecosystem studies. *Annu Rev Ecol Evol Syst* 18:293-320. <https://doi.org/10.1146/annurev.es.18.110187.001453>
- Pianka ER (1973) The structure of lizard communities. *Annu Rev Ecol Evol Syst* 4:53-74. <https://doi.org/10.1146/annurev.es.04.110173.000413>
- Plancus JA (1746) De Mola pisce. *Comment bonon Scient Inst Acad* 2:297–304.
- Phillips ND, Elliott Smith EA, Newsome SD, Houghton JDR, Carson CD, Alfaro-Shigueto J, Mangel JC, Eagling LE, Kubicek L, Harrod C (2020) Bulk tissue and amino acid stable isotope analyses reveal global ontogenetic patterns in ocean sunfish trophic ecology and habitat use. *Mar Ecol Prog Ser* 633:127-140. <https://doi.org/10.3354/meps13166>
- Phillips N, Nyegaard M, Sawai E, Chang CT, Baptista M, Thys T (2023) The ocean sunfishes (family Molidae): Recommendations from the IUCN molidae review panel. *Mar Policy* 155:105760. <https://doi.org/10.1016/j.marpol.2023.105760>
- Pope EC, Hays GC, Thys TM, Doyle TK, Sims DW, Queiroz N, Hobson VJ, Kubicek L, Houghton JDR (2010) The biology and ecology of the ocean sunfish *Mola mola*:

- A review of current knowledge and future research perspectives. *Rev Fish Biol Fisher* 20:471–487. <https://doi.org/10.1007/s11160-009-9155-9>
- Post DM (2002) Using stable isotopes to estimate trophic position: Models, methods, and assumptions. *Ecology* 83:703–718. [https://doi.org/10.1890/0012-9658\(2002\)083\[0703:USITET\]2.0.CO;2](https://doi.org/10.1890/0012-9658(2002)083[0703:USITET]2.0.CO;2)
- Purushottama GB, Chellappan A, Ramkumar C, Thakurdas S, Mhadgut B (2016) A rare occurrence and biology of the slender sunfish, *Ranzania laevis* (Actinopterygii: Tetraodontiformes: Molidae), in the coastal waters of Mumbai, North-West Coast of India. *Indian J Mar Sci* 43:1554-1559.
- Reuvens CL (1897) *Orthragoriscus nasus* Ranz. on the Dutch coast. Notes from the Leyden Museum 18:209-212.
- Robison BH (1975) Observations on living juvenile specimens of the slender mola *Ranzania laevis* (Pisces, Molidae). *Pac Sci* 29:27–29.
- Roughgarden J (1976) Resource partitioning among competing species—a coevolutionary approach. *Theor Popul Biol* 9:388-424. [https://doi.org/10.1016/0040-5809\(76\)90054-X](https://doi.org/10.1016/0040-5809(76)90054-X)
- Sawai E, Hibino Y, Iwasaki T (2019) A rare river stranding record of sharptail sunfish *Masturus lanceolatus* in Fukuoka Prefecture, Japan. *Biogeogr* 21:27-30.
- Sawai E, Yamanoue Y, Yoshita Y, Sakai Y, Hashimoto H (2011) Seasonal occurrence patterns of Mola sunfishes (*Mola* spp. A and B; Molidae) in waters off the Sanriku region, eastern Japan. *Japan J Ichthyol* 58:181–187. <https://doi.org/10.11369/jji.58.181>
- Schoener TW (1974) Resource Partitioning in Ecological Communities: Research on how similar species divide resources helps reveal the natural regulation of species diversity. *Science* 185:27-39. <https://doi.org/10.1126/science.185.4145.27>
- Seitz AC, Weng KC, Boustany AM, Block BA (2002) Behaviour of a sharptail mola in

- the Gulf of Mexico. *J Fish Biol* 60:1597–1602. <https://doi.org/10.1111/j.1095-8649.2002.tb02452.x>
- Shiple ON, Gallagher AJ, Shiffman DS, Kaufman L, Hammerschlag N (2019) Diverse resource-use strategies in a large-bodied marine predator guild: evidence from differential use of resource subsidies and intraspecific isotopic variation. *Mar Ecol Prog Ser* 623:71–83. <https://doi.org/10.3354/meps12982>
- Smith KA, Hammond M, Close PG (2010) Aggregation and stranding of elongate sunfish (*Ranzania laevis*) (Pisces: Molidae) (Pennant, 1776) on the southern coast of Western Australia. *J R Soc West Aust* 93:181–188. <https://doi.org/10.1093/acprof:oso/9780199583652.003.0012>
- Smith EP (1982) Niche breadth, resource availability, and inference. *Ecology* 63:1675–1681. <https://doi.org/10.2307/1940109>
- Sousa LL, Xavier R, Costa V, Humphries NE, Trueman C, Rosa R, Sims DW, Queiroz N (2016) DNA barcoding identifies a cosmopolitan diet in the ocean sunfish. *Sci Rep* 6:28762 <https://doi.org/10.1038/srep28762>
- Steenstrup JJS, Lütken CF (1898) *Spolia Atlantica: Bidrag til Kundskab om Klumpeller Maanefiskene (Molidae)*. Bianco Lunos Kgl. Hof-Bogtrykkeri, Copenhagen.
- Symondson WOC (2002) Molecular identification of prey in predator diets. *Mol Ecol* 11:627–641. <https://doi.org/10.1046/j.1365-294X.2002.01471.x>
- Syväranta J, Harrod C, Kubicek L, Cappanera V, Houghton JDR (2012) Stable isotopes challenge the perception of ocean sunfish *Mola mola* as obligate jellyfish predators. *J Fish Biol* 80:225–231. <https://doi.org/10.1111/j.1095-8649.2011.03163.x>
- Tirasin EM, Jørgensen T (1999) An evaluation of the precision of diet description. *Mar Ecol Prog Ser* 182: 243–252. <https://www.jstor.org/stable/24852135>
- Vander Zanden MJ, Rasmussen JB (2001) Variation in $\delta^{15}\text{N}$ and $\delta^{13}\text{C}$ trophic fractionation: Implications for aquatic food web studies. *Limnol Oceanogr* 46:2061–

2066. <https://doi.org/10.4319/lo.2001.46.8.2061>

Warrant EJ (2004) Vision in the dimmest habitats on earth. *J Comp Physiol A* 190:765–789. <https://doi.org/10.1007/s00359-004-0546-z>

Warrant EJ, Locket NA (2004) Vision in the deep sea. *Biol Rev* 79:671–712. <https://doi.org/10.1017/S1464793103006420>

Wainwright PC, Richard BA (1995) Predicting patterns of prey use from morphology of fishes. *Environ Biol Fish* 44:97-113. <https://doi.org/10.1007/BF00005909>

Yabe H (1950) Juvenile of the pointed-tailed ocean sunfish, *Masturus lanceolatus*. *Bull Jpn Soc Sci Fish* 16:40-42. <https://doi.org/10.2331/suisan.16.40>

Table 4.1. Summary of diet studies of the Family Molidae from the literature review. Bold text represents the prey that were identified as the most important (highest %IRI), abundance (%N), weight (%W) or volume (%V).

Species	Region	Sample size	Body size (total length)	Specimen/Data source	Diet composition	Reference
<i>Mola mola</i>	Taiwan	40	138-279	Collected from fishery activities	Cnidaria: scyphozoa Crustacean: amphipoda , decapoda Mollusca: cephalopoda Tunicate, Algae	This study
	Florida Atlantic coast	1	149	Collected from stranded specimen	Algae: <i>Ectocarpus</i> sp., Epiphytic diatoms Crustacean: amphipoda, copepoda, decapoda, polychaeta, osstracoda Fish: Actinopterygii Seagrass: <i>Halodule wrightii</i>	Bakenhaster & Knight-Gray (2016)

Table 4.1. (Continued) Summary of diet studies of the Family Molidae from the literature review. Bold text represents the prey that were identified as the most important (highest %IRI), abundance (%N), weight (%W) or volume (%V).

Species	Region	Sample size	Body size (total length)	Specimen/Data source	Diet composition	Reference
	Southern Portugal	57	37-110	Collected from fishery activities	Cnidaria: scyphozoa, hydrozoa Crustacean: malacostraca , maxillopoda Fish: Actinopterygii Mollusca: cephalopoda, gastropoda, Bivalvia	Sousa et al. (2016)
	Iwate, Japan	4	125-200	Recorded from bio-logging device	Cnidaria: siphonophore Ctenophora	Nakamura et al. (2015)
	Iwate, Japan	10	<50, >200	Collected from fishery activities	Cnidaria: scyphozoa Crustacean: amphipoda Mollusca: Bivalvia	Nakamura & Sato (2014)
	Dutch coast	1	184	Collected from fishery activities	Algae: <i>Fucus vesiculosus</i> , <i>Zostera marina</i> Fish: <i>Limanda limanda</i>	Reuvens (1897)

Table 4.1. (Continued) Summary of diet studies of the Family Molidae from the literature review. Bold text represents the prey that were identified as the most important (highest %IRI), abundance (%N), weight (%W) or volume (%V).

Species	Region	Sample size	Body size (total length)	Specimen/Data source	Diet composition	Reference
<i>Mola alexandrini</i>	Taiwan	34	79-322	Collected from fishery activities	Cnidaria: scyphozoa Crustacean: amphipoda , decapoda Mollusca: pteropoda Fish, Tunicate	This study
<i>Mola tecta</i>	New Zealand	3	65-169	Collected from stranded specimen and fisheries activities	Cnidaria: siphonophore Tunicate	Nyegaard et al. (2018)
<i>Masturus lanceolatus</i>	Taiwan	105	57-193	Collected from fishery activities	Cnidaria: scyphozoa Crustacean: amphipoda , decapoda, euphausiacea Mollusca: cephalopoda, pteropoda , gastropoda, heteropoda Fish, Tunicate , Algae, Sand	Chang et al. (2023)

Table 4.1. (Continued) Summary of diet studies of the Family Molidae from the literature review. Bold text represents the prey that were identified as the most important (highest %IRI), abundance (%N), weight (%W) or volume (%V).

Species	Region	Sample size	Body size (total length)	Specimen/Data source	Diet composition	Reference
	Japan	1	112	Collected from stranded specimen	Sand, Leaves	Sawai et al. (2019)
	Florida Atlantic coast	2	245, 250	Collected from stranded specimen	Crustacean: decapoda Mollusca: cephalopoda, pteropoda, gastropoda Seagrass, Fish, Tunicate	Bakenhaster & Knight-Gray (2016)
	Japan	2	3.7, 7	Collected from fishery activities	Annelida, Sponge	Yabe (1950)
<i>Ranzania laevis</i>	Australia	1	58	Collected from fishery activities	Mollusca: cephalopoda Crustacean	Nyegaard et al. (2017)
	Mumbai, India	1	52.5	Collected from fishery activities	Empty stomach with green mass, and white spongy materials	Purushottama et al. (2016)

Table 4.1. (Continued) Summary of diet studies of the Family Molidae from the literature review. Bold text represents the prey that were identified as the most important (highest %IRI), abundance (%N), weight (%W) or volume (%V).

Species	Region	Sample size	Body size (total length)	Specimen/Data source	Diet composition	Reference
	Western Australia	4	30-70	Collected from stranded specimen	Seagrass: <i>Posidonia sinuosa</i>, <i>P. australis</i> Unidentified invertebrates, Sand	Smith et al. (2010)
	Between California Current & Eastern North Pacific	7	10-11	Collected from fishery activities	Crustacean: copepoda, ostracoda, amphipoda	Robison (1975)
	California	3	26-30	Collected from fishery activities	Crustacean: natantian shrimp, hyperiid amphipod, megalopa, zoea Mollusca: pteropoda Fish: <i>Trachipterus altivelis</i> , myctophid larva, unidentified larva	Fitch (1969)

Table 4.1. (Continued) Summary of diet studies of the Family Molidae from the literature review. Bold text represents the prey that were identified as the most important (highest %IRI), abundance (%N), weight (%W) or volume (%V).

Species	Region	Sample size	Body size (total length)	Specimen/Data source	Diet composition	Reference
	South Africa	1		Collected from stranded specimen	Crustacean: crab megalopa	Barnard (1935)
	Dassen Island, South Africa	1		Collected from fishery activities	Seaweed	Barnard (1927)
	Swansea, UK	1	65	-	Shells, Decomposed matter	Steenstrup & Lütken (1898)
	Cornwall, UK	1	-	Collected from fishery activities	Crustacean: crab	Donovan (1803)
	-	1	-	-	Seaweed	Plancus (1746)

Table 4.2. Stomach contents of three collected sympatric species: *Mola mola*, *Mola alexandrini*, and *Masturus lanceolatus*. Four diet indices were calculated: %FO, frequency of occurrence; %N, numerical abundance; %W, gravimetric importance; %IRI, proportion IRI of a prey item relative to the sum of all values of the index of relative importance. The values outside and inside the parentheses represent the full size range (unrestricted data) and size-restricted data, respectively.

Prey item	<i>Masturus lanceolatus</i>				<i>Mola alexandrini</i>				<i>Mola mola</i>			
	%FO	%N	%W	%IRI	%FO	%N	%W	%IRI	%FO	%N	%W	%IRI
SCYPHOZOA												
Atollidae - <i>Atolla</i> spp.	11.8 (9.1)	1.2 (0.5)	3.2 (0.04)	0.6 (0.1)	90.0 (84.2)	95.0 (93.5)	99.9 (99.8)	98.1 (97.4)	88.2 (82.4)	93.2 (91.6)	99.7 (99.5)	96.7 (95.6)
MOLLUSCS												
Cephalopoda												
Ommastrephidae (beak)	8.2 (9.1)	0.4 (0.5)	0.6 (0.1)	0.1 (0.1)					5.9 (5.9)	0.1 (0.1)	0.1 (0.1)	0.0 (0.0)
Onychoteuthidae (beak)									2.9 (5.9)	0.1 (0.1)	0.04 (0.1)	0.0 (0.0)
Gonatidae (beak)	1.2	0.1	0.01	0.0					2.9 (5.9)	0.02 (0.1)	0.02 (0.1)	0.0 (0.0)
Pen of unidentified cephalopoda	2.4 (9.1)	0.1 (0.5)	0.0 (0.0)	0.0 (0.1)								
Eye lens of unidentified cephalopoda	10.6 (27.3)	1.6 (4.3)	0.1 (0.1)	0.2 (1.5)								

Table 4.2. (Continued) Stomach contents of three collected sympatric species: *Mola mola*, *Mola alexandrini*, and *Masturus lanceolatus*. Four diet indices were calculated: %FO, frequency of occurrence; %N, numerical abundance; %W, gravimetric importance; %IRI, proportion IRI of a prey item relative to the sum of all values of the index of relative importance. The values outside and inside the parentheses represent the full size range (unrestricted data) and size-restricted data, respectively.

Prey item	<i>Masturus lanceolatus</i>				<i>Mola alexandrini</i>				<i>Mola mola</i>			
	%FO	%N	%W	%IRI	%FO	%N	%W	%IRI	%FO	%N	%W	%IRI
Hook of unidentified cephalopoda	1.2	1.8	0.1	0.03								
Pteropoda												
Cavoliniidae - <i>Diacavolinia longirostris</i>	34.1 (54.6)	16.0 (13.4)	1.2 (0.2)	6.5 (9.1)	2.5 (5.3)	0.1 (0.1)	0.0 (0.0)	0.0 (0.0)				
Cavoliniidae - <i>Cavolinia</i> spp.	9.4	0.8	0.1	0.1								
Cavoliniidae - <i>Diacria costata</i>	4.7	0.2	0.0	0.01								
Creseidae - <i>Creseis conica</i>	30.6 (27.3)	13.1 (13.4)	1.0 (0.1)	4.8 (4.5)								
Cliidae - <i>Clio pyramidata</i>	2.4 (18.2)	0.1 (1.1)	0.0 (0.01)	0.0 (0.2)								
Carinariidae - <i>Carinaria</i> spp.	23.5 (27.3)	5.8 (4.3)	0.6 (0.1)	1.7 (1.5)								
Atlantidae	15.3 (9.1)	1.5 (2.1)	0.1 (0.)	0.3 (0.2)								

Table 4.2. (Continued) Stomach contents of three collected sympatric species: *Mola mola*, *Mola alexandrini*, and *Masturus lanceolatus*. Four diet indices were calculated: %FO, frequency of occurrence; %N, numerical abundance; %W, gravimetric importance; %IRI, proportion IRI of a prey item relative to the sum of all values of the index of relative importance. The values outside and inside the parentheses represent the full size range (unrestricted data) and size-restricted data, respectively.

Prey item	<i>Masturus lanceolatus</i>				<i>Mola alexandrini</i>				<i>Mola mola</i>			
	%FO	%N	%W	%IRI	%FO	%N	%W	%IRI	%FO	%N	%W	%IRI
Gastropoda												
Benthic gastropoda (unidentified)	2.4	0.1	0.01	0.0								
Heteropoda												
Heteropods radula	10.6 (9.1)	4.7 (8.0)	0.2 (0.01)	0.6 (0.9)								
TUNICATE												
Salpidae	63.5 (45.5)	15.3 (8.6)	31.0 (5.8)	32.5 (8.0)								
Pyrosomatidae - <i>Pyrosoma</i> spp.	56.5 (45.5)	16.0 (32.6)	55.6 (92.3)	44.7 (69.8)	2.5 (5.3)	0.02 (0.1)	0.0 (0.0)	0.0 (0.0)	2.9 (5.9)	0.1 (0.1)	0.0 (0.0)	0.0 (0.0)
Pyrosomatidae - <i>Pyrosomella</i> spp.	1.2	0.1	0.04	0.0								
Pyrosomatidae - <i>Pyrostremma</i> spp.									2.9 (5.9)	0.1 (0.2)	0.0 (0.0)	0.0 (0.0)
CRUSTACEANS												

Table 4.2. (Continued) Stomach contents of three collected sympatric species: *Mola mola*, *Mola alexandrini*, and *Masturus lanceolatus*. Four diet indices were calculated: %FO, frequency of occurrence; %N, numerical abundance; %W, gravimetric importance; %IRI, proportion IRI of a prey item relative to the sum of all values of the index of relative importance. The values outside and inside the parentheses represent the full size range (unrestricted data) and size-restricted data, respectively.

Prey item	<i>Masturus lanceolatus</i>				<i>Mola alexandrini</i>				<i>Mola mola</i>			
	%FO	%N	%W	%IRI	%FO	%N	%W	%IRI	%FO	%N	%W	%IRI
Amphipoda												
Phronimidae - <i>Phronima</i> spp.	47.1 (45.5)	10.3 (4.8)	2.1 (1.1)	6.5 (3.3)	2.5	0.1	0.0	0.0				
Hyperiididae - <i>Hyperia</i> spp.	4.7 (9.1)	0.2 (0.5)	0.0 (0.0)	0.01 (0.1)								
Lestrigonidae - <i>Lestrigonus</i> spp.					70.0 (68.4)	4.8 (6.3)	0.1 (0.2)	1.9 (2.6)	88.2 (88.2)	6.4 (8.0)	0.2 (0.2)	3.3 (4.4)
Euphausiacea												
Euphausiidae - Euphausiids	2.4	0.5	0.03	0.01								
Decapoda												
<i>Gnathophausia</i> sp.	1.2	0.1	0.2	0.0								
<i>Puerulus</i> sp.									2.9	0.02	0.0	0.0
Caridea					2.5	0.02	0.0	0.0	5.9	0.12	0.0	0.0

Table 4.2. (Continued) Stomach contents of three collected sympatric species: *Mola mola*, *Mola alexandrini*, and *Masturus lanceolatus*. Four diet indices were calculated: %FO, frequency of occurrence; %N, numerical abundance; %W, gravimetric importance; %IRI, proportion IRI of a prey item relative to the sum of all values of the index of relative importance. The values outside and inside the parentheses represent the full size range (unrestricted data) and size-restricted data, respectively.

Prey item	<i>Masturus lanceolatus</i>				<i>Mola alexandrini</i>				<i>Mola mola</i>			
	%FO	%N	%W	%IRI	%FO	%N	%W	%IRI	%FO	%N	%W	%IRI
Shrimp (unidentified)	16.5 (18.2)	1.9 (1.1)	0.3 (0.1)	0.4 (0.3)								
Crab megalopa (unidentified)	1.2	0.1	0.01	0.0								
Scyllaridae phyllosoma	12.9	1.8	0.6	0.4								
Crab zoea (unidentified)	3.5 (18.2)	0.2 (1.6)	0.01 (0.03)	0.01 (0.04)								
FISH												
Scombridae	1.2	0.1	1.4	0.02								
Lutjanidae	1.2	0.1	0.8	0.01								
Lutjanidae (teeth)	2.5	0.1	0.01	0.0								
Exocoetidae (egg)	14.1 (9.1)	4.7 (0.5)	0.04 (0.0)	0.7 (0.1)								
Fish (unidentified)	1.2	0.1	0.9	0.01	2.5 (5.3)	0.02 (0.1)	0.01 (0.02)	0.0 (0.0)				

Table 4.2. (Continued) Stomach contents of three collected sympatric species: *Mola mola*, *Mola alexandrini*, and *Masturus lanceolatus*. Four diet indices were calculated: %FO, frequency of occurrence; %N, numerical abundance; %W, gravimetric importance; %IRI, proportion IRI of a prey item relative to the sum of all values of the index of relative importance. The values outside and inside the parentheses represent the full size range (unrestricted data) and size-restricted data, respectively.

Prey item	<i>Masturus lanceolatus</i>				<i>Mola alexandrini</i>				<i>Mola mola</i>			
	%FO	%N	%W	%IRI	%FO	%N	%W	%IRI	%FO	%N	%W	%IRI
Otolith of unidentified fish	1.2	0.1	0.0	0.0								
Bone of unidentified fish	4.7	1.0	0.03	0.1								
OTHERS												
Algae									2.9	0.02	0.0	0.0
TOTAL	85 (11)	343 (187)	0.7 (0.7) kg		40 (19)	4158 (1816)	60.5 (25.2) kg		34 (17)	4268 (1911)	60.3 (26.8) kg	

Table 4.3. Diet breadth (Levin's B) calculated by %N and %W of three sympatric species: *Mola mola*, *Mola alexandrini*, and *Masturus lanceolatus*. The values outside and inside the parentheses represent the full body size range (unrestricted data) and size-restricted data, respectively.

Diet breadth	<i>Masturus lanceolatus</i>	<i>Mola alexandrini</i>	<i>Mola mola</i>
%N	0.102 (0.261)	0.010 (0.020)	0.013 (0.020)
%W	0.145 (0.019)	0.000 (0.000)	0.001 (0.001)

Table 4.4. Diet overlap calculated by stomach content analysis (SCA in %N and %W) and stable isotope analysis (SIA) of three sympatric species: *Mola mola*, *Mola alexandrini*, and *Masturus lanceolatus*. The values outside and inside the parentheses represent the full body size range (unrestricted data) and size-restricted data, respectively.

Diet overlap	SCA in %N	SCA in %W	SIA
<i>Mola mola</i> & <i>Mola alexandrini</i>	98.2 (97.9)	99.8 (99.7)	71 (71)
<i>Mola mola</i> & <i>Masturus lanceolatus</i>	7.7 (1.0)	3.3 (0.2)	38 (30)
<i>Mola alexandrini</i> & <i>Masturus lanceolatus</i>	6.2 (0.8)	3.2 (0.0)	38 (36)

Table S4.1. Sample size, body size range, and average size in both total length (outside the parentheses) and standard length (inside the parentheses) of three sympatric species – *Mola mola*, *Mola alexandrini*, and *Masturus lanceolatus* – for both the full body size range (unrestricted data) and for size-restricted data, and for both the stomach content analysis (SCA) and the stable isotope analysis (SIA).

	<i>Masturus lanceolatus</i>			<i>Mola mola</i>			<i>Mola alexandrini</i>		
SCA	n	Size range (cm)	Size average (cm)	n	Size range (cm)	Size average (cm)	n	Size range (cm)	Size average (cm)
Full size range data	85	67-193	113 ± 27	34	138-279	194 ± 27	40	79-322	189 ± 39
		(42-151)	(91 ± 21)		(106-249)	(161 ± 27)		(63-301)	(161 ± 40)
Size-restricted data	11	134-193	164 ± 18	17	155-197	177 ± 13	19	157-203	173 ± 11
		(120-151)	(133 ± 9)		(134-158)	(145 ± 7)		(124-159)	(142 ± 9)
SIA									
Full size range data	176	67-235	125 ± 31	28	80-230	178 ± 33	60	68-257	180 ± 32
		(42-220)	(101 ± 27)		(68-209)	(145 ± 28)		(60-235)	(151 ± 31)
Size-restricted data	41	134-190	165 ± 14	18	149-200	181 ± 14	33	148-192	173 ± 13
		(120-160)	(133 ± 11)		(120-160)	(144 ± 9)		(124-159)	(141 ± 11)

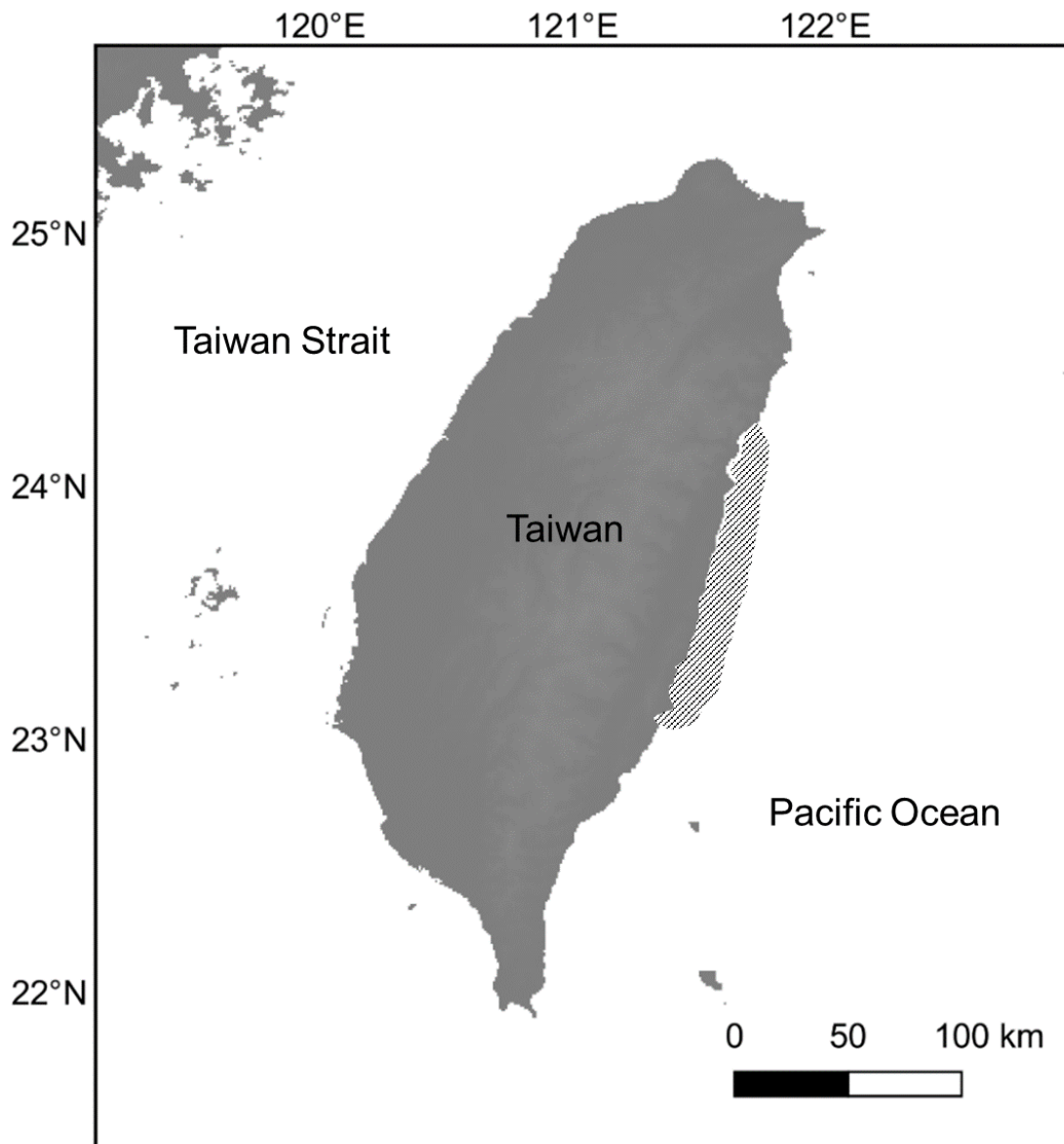


Fig. 4.1. Map of the fishing grounds (cross hatched area) for set-net and longline fishing operations in eastern Taiwan for three sympatric species: *Mola mola*, *Mola alexandrini*, and *Masturus lanceolatus*.

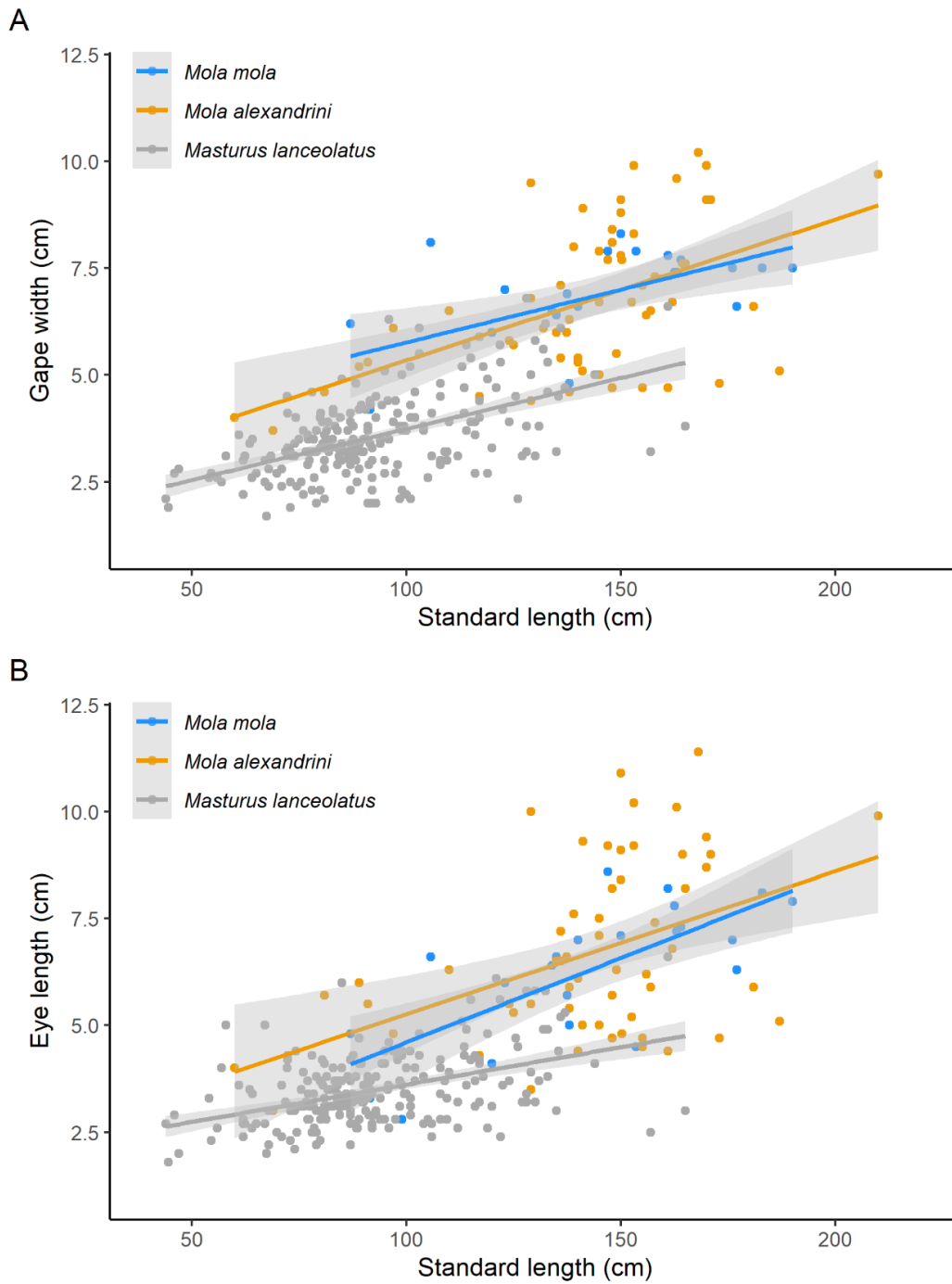


Fig. 4.2. Linear relationships between gape width and standard body length (A), and eye length and body length (B) of three sympatric species: *Mola mola*, *Mola alexandrini*, and *Masturus lanceolatus*. Each data point indicates an individual fish. Solid line is the regression line and the gray area indicates the 95% confidence interval.

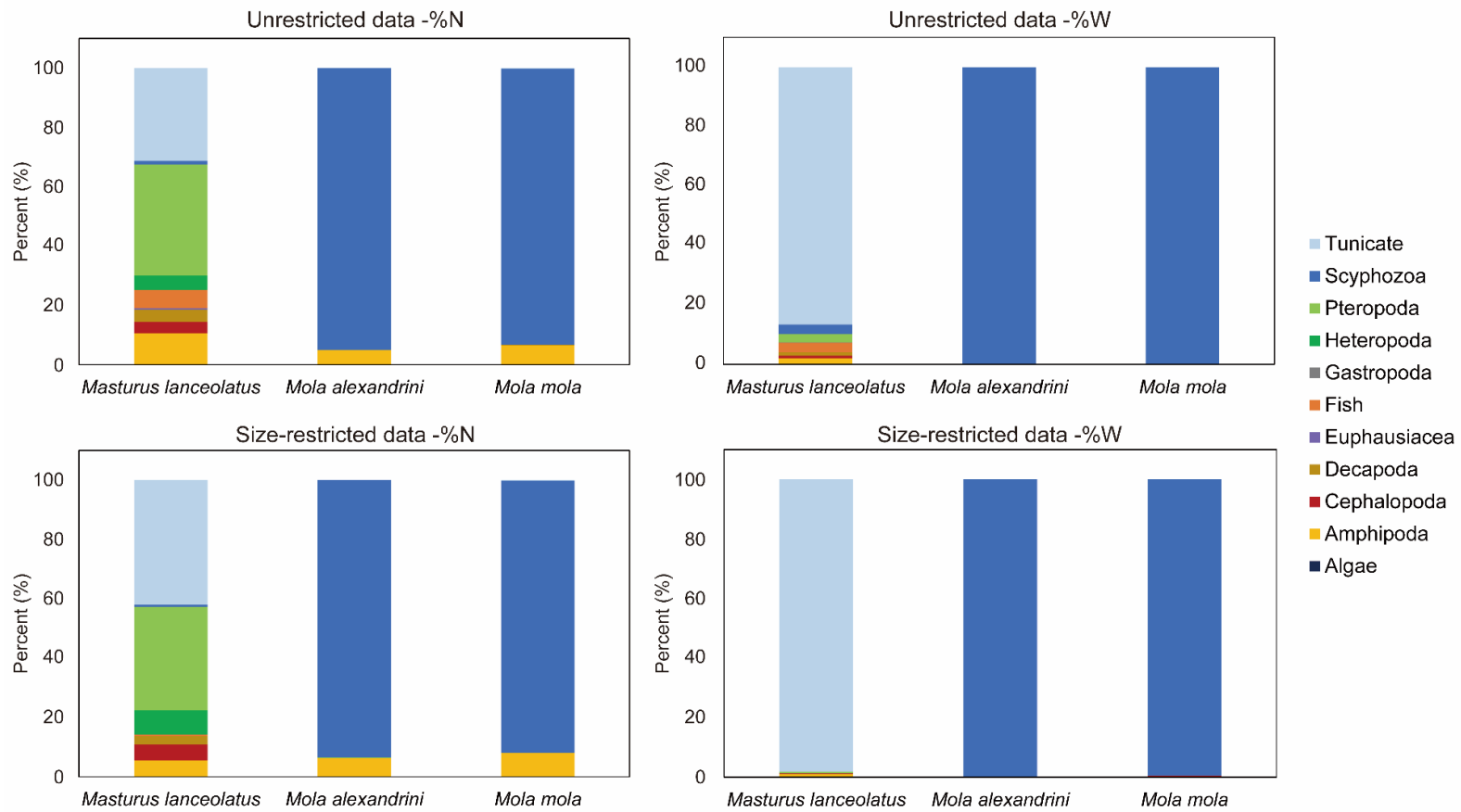


Fig. 4.3. Numeric (%N) and gravimetric (%W) diet compositions of three sympatric species – *Mola mola*, *Mola alexandrini*, and *Masturus lanceolatus* – for all sampled fishes (unrestricted data) and for size-restricted data.

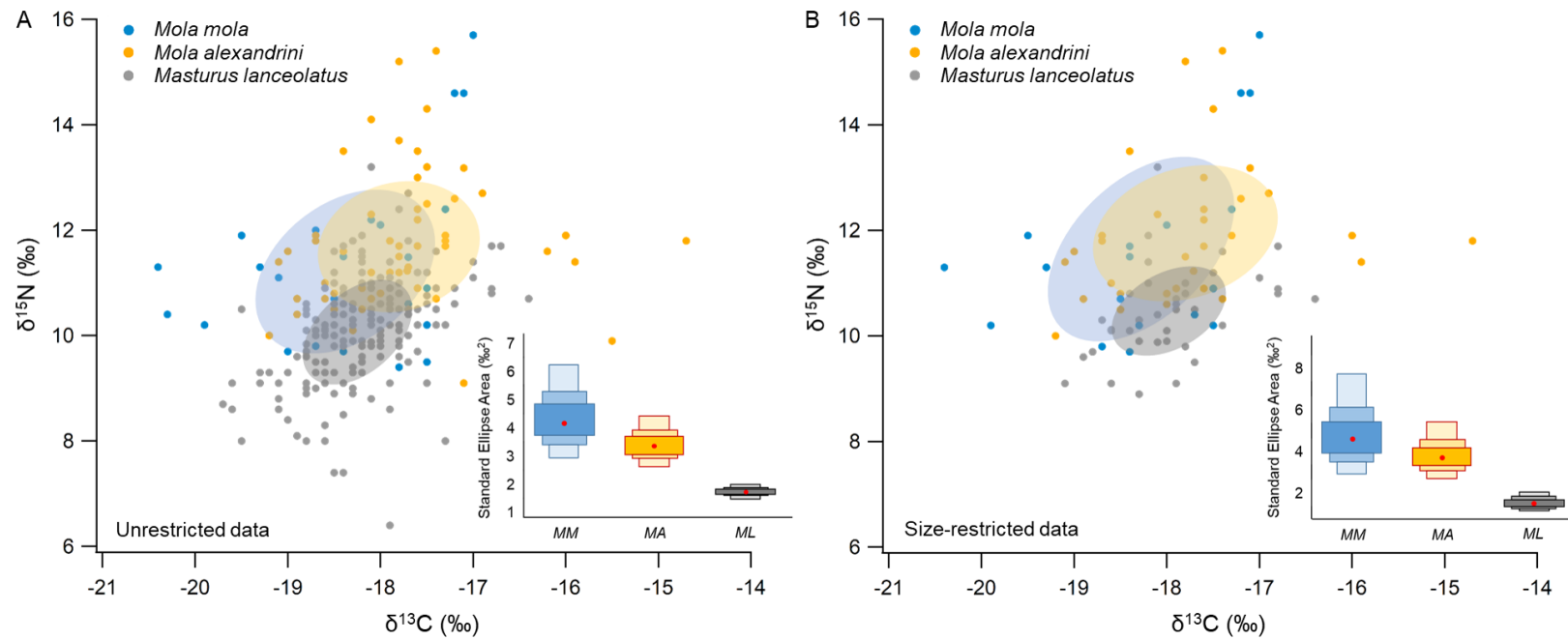


Fig. 4.4. Biplot of $\delta^{13}\text{C}$ and $\delta^{15}\text{N}$ values from three sympatric species – *Mola mola*, *Mola alexandrini*, and *Masturus lanceolatus* – for all sampled fishes (unrestricted data, A) and size-restricted data (B). Each data point indicates an individual fish. The color areas represent the isotopic diet breadths for the three sympatric species. Small plots represent isotopic diet breadth (Bayesian standard ellipse areas, SEAb) of the three sympatric species: *Mola mola* (MM), *Mola alexandrini* (MA), and *Masturus lanceolatus* (ML). (red dot: mean isotopic areas; color box: 50% credible intervals, median-light color box: 75% credible intervals; dark color box: 95% credible intervals).

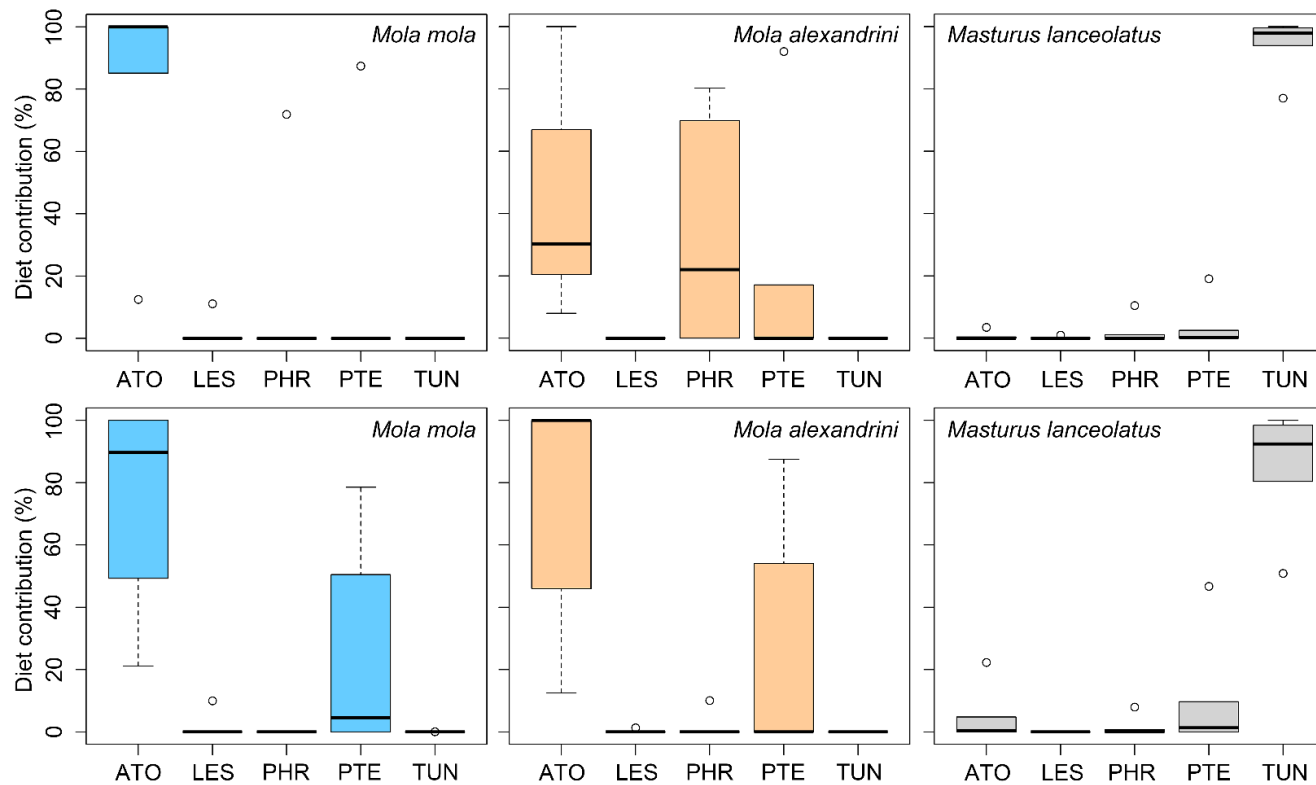


Fig. 4.5. Estimated contribution of common prey species to the diets of three sympatric species – *Mola mola*, *Mola alexandrini*, and *Masturus lanceolatus* – for all sampled fishes (unrestricted data, upper plots) and size-restricted data (lower plots), based on Bayesian isotope mixing models. Informative priors were based on diet compositions (by %W) of each species. Boxplots represent the 25th, median, and 75th quartiles of data; whiskers represent $1.5\times$ the interquartile range; and open circles represent outliers. ATO = scyphozoan *Atolla* spp., LES = amphipod *Lestrigonus* spp., PHR = amphipod *Phronima* spp., PTE = pteropods, TUN = tunicate.

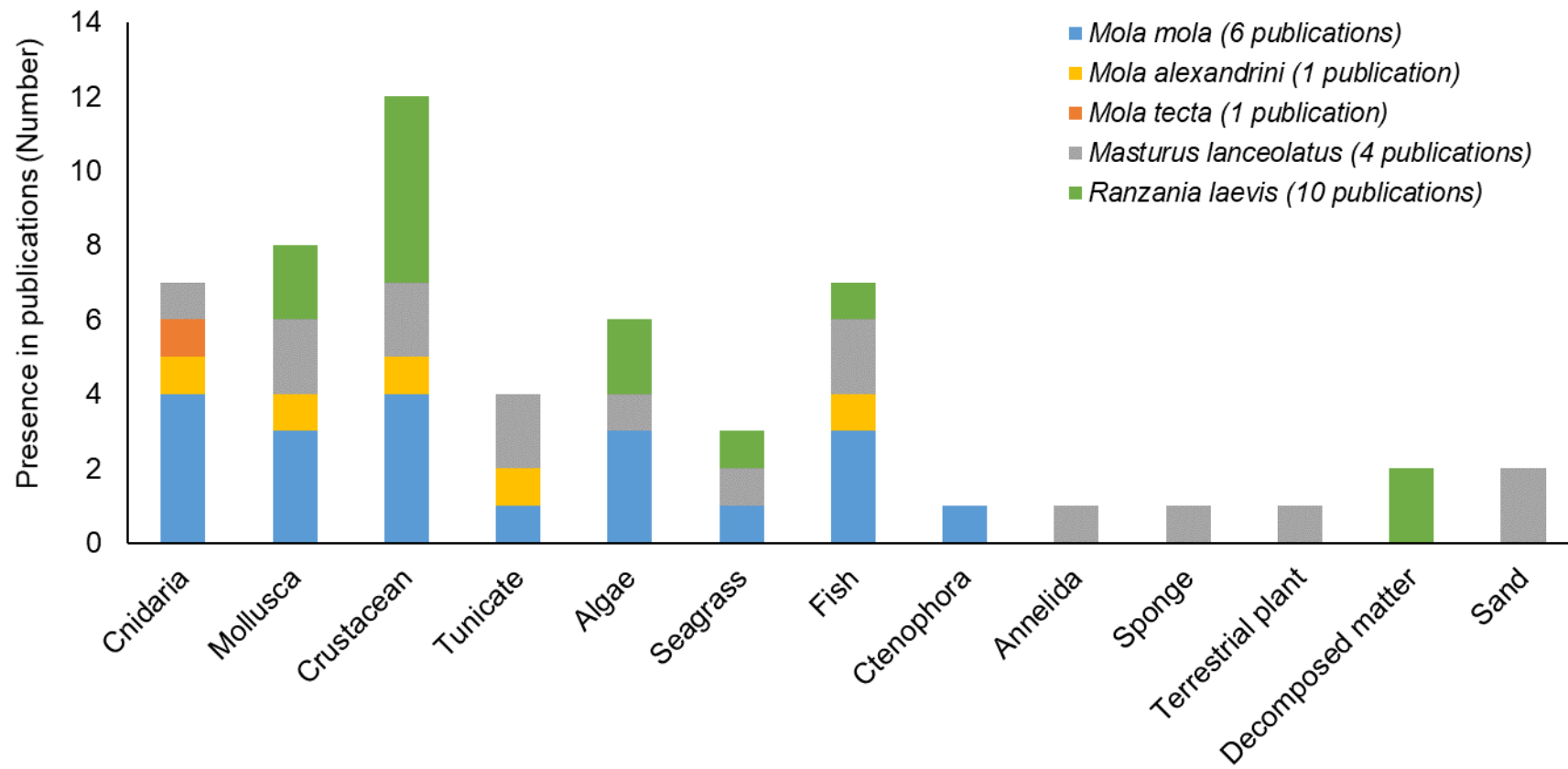


Fig. S4.1. The number of studies that report different prey types in diet composition of molids.

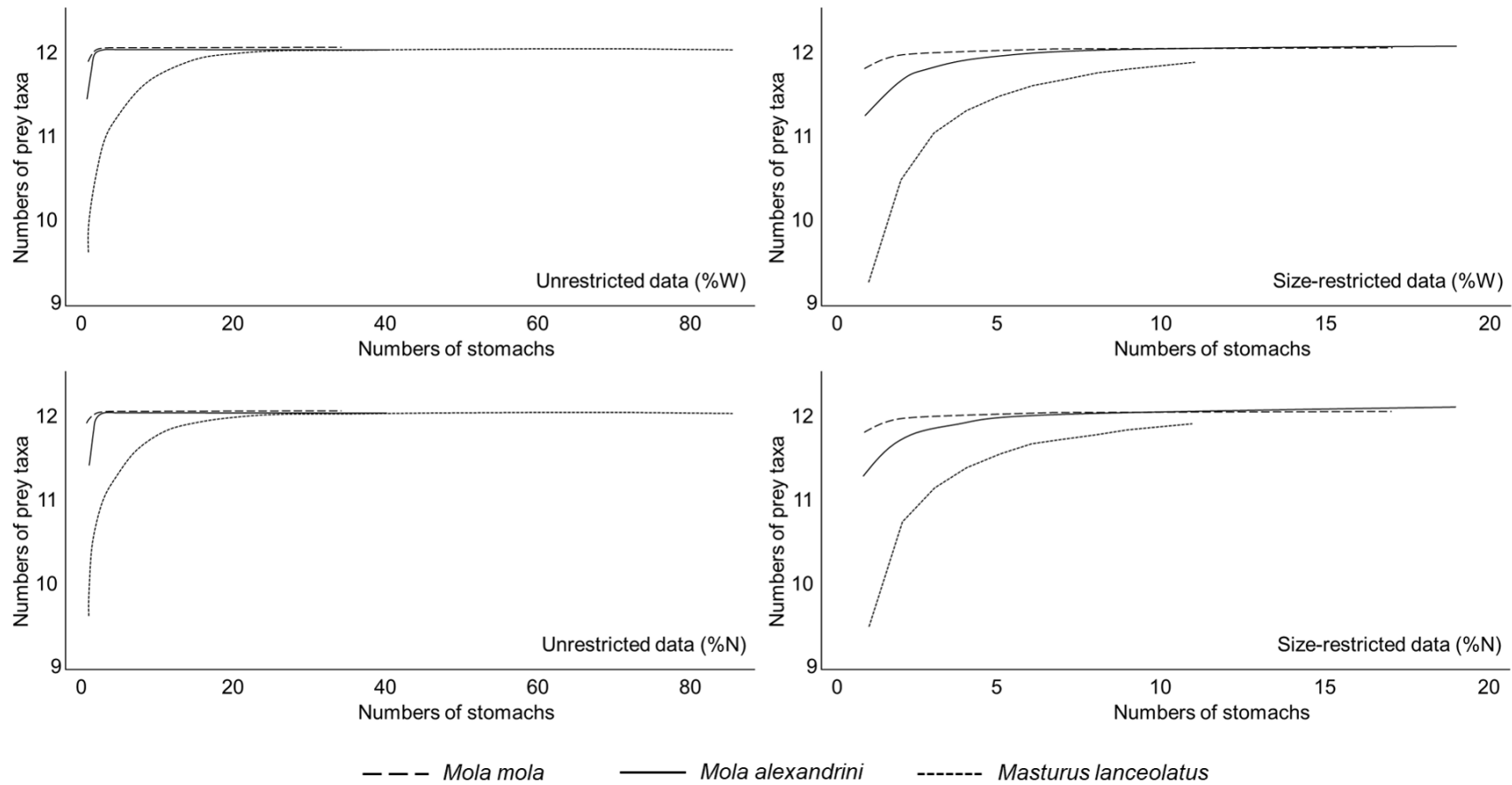


Fig. S4.2. Cumulative prey curves (%N and %W) of three sympatric species – *Mola mola*, *Mola alexandrini*, and *Masturus lanceolatus* – for all sampled fish (unrestricted data) and size-restricted data.

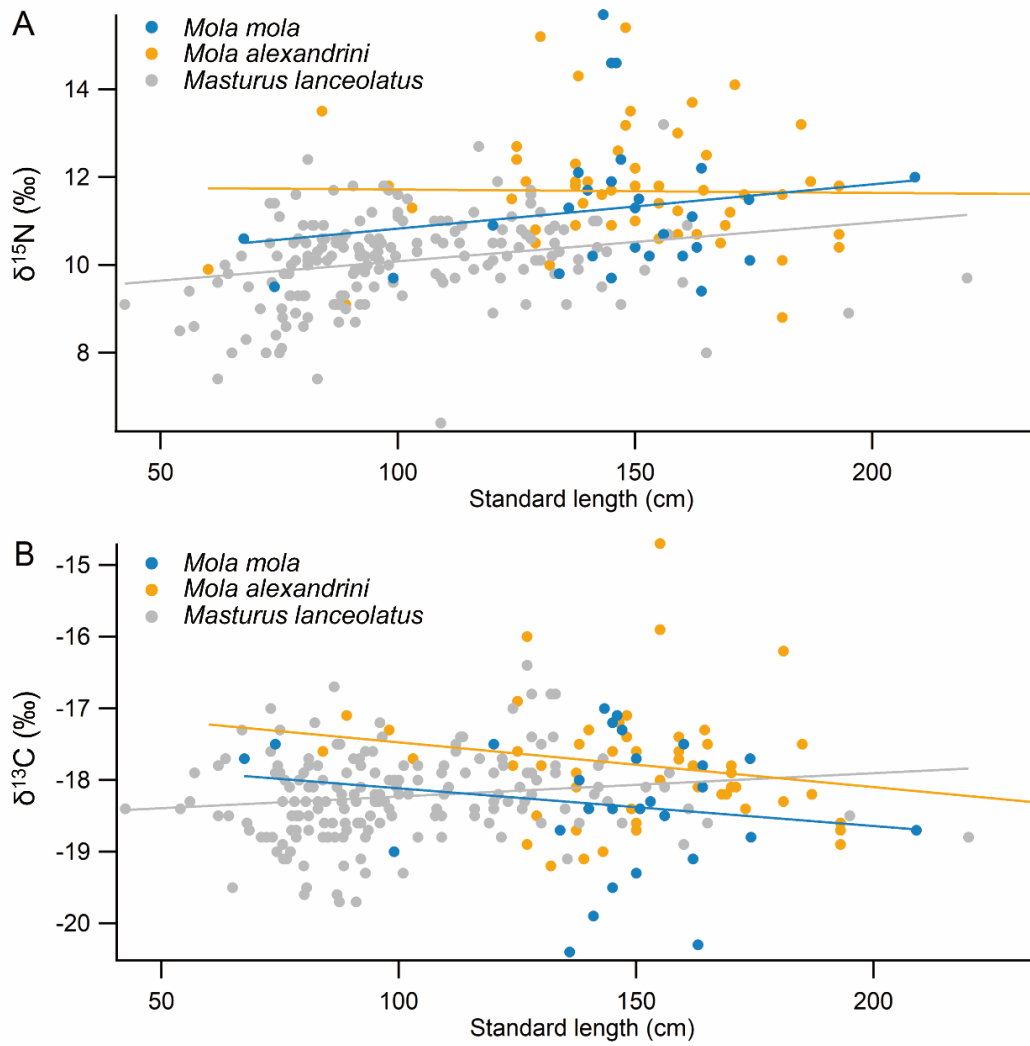


Fig. S4.3. Linear relationships between standard body length and $\delta^{15}\text{N}$ (A), and body length and $\delta^{13}\text{C}$ (B) of three sympatric species – *Mola mola*, *Mola alexandrini*, and *Masturus lanceolatus* – for all sampled fish (unrestricted data). Each data point indicates an individual fish. Solid lines are the regression lines.

CHAPTER 5 – Ontogenetic and seasonal shifts in diets of sharptail sunfish

Masturus lanceolatus in waters off Taiwan

Chang CT, Drazen JC, Chiang WC, Madigan DJ, Carlisle AB, Wallsgrove NJ, Hsu HH, Ho YH, Popp BN (2023) Marine Ecology Progress Series 715: 113-127.

5.1 Abstract

Sharptail sunfish *Masturus lanceolatus* share a circumglobal distribution with ocean sunfish *Mola mola* and are typically regarded as gelatinous plankton feeders. Both species are frequently captured as bycatch in the same areas, but sharptail sunfish are often targeted and heavily harvested in certain regions. However, the diet of sharptail sunfish remains poorly described. We examined the foraging habits and trophic dynamics of sharptail sunfish from waters off eastern Taiwan using stomach content analysis (SCA; n = 162), bulk tissue stable isotope analysis (SIA; n = 213), and compound-specific isotope analysis of amino acids (CSIA-AA; n = 10). Results demonstrated that sharptail sunfish mainly consumed tunicates, with lower dietary proportions of diverse prey from epi- and mesopelagic, coastal, and benthic habitats. The diet of sharptail sunfish changed significantly with size; small mola (<80 cm) had lower $\delta^{15}\text{N}$ and $\delta^{13}\text{C}$ values and fed on more pteropods and Salpidae, while large mola (>80 cm) fed on more Pyrosoma spp., cephalopods, and benthic organisms living on sandy substrates, with larger individuals having correspondingly higher isotope values and trophic positions. Diet compositions and $\delta^{13}\text{C}$ values also showed seasonal variations across body size, suggesting that sharptail sunfish might undergo seasonal migrations with changing availability of food resources. The results provide insights into the trophic dynamics of sharptail sunfish and suggest that their foraging behavior varies across life-history stages and seasons.

5.2 Introduction

Members of the family Molidae (genera *Mola*, *Masturus*, and *Ranzania*) are distributed worldwide from tropical to temperate regions. The family includes the world's heaviest bony fish, the bumphead sunfish *Mola alexandrini*, which weighs up to 2.7 t (Gomes-Pereira et al. 2023). The Molidae play an important ecological role as predators in the gelatinous food web (Grémillet et al. 2017), and most *Mola* species were regarded as obligate gelativores that typically feed on scyphozoan jellyfish (Fraser-Brunner 1951, Hooper et al. 1973). However, recent studies using stomach content analysis (SCA) and bulk tissue stable isotope analysis (SIA) have revealed a wider range of prey items consumed by ocean sunfish *Mola mola*, including pelagic and neritic prey such as crab megalops and amphipods (Syväranta et al. 2012, Harrod et al. 2013, Nakamura & Sato 2014). Using DNA metabarcoding, SIA, and compound-specific isotope analysis of amino acids (CSIA-AA), researchers found evidence of an ontogenetic shift in the diets of ocean sunfish. Small-sized individuals were found to have a mixed diet of both benthic and pelagic prey, while larger individuals occupied a higher trophic position and fed primarily on pelagic-derived prey (Sousa et al. 2016, Phillips et al. 2020). These observations might reflect ontogenetic dietary changes or could be related to seasonal migration patterns (Dewar et al. 2010, Chang et al. 2021) and variability in foraging behaviors across region and/or life stage. For instance, small ocean sunfish off Japan stayed near the shallow seabed, whereas larger individuals moved back and forth between surface and deeper waters (Nakamura & Sato 2014).

Sharptail sunfish *Masturus lanceolatus* share a circumglobal distribution with ocean sunfish (Caldera et al. 2020). They have similar physical features as well as behavioral and movement patterns, including migration patterns and depth distributions (Seitz et al. 2002, Dewar et al. 2010, Chang et al. 2020). Sharptail sunfish are captured as bycatch globally (Nyegaard et al. 2018, Arostegui et al. 2020) and are targeted for

human consumption regionally (e.g. Taiwan, average annual catch: 436 t in 2006–2019; Fisheries Agency 2020). While the International Union for Conservation of Nature (IUCN) assessed the conservation status of the sharptail sunfish as ‘Least Concern’ in 2015, this was largely based upon lack of available data (Leis et al. 2015). Broadly, limited data are available on sharptail sunfish, and their diets are poorly described. Bakenhaster & Knight-Gray (2016) noted that remains of fishes and some invertebrates were found in the stomach contents of 2 sharptail sunfish from waters off Florida (USA). In addition, sand and leaves were discovered in the stomach of 1 stranded sharptail sunfish in Japan (Sawai et al. 2019), although this likely reflects ingestion of these items during stranding. Overall, it is difficult to characterize sharptail sunfish diet due to lack of data and the highly digested nature of their gut contents. As such, more robust diet studies are required to understand the trophic ecology of this species and how it partitions the environment with the closely related ocean sunfish.

Coupling SCA and SIA provides insight into the feeding habits of sharptail sunfish across ontogeny and habitats. SCA provides a detailed snapshot of dietary information that reflects recent foraging (i.e. hours to days/weeks; Cortés 1997), whereas SIA can provide information on the sources of primary production that support their diet and their trophic relationships integrated over longer time scales. Stable isotope ratios ($^{13}\text{C}/^{12}\text{C}$ and $^{15}\text{N}/^{14}\text{N}$; $\delta^{13}\text{C}$ and $\delta^{15}\text{N}$) in predator tissues reflect their diets over the previous weeks, months, or >1 yr, depending on the tissue examined and its isotopic incorporation rate (Madigan et al. 2021). In particular, $\delta^{15}\text{N}$ values increase significantly (2~4‰) with each trophic level (Vander Zanden & Rasmussen 2001, Post 2002), and as a result are frequently used to examine trophic dynamics and trophic position of animals. However, it can be challenging to distinguish the relative importance of variation in baseline $\delta^{15}\text{N}$ values of the food web from increases in $\delta^{15}\text{N}$ associated with feeding at higher trophic levels. CSIA-AA is a more recently developed

tool that overcomes these limitations of bulk SIA. The $\delta^{15}\text{N}$ values in ‘source’ amino acids (e.g. lysine, phenylalanine, serine, tyrosine, and sometimes glycine) change little with increasing trophic level and reflect the baseline of food webs, whereas other amino acids, in particular the ‘trophic’ amino acids (e.g. alanine, glutamic acid, leucine, proline, valine), which exhibit high isotope fractionation, reflect an organism’s trophic level (McClelland & Montoya 2002, Popp et al. 2007, Chikaraishi et al. 2009). Therefore, $\delta^{15}\text{N}$ values of amino acids retain information about isotopic baselines and trophic isotope fractionation. Differences in $\delta^{15}\text{N}$ values of source and trophic amino acids can thus be used to determine both the $\delta^{15}\text{N}$ values at the base of the food web and trophic positions of animals (McClelland & Montoya 2002, Bradley et al. 2015).

In this study, we used SCA, bulk SIA, and CSIA-AA to reveal the trophic ecology of sharptail sunfish. We aimed to explore (1) whether sharptail sunfish feed mainly on Scyphozoa, other gelatinous taxa, or on more diverse prey and (2) potential ontogenetic or seasonal shifts in sharptail sunfish diet. The results will provide new insights into the trophic ecology of sharptail sunfish in oceanic food webs.

5.3 Materials and methods

5.3.1 Sample collection

We collected tissue and stomach samples from sharptail sunfish at fish markets in eastern Taiwan from 2017 to 2021. All sharptail sunfish were caught off eastern Taiwan by set-net and longline fisheries (Fig. 5.1), preserved on ice, and brought back to local fish markets for sale on the same day. Total length (TL, from the tip of the snout to the end of the caudal fin) and standard length (SL, from the tip of the snout to the line in front of the caudal fin) were measured. We used SL in analyses here, as in some cases, caudal fins had been removed and discarded before landing. Stomach contents ($n = 162$) and white muscle samples ($n = 213$, collected from the abdomen) were collected, and

muscle samples were frozen at -80°C . Stomach contents were processed immediately due to the rapid digestion of gelatinous prey (Arai et al. 2003).

Prey items for SIA were collected to match, as closely as possible, prey found in stomach contents of sharptail sunfish. Scyphozoa (*Atolla* spp.) ($n = 8$) were collected with hand-nets from a boat during the summer in the waters off eastern Taiwan in 2019, and the whole body was processed immediately. Cephalopods ($n = 4$) were collected from fish markets in eastern Taiwan from the same fishing regions as those for sharptail sunfish. Mantle tissues of cephalopods were taken and frozen at -80°C until processing. Undigested tunicates (*Pyrosoma* spp. and Salpidae, $n = 16$), amphipods *Phronima* spp. ($n = 7$), and pteropods ($n = 10$) were collected directly from stomach contents of sharptail sunfish and preserved at -80°C for processing.

5.3.2 Stomach content analysis

In the laboratory, prey items were identified to the lowest possible taxon, and their abundance and weight were measured. Cephalopods were identified from beaks. After measurement, the prey items were preserved in 95% ethanol. All prey items were categorized into 9 functional groups based on their habitat and taxon (Table S5.1 in the Supplement at www.int-res.com/articles/suppl/m715p113_supp.pdf). Unidentified items, sand, and plastics were not included in these functional groups and the analyses, and a stomach without any prey was counted as an empty stomach.

5.3.3 Bulk tissue stable isotope analysis

Sharptail sunfish muscle tissue and prey items were rinsed with distilled water and dried for 48 h at 60°C and then ground into a homogeneous powder. Approximately 0.4–0.8 mg (depending on the species) of powder were packed into ultra-clean tin capsules. Pteropods and *Phronima* spp. were weighed into silver cups and acidified with 10% HCl for removing the carbonate, after which the samples were dried for 24 h at 60°C . $\delta^{13}\text{C}$ and $\delta^{15}\text{N}$ values were determined using an elemental analyzer (Costech

ECS 4010 Elemental Combustion System using a Zero Blank Autosampler) and mass spectrometer (Thermo-Delta V Advantage). The bulk isotope values were expressed in standard ‰ notation relative to Vienna Pee Dee belemnite (V-PDB) for carbon and atmospheric N₂ for nitrogen. The analytical error derived from multiple analyses of reference materials for both $\delta^{13}\text{C}$ and $\delta^{15}\text{N}$ was <0.2‰. Because lipids have lower $\delta^{13}\text{C}$ values relative to other animal tissues, and the variability in tissue lipid content can affect $\delta^{13}\text{C}$ values (Focken & Becker 1998), the $\delta^{13}\text{C}$ values of sharptail sunfish muscle (C:N > 3.5) and invertebrate prey items (C:N > 3.8) were normalized using lipid normalization algorithms for muscle from Atlantic bluefin tuna *Thunnus thynnus* (Logan et al. 2008) and from zooplankton (Syväranta & Rautio 2010), respectively.

5.3.4 Nitrogen isotope analysis of individual amino acids

Ten sharptail sunfish across size classes were selected for CSIA-AA. The preparation for CSIA-AA followed the methods of Hannides et al. (2009). Approximately 10–15 mg of homogenized white muscle tissue were hydrolyzed, then esterification and trifluoroacetylation were undertaken. The $\delta^{15}\text{N}$ values of individual amino acids were analyzed using a Delta V Plus mass spectrometer interfaced to a Trace GC gas chromatograph. All samples were analyzed in triplicate, and measured $\delta^{15}\text{N}$ values were corrected relative to the known $\delta^{15}\text{N}$ values of a norleucine internal reference. Standard deviation for triplicate injections of each sample averaged 0.55‰ ($\pm 0.3\%$) and ranged from 0.03 to 1.95‰. Three trophic amino acids (alanine, leucine, glutamic acid) and 3 source amino acids (glycine, phenylalanine, lysine) were selected to calculate a weighted average for trophic position (TP) estimation based on Bradley et al. (2015).

5.3.5 Data analysis

To classify sharptail sunfish into ecologically relevant size groupings, we used LOESS smoothing and a piecewise linear regression model in R version 4.0.4

(‘fANCOVA’ and ‘segmented’ packages) (Cleveland et al. 1992, Muggeo 2008) to find breakpoints in the relationship between isotopic data and body size of sharptail sunfish. The discontinuous values in $\delta^{13}\text{C}$ and $\delta^{15}\text{N}$ implied a change in diet of sharptail sunfish across size, with breakpoints found at approximately 80 and 120 cm for both $\delta^{13}\text{C}$ and $\delta^{15}\text{N}$ values (Fig. S5.1). Thus, sharptail sunfish were categorized into 3 size classes: Class I (<80 cm SL), Class II (80–120 cm SL), and Class III (>120 cm SL). Subsequent diet compositions and isotopic values of sharptail sunfish were analyzed by these 3 size classes. The analysis did not include the interannual variation in diets of sharptail with the assumption of similar prey availability across years.

For SCA, 5 diet indices were calculated: frequency of occurrence (%FO) as the proportion of predator stomachs containing a prey item; gravimetric importance (%W) as the proportion of the weight of a prey item in the total weight of stomach contents; numerical abundance (%N) as the proportion of the number of a prey item in the total number of all prey; the index of relative importance (IRI) as an index of the combination of these 3 metrics (Pianka 1973); and %IRI as the proportion of IRI of a prey item in the sum of all IRI values. The indices for prey composition and proportion for functional prey groups among each size class and seasons of sharptail sunfish were calculated. Diets (%N and %W) among size classes and seasons were compared using a percent similarity index (PSI, Hurlbert 1978). Cumulative prey curves were used to determine whether there was a sufficient number of stomach samples across size and seasons to describe the diet of sharptail sunfish. The diet compositions (%N and %W) of sharptail sunfish across all size classes and seasons were compared using a 2-way nested analysis of similarities (ANOSIM, 9999 permutations) with pairwise tests, all based upon a Bray-Curtis similarity matrix. This analysis was done using PRIMER software (version 6, Plymouth Marine Laboratory; Clarke 1993).

For bulk SIA, nonlinear regression was used to test the relationships between $\delta^{13}\text{C}$

and $\delta^{15}\text{N}$ values and SL for sharptail sunfish. Differences in $\delta^{13}\text{C}$ and $\delta^{15}\text{N}$ values between body size and seasons were tested using ANOVA (mixed design; Underwood 1997), with size class and season as fixed effects, and Tukey's post hoc test in R version 4.0.4. The differences in $\delta^{13}\text{C}$ and $\delta^{15}\text{N}$ values among prey categories and sharptail sunfish were tested using 1-way ANOVA with Tukey's post hoc tests in R version 4.0.4. TP_{bulk} using bulk $\delta^{15}\text{N}$ values was estimated using the equation:

$$TP_{\text{bulk}} = TP_{\text{base}} + \frac{\delta^{15}N_{\text{consumer}} - \delta^{15}N_{\text{baseline}}}{TDF} \quad (1)$$

where $\delta^{15}\text{N}_{\text{consumer}}$ represents the $\delta^{15}\text{N}$ value of sharptail sunfish and $\delta^{15}\text{N}_{\text{baseline}}$ represents the baseline species $\delta^{15}\text{N}$ values. Here, we used $\delta^{15}\text{N}$ values (5.1‰) of zooplankton from the waters off Taiwan as $\delta^{15}\text{N}_{\text{baseline}}$ and a trophic level of 2 ($TP = 2$) for TP_{base} (Weng et al. 2015). The trophic discrimination factor (TDF) for ocean sunfish muscle (3‰) was used (Phillips et al. 2020). Differences in TP across size classes were tested using 1-way ANOVA in R version 4.0.4.

Due to the high variability in bulk $\delta^{15}\text{N}$ values of zooplankton as the base of food webs, CSIA-AA was used to estimate a more accurate TP for sharptail sunfish. TP_{AA} using $\delta^{15}\text{N}$ values of amino acids was estimated using the equation:

$$TP_{\text{AA}} = 1 + \frac{\delta^{15}N_{\text{Trp}} - \delta^{15}N_{\text{Src}} - \beta}{TDF_{\text{AA}}} \quad (2)$$

where $\delta^{15}\text{N}_{\text{Trp}}$ and $\delta^{15}\text{N}_{\text{Src}}$ are the weighted averages of selected trophic and source amino acids. β (3.6‰; Bradley et al. 2015) represents the difference between the $\delta^{15}\text{N}$ values of trophic and source amino acids in primary producers. TDF_{AA} (5.7‰; Bradley et al. 2015) represents the TDF for the $\delta^{15}\text{N}$ values of trophic (alanine, leucine, glutamic acid) and source (glycine, phenylalanine, lysine) amino acids for each trophic level.

The Bayesian mixing model in the 'MixSIAR' package (Stock & Semmens 2013) was applied in R version 3.6.0 to estimate relative contributions of prey taxa to each

sharptail sunfish size class. The most common prey items found in the stomach contents of sharptail sunfish were used, including *Phronima* spp. (n = 7), tunicates (*Pyrosoma* spp. and Salpidae, n = 16), and pteropods (n = 10). Scyphozoa (*Atolla* spp.; n = 8) were selected because Scyphozoa are regarded as the major food source for other mollusks. *Pyrosoma* spp. and Salpidae had similar isotopic values and ecological niche. They were weighted equally in calculated tunicate values. Cephalopods (n = 4) were used because the proportion of cephalopods in the gut contents of sharptail sunfish increased with size, reflecting increased contribution to the diets of large sharptail sunfish. Gravimetric importance (%W) represents the total mass or energy transferred from prey to sharptail sunfish. We constructed the informative priors based on the diet compositions (by %W) of sharptail sunfish in this study. The informative priors were scaled to have a total weight equal to the number of sources (Stock et al. 2018). We used bulk tissue TDF values for ocean sunfish, where $\Delta^{13}\text{C} = 2 \pm 1.3\text{‰}$ and $\Delta^{15}\text{N} = 3 \pm 1.2\text{‰}$ (Phillips et al. 2020). For model inputs, Markov chain Monte Carlo was set to normal length. Both Gelman-Rubin (Gelman et al. 2013) and Geweke diagnostics (Geweke 1991) were used to test for model convergence.

Stable Isotope Bayesian Ellipses in R version 4.0.4 (SIBER; Jackson et al. 2011) was used to calculate the isotopic niche width among 3 size classes. Specifically, we estimated trophic niche metrics including a convex hull (Layman et al. 2007), a corrected standard ellipse area (SEAc), and a Bayesian standard ellipse area (SEAb) (Jackson et al. 2011, 2012).

5.4 Results

5.4.1 Diet composition across size classes

A total of 162 stomachs of sharptail sunfish were collected, of which 57 were empty (35%). A wide variety of prey taxa were identified in stomachs, including gelatinous organisms, mollusks, crustaceans, and fishes (Table 5.1). One of the stomach

samples was excluded from analysis because it contained a relatively large abundance of flying fish eggs compared to other stomachs, which led to a disproportionate influence of this single fish on overall diet estimates. Tunicates (both salps and pyrosomes), *Phronima* spp. amphipods, and pteropods were the most frequently consumed prey. Pteropods (35%N) and tunicates (29%N) were the most numerically abundant. Based on weight, all predators fed predominantly on epi- and mesopelagic tunicates (Pyrosomatidae: 48%W; Salpidae: 33%W) that made up a total of 80% in weight and 75% in %IRI of the prey.

Cumulative prey curves indicated that sample size for sharptail sunfish <80 cm and 80–120 cm reached an asymptotic relationship (Fig. S5.2A). Thus, the sample sizes were sufficient to describe the diets of sharptail sunfish <120 cm. The stomach samples of sharptail sunfish >120 cm were probably not adequate to fully describe the diets. Sharptail sunfish diet compositions by %N (ANOSIM: $R = 0.78$, $p = 0.001$) and %W ($R = 0.09$, $p = 0.017$) showed significant differences among size classes (Table 5.2A). The diets were more similar across all size classes by %N (higher PSI values) than %W (Table 5.2A). Sharptail sunfish <80 cm fed mainly on prey from offshore, epi- and mesopelagic habitats, and sharptail sunfish >80 cm fed on prey from coastal, benthic, and epi- and mesopelagic habitats (Fig. 5.2). Tunicates were the most important prey in diets of sharptail sunfish across size groups. Within this prey category (epi-/mesopelagic tunicates), small sharptail sunfish (<80 cm) fed mainly on Salpidae (57 %W) compared to larger individuals (80–120 cm: 40 %W; >120 cm: 5 %W), which primarily fed on Pyrosoma (80–120 cm: 38 %W; >120 cm: 79 %W) (Table S5.2). The weight proportions of pteropods and amphipods *Phronima* spp. (epi/mesopelagic crustaceans) in diets decreased with increasing sharptail sunfish size. The occurrences and abundances of crustacean juveniles were mainly composed of crab zoea in the guts of sharptail sunfish >120 cm and were mainly composed of phyllosoma in the guts of

mola <80 cm. Sharptail sunfish 80–120 cm fed more on fish (Scombridae and Lutjanidae) than those <80 cm and >120 cm. In addition, sharptail sunfish >80 cm individuals foraged more on cephalopods than those <80 cm, although they were still only a minor component of the diet. A large amount of sand was found in stomachs of sharptail sunfish >120 cm (20% FO, Table S5.2).

5.4.2 Seasonal trend in diet composition across size classes

Cumulative prey curves indicated that sample size for sharptail sunfish in autumn, summer, and spring were sufficient to describe their diet (Fig. S5.2B). Overall, the diets of all sharptail sunfish showed seasonal variations by %N ($R = 0.17$, $p = 0.002$) and %W ($R = 0.18$, $p = 0.001$) (Table 5.2B). Summer diets were similar to autumn diets with high PSI values (%W: 72.5; %N: 63.3), and sharptail sunfish consumed more crustacean juveniles and cephalopods than during other seasons (Fig. S5.3). Most of the flying fish eggs were consumed in summer and autumn, including the one stomach sample with a large abundance of eggs. Autumn diets differed from spring diets in terms of %W (ANOSIM pairwise-test: $R = 0.235$, $p = 0.007$) and %N ($R = 0.328$, $p = 0.002$), and sand was found in the stomachs of sharptail sunfish in summer and autumn.

Seasonal variation in sharptail sunfish diets was examined by size group. The diet composition of sharptail sunfish <120 cm displayed seasonal variation (%N, 80 cm: $R = 0.32$, $p = 0.005$, 120 cm: $R = 0.16$, $p = 0.013$; %W, 80 cm: $R = 0.2$, $p = 0.01$, 120 cm: $R = 0.15$, $p = 0.039$) whereas that of mola >120 cm did not (%N, $R = 0.17$, $p = 0.227$; %W, $R = 0.1$, $p = 0.281$) (Table 5.2C-E). In sharptail sunfish <80 cm, most diets were distinct among seasons (%N, $R = 0.316$, $p < 0.001$; %W, $R = 0.198$, $p = 0.01$) (Table 5.2C). The proportion of pteropods was lower in summer diets than in other seasons in terms of %N (Fig. 5.3). Few crustacean juveniles (predominately phyllosoma) were found in summer and autumn diets, and a high mass of *Phronima* spp. was found in winter diets. In diets of sharptail sunfish 80–120 cm, spring diets significantly differed

from autumn diets in terms of numerical index ($R = 0.162$, $p = 0.013$); these fish fed on numerous tunicates in spring and shifted to pteropods in summer, autumn, and winter. Numerous cephalopods and fish were also found during summer, autumn, and winter. The %W of Scyphozoa was higher in summer, autumn, and winter compared to spring.

5.4.3 Seasonal variation in bulk isotope values across size classes

Isotopic compositions of carbon and nitrogen in bulk tissues were positively related to body size of sharptail sunfish (nonlinear regression: $\delta^{13}\text{C}$: $R^2 = 0.07$, $p = 0.007$; $\delta^{15}\text{N}$: $R^2 = 0.14$, $p < 0.001$). The $\delta^{15}\text{N}$ values for sharptail sunfish >80 cm were significantly higher than those for mola <80 cm (ANOVA: $F_{2, 202} = 4.646$, $p = 0.011$), and values did not differ across seasons ($F_{3, 202} = 1.074$, $p = 0.361$) with no interaction between size and season ($F_{5, 202} = 0.75$, $p = 0.587$). $\delta^{13}\text{C}$ values significantly differed across size groups, increasing with body size ($F_{2, 202} = 4.164$, $p = 0.017$). $\delta^{13}\text{C}$ values also differed significantly across seasons ($F_{3, 202} = 5.777$, $p = 0.001$). $\delta^{13}\text{C}$ values in spring were the highest and those in autumn were the lowest across all size classes. Seasonal patterns of $\delta^{13}\text{C}$ values in sharptail sunfish evaluated by size groups showed significant seasonal variations in individuals <120 cm (<80 cm: $F_{3, 45} = 4.897$, $p = 0.005$; 80–120 cm: $F_{3, 114} = 3.001$, $p = 0.034$). In mola <80 cm, $\delta^{13}\text{C}$ values in spring were significantly higher than the values in autumn (post hoc test: $p = 0.004$), whereas in mola 80–120 cm, none of the pairwise tests between seasons showed significant differences.

5.4.4 $\delta^{15}\text{N}$ values of amino acids and TP estimates

Similar to observed patterns for bulk $\delta^{15}\text{N}$ values, mean $\delta^{15}\text{N}$ values of trophic and source amino acids in sharptail sunfish slightly increased with size, from 21.5 to 23.6‰, and from 3.2 to 4‰, respectively (Table 5.3). TP_{AA} across size classes of sharptail sunfish were consistent with TP_{bulk} estimates. Mola >120 cm had higher mean TP than size classes of 80–120 cm and <80 cm (Table 5.3). Mean TP_{bulk} showed significant

differences across size class ($F_{2, 210} = 11.601, p < 0.001$), whereas mean TP_{AA} did not ($F_{2,7} = 1.658, p = 0.26$). Mean $\delta^{15}N$ values of all prey items (except for cephalopods) were significantly lower than those of sharptail sunfish ($F_{5, 252} = 77.811, p < 0.001$; post hoc test: $p < 0.05$) (Fig. 5.4A). Across prey items, the lowest mean $\delta^{15}N$ value and TP_{bulk} were observed in *Phronima* spp., and the highest values and $\delta^{15}N$ were observed in cephalopods (Fig. 5.4B). The lowest mean $\delta^{13}C$ values were found in pteropods, and the highest $\delta^{13}C$ values were found in *Atolla* spp. (epi/mesopelagic Scyphozoa).

5.4.5 Isotopic niche width across size classes

Results of isotopic niche area across 3 size classes of sharptail sunfish, calculated using SEA_c and SEA_b , were similar (Fig. 5.4A). The trophic isotopic niche decreased gradually with increasing size (SEA_c : <80 cm: 1.85, 80–120 cm: 1.72, >120 cm: 1.56) (Fig. S5.4). The overlap in SEA_c among the 3 size classes was high, with overlap percentage estimates between <80 cm and 80–120 cm, 80–120 cm and >120 cm, and <80 cm and >120 cm of 78, 85, and 70%, respectively.

5.4.6 Mixing models

Mixing model results indicated that prey contributions varied across size classes of sharptail sunfish (Fig. 5.5). The most important prey items for all size classes were tunicates, with decreasing proportions (median) with increasing size (92, 82, and 75% for <80, 80–120 and >120 cm size classes, respectively). The relative proportion of cephalopods increased across mola size, from 0.4% in fish <80 cm to 10 and 17% in fish 80–120 and >120 cm, respectively. The contributions of *Atolla* spp., pteropods, and *Phronima* spp. to the diets of sharptail sunfish were low for all 3 size groups (Fig. 5.5).

5.5 Discussion

Sharptail sunfish from waters off Taiwan fed extensively on gelatinous organisms, similar to observations of diet in other molids. However, unlike other molids that

typically feed on scyphozoans, tunicates were the most important gelatinous prey in the diets of sharptail sunfish in this study. The TP estimated from $\delta^{15}\text{N}$ values in bulk tissues and amino acids slightly increased with the increase in size, suggesting a continuous ontogenetic shift in their diet.

5.5.1 Diets of sharptail sunfish

Sharptail sunfish principally fed on gelatinous prey, mainly salps and pyrosomes, which corroborates sparse prior observations and suggests that they are selective and targeted predators (Harbison & Janssen 1987, Bakenhaster & Knight-Gray 2016). This feeding strategy is similar to other mollids with described diets, such as the ocean sunfish (Pope et al. 2010). In our study, sharptail sunfish principally consumed tunicates, but also salps and pyrosomes, as demonstrated by SCA and SIA. Typically, due to high water content, gelatinous species have low energy density and are regarded as unfavorable foods in pelagic food webs (Larson 1986). However, some studies (Davenport & Balazs 1991, Davenport 1998, Doyle et al. 2007) have indicated that leatherback sea turtles *Dermochelys coriacea* are able to consume enough Scyphozoa daily to maintain sufficient energy intake. Like sea turtles, sharptail sunfish consume huge quantities and biomass of gelatinous food (tunicates) which are likely their main energy source.

Sharptail sunfish mainly consumed gelatinous prey but augmented their diet with various other prey from epi- and mesopelagic, coastal, and benthic habitats, suggesting they search for prey sources in various habitats and thus expand their feeding niche. Similar dietary observations were reported for 2 stranded sharptail sunfish on the Atlantic coast of Florida, which fed on prey from pelagic (tunicates) and benthic habitats (various invertebrates) (Bakenhaster & Knight-Gray 2016). Foraging in diverse habitats (from epi- to mesopelagic, and from pelagic to benthic) might be relevant to the wide-ranging vertical movement behavior of sharptail sunfish, which potentially

track prey on the seafloor, surface, and deep water (Cartamil & Lowe 2004, Dewar et al. 2010). These vertically variable foraging strategies have been observed in other mollids and in other consumers of gelatinous prey, such as loggerhead sea turtles *Caretta caretta* and leatherback sea turtles, that search for prey in various habitats (Houghton et al. 2006, Marshall et al. 2012, Nakamura & Sato 2014).

While both sharptail sunfish and ocean sunfish are gelativores, their diets and habitat uses across ontogeny differ. Notably, a small amount of Scyphozoa was found in the stomachs of sharptail sunfish across size groups, in contrast to the diets of ocean sunfish, which are dominated by this prey group (Pope et al. 2010, Nakamura & Sato 2014). There are 2 possible explanations for this difference. One is that sharptail sunfish have a selective preference for other gelatinous species and invertebrates, suggesting potential resource partitioning from ocean sunfish. Indeed, tunicates have rarely been found in the stomachs of *Mola* spp. captured in the same location off east Taiwan (C.T. Chang unpubl. data). Another reason might be underestimation of Scyphozoa from stomach contents. Systematically underestimating soft-bodied prey is a well-documented problem in diet studies based on SCA (Symondson 2002). However, such prey are regularly recognized in ocean sunfish stomachs, suggesting they would be present in sharptail sunfish stomachs if they were being consumed. Further, the low contribution of Scyphozoa from Bayesian mixing models indicated minimal importance of Scyphozoa in sharptail sunfish diet, so the lack of Scyphozoa in stomachs might not be due to poor preservation but to actual infrequency in overall diet.

5.5.2 Size effects

Size-related changes in sharptail sunfish diets suggest intraspecific resource partitioning. In our study, the diet composition of sharptail sunfish changed with increasing sizes from low-mobility prey (e.g. small invertebrates) to include more active prey (e.g. cephalopods and fish), from epi- and mesopelagic habitats to pelagic,

benthic, and coastal regions. These changes are likely related to body size and swimming performance of sharptail sunfish. Molas are thought to be suction feeders (Gregory 1933), and prey availability is constrained by gape size, similar to tunas (Ménard et al. 2006). Increased swimming ability of fish may enable them to forage in various habitats or on higher-mobility prey (Sánchez-Hernández et al. 2019). Further increasing body size may increase competitive performance and decrease predation risk, thus expanding the habitats (pelagic, benthic, and coastal habitats) within which they can forage. Similar patterns were found in studies of ocean sunfish, with small fish targeting a mixed diet in nearshore waters and large individuals exploiting prey from a broad depth range from epipelagic to mesopelagic zones (Nakamura & Sato 2014, Sousa et al. 2016, Phillips et al. 2020).

Despite these slight but significant changes in diet with size, all sharptail sunfish predominately fed on tunicates. Little variance in niche width across sharptail sunfish size groups also suggested high similarity of food sources (gelatinous prey) at all life stages, and the $\delta^{15}\text{N}_{\text{Src}}$ values suggest they feed from the same habitats, similar to sea turtles, which have been shown to feed mainly on Scyphozoa throughout their lifespans (Pate & Salmon 2017). This high utilization of gelatinous prey regardless of size was also demonstrated in mixing model diet estimates, which suggested dominance of tunicates across sizes. Large sharptail sunfish did have slightly higher TPs (in both TP_{AA} and TP_{bulk}) and $\delta^{15}\text{N}_{\text{TP}}$ values than small individuals, which may result from their ability to capture slightly higher quantities of higher-mobility prey of higher TP.

5.5.3 Seasonal effect

Seasonal shifts in diets and isotopic compositions of sharptail sunfish were observed, suggesting that sharptail sunfish may adjust their diets to seasonally abundant or particularly energy-rich prey when they are available. During spring, $\delta^{13}\text{C}$ values of mola were highest, and the very high mass of tunicates found (especially for small mola)

suggests that they fed on these filter-feeding prey during the high-productivity spring season (González et al. 2000, Czudaj et al. 2020, Lan et al. 2020). Moreover, a regular seasonal bloom of tunicates occurs on the waters off Taiwan in the high-productivity season, suggesting that sharptail sunfish may advantageously feed on highly abundant prey when available (Kuo et al. 2015, Franco et al. 2016, 2019), similar to observations of mesopelagic fishes (Cailliet 1972). During summer and autumn, sharptail sunfish had low $\delta^{13}\text{C}$ values, suggesting feeding in different habitats or on different seasonally available resources. This difference was consistent with SCA results that showed mola feeding on more pelagic prey in winter and spring and more coastal, benthic, and pelagic prey in summer and autumn. Additionally, the fact that most flying fish eggs were found in summer and autumn diets is further evidence for opportunistic feeding on pulses of available prey abundance; similar foraging patterns were observed in green turtles *Chelonia mydas* off Taiwan, which fed on eggs during flying fish egg-harvest seasons (Ng et al. 2014). We propose that in high-productivity seasons (spring and winter), sharptail sunfish (especially larger individuals) can obtain adequate energy from tunicates from pelagic regions. In low-productivity seasons (summer and autumn), they might move closer inshore, where productivity is higher (Guo 1991, Chung et al. 2007), or move back and forth between the surface and benthic habitats to expand available prey resources.

Additionally, seasonal shifts in $\delta^{13}\text{C}$ values of sharptail sunfish might be affected by the seasonal variability in the carbon isotopic composition of lower trophic level prey or particulate organic matter (POM). The $\delta^{13}\text{C}$ values of POM showed seasonal variations due to different oceanographic processes near the waters surrounding Taiwan (Lin et al. 2014, Ho et al. 2021). The seasonal variabilities in the base of the food web propagate to the consumer, i.e. mola, via foraging.

5.5.4 Integrating SCA and SIA in estimating diets of sharptail sunfish

There were some discrepancies between SCA and SIA that highlighted the differences in dietary resolution between the 2 approaches and the importance of integrating them in studying foraging ecology. The importance of tunicates in diets of sharptail sunfish were shown in both approaches, whereas other organisms like cephalopods or benthic organisms were shown only using SCA. SCA results can provide a snapshot of diets but cannot reflect long-term dietary prey proportions (e.g. %N or %W) because of variability in digestibility of prey items. In addition, multiple indices (number, weight, occurrence, IRI, PSI) and approaches (ANOSIM) were combined and used to fully describe the diet composition in SCA due to the high variability of gut contents between individual fish. In diet compositions of sharptail sunfish, some groups' diets had high/low PSI but significant/non-significant differences in ANOSIM. It may seem counterintuitive that the diet between groups with low PSI (low overlap) would not have a significant difference and vice versa. This could be due to inherent differences in both approaches. PSI is a comparison of diet overlap between groups using overall %N or %W values (Hurlbert 1978), while ANOSIM uses all diet data, including the variability, in a statistical test (Anderson & Walsh 2013). When a group's diets has low PSI values but the result of ANOSIM is non-significant, it implies a large variation in diets within the group. Therefore, a lower overlap (low PSI values) may not accurately reflect the diets.

SIA results provide time-integrated information on assimilated prey and their energy contribution (Peterson & Fry 1987). For example, in our study, cephalopods contributed little to the diets (based on %FO, %N, and %W) of large sharptail sunfish because they were only occasionally observed and highly digested. However, SIA results indicated that cephalopods were more important to the long-term diet of large sharptail sunfish than apparent from SCA. The inconsistency between SIA and SCA was also found in the trophic niche widths across the size of sharptail sunfish. The

decrease in trophic niche widths with body size was not shown in the SCA results in our study. Instead, large sharptail sunfish exploit their diets in different habitats. Newsome et al. (2007) mentioned that the limitation of an SIA-derived niche is that a small niche width of a consumer would result from consumers feeding on varied resources that have similar isotopic compositions. These types of discrepancies have also been described in studies of apex predators (Chiang et al. 2020, Petta et al. 2020). Thus, integrating the SCA and SIA provides a more holistic view of the trophic ecology of sharptail sunfish.

There are some limitations in this study. First, we did not explore the interannual variation in diets due to the small sample size, and we assumed that prey availabilities are similar across years. Second, the sample sizes in different seasons across all size groups were unbalanced because of the seasonal occurrence of sharptail sunfish in waters off Taiwan. However, an unbalanced design might decrease the statistical power and the robustness (Anderson & Walsh 2013), and increasing the sample size would improve the robustness of the method. Additionally, some gut contents were not identifiable because they were highly digested. DNA metabarcoding could be used to cope with unidentified prey and improve the accuracy of the diet estimates in future work. Last, similar isotopic values of tunicates and pteropods contribute to the uncertainties of the mixing model results (Phillips et al. 2005). The model can perform well when prey sources have dissimilar isotopic values, and vice versa. If tunicates and pteropods, which have similar isotopic values, are combined (resulting in a total of 4 prey sources), the contribution of tunicates is slightly higher than the results with 5 prey sources due to the increase in the percentage of tunicates + pteropods (%W). However, in the present study, we chose not to combine these 2 prey sources because of the differences in their trophic niche and taxonomy.

5.6 Conclusions

We found that sharptail sunfish predominately fed on tunicates, although increasing diet diversity with increasing body size and seasonal shifts in diet suggest the possibility of reducing intra- and inter-specific competition for prey resources. Sharptail sunfish diets differed unexpectedly from co-occurring ocean sunfish in that they did not feed extensively on scyphozoans, suggesting a potential for resource or trophic niche partitioning among Molidae. The present study further describes the resource use and ecological role of the poorly studied sharptail sunfish, adding to the understanding of trophic interactions of Molidae in marine ecosystems. Understanding pelagic predator feeding strategies helps clarify how species modify diet and behavior across ontogeny and seasons, identifying key prey species and feeding habitat that may be integrated into more holistic population assessments and conservation and management initiatives.

5.7 References

- Anderson MJ, Walsh DCI (2013) PERMANOVA, ANOSIM, and the Mantel test in the face of heterogeneous dispersions: What null hypothesis are you testing? *Ecol Monogr* 83: 557–574.
- Arai MN, Welch DW, Dunsmuir AL, Jacobs MC, Ladouceur AR (2003) Digestion of pelagic Ctenophora and Cnidaria by fish. *Can J Fish Aquat Sci* 60: 825–829.
- Arostegui MC, Braun CD, Woodworth-Jefcoats PA, Kobayashi DR, Gaube P (2020) Spatiotemporal segregation of ocean sunfish species (Molidae) in the eastern North Pacific. *Mar Ecol Prog Ser* 654: 109–125.
- Bakenhaster MD, Knight-Gray JS (2016) New diet data for *Mola mola* and *Masturus lanceolatus* (Tetraodontiformes: Molidae) off Florida's Atlantic coast with discussion of historical context. *Bull Mar Sci* 92: 497–511.

- Bradley CJ, Wallsgrove NJ, Choy CA, Drazen JC, Hetherington ED, Hoen DK, Popp BN (2015) Trophic position estimates of marine teleosts using amino acid compound specific isotopic analysis. *Limnol Oceanogr Methods* 13: 476–493.
- Cailliet GM (1972) The study of feeding habits of two marine fishes in relation to plankton ecology. *Trans Am Microsc Soc* 91: 88–89.
- Caldera EJ, Whitney JL, Nyegaard M, Ostalé-Valriberas E, Kubicek L, Thys TM (2020) Genetic insights regarding the taxonomy, phylogeography and evolution of the ocean sunfishes (Molidae: Tetraodontiformes). In: Thys TM, Hays GC, Houghton JDR (eds) *The ocean sunfishes: evolution, biology and conservation*. CRC Press, Boca Raton, FL, p 37–54
- Cartamil DP, Lowe CG (2004) Diel movement patterns of ocean sunfish *Mola mola* off southern California. *Mar Ecol Prog Ser* 266: 245–253.
- Chang CT, Lin SJ, Chiang WC, Musyl MK, Lam CH, Hsu HH, Chang YC, Ho YS (2020) Horizontal and vertical movement patterns of sunfish off eastern Taiwan. *Deep-Sea Res II: Top Stud Oceanogr* 175: 104683.
- Chang CT, Chiang WC, Musyl MK, Popp BN and others (2021) Water column structure influences long-distance latitudinal migration patterns and habitat use of bumphead sunfish *Mola alexandrini* in the Pacific Ocean. *Sci Rep* 11: 21934.
- Chiang WC, Chang CT, Madigan DJ, Carlisle AB and others (2020) Stable isotope analysis reveals feeding ecology and trophic position of black marlin off eastern Taiwan. *Deep-Sea Res II: Top Stud Oceanogr* 175 :104821.
- Chikaraishi Y, Ogawa NO, Kashiyama Y, Takano Y and others (2009) Determination of aquatic food-web structure based on compound-specific nitrogen isotopic composition of amino acids. *Limnol Oceanogr Methods* 7: 740–750.
- Chung IC, Hwang RL, Lin SH, Wu TM and others (2007) Nutrients, temperature, and salinity as primary factors influencing the temporal dynamics of macroalgal

- abundance and assemblage structure on a reef of Du-Lang Bay in Taitung in southeastern Taiwan. *Bot Stud* 48: 419–433.
- Clarke KR (1993) Non-parametric multivariate analyses of changes in community structure. *Aust J Ecol* 18: 117–143.
- Cleveland WS, Grosse E, Shyu WM (1992) Local regression models. In: Chambers JM, Hastie TJ (eds) *Statistical models in S*. Wadsworth & Brooks/Cole, Pacific Grove, CA, p 309–376
- Cortés E (1997) A critical review of methods of studying fish feeding based on analysis of stomach contents: application to elasmobranch fishes. *Can J Fish Aquat Sci* 54: 726–738.
- Czudaj S, Gieseemann A, Hoving HJ, Koppelman R, Luskow F, Möllmann C, Fock HO (2020) Spatial variation in the trophic structure of micronekton assemblages from the eastern tropical North Atlantic in two regions of differing productivity and oxygen environments. *Deep Sea Res I* 163:103275.
- Davenport J (1998) Sustaining endothermy on a diet of cold jelly: energetics of the leatherback turtle *Dermochelys coriacea*. *Brit Herp Soc Bull* 62: 4–8.
- Davenport J, Balazs GH (1991) ‘Fiery bodies’ — Are pyrosomas an important component of the diet of leatherback turtles? *Brit Herp Soc Bull* 37: 33–38.
- Dewar H, Thys T, Teo SLH, Farwell C and others (2010) Satellite tracking the world’s largest jelly predator, the ocean sunfish, *Mola mola*, in the Western Pacific. *J Exp Mar Biol Ecol* 393: 32–42.
- Doyle TK, Houghton JDR, McDevitt R, Davenport J, Hays GC (2007) The energy density of jellyfish: estimates from bomb-calorimetry and proximate-composition. *J Exp Mar Biol Ecol* 343: 239–252.
- Fisheries Agency (2020) *Fisheries statistical yearbook—Taiwan, Kinmen and Matsu Area, 2020*. Fisheries Agency, Council of Agriculture, Taipei.

- Focken U, Becker K (1998) Metabolic fractionation of stable carbon isotopes: implications of different proximate compositions for studies of the aquatic food webs using $\delta^{13}\text{C}$ data. *Oecologia* 115: 337–343.
- Franco P, Chen HJ, Hwang JS (2016) Taxonomic composition and seasonal distribution changes of pelagic tunicates in the waters off nuclear power plants in northern Taiwan in relation to environmental conditions. *Zool Stud* 55: e28.
- Franco P, Dahms HU, Hwang JS (2019) Pelagic tunicates at shallow hydrothermal vents of Kueishantao. *PLOS ONE* 14: e0225387.
- Fraser-Brunner A (1951) The ocean sunfishes (Family Molidae). *Bull Br Mus Nat Hist* 1: 87–121.
- Gelman A, Carlin JB, Stern HS, Dunson DB, Vehtari A, Rubin DB (2013) Bayesian data analysis. CRC Press, Boca Raton, FL.
- Geweke J (1991) Evaluating the accuracy of sampling-based approaches to the calculation of posterior moments. Research Department Staff Report 148. Federal Reserve Bank of Minneapolis, Minneapolis, MN.
- Gomes-Pereira JN, Pham CK, Miodonski J, Santos MAR and others (2023) The heaviest bony fish in the world: a 2744 kg giant sunfish *Mola alexandrini* (Ranzani, 1839) from the North Atlantic. *J Fish Biol* 102: 290–293.
- González HE, Sobarzo M, Figueroa D, Nöthig EM (2000) Composition, biomass and potential grazing impact of the crustacean and pelagic tunicates in the northern Humboldt Current area off Chile: differences between El Niño and non-El Niño years. *Mar Ecol Prog Ser* 195: 201–220.
- Gregory WK (1933) Fish skulls: a study of the evolution of natural mechanisms. The American Philosophical Society, Philadelphia, PA
- Grémillet D, White CR, Authier M, Doremus G, Ridoux V, Pettex E (2017) Ocean sunfish as indicators for the rise of slime. *Curr Biol* 27: R1263–R1264.

- Guo YJ (1991) The Kuroshio. Part II. Primary productivity and phytoplankton. *Oceanogr Mar Biol Annu Rev* 29: 155–189.
- Hannides CCS, Popp BN, Landry MR, Graham BS (2009) Quantification of zooplankton trophic position in the North Pacific Subtropical Gyre using stable nitrogen isotopes. *Limnol Oceanogr* 54: 50–61.
- Harbison GR, Janssen J (1987) Encounters with a swordfish (*Xiphias gladius*) and sharptail sunfish (*Masturus lanceolatus*) at depths greater than 600 meters. *Copeia* 1987: 511–513.
- Harrod C, Syväranta J, Kubicek L, Cappanera V, Houghton JDR (2013) Reply to Logan & Dodge: ‘Stable isotopes challenge the perception of ocean sunfish *Mola mola* as obligate jellyfish predators’. *J Fish Biol* 82: 10–16.
- Ho PC, Okuda N, Yeh CF, Wang PL, Gong GC, Hsieh CH (2021) Carbon and nitrogen isoscape of particulate organic matter in the East China Sea. *Prog Oceanogr* 197: 102667.
- Hooper SN, Paradis M, Ackman RG (1973) Distribution of trans-6-hexadecenoic acid, 7-methyl-7-hexadecenoic acid and common fatty acids in lipids of ocean sunfish *Mola mola*. *Lipids* 8: 509–516.
- Houghton JDR, Doyle TK, Wilson MW, Davenport J, Hays GC (2006) Jellyfish aggregations and leatherback turtle foraging patterns in a temperate coastal environment. *Ecology* 87: 1967–1972.
- Hurlbert SH (1978) The measurement of niche overlap and some relatives. *Ecology* 59: 67–77.
- Jackson AL, Inger R, Parnell AC, Bearhop S (2011) Comparing isotopic niche widths among and within communities: SIBER – Stable Isotope Bayesian Ellipses in R. *J Anim Ecol* 80 :595–602.
- Jackson MC, Donohue I, Jackson AL, Britton JR, Harper DM, Grey J (2012)

- Population-level metrics of trophic structure based on stable isotopes and their application to invasion ecology. *PLOS ONE* 7: e31757.
- Kuo CY, Fan TY, Li HH, Lin CW, Liu LL, Kuo FW (2015) An unusual bloom of the tunicate, *Pyrosoma atlanticum*, in southern Taiwan. *Bull Mar Sci* 91: 363–364.
- Lan KW, Lian LJ, Li CH, Hsiao PY, Cheng SY (2020) Validation of a primary production algorithm of vertically generalized production model derived from multi-satellite data around the waters of Taiwan. *Remote Sens* 12: 1627.
- Larson RJ (1986) Water content, organic content, and carbon and nitrogen composition of medusae from the northeast Pacific. *J Exp Mar Biol Ecol* 99: 107–120.
- Layman CA, Arrington DA, Montaña CG, Post DM (2007) Can stable isotope ratios provide for community-wide measures of trophic structure? *Ecology* 88: 42–48.
- Leis JL, Matsuura K, Shao KT, Hardy G and others (2015) Sharptail sunfish *Masturus lanceolatus* (errata version published in 2017). The IUCN Red List of Threatened Species: e.T193634A115330232.
- Lin HY, Lin PY, Chang NN, Shiao JC, Kao SJ (2014) Trophic structure of megabenthic food webs along depth gradients in the South China Sea and off northeastern Taiwan. *Mar Ecol Prog Ser* 501: 53–66.
- Logan JM, Jardine TD, Miller TJ, Bunn SE, Cunjak RA, Lutcavage ME (2008) Lipid corrections in carbon and nitrogen stable isotope analyses: comparison of chemical extraction and modelling methods. *J Anim Ecol* 77: 838–846.
- Madigan DJ, Snodgrass OE, Hyde JR, Dewar H (2021) Stable isotope turnover rates and fractionation in captive California yellowtail (*Seriola dorsalis*): insights for application to field studies. *Sci Rep* 11: 4466.
- Marshall CD, Guzman A, Narazaki T, Sato K, Kane EA, Sterba-Boatwright BD (2012) The ontogenetic scaling of bite force and head size in loggerhead sea turtles (*Caretta caretta*): implications for durophagy in neritic, benthic habitats. *J Exp Biol*

215: 4166–4174.

McClelland JW, Montoya JP (2002) Trophic relationships and the nitrogen isotopic composition of amino acids in plankton. *Ecology* 83: 2173–2180.

Ménard F, Labrune C, Shin YJ, Asine AS, Bard FX (2006) Opportunistic predation in tuna: a size-based approach. *Mar Ecol Prog Ser* 323: 223–231.

Muggeo VMR (2008) Segmented: an R package to fit regression models with broken-line relationships. *R News* 8: 20–25

Nakamura I, Sato K (2014) Ontogenetic shift in foraging habit of ocean sunfish *Mola mola* from dietary and behavioral studies. *Mar Biol* 161: 1263–1273.

Newsome SD, Martinez del Rio C, Bearhop S, Phillips DL (2007) A niche for isotopic ecology. *Front Ecol Environ* 5: 429–436.

Ng KY, Chen TH, Balazs GH (2014) Flying fish egg harvest off Keelung, Taiwan uncovers occurrence of pelagic-phase green turtles. *Mar Turtle Newsl* 143: 14–15.

Nyegaard M, Loneragan N, Hall S, Andrew J, Sawai E, Nyegaard M (2018) Giant jelly eaters on the line: species distribution and bycatch of three dominant sunfishes in the Southwest Pacific. *Estuar Coast Shelf Sci* 207: 1–15.

Pate JH, Salmon M (2017) Ontogenetic niches and the development of body shape in juvenile sea turtles. *Chelonian Conserv Biol* 16: 185–193.

Peterson BJ, Fry B (1987) Stable isotopes in ecosystem studies. *Annu Rev Ecol Syst* 18: 293–320.

Petta JC, Shipley ON, Wintner SP, Cliff G, Dicken ML, Hussey NE (2020) Are you really what you eat? Stomach content analysis and stable isotope ratios do not uniformly estimate dietary niche characteristics in three marine predators. *Oecologia* 192: 1111–1126.

Phillips DL, Newsome SD, Gregg JW (2005) Combining sources in stable isotope mixing models: alternative methods. *Oecologia* 144: 520–527.

- Phillips ND, Elliott Smith EA, Newsome SD, Houghton JDR and others (2020) Bulk tissue and amino acid stable isotope analyses reveal global ontogenetic patterns in ocean sunfish trophic ecology and habitat use. *Mar Ecol Prog Ser* 633: 127–140.
- Pianka ER (1973) The structure of lizard communities. *Annu Rev Ecol Evol Syst* 4: 53–74.
- Pope EC, Hays GC, Thys TM, Doyle TK and others (2010) The biology and ecology of the ocean sunfish *Mola mola*: a review of current knowledge and future research perspectives. *Rev Fish Biol Fish* 20: 471–487.
- Popp BN, Graham BS, Olson RJ, Hannides CCS and others (2007) Insight into the trophic ecology of yellowfin tuna, *Thunnus albacares*, from compound-specific nitrogen isotope analysis of proteinaceous amino acids. In: Dawson TE, Siegwolf RTW (ed) *Stable isotopes as indicators of ecological change*. Elsevier, Amsterdam, p 173-190.
- Post DM (2002) Using stable isotopes to estimate trophic position: models, methods, and assumptions. *Ecology* 83: 703–718.
- Sánchez-Hernández J, Nunn AD, Adams CE, Amundsen PA (2019) Causes and consequences of ontogenetic dietary shifts: a global synthesis using fish models. *Biol Rev Camb Philos Soc* 94: 539–554.
- Sawai E, Hibino Y, Iwasaki T (2019) A rare river stranding record of sharptail sunfish *Masturus lanceolatus* in Fukuoka Prefecture, Japan. *Biogeography* 21: 27–30.
- Seitz AC, Weng KC, Boustany AM, Block BA (2002) Behaviour of a sharptail sunfish in the Gulf of Mexico. *J Fish Biol* 60: 1597–1602.
- Sousa LL, Xavier R, Costa V, Humphries NE and others (2016) DNA barcoding identifies a cosmopolitan diet in the ocean sunfish. *Sci Rep* 6: 28762.
- Stock BC, Semmens BX (2013) *MixSIAR GUI user manual: version 3.1*.
<https://github.com/brianstock/MixSIAR/>

- Stock BC, Jackson AL, Ward EJ, Parnell AC, Phillips DL, Semmens BX (2018) Analyzing mixing systems using a new generation of Bayesian tracer mixing models. *PeerJ* 6: e5096.
- Symondson WOC (2002) Molecular identification of prey in predator diets. *Mol Ecol* 11: 627–641.
- Syväranta J, Rautio M (2010) Zooplankton, lipids and stable isotopes: importance of seasonal, latitudinal, and taxonomic differences. *Can J Fish Aquat Sci* 67: 1721–1729.
- Syväranta J, Harrod C, Kubicek L, Cappanera V, Houghton JDR (2012) Stable isotopes challenge the perception of ocean sunfish *Mola mola* as obligate jellyfish predators. *J Fish Biol* 80: 225–231.
- Underwood AJ (1997) Experiments in ecology: their logical design and interpretation using analysis of variance. Cambridge University Press, Cambridge
- Vander Zanden MJ, Rasmussen JB (2001) Variation in $\delta^{15}\text{N}$ and $\delta^{13}\text{C}$ trophic fractionation: implications for aquatic food web studies. *Limnol Oceanogr* 46: 2061–2066.
- Weng JS, Lee MA, Liu KM, Hsu MS, Hung MK, Wu LJ (2015) Feeding ecology of juvenile yellowfin tuna from waters southwest of Taiwan inferred from stomach contents and stable isotope analysis. *Mar Coast Fish* 7: 537–548.

Table 5.1. Prey items of collected sharptail sunfish with stomach contents. Five diet indices were calculated: %FO: frequency of occurrence; %N: numerical abundance; %W: gravimetric importance; IRI: index of relative importance; %IRI: proportion IRI of a prey item relative to the sum of all IRI values

Prey item	%FO	%N	%W	IRI	%IRI
SCYPHOZOA					
Atollidae - <i>Atolla</i> spp.	10.48	1.03	3.10	43.35	0.52
MOLLUSCS					
Cephalopoda					
Ommastrephidae (beak)	7.62	0.38	0.51	6.77	0.08
Gonatidae (beak)	0.95	0.05	0.00	0.05	0.00
Pen of unidentified cephalopod	1.90	0.09	0.00	0.18	0.00
Eye lens of unidentified cephalopod	12.38	1.60	0.12	21.23	0.26
Hook of unidentified cephalopod	0.95	1.46	0.09	1.47	0.02
Pteropoda					
Cavoliniidae - <i>Diacavolinia longirostris</i>	36.19	13.91	1.02	540.45	6.54
Cavoliniidae - <i>Cavolinia</i> spp.	10.48	2.30	0.16	25.78	0.31
Cavoliniidae - <i>Diacria costata</i>	6.67	0.42	0.01	2.87	0.03
Creseidae - <i>Creseis conica</i>	27.62	11.00	0.82	326.22	3.95
Cliidae - <i>Clio pyramidata</i>	2.86	0.14	0.00	0.41	0.00
Carinariidae - <i>Carinaria</i> spp.	23.81	5.50	0.61	145.46	1.76
Atlantidae	17.14	1.60	0.08	28.76	0.35
Gastropoda					
Benthic gastropod (unidentified)	3.81	0.23	0.02	0.96	0.01

Table 5.1. (Continued) Prey items of collected sharptail sunfish with stomach contents. Five diet indices were calculated: %FO: frequency of occurrence; %N: numerical abundance; %W: gravimetric importance; IRI: index of relative importance; %IRI: proportion IRI of a prey item relative to the sum of all IRI values

Prey item	%FO	%N	%W	IRI	%IRI
Heteropoda					
Heteropod radula	12.38	4.28	0.18	55.18	0.67
TUNICATES					
Salpidae	60.95	15.55	32.81	2948.11	35.67
Pyrosomatidae - <i>Pyrosoma</i> spp.	52.38	13.67	48.02	3231.48	39.09
Pyrosomatidae - <i>Pyrosomella</i> spp.	0.95	0.05	0.03	0.07	0.00
CRUSTACEANS					
Amphipoda					
Phronimidae - <i>Phronima</i> spp.	47.62	11.56	3.56	719.82	8.71
Hyperiididae - <i>Hyperia</i> spp.	4.76	0.23	0.00	1.12	0.01
Euphausiacea					
Euphausiidae - euphausiids	1.90	0.38	0.02	0.76	0.01
Decapoda					
<i>Gnathophausia</i> sp.	0.95	0.05	0.16	0.20	0.00
Shrimp (unidentified)	14.29	1.79	0.26	29.25	0.35
Crab megalopa (unidentified)	0.95	0.09	0.01	0.10	0.00
Scyllaridae phyllosoma	10.48	1.46	0.49	20.39	0.25
Crab zoea (unidentified)	3.81	0.23	0.01	0.95	0.01
FISH					
Scombridae	0.95	0.05	1.19	1.18	0.01

Table 5.1. (Continued) Prey items of collected sharptail sunfish with stomach contents. Five diet indices were calculated: %FO: frequency of occurrence; %N: numerical abundance; %W: gravimetric importance; IRI: index of relative importance; %IRI: proportion IRI of a prey item relative to the sum of all IRI values

Prey item	%FO	%N	%W	IRI	%IRI
Lutjanidae	0.95	0.05	0.68	0.69	0.01
Lutjanidae (teeth)	1.90	0.09	0.01	0.19	0.00
Exocoetidae (egg)	12.38	4.79	0.39	64.23	0.78
Fish (unidentified)	1.90	0.09	0.73	1.58	0.02
Otolith of unidentified fish	1.90	0.19	0.00	0.36	0.00
Bone of unidentified fish	4.76	1.08	0.03	5.28	0.06
OTHER					
Sand	1.90	-	4.49	8.55	0.10
Plastics	6.67	3.95	0.05	26.68	0.32
Unidentified organisms	5.71	0.66	0.32	5.61	0.07
TOTAL	105	2128	821 g		

Table 5.2. Percent similarity index (PSI) values among size classes of sharptail sunfish and seasons; measured in terms of prey numbers (%N, below diagonal dashes) and weights (%W, above diagonal dashes). Comparisons do not include unidentified organisms, plastics, and sand. *represents significant differences in ANOSIM results ($p < 0.05$) between groups in terms of %N and %W

(A) Size class (ANOSIM: $p < 0.05$)				
	<80 cm	80–120 cm	>120 cm	
<80 cm	–	76.6*	33.4*	
80–120 cm	58.9*	–	44.3*	
>120 cm	59.8*	51.2*	–	
(B) Season (ANOSIM: $p < 0.05$)				
	Spring	Summer	Autumn	Winter
Spring	–	37.9	55.9*	26.9
Summer	64.7	–	72.5	57.3
Autumn	50.5*	63.3	–	60.0*
Winter	38.8	48.3	50.3	–
(C) <80 cm (ANOSIM: $p < 0.05$)				
	Spring	Summer	Autumn	Winter
Spring	–	66.4	61.7*	37.4
Summer	22.4	–	81.5*	36.8
Autumn	43*	29*	–	40.5*
Winter	23.7	21.5*	30.1*	–
(D) 80–120 cm (ANOSIM: $p < 0.05$)				
	Spring	Summer	Autumn	Winter
Spring	–	44.7	38.9	63.6

Table 5.2. Percent similarity index (PSI) values among size classes of sharptail sunfish and seasons; measured in terms of prey numbers (%N, below diagonal dashes) and weights (%W, above diagonal dashes). Comparisons do not include unidentified organisms, plastics, and sand. *represents significant differences in ANOSIM results ($p < 0.05$) between groups in terms of %N and %W

Summer	26.9	–	78.5	63.2
Autumn	44.6*	56	–	57.3
Winter	40	45.9	57.7	–
(E) >120 cm (ANOSIM: $p > 0.05$)				
	Spring	Summer	Autumn	Winter
Spring	–	12.4	5.7	–
Summer	12.9	–	76.1	–
Autumn	3	56.9	–	–
Winter	–	–	–	–

Table 5.3. Mean \pm SD $\delta^{15}\text{N}$ values of trophic ($\delta^{15}\text{N}_{\text{Trp}}$) and source amino acids ($\delta^{15}\text{N}_{\text{Src}}$), and trophic positions (TPs) estimated by isotopic data from individual amino acids (TP_{AA}) and bulk tissues (TP_{bulk}) across size classes of sharptail sunfish

Size class	$\delta^{15}\text{N}_{\text{Trp}}$ (‰)	$\delta^{15}\text{N}_{\text{Src}}$ (‰)	TP_{AA}	TP_{bulk}
<80 cm	21.49 \pm 1.4	3.51 \pm 0.2	3.5 \pm 0.3	3.5 \pm 0.4
80–120 cm	22.00 \pm 2.0	3.48 \pm 3.8	3.6 \pm 0.4	3.7 \pm 0.3
>120 cm	24.41 \pm 1.0	4.52 \pm 1.1	3.9 \pm 0.2	3.8 \pm 0.3

Table S5.1. Habitat and functional groups for prey items of sharptail sunfish

Species	Habitat	Functional group
Atollidae - <i>Atolla</i> spp.	Epi- and mesopelagic	Epi- and mesopelagic scyphozoan
Ommastrephidae (beak)	Epi- and mesopelagic	Epi- and mesopelagic cephalopoda
Gonatidae (beak)	Epi- and mesopelagic	Epi- and mesopelagic cephalopoda
Pen of unidentified cephalopoda	Epi- and mesopelagic	Epi- and mesopelagic cephalopoda
Eye lens of unidentified cephalopoda	Epi- and mesopelagic	Epi- and mesopelagic cephalopoda
Hook of unidentified cephalopoda	Epi- and mesopelagic	Epi- and mesopelagic cephalopoda
Cavoliniidae - <i>Diacavolinia longirostris</i>	Epi- and mesopelagic	Epi- and mesopelagic pteropoda
Cavoliniidae - <i>Cavolinia</i> spp.	Epi- and mesopelagic	Epi- and mesopelagic pteropoda
Cavoliniidae - <i>Diacria costata</i>	Epi- and mesopelagic	Epi- and mesopelagic pteropoda
Creseidae - <i>Creseis conica</i>	Epi- and mesopelagic	Epi- and mesopelagic pteropoda
Cliidae - <i>Clio pyramidata</i>	Epi- and mesopelagic	Epi- and mesopelagic pteropoda
Carinariidae - <i>Carinaria</i> spp.	Epi- and mesopelagic	Epi- and mesopelagic pteropoda
Atlantidae	Epi- and mesopelagic	Epi- and mesopelagic pteropoda
Benthic gastropoda (unidentified)	Benthic	Benthic organism
Heteropods radula	Epi- and mesopelagic	Epi- and mesopelagic pteropoda
Salpidae	Epi- and mesopelagic	Epi- and mesopelagic tunicate
Pyrosomatidae - <i>Pyrosoma</i> spp.	Epi- and mesopelagic	Epi- and mesopelagic tunicate
Pyrosomatidae - <i>Pyrosomella</i> spp.	Epi- and mesopelagic	Epi- and mesopelagic tunicate
Phronimidae - <i>Phronima</i> spp.	Epi- and mesopelagic	Epi- and mesopelagic crustacean
Hyperiididae - <i>Hyperia</i> spp.	Epi- and mesopelagic	Epi- and mesopelagic crustacean
Euphausiidae - Euphausiids	Epi- and mesopelagic	Epi- and mesopelagic crustacean
<i>Gnathophausia</i> sp.	Epi- and mesopelagic	Epi- and mesopelagic crustacean
Shrimp (unidentified)		Unidentified shrimp

Table S5.1. (Continued) Habitat and functional groups for prey items of sharptail sunfish

Species	Habitat	Functional group
Crab megalopa (unidentified)	Coastal	Crustacean juvenile
Scyllaridae phyllosoma	Coastal and offshore	Crustacean juvenile
Crab zoea (unidentified)	Coastal	Crustacean juvenile
Scombridae	Epi- and mesopelagic	Fish
Lutjanidae	Coastal	Fish
Lutjanidae (teeth)	Coastal	Fish
Exocoetidae (egg)	Epipelagic	Fish
Fish (unidentified)		Fish
Otolith of unidentified fish		Fish
Bone of unidentified fish		Fish

Table S5.2. Prey tables for stomach contents of sharptail sunfish across three size classes

Size class	<80 cm					80-120 cm					>120 cm				
Prey item	%FO	%N	%W	IRI	%IRI	%FO	%N	%W	IRI	%IRI	%FO	%N	%W	IRI	%IRI
SCYPHOZOA															
Atollidae - <i>Atolla</i> spp.	5.88	0.25	0.24	2.89	0.03	13.11	1.68	6.56	108.04	1.26	10.00	0.54	0.03	5.70	0.07
MOLLUSCS															
Cephalopoda															
Ommastrephidae (beak)	8.82	0.37	0.17	4.80	0.05	6.56	0.35	0.98	8.72	0.10	10.00	0.54	0.06	6.00	0.07
Gonatidae (beak)	0.00	0.00	0.00	0.00	0.00	1.64	0.09	0.01	0.16	0.00	0.00	0.00	0.00	0.00	0.00
Pen of unidentified cephalopoda	0.00	0.00	0.00	0.00	0.00	1.64	0.09	0.00	0.15	0.00	10.00	0.54	0.00	5.40	0.06
Eye lens of unidentified cephalopoda	8.82	0.50	0.19	6.09	0.07	11.48	1.94	0.12	23.65	0.28	30.00	4.30	0.06	130.80	1.56
Hook of unidentified cephalopoda	0.00	0.00	0.00	0.00	0.00	1.64	2.73	0.19	4.79	0.06	0.00	0.00	0.00	0.00	0.00
Pteropoda															
Cavoliniidae - <i>Diacavolinia longirostris</i>	35.29	14.60	1.76	577.34	6.56	32.79	13.49	1.21	482.01	5.61	60.00	13.44	0.19	817.80	9.74
Cavoliniidae - <i>Cavolinia</i> spp.	11.76	4.95	0.39	62.80	0.71	11.48	0.79	0.15	10.79	0.13	0.00	0.00	0.00	0.00	0.00

Table S5.2. (Continued) Prey tables for stomach contents of sharptail sunfish across three size classes

Size class	<80 cm					80-120 cm					>120 cm				
Prey item	%FO	%N	%W	IRI	%IRI	%FO	%N	%W	IRI	%IRI	%FO	%N	%W	IRI	%IRI
Cavoliniidae - <i>Diacria costata</i>	17.65	0.99	0.03	18.00	0.20	1.64	0.09	0.00	0.15	0.00	0.00	0.00	0.00	0.00	0.00
Creseidae - <i>Creseis conica</i>	23.53	14.48	1.85	384.24	4.36	29.51	8.11	0.76	261.84	3.05	30.00	13.44	0.12	406.83	4.84
Cliidae - <i>Clio pyramidata</i>	2.94	0.12	0.00	0.35	0.00	0.00	0.00	0.00	0.00	0.00	20.00	1.08	0.00	21.60	0.26
Carinariidae - <i>Carinaria</i> spp.	26.47	6.19	1.63	207.00	2.35	21.31	5.2	0.45	120.40	1.40	30.00	4.30	0.10	132.00	1.57
<i>Atlantidae</i>	17.65	0.99	0.18	20.65	0.23	18.03	1.94	0.06	36.06	0.42	10.00	2.15	0.04	21.90	0.26
Gastropoda															
Benthic gastropods (unidentified)	8.82	0.37	0.05	3.70	0.04	1.64	0.18	0.01	0.31	0.00	0.00	0.00	0.00	0.00	0.00
Heteropoda															
Heteropods radula	17.65	5.57	0.56	108.19	1.23	9.84	2.73	0.11	27.95	0.33	10.00	8.06	0.01	80.70	0.96
TUNICATE															
Salpidae	67.65	16.34	56.62	4935.74	56.05	60.66	16.23	39.59	3386.04	39.44	40.00	8.06	4.90	518.40	6.17
Pyrosomatidae - <i>Pyrosoma</i> spp.	41.18	7.05	27.02	1403.00	15.93	59.02	15.26	37.88	3136.32	36.53	50.00	32.80	78.89	5584.50	66.50

Table S5.2. (Continued) Prey tables for stomach contents of sharptail sunfish across three size classes

Size class	<80 cm					80-120 cm					>120 cm				
Prey item	%FO	%N	%W	IRI	%IRI	%FO	%N	%W	IRI	%IRI	%FO	%N	%W	IRI	%IRI
Pyrosomatidae - <i>Pyrosomella</i> spp.	0.00	0.00	0.00	0.00	0.00	1.64	0.09	0.07	0.26	0.00	0.00	0.00	0.00	0.00	0.00
CRUSTACEANS															
Amphipoda															
Phronimidae - <i>Phronima</i> spp.	50.00	10.52	6.88	870.00	9.88	45.90	13.40	3.68	783.97	9.13	50.00	4.84	0.89	286.50	3.41
Hyperiididae - <i>Hyperia</i> spp.	2.94	0.12	0.00	0.35	0.00	4.92	0.26	0.00	1.28	0.01	10.00	0.54	0.00	5.40	0.06
Euphausiacea															
Euphausiidae - Euphausiids	0.00	0.00	0.00	0.00	0.00	3.28	0.71	0.04	2.46	0.03	0.00	0.00	0.00	0.00	0.00
Decapoda															
<i>Gnathophausia</i> sp.	0.00	0.00	0.00	0.00	0.00	1.64	0.09	0.36	0.74	0.01	0.00	0.00	0.00	0.00	0.00
Shrimp (unidentified)	11.76	1.36	0.49	21.76	0.25	14.75	2.20	0.26	36.29	0.42	20.00	1.08	0.09	23.40	0.28
Crab megalopa (unidentified)	2.94	0.25	0.05	0.88	0.01	0.00	0.00	0.00	0.00	0.00	0.00	0.00	0.00	0.00	0.00
Scyllaridae phyllosoma	20.59	2.60	1.47	83.80	0.95	6.56	0.88	0.33	7.94	0.09	0.00	0.00	0.00	0.00	0.00

Table S5.2. (Continued) Prey tables for stomach contents of sharptail sunfish across three size classes

Size class	<80 cm					80-120 cm					>120 cm				
Prey item	%FO	%N	%W	IRI	%IRI	%FO	%N	%W	IRI	%IRI	%FO	%N	%W	IRI	%IRI
Crab zoea (unidentified)	2.94	0.12	0.00	0.35	0.00	1.64	0.09	0.01	0.16	0.00	20.00	1.61	0.03	32.80	0.39
FISH															
Scombridae	0.00	0.00	0.00	0.00	0.00	1.64	0.09	2.56	4.35	0.05	0.00	0.00	0.00	0.00	0.00
Lutjanidae	0.00	0.00	0.00	0.00	0.00	1.64	0.09	1.47	2.56	0.03	0.00	0.00	0.00	0.00	0.00
Lutjanidae (teeth)	0.00	0.00	0.00	0.00	0.00	3.28	0.18	0.02	0.66	0.01	0.00	0.00	0.00	0.00	0.00
Exocoetidae (egg)	11.76	3.34	0.01	39.40	0.45	13.11	6.53	0.85	96.75	1.13	10.00	0.54	0.00	5.40	0.06
Fish (unidentified)	0.00	0.00	0.00	0.00	0.00	3.28	0.18	1.58	5.77	0.07	0.00	0.00	0.00	0.00	0.00
Otolith of unidentified fish	2.94	0.25	0.01	0.76	0.01	1.64	0.18	0.00	0.30	0.00	0.00	0.00	0.00	0.00	0.00
Bone of unidentified fish	0.00	0.00	0.00	0.00	0.00	6.56	1.68	0.06	11.41	0.13	10.00	2.15	0.00	21.50	0.26
OTHERS															
Sand	0.00	0.00	0.00	0.00	0.00	0.00	0.00	0.00	0.00	0.00	20.00	-	14.57	291.40	3.47
Plastics	5.88	8.29	0.01	48.80	0.55	8.20	1.50	0.11	13.20	0.15	0.00	0.00	0.00	0.00	0.00

Table S5.2. (Continued) Prey tables for stomach contents of sharptail sunfish across three size classes

Size class	80 cm					80-120 cm					>120 cm				
Prey item	%FO	%N	%W	IRI	%IRI	%FO	%N	%W	IRI	%IRI	%FO	%N	%W	IRI	%IRI
Unidentified organisms	5.88	0.37	0.38	4.41	0.05	6.56	0.97	0.51	9.71	0.11	0.00	0.00	0.00	0.00	0.00
TOTAL	34	808	188.1			61	1134	380.2			10	186	252.8		

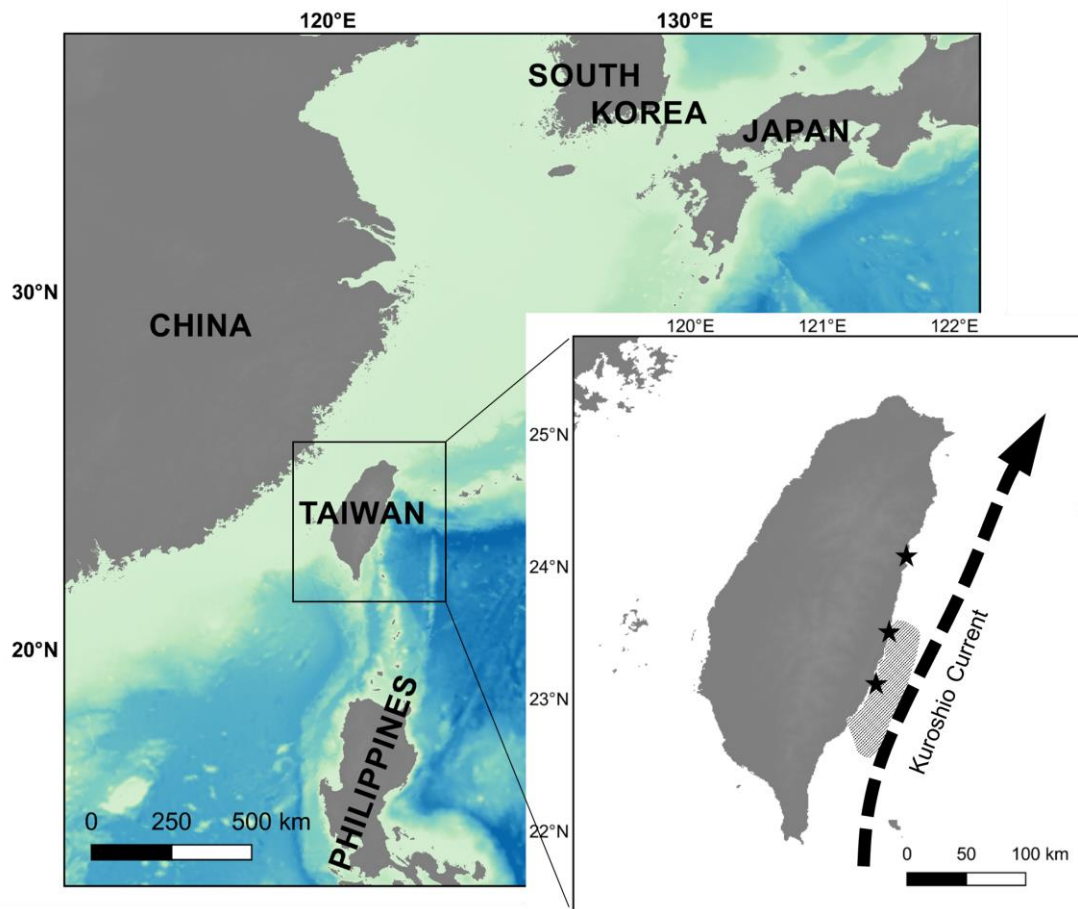


Fig. 5.1. Sharptail sunfish fishing grounds for set-net (stars) and longline (hatched area) fishing operations in eastern Taiwan

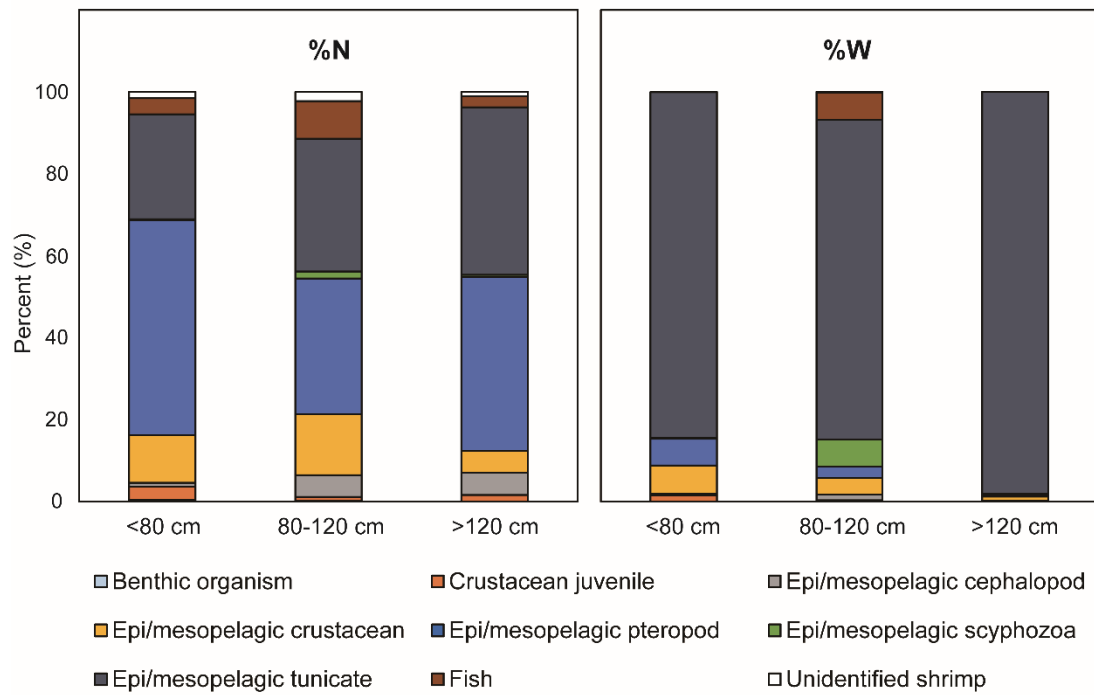


Fig. 5.2. Numerical (%N) and gravimetric (%W) diet compositions of sharptail sunfish for each size class (sample sizes: <80 cm, n = 34; 80–120 cm, n = 61; >120 cm, n = 10). Prey items were categorized into different functional groups

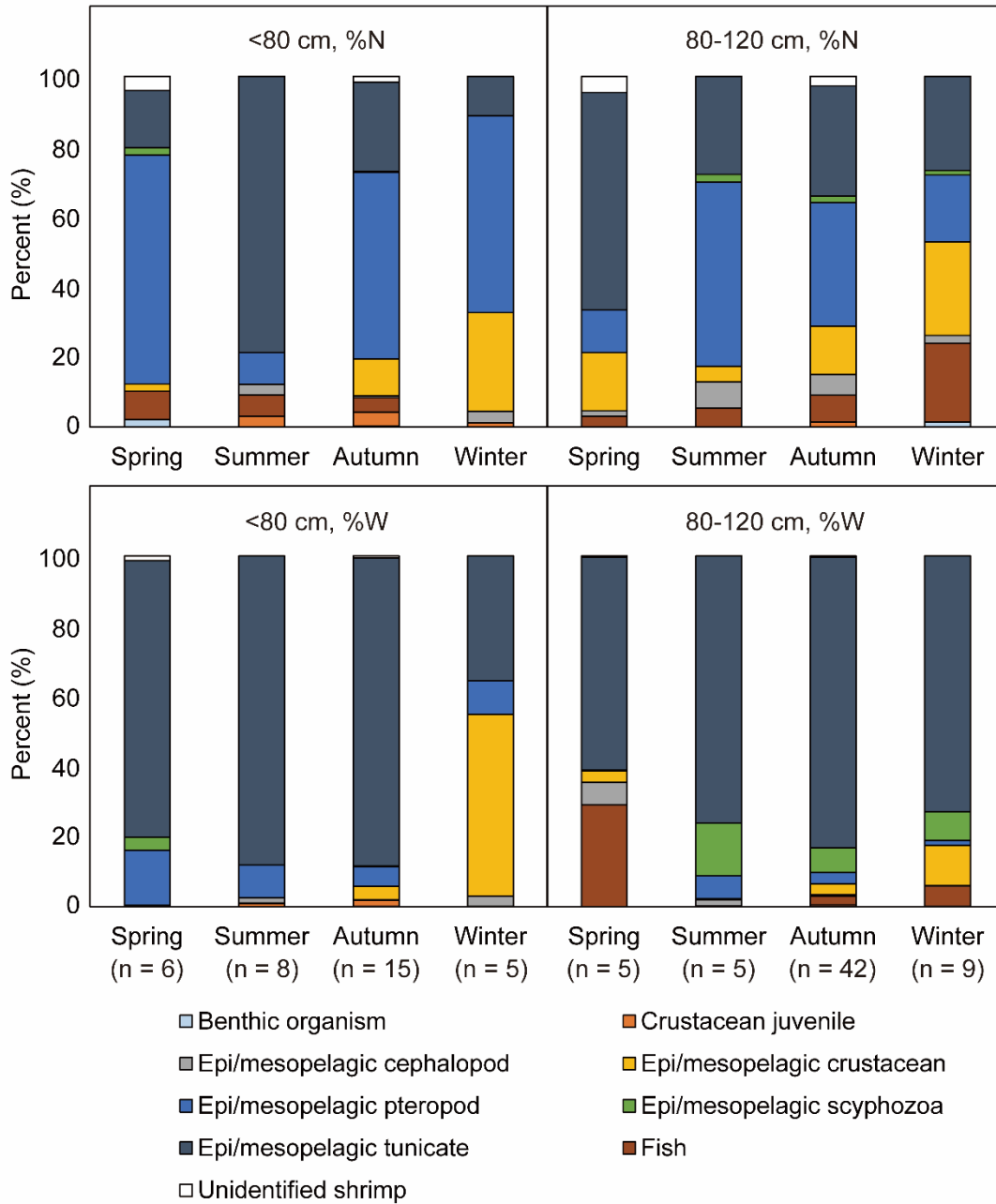


Fig. 5.3. Seasonal diet composition of sharptail sunfish <80 cm and 80–120 cm in terms of numerical (%N) and gravimetric (%W) indices. Sample size (n) represents sample size for each size class in each season. Individuals >120 cm were excluded because their diet compositions were not significantly different among seasons ($p > 0.05$)

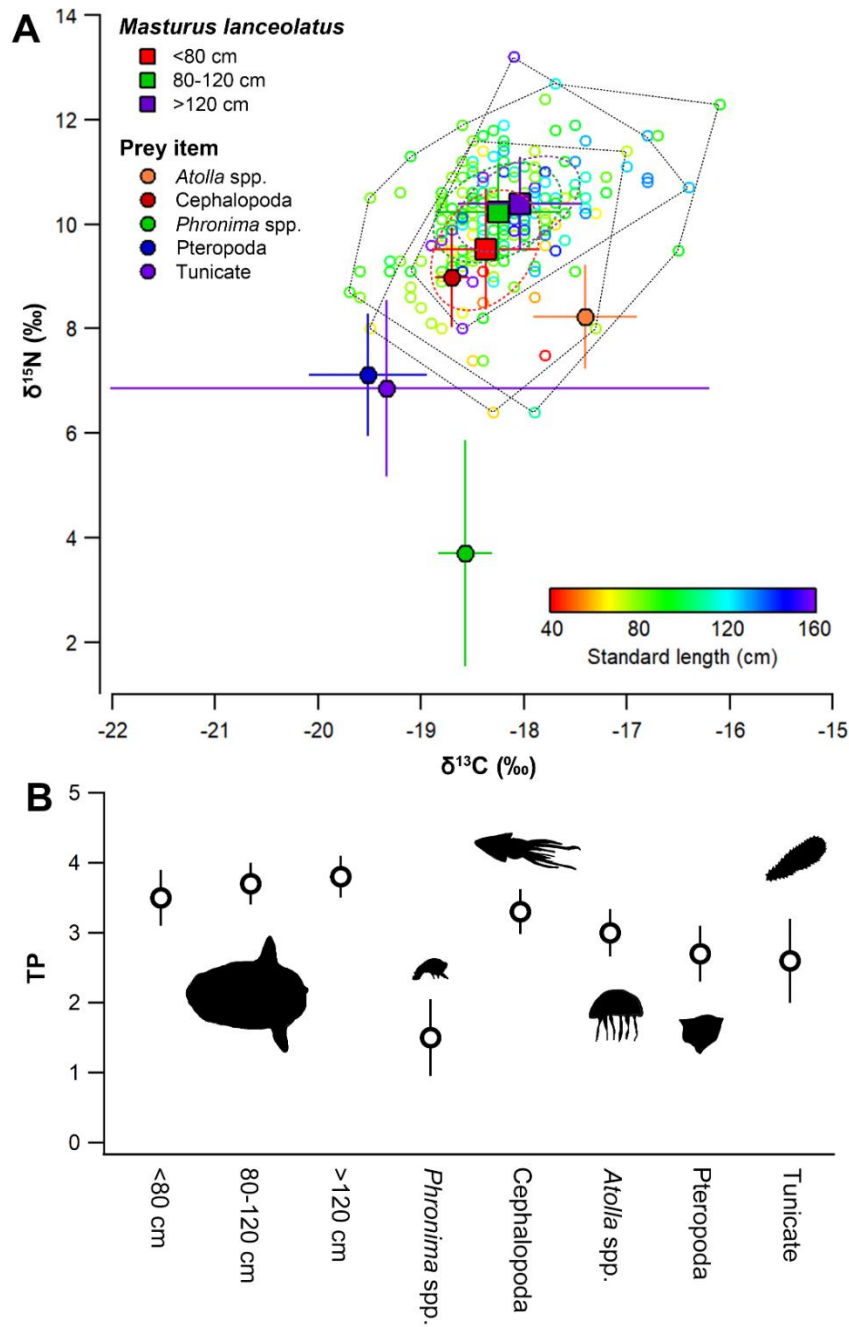


Fig. 5.4. (A) Biplot of $\delta^{13}\text{C}$ and $\delta^{15}\text{N}$ values from sharptail sunfish and their prey items (mean \pm 1 SD) off eastern Taiwan and (B) trophic position (TP) estimates in bulk tissues of sharptail sunfish and their prey items. Isotopic niche for sharptail sunfish across size classes in (A) shows corrected standard ellipse areas (SEAc, dashed lines) and total area of convex hull (dotted lines). Open circles in (A) represent the $\delta^{13}\text{C}$ and $\delta^{15}\text{N}$ values for all specimens of sharptail sunfish

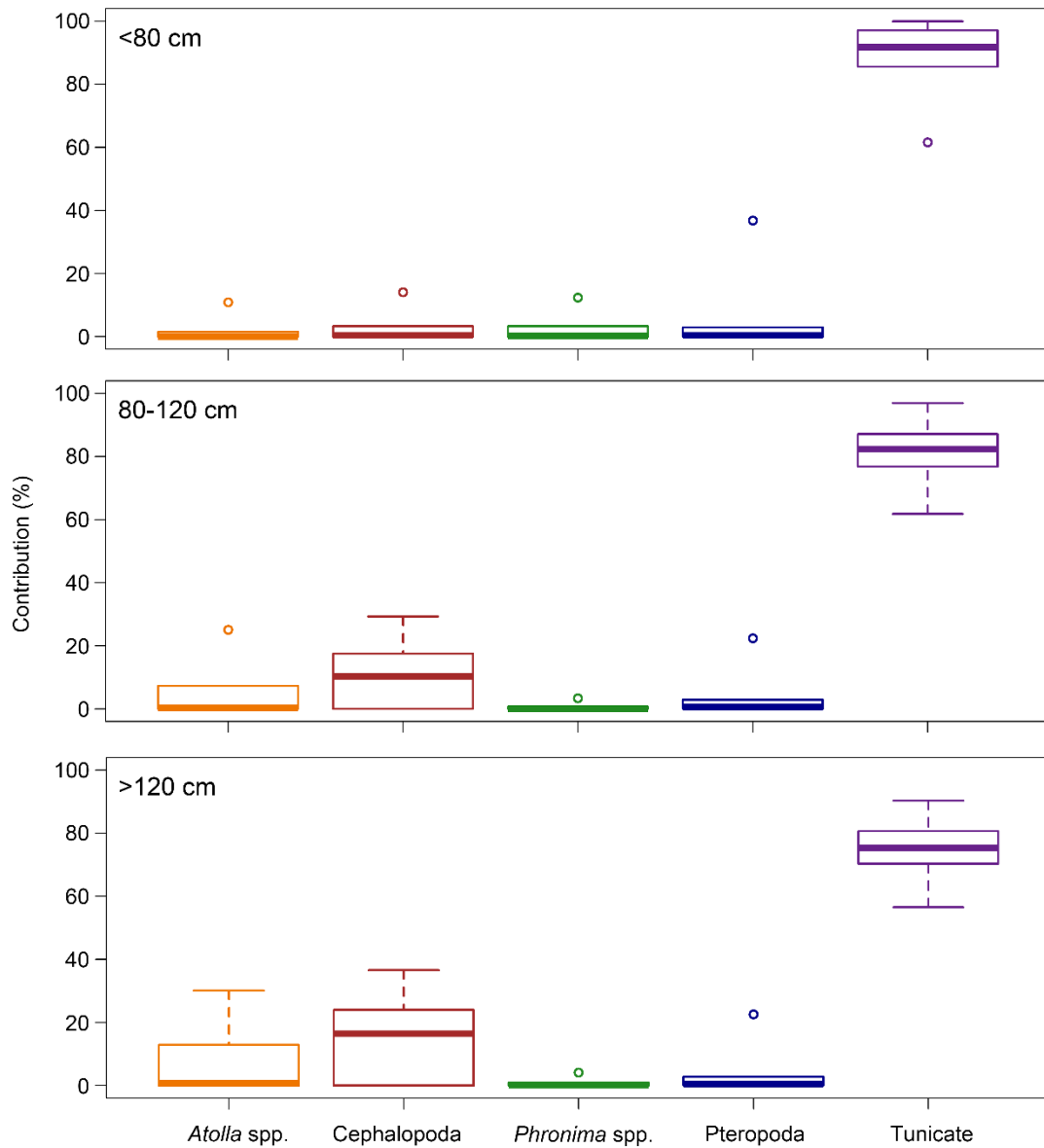


Fig. 5.5. Estimated contribution of common prey species to sharptail sunfish diet based on Bayesian isotope mixing models. Informative priors were based on diet compositions (by % weight, %W) of sharptail sunfish. Boxplots represent the 25th, median, and 75th quartiles of data; whiskers represent 1.5× the interquartile range; and open circles represent outliers

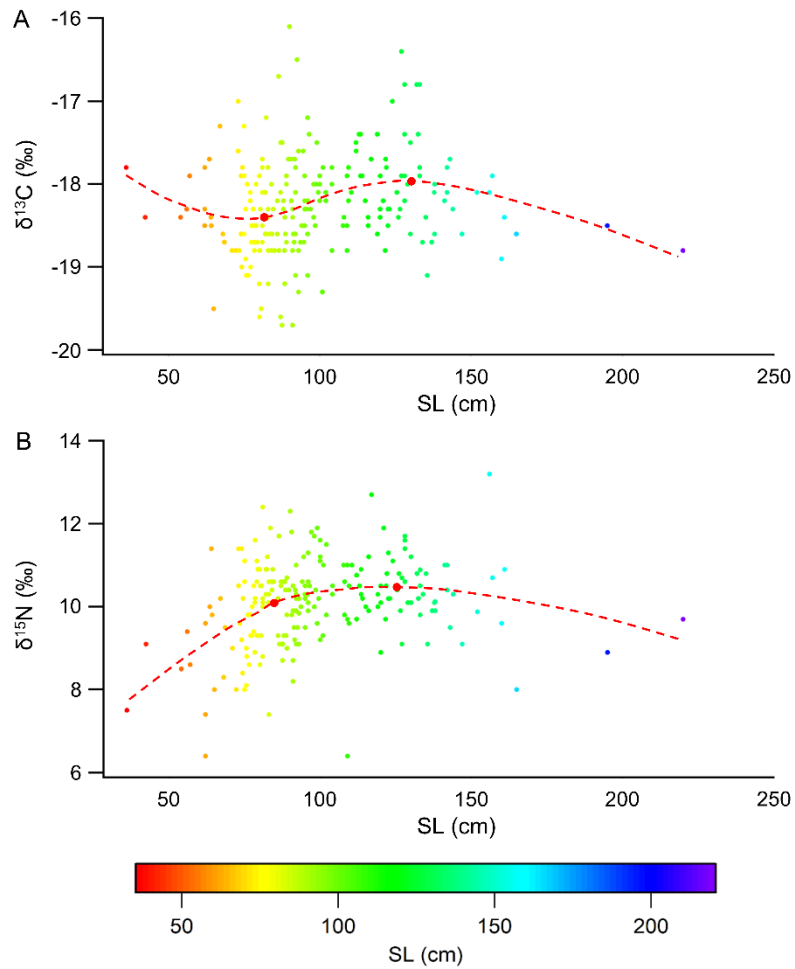


Fig. S5.1. Relationships between standard length (SL) and values of (A) $\delta^{13}\text{C}$ and (B) $\delta^{15}\text{N}$ of sharptail sunfish. Dashed lines show estimates from LOESS smoothing, with red dots showing breakpoints.

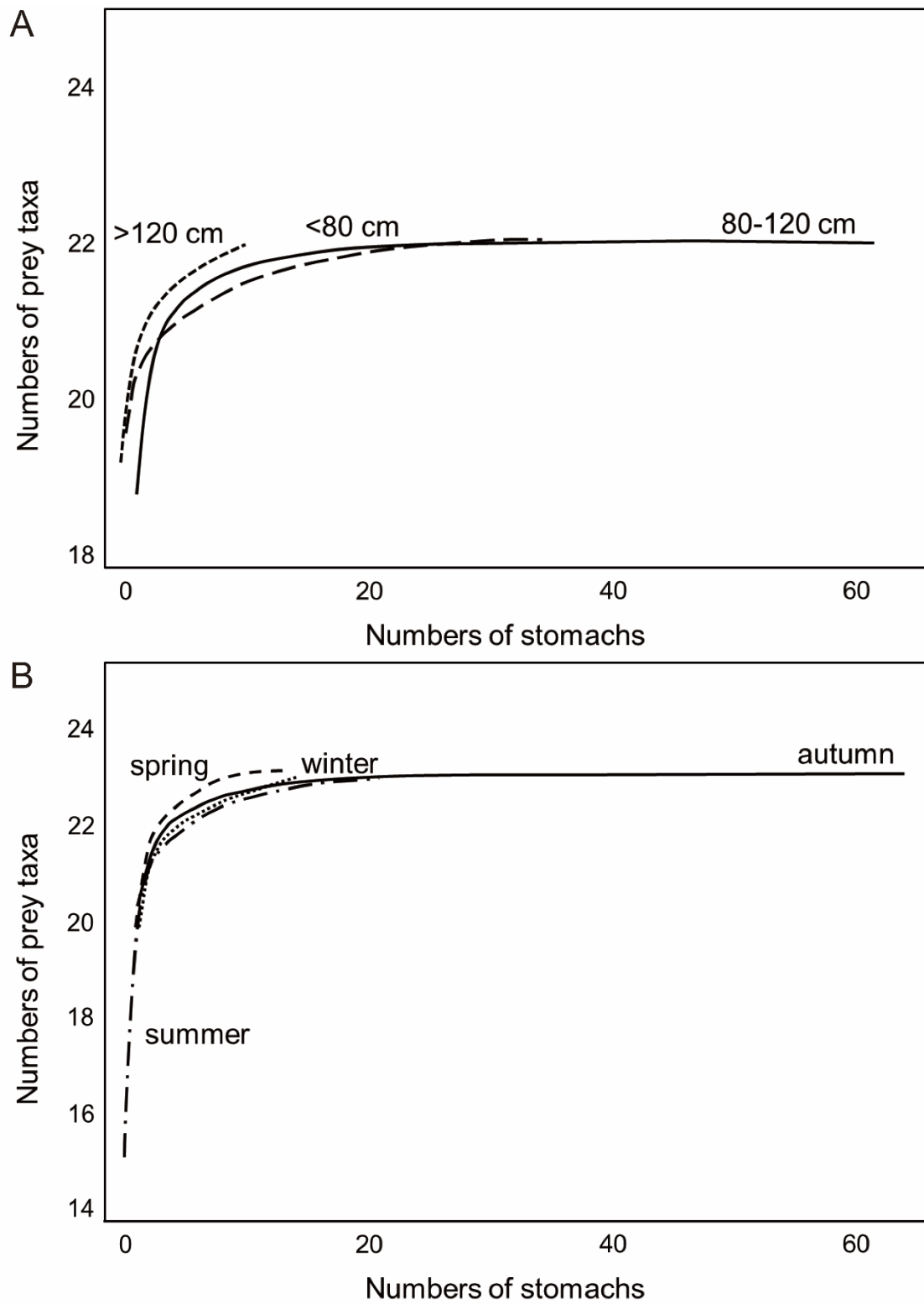


Fig. S5.2. Cumulative prey curves of sharptail sunfish across sizes (A) and seasons (B).

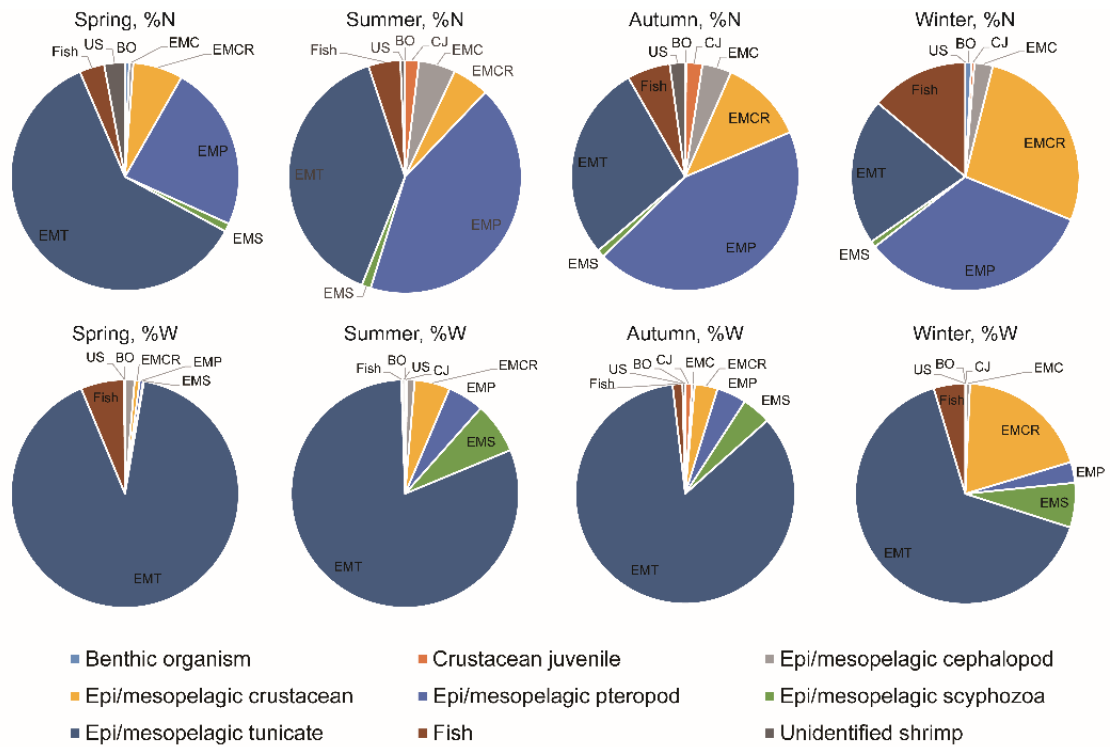


Fig. S5.3. Numerical (%N) and gravimetric (%W) diet compositions of sharptail sunfish among seasons (sample size: spring, n = 13; summer, n = 15; autumn, n = 63; winter, n = 14). Prey items were categorized into different functional groups as in Figure 5.2. Functional group abbreviations are as follows: BO = benthic organism, EMCR = epi/mesopelagic crustacean, EMS = epi/mesopelagic scyphozoa, CJ = crustacean juvenile, EMC = epi/mesopelagic cephalopod, EMP = epi/mesopelagic pteropods, EMT = epi/mesopelagic tunicate, US = unidentified shrimp.

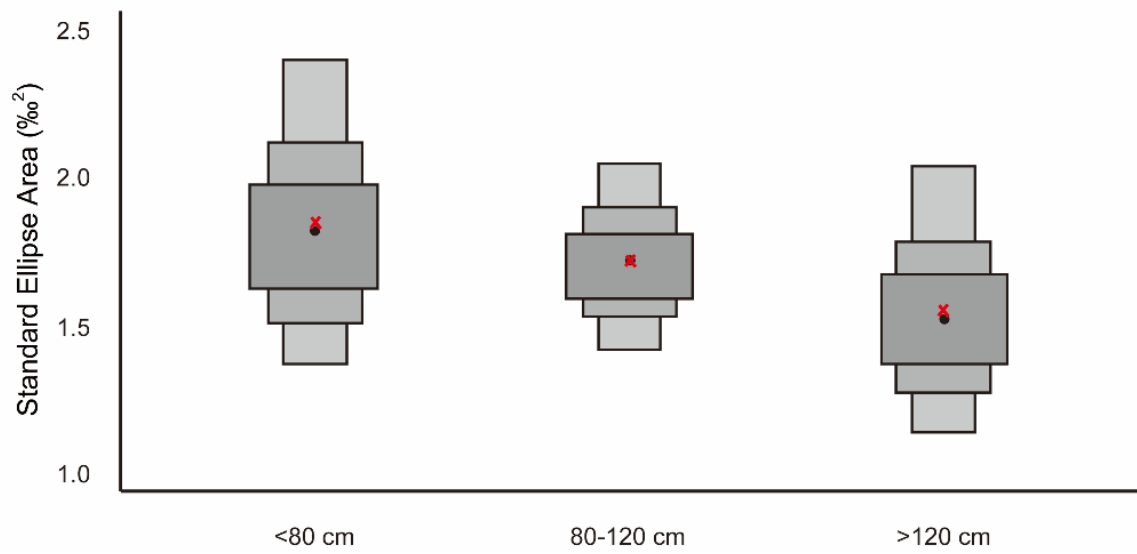


Fig. S5.4. Bayesian standard ellipse areas (SEA_b) of each size class (black dot: mean isotopic areas; red cross: estimated isotopic areas; dark gray box: 50% credible intervals, gray box: 75% credible intervals; light gray box: 95% credible intervals)

CHAPTER 6 – Conclusions and Future Directions

Highly migratory species travel long distances, migrating across international boundaries and can display different habitat uses across their life histories, related to foraging, spawning, or maintenance of thermal preferences. Many migratory species are endangered or threatened with overfishing. The molids are distributed circumglobally from tropical to temperate regions, with highly migratory behavior. Molids are caught globally as bycatch in several fisheries across their distribution range, including the longline, set net, drift net, trawl fisheries (Pope et al. 2010). They are targeted as commercial species in several countries of northwestern Pacific Ocean such as Taiwan, Japan, and South Korea (Chang et al. 2018, Nyegaard et al. 2020). The conservation of molids is especially important due to their special ecological roles as predators of gelatinous zooplankton and their highly migratory nature. Understanding their migrations, trophic dynamics and habitat use is imperative for effective conservation and can help us to develop management strategies and policies.

The overarching goal of this research is to explore the migration patterns, habitat use and feeding ecology of molids using electronic tagging, stomach content and stable carbon and nitrogen isotopic data in the western Pacific Ocean. The specific objectives of my research were as follows: i) explore the migration patterns and habitat uses of molids using electronic tags, isoscapes, CSIA-AA, and a Bayesian mixing model (Chapter 2 and 3), ii) reveal the feeding ecology of molids using literature review, SIA, SCA, and CSIA-AA, including breadth, overlap, and ontogenetic shift in the diets of molids (Chapter 4 and 5).

In this chapter, I conclude the key findings from each research chapter to examine the movement and feeding ecology of molids, and identify the potential direction of future research.

6.1 Research conclusion

Tagging technology was used to explore the migration path and the relationships of the migratory and environments of molids (Chapter 2). This study documented the first long-distance latitudinal movement patterns of molids tagged in waters off Taiwan. Two molids made northward movements from Taiwan to Japan and two made southward movement from Taiwan to the southern hemisphere. These molids exhibited different habitat utilization patterns between southward and northward migrations. The northward movement behaviors showed an affinity to mesoscale eddies and thermal preferences while the southward movements were possibly related to the ocean currents and thermal stratification of the water column. Although only four molids were tagged in this study, they showed similar migration paths especially the molids, which made southward movements.

Additionally, isotope analyses, including isoscapes of bulk tissue, CSIA-AA, and Bayesian mixing models, were used to examine the migration patterns and habitat uses of molids at a population level (Chapter 3). One notable finding of this research was the evidence suggesting that some large molids found in Taiwan and Japan might migrate from the warm pool region, and one molid found in New Caledonia might migrate from Taiwan, consistent with the tracks of molids in Chapter 2. These findings suggest these molids may be potential migrants from warm pool regions. Coupled with the captured timing of these potential large migrants and the spawning period of molids in Taiwan and Japan (Nakatsubo et al. 2007, Sawai & Chang 2018, Chang unpublished data), as determined by gonadal indices and the histological observation of gonad tissues, it is suggested that the migration of the molids from the warm pool is likely related to spawning behavior.

Diets description, breadth and overlap of molids were examined in this research using literature review, SIA and SCA (Chapter 4). This chapter provided a

comprehensive diet description of each species in the Family Molidae and the diet separation among sympatric species. The literature review revealed that molids exhibit broader diets than previously characterized as predators of gelatinous plankton almost exclusively. Ocean sunfish, bumphead sunfish, and hoodwinker sunfish reportedly consume prey from epi/mesopelagic environments, while sharptail sunfish and slender sunfish consume prey from both epi/mesopelagic environments and benthic habitats. No gelatinous prey was found in the stomachs of slender sunfish. Off Taiwan, ocean sunfish and bumphead sunfish had similar and relatively narrow diet breadths, differing from sharptail sunfish displayed a broader diet, mainly consuming tunicates and augmenting their diet from epi- and mesopelagic, coastal, and benthic habitats. This study provides an insight into the diet and trophic role of molids.

Chapter 5 provided a detailed diet description of sharptail sunfish, mainly distributed in the tropical and subtropical regions. Sharptail mola are captured as bycatch globally (Nyegaard et al. 2018, Arostegui et al. 2020) and are targeted for human consumption regionally (e.g. Taiwan, Fisheries Agency 2020). Broadly, prior to this work limited data were available on sharptail mola, and their diets were poorly described. In this study, sharptail sunfish from waters off Taiwan fed extensively on gelatinous organisms, similar to observations of diet in other molids. However, unlike other molids that typically feed on scyphozoans, tunicates were the most important gelatinous prey in the diets of sharptail mola in this study. The diet of sunfish mola changed significantly with size and seasons.

Overall, this study contributes to our understanding of the migratory behaviors, habitat uses and trophic interactions of molids in marine ecosystems. The population of molids face several threats, primarily from fishing activities and climate change. Molids are frequently caught as bycatch in various fisheries, including longline, set-net, dtift net, and trawl fisheries across different countries. Despite the overlap between their

distributions and some marine protected areas (MPAs) (Table 6.1), there are currently no species-specific conservation measures in place for molids. Furthermore, MPAs have yet to be established in some Asian countries where molids are extensively captured.

Climate change further exacerbates the challenges faced by pelagic fish like molids. The spatiotemporal distributions, migration pathways, and habitats uses of pelagic fishes may be susceptible to changes in the marine environment, such as ocean warming and deoxygenation (Ravier & Fromentin 2004, Stramma et al. 2012, Chang et al. 2013, Skubel et al. 2018). For example, the ocean warming increases water stratification, and further influences the horizontal and vertical distributions of molids in the water columns. Dissolved oxygen (DO) levels in the water are another critical factor, as many pelagic fishes tend to avoid hypoxia zones where oxygen concentrations < 2.5 ml L⁻¹ (Brill 1994). Molids preferred to stay in areas with higher DO concentration (4 to 5 ml L⁻¹), although they display a broad range of vertical movements (Chang et al. 2021). Ocean deoxygenation and warming are expected to expand the oxygen minimum zones and intensify thermal stratification in the water column, thereby compressing the available habitat for molids, especially in the vertical water column (Prince et al. 2010). The major consequence of habitat compression is that molids become more vulnerable to surface fishing gear. As their habitat range becomes shallower, they are more susceptible to capture by the fisheries. Additionally, pelagic fishes may alter their migration pathways due to the influence of rising water temperature. Some pelagic fishes such as tuna, billfish migrate into cooler regions in response to ocean warming (Gilman et al. 2016, Erauskin-Extramiana et al. 2019). Both threats from fishing activities and the impacts of climate change pose a risk to molid populations. Without the species-specific conservation measures, particularly in regions where molids are targeted species, these pressures could lead to declines in molid populations and their

long-term survival.

Understanding the migratory patterns and diets of molids is crucial for developing effective conservation measures. Molids migrate long distances for spawning, feeding, or in response to seasonal changes in water temperature and food availability. By knowing their migratory routes and critical habitats, we can implement measures to protect them from fishing activities and habitat degradation. For example, spatial management strategies, such as the designation of MPAs and the implementation of fishing restrictions in key habitats, can help mitigate the impacts of fishing and environmental changes. Nusa Penida Marine Protected Area in Indonesia is a successful example of spatial management that is developing species-specific tourism management for pelagic fishes including the molids and manta ray (Carter et al. 2014). This MPA not only protects critical habitats for marine organisms but also promotes sustainable tourism, benefiting both the marine ecosystem and the local economy.

6.2. Future Research

There are several promising directions for future research. Firstly, expanding the research regions to explore the migration patterns and habitat uses of molids across the Pacific Ocean would be beneficial. In the western Pacific Ocean, molids are captured as targeted species, with the average annual catch exceeding 400 tonnes from 2010 to 2021 (FAO, 2024). Previous studies have indicated that the western Pacific Ocean (South Korea and Japan) may be the spawning ground of molids (Nakatsubo et al. 2007, Kang et al. 2015). Molids' larvae have been observed and collected in various regions across the Pacific Ocean, including Hawaii (Sherman 1961, Leis & Miller 1976, Leis 1977), the northwestern Pacific near the Mariana Archipelago (Sokolovskaya & Sokolovskiy 1975, Kawakami et al. 2010) and the southwestern Pacific (Wan & Zhang 2005). Therefore, increasing the sample sizes from the western, eastern, central, and

southern Pacific Ocean could provide valuable insights into spawning areas and juvenile habitat use.

Secondly, studying the migratory patterns and movement behaviors of moids in different body size can help us to understand the habitat uses of moids across their life stages. Previous tagging studies have revealed the migration patterns of moids in the northwestern and eastern Pacific Ocean (Dewar et al. 2010, Thys et al. 2013, 2015, 2016, 2017, Chang et al. 2020, 2021). These studies have shown that most small moids exhibit site fidelity and make seasonal migrations within a limited region. These migration patterns are likely driven by the temperature changes and food availability (Dewar et al., Thys et al. 2015, 2016). Chang et al. (2021) and findings in Chapter 3 revealed that some large moids migrated across the ocean basins in the western Pacific Ocean, and the migration patterns may be related to the spawning behavior. The observed difference in movement behaviors between large and small moids suggest different habitat uses of moids across their size ranges. Large moids tend to undertake long distance migrations, possibly related to their reproductive strategies, whereas small moids show more localized movement patterns influenced by environments and resource availability. Thus, exploring the movement behavior of moids in different body size would provide a more comprehensive picture of the migratory paths and habitat uses of moids across their life stages.

Thirdly, incorporating more isotopic tracers, such as carbon or oxygen, could improve our understanding the migratory patterns of moids. In this study, we used nitrogen isotope ratios as a tracer to examine the migration patterns of moids. Carbon isotope ratio can be used as another trace. Carbon isotopes are fractionated during several processes when they move through the environment and into food webs, including the equilibrium between atmosphere and the ocean DIC pool (Boutton 1991) and photosynthesis process in primary producers (Popp et al. 1999). Furthermore, $\delta^{13}\text{C}$

of essential amino acids ($\delta^{13}\text{C}_{\text{EAA}}$) can be regarded as fingerprints to trace the sources of primary producers (Larson et al. 2009, 2020). Primary producers can generate unique $\delta^{13}\text{C}_{\text{EAA}}$ fingerprints and those fingerprints can be preserved in the tissue of consumers because the consumers obtain EAA from primary producers and they cannot synthesize EAA by themselves (McMahon 2010). Thus, increasing multiple tracers can improve the accuracy of the potential habitats and migratory paths of mollids.

Lastly, the diet study of most species within the Family Mollidae requires further investigation. For instance, *Mola alexandrini*, a species often misidentified as *M. mola*, and *M. tecta*, a new species discovered in 2018, each have only one diet study to date (Nyegaard et al. 2018, Chang 2024. in review). Additionally, the sample sizes in most diet studies of *Masturus lanceolatus* are relatively small, and most samples are stranding (Yabe 1950, Bakenhaster & Knight-Gray 2016, Sawai et al. 2019). Although there are ten diet studies for *Ranzania laevis*, most were conducted from 1800s to 1900s. There is still a lack of comprehensive diet information for these species across different regions, seasons, and life stages. Gathering more data on the dietary of these species across various environments and time periods is important for understanding their ecological roles in the marine ecosystems.

In conclusion, by implementing these future research directions, we can enhance our understanding of the movement and feeding ecology of mollids. By knowing their migration patterns, potential spawning areas, and feeding ecology, we can provide insight into the interactions of mollids, prey, and habitat across mollids' life stages. This knowledge is important for developing effective conservation measures and sustainable management practices to protect mollid populations in marine ecosystems.

6.3 References

Arostegui MC, Braun CD, Woodworth-Jefcoats PA, Kobayashi DR, Gaube P (2020)

- Spatiotemporal segregation of ocean sunfish species (Molidae) in the eastern North Pacific. *Mar Ecol Prog Ser* 654:109-125.
- Boutton TW (1991) Stable carbon isotope ratios of natural materials: II. Atmospheric, terrestrial, marine and freshwater environments. In *Carbon Isotope Techniques*, DC Coleman & B Fry (eds). San Diego, ca: academic Press, 173–186.
- Brill RW (1994) A review of temperature and oxygen tolerance studies of tunas pertinent to fisheries oceanography, movement models and stock assessments. *Fish Oceanogr* 3: 204-216.
- Carter E, Welly M, Sanjaya W (2014) Lessons learned in the development and establishment of the Nusa Penida Marine Protected Area, 2008 – 2014. Coral Triangle Center.
- Chang CT, Chiang WC, Musyl MK, Popp BN, Lam CH, Lin SJ, Watanabe YY, Ho YH, Chen JR (2021) Water column structure influences long-distance latitudinal migration patterns and habitat use of bumphead sunfish *Mola alexandrini* in the Pacific Ocean. *Sci Rep* 11:21934.
- Chang CT, Chih CH, Chang YC, Chiang WC, Tsai FY, Hsu HH, Wu JH, Ho YH (2018) Seasonal variations of species, abundance and size composition of Molidae in eastern Taiwan. *J Taiwan Fish Res* 26: 27-42.
- Chang CT, Lin SJ, Chiang WC, Musyl MK, Lam CH, Hsu HH, Chang YC, Ho YS (2020) Horizontal and vertical movement patterns of sunfish off eastern Taiwan. *Deep-Sea Res II: Top Stud Oceanogr* 175:104683.
- Chang YL, Sun CL, Chen Y, Yeh SZ, DiNardo G, Su NJ (2013) Modelling the impacts of environmental variation on the habitat suitability of swordfish, *Xiphias gladius*, in the equatorial Atlantic Ocean. *ICES J Mar Sci* 70: 1000–1012.
- Dewar H, Thys T, Teo SLH, Farwell C, O'Sullivan J, Tobayama T, Soichi M, Nakatsubo T, Kondo Y, Okada Y, Lindsay DJ, Hays GC, Walli A, Weng K, Streelmanand JT,

- Karl SA (2010) Satellite tracking the world's largest jelly predator, the ocean sunfish, *Mola mola*, in the Western Pacific. *J Exp Mar Biol Ecol* 393:32–42.
- Erauskin-Extramiana M, Arrizabalaga H, Hobday AJ, Cabré A, Ibaibarriaga L, Arregui I, Murua H, Chust G (2019) Large-scale distribution of tuna species in a warming ocean. *Glob Change Biol* 25: 2043-2060.
- FAO (2024) Fishery and Aquaculture Statistics – Yearbook 2021. FAO Yearbook of Fishery and Aquaculture Statistics. Rome.
- Fisheries Agency (2020) Fisheries statistical yearbook – Taiwan, Kinmen and Matsu Area, 2020. Fisheries Agency, Council of Agriculture, Taipei/Taiwan.
- Gilman E, Allain V, Collette BB, Hampton J, Lehodey P (2016) Effects of ocean warming on Pelagic tunas, a review. In Laffole D, Baxter J (eds) *Explaining ocean warming: Causes, scale, effects and consequences*. Gland, Switzerland: IUCN – International Union for the Conservation of Nature, pp 254-270.
- Kang MJ, Baek HJ, Lee DW, Choi JH (2015) Sexual maturity and spawning of ocean sunfish *Mola mola* in Korean waters. *Korean J Fish Aquat Sci* 48: 739–744.
- Kawakami T, Aoyama J, Tsukamoto K (2010) Morphology of pelagic fish eggs identified using mitochondrial DNA and their distribution in waters west of the Mariana Islands. *Environ Biol Fish* 87: 221–235.
- Larsen T, Hansen T, Dierking J (2020) Characterizing niche differentiation among marine consumers with amino acid $\delta^{13}\text{C}$ fingerprinting. *Ecol Evol* 10: 7768-7782.
- Larsen T, Taylor DL, Leigh MB, O'Brien DM (2009) Stable isotope fingerprinting: A novel method for identifying plant, fungal or bacterial origins of amino acids. *Ecology* 90: 3526–3535.
- Leis JM (1977) Development of the eggs and larvae of the slender mola, *Ranzania laevis* (Pisces, Molidae). *Bull Mar Sci* 27: 448–466.
- Leis JM, Miller JM (1976) Offshore distributional patterns of Hawai'ian fish larvae.

Mar Biol 36: 359–367.

Madigan DJ, Baumann Z, Carlisle AB, Hoen DK, Popp BN, Dewar H, Snodgrass OE, Block BA, Fisher NS (2014) Reconstructing transoceanic migration patterns of Pacific bluefin tuna using a chemical tracer toolbox. *Ecology* 95: 1674-1683.

Madigan DJ, Chiang WC, Wallsgrove NJ, Popp BN, Kitagawa T (2016) Intrinsic tracers reveal recent foraging ecology of giant Pacific bluefin tuna at their primary spawning grounds. *Mar Ecol Prog Ser*: 553, 253-266.

Madigan DJ, Shipley ON, Carlisle AB, Dewar H, Snodgrass OE, Hussey NE (2021) Isotopic tracers suggest limited trans-oceanic movements and regional residency in North Pacific blue sharks (*Prionace glauca*). *Front Mar Sci* 8: 653606.

McMahon KW, Fogel ML, Elsdon TS, Thorrold SR (2010) Carbon isotope fractionation of amino acids in fish muscle reflects biosynthesis and isotopic routing from dietary protein. *J Anim Ecol* 79: 1132–1141.

Nakatsubo T, Kawachi M, Mano N, Hirose H (2007) Spawning period of ocean sunfish *Mola mola* in waters of the eastern Kanto Region, Japan. *Aquac Sci* 55: 613-618.

Nakatsubo T, Kawachi M, Mano N, Hirose H (2007) Spawning period of ocean sunfish *Mola mola* in waters of the eastern Kanto region, Japan. *Aquat Sci* 55: 613–618.

Nyegaard M, Loneragan N, Hall S, Andrew J, Sawai E, Nyegaard M (2018) Giant jelly eaters on the line: Species distribution and bycatch of three dominant sunfishes in the Southwest Pacific. *Estuar Coast Shelf Sci* 207:1-15.

Office of National Marine Sanctuaries (2024) Marine Protected Areas (MPA) Inventory 2023-2024, <https://www.fisheries.noaa.gov/inport/item/69506>.

Pope EC, Hays G, Thys T, Doyle T, Sims D, Queiroz N (2010) The biology and ecology of the ocean sunfish *Mola mola*: A review of current knowledge and future research perspectives. *Rev Fish Biol Fish* 20:471–487.

Popp BN, Trull T, Kenig F, Wakeham SG, Rust TM, Tilbrook B, Griffiths B, Wright SW,

- Marchant HJ, Bidigare RR, Laws EA (1999) Controls on the carbon isotopic composition of Southern Ocean phytoplankton. *Global Biogeochem Cycles* 13: 827–843.
- Prince ED, Luo J, Goodyear CP, Hoolihan JP, Snodgrass D, Orbesen ES, Serafy JE, Ortiz M, Schirripa MJ (2010) Ocean scale hypoxia-based habitat compression of Atlantic istiophorid billfishes. *Fish Oceanogr* 19: 448-462.
- Ravier C, Fromentin JM (2004) Are the long-term fluctuations in Atlantic bluefin tuna (*Thunnus thynnus*) population related to environmental changes? *Fish Oceanogr* 13: 145–160.
- Sawai E, Chang YC (2018) A rare record of the bump-head sunfish, *Mola alexandrini* (Tetraodontiformes: Molidae) with a 117 kg ovary from Hualien, Taiwan. *Biogeography* 20: 73-77.
- Sherman K (1961) Occurrence of early developmental stages of the oblong ocean sunfish *Ranzania laevis* (Pennant) in the Central North Pacific. *ASIH*: 467–470.
- Skubel RA, Kirtman BP, Fallows C, Hammerschlag N (2018) Patterns of long-term climate variability and predation rates by a marine apex predator, the white shark. *Carcharodon carcharias*. *Mar Ecol Progr Ser* 587: 129–139.
- Sokolovskaya TS, Sokolovskiy AS (1975) New data on expansion of the area of reproduction of ocean sunfishes (Pisces, Molidae) in the Northwestern Part of the Pacific Ocean. *J Ichthyol* 15: 675-678.
- Stramma L, Prince ED, Schmidtko S, Luo J, Hoolihan JP, Visbeck M, Wallace DWR, Brandt P, Körtzinger A (2012) Expansion of oxygen minimum zones may reduce available habitat for tropical pelagic fishes. *Nat Clim Change* 2: 33-37.
- Thys TM, Hearn AR, Weng KC, Ryan JP, Penaherrera-Palma C (2017) Satellite tracking and site fidelity of short ocean sunfish, *Mola ramsayi*, in the Galapagos Islands. *J Mar Biol* 2017: 7097965.

- Thys TM, Ryan JP, Dewar H, Perle CR, Lyons K (2015) Ecology of the ocean sunfish, *Mola mola*, in the southern California Current System. *J Exp Mar Biol Ecol* 471: 64-76.
- Thys TM, Ryan JP, Weng KC, Erdmann M, Tresnati J (2016) Tracking a marine ecotourism star: Movements of the short ocean sunfish *Mola ramsayi* in Nusa Penida, Bali, Indonesia. *J Mar Biol* 2016: 8750193.
- Thys TM, Whitney J, Hearn A, Weng KC, Peñaherrera C, et al. (2013) First record of the southern ocean sunfish, *Mola ramsayi*, in the Galápagos Marine Reserve. *Mar Biodivers Rec* 6: e70.
- Wan RJ, Zhang RZ (2005) Spatial distribution and morphological characters of the eggs and larvae of the slender mola *Ranzania laevis* from the tropical waters of the western Pacific Ocean. *Acta Zool Sin* 51: 1034–1043.

Table 6.1. The overlap of marine protected areas with mollids' distributions. The distributions of mollids are identified from the occurrence of record in iNaturalist <https://www.inaturalist.org/>

Area	Marine Protected Area
USA	Papahānaumokuākea Marine National Monument, Pacific Remote Islands Marine National Monument, Northeast Canyons and Seamounts Marine National Monument, Gerry E. Studds/Stellwagen Bank National Marine Sanctuary, North Shore Ocean Sanctuary, South Essex Ocean Sanctuary, Cape Cod Bay Ocean Sanctuary, Cape and Islands Ocean Sanctuary, Greater Farallones National Marine Sanctuary, Cordell Bank National Marine Sanctuary, Monterey Bay National Marine Sanctuary, Channel Islands National Marine Sanctuary, Channel Islands National Park, Santa Barbara Island Federal Marine Reserve, Olympic Coast National Marine Sanctuary, Flower Garden Banks National Marine Sanctuary, Gulf of the Farallones
Canada	St Anns Bank Marine Protected Area, The Gully Marine Protected Area, SGAan Kinghlas-Bowie Seamount Marine Protected Area, Gwaii Haanas National Marine Conservation Area Reserve & Haida Heritage Site, Hecate Strait and Queen Charlotte Sound Glass Sponge Reefs Marine Protected Areas
Japan	Izu-Ogasawara Trench Offshore Seabed Nature Conservation Area, Nishi-Shichito Ridge Offshore Seabed Nature Conservation Area

Table 6.1. (Continued) The overlap of marine protected areas with mollids' distributions. The distributions of mollids are identified from the occurrence of record in iNaturalist <https://www.inaturalist.org/>

Area	Marine Protected Area
Philippines	Tubbataha Reefs Natural Park
France	Natural Parck of the Croal Sea
Australia	Coral Sea Commonwealth Marine Reserve, Great Barrier Reef Marine Park, Norfolk Commonwealth Marine Reserve, Argo-Rowley Terrace Commonwealth Marine Reserve, Lord Howe Commonwealth Marine Reserve
UK	Pitcairn Islands Marine Reserve, Charlie Gibbs North High Seas Area, Southern North Sea Marine Protected Area
Palau	Palau National Marine Sanctuary
Chile	Juan Fernandez Marine Park, Nazca-Desventuradas Marine Park, Motu Motiro Hiva Marine Park
Mexico	Pacifico Mexicano Profundo, Revillagigedo National Park
Brazil	Sao Pedro & Sao Paulo Environment Protection Area
Ecuador	Galapagos Marine Reserve

Table 6.1. (Continued) The overlap of marine protected areas with mollids' distributions. The distributions of mollids are identified from the occurrence of record in iNaturalist <https://www.inaturalist.org/>

Area	Marine Protected Area
Christmas Island	Christmas Island Marine Park
Spain	Corredor de migración de cetáceos del Mediterráneo Marine Protected Area
France, Italy, Monaco	Pelagos Sanctuary For The Conservation Of Marine Mammals
Greece	NISOS GYAROS KAI THALASSIA ZONI Sites of Community Importance
Indonesia	Nusa Penida Marine Protected Area
Portugal	Ilhas Selvagens Natural Reserve, Arquipélago Submarino do Meteor Resource Management Protected Area, Faial-Pico Channel Marine Protected Area
South Africa	Helderberg Marine Protected Area